

INFORMATION TO USERS

This manuscript has been reproduced from the microfilm master. UMI films the text directly from the original or copy submitted. Thus, some thesis and dissertation copies are in typewriter face, while others may be from any type of computer printer.

The quality of this reproduction is dependent upon the quality of the copy submitted. Broken or indistinct print, colored or poor quality illustrations and photographs, print bleedthrough, substandard margins, and improper alignment can adversely affect reproduction.

In the unlikely event that the author did not send UMI a complete manuscript and there are missing pages, these will be noted. Also, if unauthorized copyright material had to be removed, a note will indicate the deletion.

Oversize materials (e.g., maps, drawings, charts) are reproduced by sectioning the original, beginning at the upper left-hand corner and continuing from left to right in equal sections with small overlaps.

Photographs included in the original manuscript have been reproduced xerographically in this copy. Higher quality 6" x 9" black and white photographic prints are available for any photographs or illustrations appearing in this copy for an additional charge. Contact UMI directly to order.

ProQuest Information and Learning
300 North Zeeb Road, Ann Arbor, MI 48106-1346 USA
800-521-0600

UMI[®]

UNIVERSITY OF ALBERTA

Synthesis and Conformational Studies of Constrained Oligosaccharides

by

Shirley Ann Wacowich-Sgarbi

A thesis submitted to the faculty of Graduate Studies and Research in partial fulfillment of the requirements for the degree of Doctor of Philosophy.

DEPARTMENT OF CHEMISTRY

Edmonton, Alberta

Spring, 2000



National Library
of Canada

Acquisitions and
Bibliographic Services

395 Wellington Street
Ottawa ON K1A 0N4
Canada

Bibliothèque nationale
du Canada

Acquisitions et
services bibliographiques

395, rue Wellington
Ottawa ON K1A 0N4
Canada

Your file Votre référence

Our file Notre référence

The author has granted a non-exclusive licence allowing the National Library of Canada to reproduce, loan, distribute or sell copies of this thesis in microform, paper or electronic formats.

The author retains ownership of the copyright in this thesis. Neither the thesis nor substantial extracts from it may be printed or otherwise reproduced without the author's permission.

L'auteur a accordé une licence non exclusive permettant à la Bibliothèque nationale du Canada de reproduire, prêter, distribuer ou vendre des copies de cette thèse sous la forme de microfiche/film, de reproduction sur papier ou sur format électronique.

L'auteur conserve la propriété du droit d'auteur qui protège cette thèse. Ni la thèse ni des extraits substantiels de celle-ci ne doivent être imprimés ou autrement reproduits sans son autorisation.

0-612-60036-X

Canada

UNIVERSITY OF ALBERTA
LIBRARY RELEASE FORM

NAME OF AUTHOR: Shirley Ann Wacowich-Sgarbi
TITLE OF THESIS: Synthesis and Conformational Studies of Constrained
Oligosaccharides.
DEGREE: Doctor of Philosophy
YEAR THIS DEGREE GRANTED: 2000

Permission is hereby granted to the University of Alberta Library to reproduce single copies of this thesis and to lend or sell such copies for private, scholarly or scientific research purposes only.

The author reserves all other publication and other rights in association with the copyright in the thesis, and except as hereinbefore provided, neither the thesis nor any substantial portion thereof may be printed or otherwise reproduced in any material form whatever without the author's prior written permission.



84 St. Andrew's

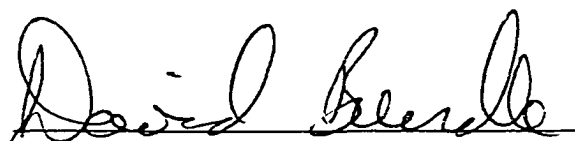
Baie D'Urfé, Québec

Canada, H9X 2V1

Date: *Jan 19, 2000*

UNIVERSITY OF ALBERTA
FACULTY OF GRADUATE STUDIES AND RESEARCH

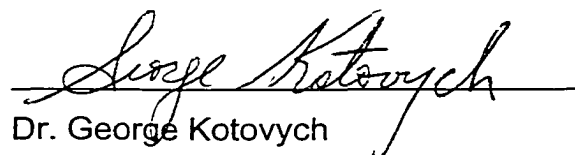
The undersigned certify that they have read, and recommended to the Faculty of Graduate Studies and Research for acceptance, a thesis entitled **Synthesis and Conformational Studies of Constrained Oligosaccharides** by **Shirley Ann Wacowich-Sgarbi** in partial fulfillment of the requirements for the degree of **Doctor of Philosophy**.



Dr. David R. Bundle (Supervisor)



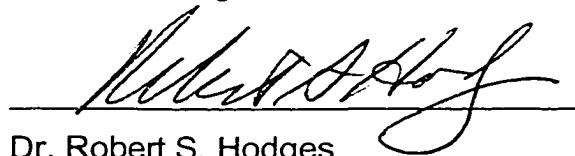
Dr. Dennis G. Hall (Chair)



Dr. George Kotovych



Dr. Ole Hindsgaul



Dr. Robert S. Hodges



Dr. B. Mario Pinto (External Examiner)

Dated: December 10th, 1999

Abstract

The possibility that the low affinity of oligosaccharide-protein interactions originates from the flexibility about the glycosidic linkage has been investigated by the synthesis and bioassay of tethered oligosaccharides. Tethered analogues of the human blood group H-type 2 trisaccharide α -L-Fucp(1→2)- β -D-Galp(1→4) β -D-GlcpNAc1→OMe (**1**), that constrain the β Galp(1→4)GlcpNAc glycosidic linkage were synthesized via intramolecular glycosylation. Attempts to tether the α Fuc to β GlcNAc residue are also reported. Dramatic changes in the stereochemical outcome of the intramolecular glycosylation were observed when the protecting groups on the donor moiety of the tethered monosaccharides were changed. An investigation was performed in order to determine the factors which control the stereoselectivity of these reactions.

The tethered oligosaccharides were assayed for activity with H-type 2 specific lectins, such as: *Ulex europaeus* I, *Psophocarpus tetragonolobus* II, and *Erythrina corallodendron* lectins. In the *Ulex* system, tethered trisaccharide **28** was almost as good an inhibitor as the native trisaccharide **1**. However, for all lectin-inhibitor combinations, none of the tethered trisaccharides were as active as the native epitope.

Modeling showed that the solution conformations of tethered trisaccharide **28** and to a lesser extent **29** matched that of native trisaccharide **1**. This data also suggests that tethering of the H-type 2 trisaccharide did succeed in reducing the flexibility about the β Galp(1→4)GlcpNAc glycosidic linkage, but that the rotational freedom about the α Fucp(1→2)Galp linkage was increased. The increase in rotational freedom of the fucose residue is attributed to the decrease in activity of the tethered trisaccharides.

A tethered α -disaccharide (**82**) with the *anti*-conformation was synthesized and used to calibrate the heteronuclear three bond coupling constant. Disaccharide **82** is the first example of a deprotected disaccharide “frozen” in the high-energy *anti*-conformation.

The bioactivities and conformational results highlight the challenge in design and synthesis of oligosaccharides that are pre-organized in a bioactive conformation. The absence of substantial free energy gains in this and other studies of pre-organized ligands, reinforces the hypothesis that solvent reorganization rather than conformational entropy is the major contributor to the low affinity of protein-carbohydrate interactions.

Acknowledgements

I would like to thank my best friend, my confidant, my husband Paulo Sgarbi for the love and support he has given me throughout our time together and apart. Thanks to my Mom, Dad and Mathieu for cheering on the sidelines, and Dave who had to deal with my craziness. I'll never forget my best friends EJMD and Chi-Chenne.

Many thanks go out to my colleagues and friends in the Bundle-clan, who have contributed to my scientific growth. Particularly thanks to Lesley Liu, Joanna Sadowska, and Dr. Chang-Chun Ling. A special thanks to Dr. Albin Otter for the invaluable instruction and advice throughout the years.

I would like to thank my supervisor Dr. D. R. Bundle for the challenge, and for giving me the opportunity to explore different areas in chemistry.

Table of Contents

	Page
<i>Chapter 1 - Introduction</i>	
1.1: Carbohydrates	1
1.2: Current Project	2
1.3: Protein-Carbohydrate Interactions	2
1.4: Carbohydrate Antigens	3
1.4.1: Glycoproteins	4
1.4.2: Glycolipids	5
1.4.3: Human Blood Group ABO(H) Antigens	7
1.4.4: Basis of the A, B, O Histo-Blood Groups	9
1.5: Lectin	10
1.5.1: Lectins and their Function	10
1.5.2: General Structure of Legume Lectins	11
1.5.3: Lectin Specificity	15
1.5.4: Ligand Multivalency	16
1.5.5: Lectins and Medicine	17
1.6: Lectin-Carbohydrate Interactions	18
1.6.1: Thermodynamics	20
1.7: Constrained Oligosaccharides	22
1.7.1: Overview on Constrained Oligosaccharides	29
<i>Chapter 2 - Design of Constrained H-type 2 Derivatives</i>	
2.1: Pre-Organisation of H-type 2 Trisaccharide	31
2.2: Mapping Study of the H-type 2 Trisaccharide	32
2.2.1: Tethering Sites on the H-type 2 Trisaccharide	33
2.3: Computer Modeling	35

**Chapter 3 - Synthesis of Constrained Trisaccharides via
Intramolecular Glycosylation**

3.1: Introduction	41
3.1.1: Glycoside Synthesis – General Concepts	41
3.1.2: Review of Intramolecular O-Glycosylation	42
3.1.2a: Category 1 - Temporary Tethers	43
3.1.2b: Category 2 - Permanent Tethers	48
3.1.2c: Overview on Intramolecular O-Glycosylation	55
3.2: Synthesis of Constrained H-type 2 Trisaccharides	56
3.2.1: Synthesis of Constrained H-type 2 Trisaccharide 28	58
3.2.1a: Strategy	58
3.2.1b: Preparation of the Linker	61
3.2.1c: Tethering the Monosaccharide Synthons	61
a) Route 1a	61
b) Route 1b	63
c) Route 2	66
3.2.1d: Intramolecular Glycosylations	68
3.2.1e: Assembly and Deprotection of the Tethered Trisaccharide	69
3.2.2: Synthesis of Constrained H-type 2 Trisaccharide 29	71
3.2.2a: Preparation of the Linker	72
3.2.2b: Preparation of the Galactose Donor	73
3.2.2c: Tethering the Monosaccharide Synthons	74
3.2.2d: Intramolecular Glycosylations	76
3.2.2e: Assembly and Deprotection of the Tethered Trisaccharide	78
3.2.3: Synthesis of Lactosamine Derivatives	80
3.2.4: Influence of Substituents at C-6 of Fucose on Binding to <i>Ulex</i>	82
3.2.4a: Preparation of Fucose Derivative 93	83
3.2.4b: Preparation of Fucose Derivative 94	84

3.2.4c: Biological Activity	85
3.2.5: Synthesis of Constrained H-type 2 Trisaccharide 31	86
3.2.5a: Strategy	86
3.2.5b: Preparation of the Fucose Donor	88
3.2.5c: Tethering the Monosaccharide Synthons	93
3.2.5d: Glycosylation	94
3.3: Investigation of the Intramolecular Glycosylation	96
3.3.1: Observation	96
3.3.2: Synthesis of the Intramolecular Glycosylation Precursors	98
3.3.3: Intramolecular Glycosylation	102
Chapter 4 - Biological Activity of the Constrained Carbohydrates:	
4.1: Introduction	105
4.2: Solid-Phase Immunoassay	105
4.2.1: Basic Principles of EIA	105
4.2.2: Competition EIA	107
4.2.3: Protocol	107
4.3: Results	109
4.3.1: Binding Studies of the Constrained Trisaccharides 28 and 29 with <i>Ulex europaeus</i> l and Winged Bean	109
4.3.2: Binding Studies of the Constrained Di- and Trisaccharides with <i>Erythrinia corallodendron</i>	110
4.4: Conclusion	111

Chapter 5 - NMR and Modeling Studies of the Free Conformations of H-type 2 Trisaccharide and Constrained Derivatives

5.1: Introduction	114
5.1.1: Conformational Parameters of Oligosaccharides	114
5.1.2: Anomeric Effect	116
5.1.3: Determination of the Solution Conformation of Oligosaccharides	118
5.1.3a: Nuclear Magnetic Resonance	118
5.1.3b: Theoretical Predictions	118
5.1.4: Outline of Investigation	121
5.2: Determination of Solution Conformation of H-type 2 Trisaccharide	121
5.2.1: Proton and Carbon Assignments for H-type 2 Trisaccharide	122
5.2.2: T-ROESY Distance Measurements for H-type 2 Trisaccharide 1	126
5.2.3: Solution Conformation of the Trisaccharide 1	128
5.3: The Solution Conformation of Constrained Trisaccharides 28 and 29	131
5.3.1: Proton and Carbon Assignments for Trisaccharides 28 and 29	132
5.3.2: T-ROESY Distance Measurements for Constrained Trisaccharides 28 and 29	133
5.3.3: Solution Conformation of the Constrained Trisaccharides 28 and 29	134
5.4: Comparison of Solution Conformation of 1 and its Tethered Derivatives 28 and 29	139
5.5: Conformational Analysis of a $\alpha\text{Galp}(1\rightarrow4)\beta\text{Glc}p\text{NAC}\rightarrow\text{OCH}_3$ Disaccharide that Adopts the <i>ANTI</i> -Conformation	143
5.5.1: Proton and Carbon Assignments for Tethered	144

Disaccharide 82	
5.5.2: Proton and Carbon Assignments for Untethered Disaccharide 92	146
5.5.3: T-ROESY Distance Measurements for Tethered Disaccharide 82	146
5.5.4: T-ROESY Distance Measurements for Untethered Disaccharide 92	148
5.5.5: EXSIDE Experiments	150
5.5.6: Conformation of the Disaccharide 92	153
5.5.7: Conformation of the Tethered Disaccharide 82	154
5.5.8: Solution Dynamics of Tethered Disaccharide 82	157
5.5.9: Conclusion	158

Chapter 6 - NMR and Theoretical Studies of the Bound Conformations of H-type 2 and its Constrained Derivatives

6.1: Introduction	160
6.2: NMR Investigation of Protein-Carbohydrate Interactions	160
6.2.1: Different NMR Protocols	160
6.2.2: Titration NMR Experiments	161
6.2.3: Chemically Induced Dynamic Nuclear Polarization	161
6.2.4: NMR Relaxation Experiments	162
6.2.5: Transferred Nuclear Overhauser Enhancement Studies	162
6.2.5a: Required Conditions for TRNOE	164
6.2.5b: Observation of Transferred NOEs	164
6.2.5c: Quantitative Interpretation of Transferred NOEs	165
6.3: Molecular Modeling of Carbohydrate-Protein Complexes	166
6.4: Outline of Investigation	167
6.5: Results and Discussion	167
6.5.1: Determination of the Bound Conformation of the	167

Trisaccharide 1	
6.5.2: NMR Studies of the Bound Conformation of the Trisaccharide 1	168
6.5.2a: Experimental Protocol	168
6.5.2b: Results	169
6.5.3: Determination of the Bound Conformation of Tethered Trisaccharide 28	169
6.5.3a: NMR studies of the Bound Conformation of Trisaccharide 28	170
6.5.3b: Experimental Protocol	170
6.5.3c: Results	171
6.5.3d: Binding of native H-type 2 Trisaccharide 75°C with <i>Ulex</i>	172
6.5.4: Modeling Studies of the Bound Conformation of Trisaccharides 1 and 28	173
6.6: Conclusion	176
Chapter 7 – Conclusions	
7.1: Studies of the Carbohydrate- <i>Ulex</i> Complexes	177
7.2: Binding of the H-type 2 trisaccharides to <i>Winged Bean</i>	178
7.3: Binding of the H-type 2 trisaccharides to <i>Erythrinia corallodendron</i>	178
7.4: Calibration of Heteronuclear Coupling Constants	179
7.5: Tethering as a Means to Reduce Entropy	179
Chapter 8 – Experimental	
8.1: Isolation and Purification of Lectins	182
8.2: Solid Phase Immunoassay	183
8.3: NMR Measurements of Oligosaccharide Solution Conformation	184
8.4: NMR Measurements of Trisaccharides Bound to <i>Ulex europaeus</i> I	186

8.5: Molecular Modeling	187
8.6: General Methods for Synthesis	190
8.7: Synthesis of Constrained H-type 2 Trisaccharides	191
8.8: Investigation of the Intramolecular Glycosylation	245
References	260

List of Figures

Figure		Page
Figure 1.1	Schematic of the location of glycoproteins and Glycosphingolipids in a plasma membrane.	3
Figure 1.2:	N- and O-linkages of glycoproteins.	4
Figure 1.3:	Type 1 and type 2 core structures of cell surface mucins.	5
Figure 1.4:	Structures of glycosphingolipids: (A) ceramide portion of glycosphingolipids; (B) tetrasaccharide core sequences (R group attached to the ceramide) found in glycosphingolipids (i) lactotetraosylceramide, (ii) neolactotetraosylceramide, (iii) gangliotetraosylceramide, and (iv) globotetraosylceramide.	6
Figure 1.5:	Terminal structures of the AB(O) blood group determinants.	9
Figure 1.6:	Structure of the <i>Ulex europaeus</i> I lectin in ribbon representation. Large sphere represents Ca^{2+} and small sphere depicts Mn^{2+} .	13
Figure 1.7:	Two views of a canonical legume lectin dimer.	14
Figure 1.8:	Tetramers formed from two canonical dimers of <i>Concanavalin A</i> . Spheres represent cations Ca^{2+} and Mn^{2+} .	15

Figure 1.9: Monovalency versus polyvalency.	17
Figure 1.10: Examples of sugar-protein hydrogen bond types.	19
Figure 1.11: Galabiose 2 and the tethered galabiose analogues 3 and 4 prepared by Magnusson <i>et al.</i> .	23
Figure 1.12: Native trisaccharide 5 , and structures of the tethered ligands 6 to 11 .	25
Figure 1.13: Native β -D-GlcNAc(1 \rightarrow 2)- α -D-Man(1 \rightarrow 3)-D-Man (12) and its tethered analogues (13 and 14).	26
Figure 1.14: Sialyl Lewis x 16 and SLe ^x analogues 15 and 17 .	27
Figure 1.15: Parent substrate for GlcNAc transferase-V 18 and analogue substrates 19 and 20 .	29
Figure 2.1: Congener mapping of the H-type 2 epitope.	33
Figure 2.2: Possible tethered trisaccharides predicted from Lemieux's work.	34
Figure 2.3: Ribbon representation of the <i>Ulex europaeus</i> I lectin with docked H-type 2 trisaccharide. Spheres represent cations Ca ²⁺ and Mn ²⁺ .	36
Figure 2.4: Computer modeling: binding site amino acids of the <i>Ulex</i> lectin co-crystallized with a molecule of (R)-2,4-dihydroxy-2-methylpentane and superimposed H-type 2 trisaccharide.	37

Figure 2.5:	Computer modeling: a stereo plot of the binding site amino acids (mid grey lines) of the <i>Ulex europaeus</i> I lectin co-crystallized with a molecule of 2,4-dihydroxy-2-methylpentane (light gray lines) and superimposed H-type 2 trisaccharide (black lines).	38
Figure 2.6:	Potential tethered trisaccharides suggested by computer modeling.	39
Figure 3.1:	Glycosylation reaction.	42
Figure 3.2:	Various attachments of the acceptor.	53
Figure 3.3:	Retrosynthesis of the tethered H-type 2 trisaccharide 28 .	59
Figure 3.4:	Potential strategies for tethering two monosaccharides.	60
Figure 3.5:	Confirmation of the regioselectivity of the benzylidene acetal reductive ring opening.	68
Figure 3.6:	Modified galactose donor.	72
Figure 3.7:	Inhibitor activities of fucose derivatives 93 and 94 relative to methyl α -L-fucopyranoside (95) obtained by competition ELISA.	86
Figure 3.8:	Retrosynthesis of the tethered H-type 2 trisaccharide 31 .	87

Figure 3.9: Interconversion of D- and L-hexoses.	88
Figure 3.10: Conversion of D-galactose to L-galactose.	89
Figure 3.11: Proposed route to constrained trisaccharide 31 .	96
Figure 3.12: Intramolecular glycosylations involving the three carbon linker.	97
Figure 4.1: The enzyme immunosorbent assay (EIA).	106
Figure 4.2: Direct competition assay format to determine IC ₅₀ values.	108
Figure 4.3: Biological activity of the tethered 28 and 29 relative to native trisaccharide 1 assayed with the <i>Ulex europaeus</i> I and WBA lectins.	110
Figure 5.1: Absolute configuration of monosaccharides found in the H-type 2 trisaccharide: a) β -D-N-acetylglucosamine; b) β -D-galactopyranose; c) α -L-fucopyranose.	115
Figure 5.2: The torsion angles ϕ (phi) and ψ (psi) shown for a (1 \rightarrow 4) linked disaccharide; $\phi_H = \text{H1-C1-O1-C4}$; $\psi_H = \text{C1-O1-C4-H4}$. The torsional angle ω (omega) is shown for a (1 \rightarrow 6) linked disaccharide; $\omega = \text{O5-C5-C6-O6}$.	115

Figure 5.3:	Rotamer states preferentially adopted by glycosides with axial and equatorial groups due to the <i>exo</i> -anomeric effect.	116
Figure 5.4:	$^3J_{C,H}$ coupling constants about the glycosidic linkage.	119
Figure 5.5:	1D 1H -NMR spectrum of H-type 2 trisaccharide 1 in D_2O .	123
Figure 5.6:	GCOSY spectrum of H-type 2 trisaccharide 1 in D_2O .	124
Figure 5.7:	Decoupled HMQC spectrum of H-type 2 trisaccharide 1 in D_2O .	125
Figure 5.8:	HMBC spectrum of H-type 2 trisaccharide 1 in D_2O .	126
Figure 5.9:	T-ROESY spectrum of H-type 2 trisaccharide 1 in D_2O .	127
Figure 5.10:	Energy minimization of trisaccharide 1 using ROE restraints produced a) a major family of structures, and b) a minor family of structures.	129
Figure 5.11:	Lowest energy structure of 1 with graphs that depict the trajectory of a 5000 ps MD simulation about both glycosidic linkages.	130

Figure 5.12: The minimization of constrained trisaccharide 28 using its ROE restraints produced a) a major, and b) a minor family of structures.	135
Figure 5.13: The minimization of constrained trisaccharide 29 using its ROE restraints produced a) a major, and b) a minor family of structures.	136
Figure 5.14: Lowest energy structure obtained from the minimization used as a starting point for the MD simulations of the constrained trisaccharide a) 28 and b) 29 . Graphs depict the trajectory of a 5000 ps MD simulation of the constrained trisaccharides about both glycosidic linkages.	138
Figure 5.15: Superimpositions of the NMR derived lowest energy conformation of the native H-type 2 trisaccharide 1 (AMBER forcefield) with a) 28 , b) 29 , and c) the GEGOP global minimum for 1 .	141
Figure 5.16: Graphs depicting the glycosidic linkage trajectory of the 5000 ps MD simulation of a) 1 , b) 28 and c) 29 .	142
Figure 5.17: T-ROESY spectrum of tethered disaccharide 82 in CD ₃ OD.	147
Figure 5.18: Diagnostic inter- and intra-residue ROE connectivities of compound 82 .	148
Figure 5.19: T-ROESY spectrum of untethered disaccharide 92 in CD ₃ OD:	149

Figure 5.20: Inter- and intra-residue ROE connectivities observed in disaccharide 92 .	150
Figure 5.21: Two-dimensional EXSIDE spectra in pyridine-d ₅ used to obtain the H'1-C'1-O1-C4 and b) C'1-O1-C4-H4 coupling constants.	152
Figure 5.22: Structures resulting from the minimization of disaccharide 92 : a) using ROE restraints obtained from the tethered disaccharide 82 ; b) without using any restraints.	154
Figure 5.23: Structures resulting from the minimization of: a) <i>anti</i> -conformer 82a using ROE restraints; b) minimized <i>syn</i> -conformer 82b , which anneals to c) 82b using ROE restraints and d) 82b without using restraints.	156
Figure 5.24: Lowest energy structure of 82 with graphs depict the trajectory of a 5000 ps MD simulation about both glycosidic linkages.	158
Figure 6.1: Representation of a protein-ligand complex in dynamic exchange with a large excess of the free ligand.	163
Figure 6.2: Comparison of the model for <i>Ulex</i> lectin docked with trisaccharide 1 (GEGOP) and the NMR derived conformation of bound 1 .	175

Figure 6.3: Comparison of the models for the bound trisaccharides **1** and **28**.

176

List of Tables

Table		Page
Table 1.1:	Structures of the human blood group ABH and Lewis antigenic determinants.	8
Table 1.2:	Lectins used for blood typing.	18
Table 3.1:	Summary of the different activation methods used in the glycosylation of compound 77 .	76
Table 5.1:	Proton and carbon assignments and coupling constants for H-type 2 trisaccharide 1 in D ₂ O at 300K.	122
Table 5.2:	Experimental ROE values and distance restraints (Å) for modeling studies of H-type 2 trisaccharide 1 .	127
Table 5.3:	Calculated and experimental inter-proton distances for the H-type 2 trisaccharide.	131
Table 5.4:	Proton and carbon assignments with coupling constants for constrained trisaccharide 28 in D ₂ O at 300K.	132
Table 5.5:	Proton and carbon assignments with coupling constants for constrained trisaccharide 29 in D ₂ O at 300K.	133
Table 5.6:	Interproton distances (Å) derived from experimental ROE values for constrained trisaccharides 28 and 29 .	134

Table 5.7:	Calculated and experimental interproton distances (Å) obtained for constrained trisaccharides 28 and 29 .	139
Table 5.8:	NOE distances obtained from NMR and theoretical investigation of the solution conformation of H-type 2 trisaccharide 1 , and constrained trisaccharides 28 and 29 .	139
Table 5.9:	Torsional angles obtained from theoretical calculations for the solution conformation of trisaccharide 1 , tethered trisaccharides 28 and 29 .	140
Table 5.10:	Proton and carbon assignments with $^3J_{H,H}$ coupling constants for tethered disaccharide 82 in D ₂ O at 300K.	144
Table 5.11:	Proton and carbon assignments with $^3J_{H,H}$ coupling constants for tethered disaccharide 82 in CD ₃ OD at 300K.	145
Table 5.12:	Proton and carbon assignments with $^3J_{H,H}$ coupling constants for disaccharide 92 in CD ₃ OD at 300K.	146
Table 5.13:	Experimental ROE values and distance restraints (Å) for modeling studies of tethered disaccharide 82 .	148
Table 5.14:	Experimental ROE values and inter-proton distances (Å) for untethered α -disaccharide 92 .	148

Table 5.15:	Summary of results from molecular modeling indicating the major and minor families of conformers found for each structure.	157
Table 5.16:	Theoretical and experimental ROE values of tethered disaccharide 82 .	157
Table 6.1:	Interproton distances (Å) derived from experimental ROE values for free and bound H-type 2 trisaccharide.	169
Table 6.2:	Interproton distances (Å) derived from experimental ROE values for free and bound tethered H-type 2 trisaccharide 28 .	172
Table 6.3:	Experimental inter-proton distances for free H-type 2 trisaccharide 1 at 27°C and 75°C, and for 1 bound to <i>Ulex europaeus</i> I at 45°C and 75°C.	173
Table 6.4:	Torsional angles obtained for the solution and bound conformations of trisaccharide 1 and tethered trisaccharide 28 .	174

List of Abbreviations

Abe	abequose, 3,6-di-deoxy-D-xylo-hexose
All	allyl
AMBER	assisted model building with energy refinement
APT	attached proton test
Bn	benzyl
BSA	bovine serum albumin
Bu	butyl
Bz	benzoyl
CAN	cerium ammonium nitrate
cDNA	complementary deoxyribonucleic acid
CHARMM	chemistry in Harvard macromolecular mechanics
CIDNP	chemically induced dynamic nuclear polarization
ConA	<i>Concanavalin A</i>
CVFF	consistent valence forcefield
2D	two dimensional
DBU	1,8-diazabicyclo[5,4,0]undec-7-ene
DCC	1,3-dicyclohexylcarbodiimide
DDQ	2,3-dichloro-5,6-dicyano-1,4-benzoquinone
DMAP	4-dimethylaminopyridine
DMF	<i>N,N</i> -dimethylformamide
DMSO	methyl sulphoxide
DMTST	dimethyl(methylthio)sulfonium triflate
DTBMP	2,6-di- <i>t</i> -butyl-4-methylpyridine
EIA	enzyme immunosorbent assay
ES HRMS	electrospray high resolution mass spectrometry
ESMS	electrospray mass spectrometry
EXSIDE	excitation-sculptured indirect-detection
Fuc	fucose, 6-deoxy-galactose
Gal	galactose

GalNAc	<i>N</i> -acetylgalactosamine, 2-acetamido-2-deoxy-galactose
GCOSY	gradient coupling correlated spectroscopy
GEGOP	geometry of glycopeptides
Glc	glucose
GlcNAc	<i>N</i> -acetylglucosamine, 2-acetamido-2-deoxy-glucose
GROMOS	Groningen molecular simulation forcefield
GTOCSY	gradient total correlation spectroscopy
HMBC	heteronuclear multiple-bond coherence
HMQC	heteronuclear multiple quantum coherence
HPLC	high pressure liquid chromatography
HRP	horseradish peroxidase
HSEA	hard sphere <i>exo</i> -anomeric effect
IC ₅₀	inhibitor concentration required to give 50% inhibition
IUPAC	International Union of Pure and Applied Chemistry
LAH	lithium aluminum hydride
Man	mannose
MC	Monte Carlo
MCPBA	<i>m</i> -chloroperbenzoic acid
MD	molecular dynamics
MM3	molecular mechanics 3 forcefield
MS	molecular sieves
Ms	methanesulphonyl
NIS	<i>N</i> -iodosuccinamide
NOE	nuclear Overhauser effect
NOESY	nuclear Overhauser effect spectroscopy
PBS	phosphate buffer saline
PBST	phosphate buffer saline containing Tween 20
PFOS	potential functions for oligosaccharide structures
Ph	phenyl
PhthN	phthalimido
PMB	<i>p</i> -methoxybenzyl

ppm	parts per million
Pyr	pyridine
ROE	rotating-frame nuclear Overhauser effect
R _f	retention factor
rt	room temperature
Ser	serine
SLe ^x	sialyl Lewis x
S _N 2	bimolecular nucleophilic substitution
TBAF	tetra-butyl ammonium fluoride
TBDMS	<i>t</i> -butyl-di-methylsilyl
TDA-1	tris[2-(2-methoxyethoxy)ethyl]amine
Tf	trifluoromethanesulphonate
THF	tetrahydrofuran
TLC	thin layer chromatography
TMB	3,3',5,5'-tetramethylbenzidine
TMS	trimethylsilyl
Tr	triphenylmethyl
TRNOE	transferred nuclear Overhauser effect
T-ROESY	transverse rotating-frame nuclear Overhauser effect
TR-ROESY	transferred transverse rotating-frame nuclear Overhauser effect
Ts	toluenesulphonyl
UV	ultraviolet
WBA	wing bean agglutinin (<i>Psophocarpus tetragonolobus</i>)

Introduction

1.1: Carbohydrates

Carbohydrates display an enormous structural and functional diversity, fulfilling roles as energy sources, as structural material (cellulose), as elements of molecular recognition, and as factors in the control of protein structure and function. Vital biological functions, both within and at the surface of the cell, depend on the molecular recognition events, which arise from the interaction between carbohydrates and proteins.

The three-dimensional structure of the carbohydrate is translated by a protein receptor into a signal, which determines the fate of a cell or glycoprotein. The asialoglycoprotein receptor, a mammalian lectin found in the plasma membranes on liver cells recognizes galactose at the non-reducing terminus of oligosaccharide units on certain glycoproteins following loss of sialic acid.¹ Once bound, the glycoprotein is removed from the blood by a process called endocytosis.¹ Due to the physiological importance of such non-covalent interactions in embryogenesis, fertilization,² neuronal development, hormonal activities, blood clotting, and cell proliferation, much time has been spent studying the interactions of carbohydrates with enzymes,^{3,4} lectins,⁵⁻⁸ and antibodies.^{9,10} Results from some of these studies have found that, typically, only one or two edges - or faces - of the carbohydrate ligand are bound by protein, and the recognition element or epitope is often limited to a disaccharide or trisaccharide unit. Since disaccharides and trisaccharides are synthetically accessible, these oligosaccharide recognition elements are not only attractive, but also potentially attainable targets for carbohydrate-based therapeutics. Some examples of such therapeutics that have reached advanced stages of development are the anti-inflammatory sialyl Lewis X tetrasaccharide,¹¹ monosaccharide drugs for influenza treatment,¹² glycosphingolipid-protein conjugates used in cancer therapy,¹³ antidiabetic α -glucosidase inhibitors,¹⁴⁻¹⁶ anti-HIV agents^{16,17} and heparin analogues.¹⁸⁻²³

1.4: Carbohydrate Antigens

Carbohydrate antigens are cell surface polysaccharides, glycoproteins or glycolipids that invoke oligosaccharide-specific antibody responses or react with antibodies. While capsular and cell wall polysaccharides of bacteria and fungi fulfill this role during infection, in human blood transfusion and organ transplantation, these cell surface antigens exist as glycoconjugates on tissues, leukocytes, and red blood cells. Mammalian glycoconjugates also function in cell-cell interactions.

The surface of cells may be regarded as being sugar coated. Cell membranes are perceived as fluid, two-dimensional viscous solutions of oriented proteins and lipids in a phospholipid bilayer (Figure 1.1).

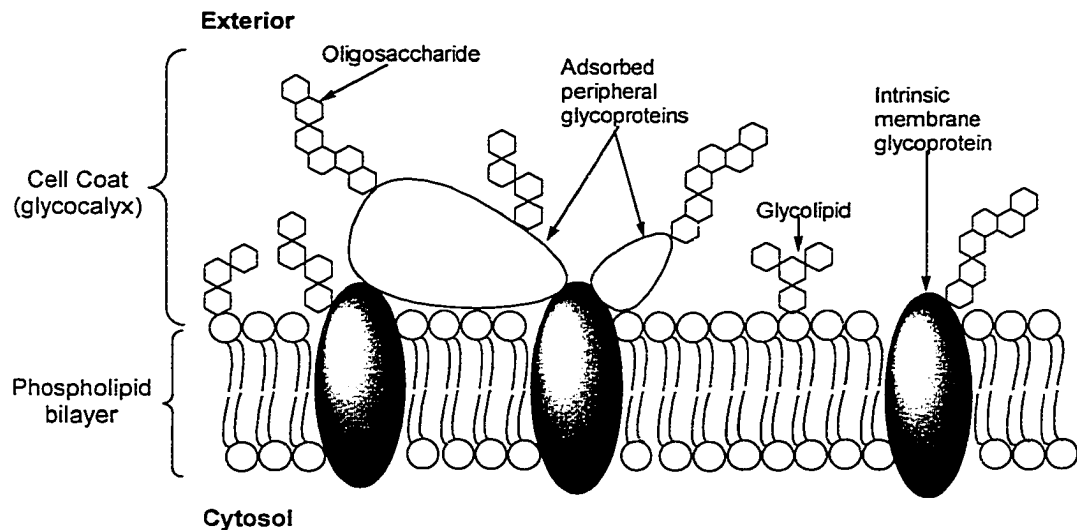


Figure 1.1: Schematic of the location of glycoproteins and glycosphingolipids in a plasma membrane.

The structural polymorphism of oligosaccharide chains of glycolipids or glycoproteins is extensive due to variations in monosaccharide composition, sequence and branching, linkage position and anomeric configuration of glycosidic linkages. The monosaccharide composition mainly consists of galactose, glucose, *N*-acetylgalactosamine, *N*-acetylglucosamine, fucose and sialic acid.

Both glycoproteins and glycolipids are especially abundant in the plasma membranes of eukaryotic cells but are absent from the inner mitochondrial membrane, the chloroplast lamellae, and several other intracellular membranes.³² Bound carbohydrates increase the hydrophilic character of lipids and proteins and help stabilize many membrane protein structures. In mammals, certain glycolipids or glycoproteins behave as blood-group antigens.

1.4.1: Glycoproteins

In the case of protein-bound cell surface oligosaccharides, the carbohydrate chain is most frequently linked to the peptide moiety either via an *N*-acetylglucosamine to the amide group of an asparagine residue (*N*-linked), or via an *N*-acetylgalactosamine to the hydroxyl group of a serine or threonine residue (*O*-linked)(Figure 1.2).

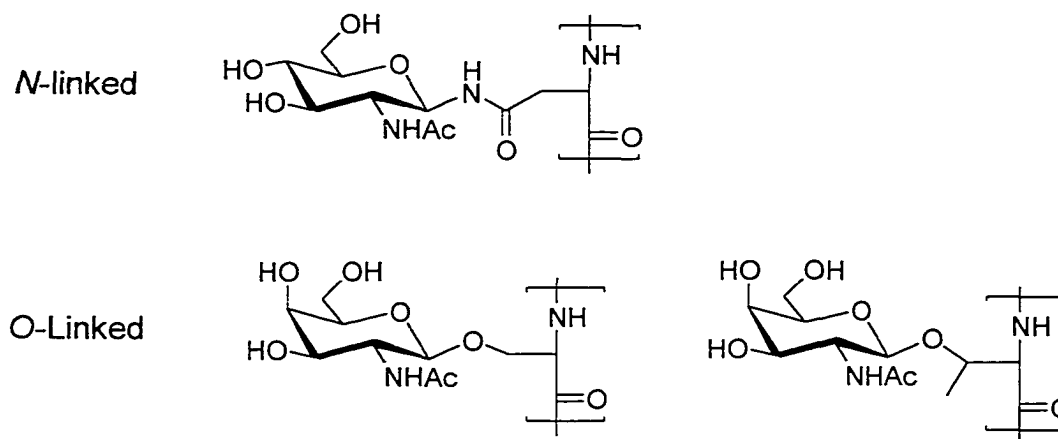


Figure 1.2: N- and O-linkages of glycoproteins.

N-linked oligosaccharides are either of the high-mannose type, the complex type, or the hybrid type.³³ In many cases, *N*-linked oligosaccharides are important in the folding of the glycoprotein³⁴ and have been shown to be important for the biological activity of certain hormones.³⁵ Though the complex type of *N*-linked oligosaccharides may carry blood group

determinants, as found in the human small intestine,³⁶ it is more common that O-linked sugar chains constitute blood group reactivity.

Some O-linked glycoproteins, the mucins, form prominent glycoprotein antigens and tumor-associated carbohydrate antigens. They constitute the major glycoproteins of mucus secretions, and are found to have high apparent molecular weights and carbohydrate contents exceeding 50%. Cell surface mucins are grouped into two different classes characterized as type 1 and type 2 core structures (Figure 1.3). Polylactosamine chains occur on the β -D-GlcNAc arm of the type 2 core structure. These mucins are important markers for cancer diagnosis and potential targets for treatments that attempt to induce T-cell responses.^{37,38} The physiological function of O-linked oligosaccharides is still not clear, though they are thought to induce a stiff and extended conformation of the peptide³⁹ by virtue of the multiple substitution within a short span of peptide.

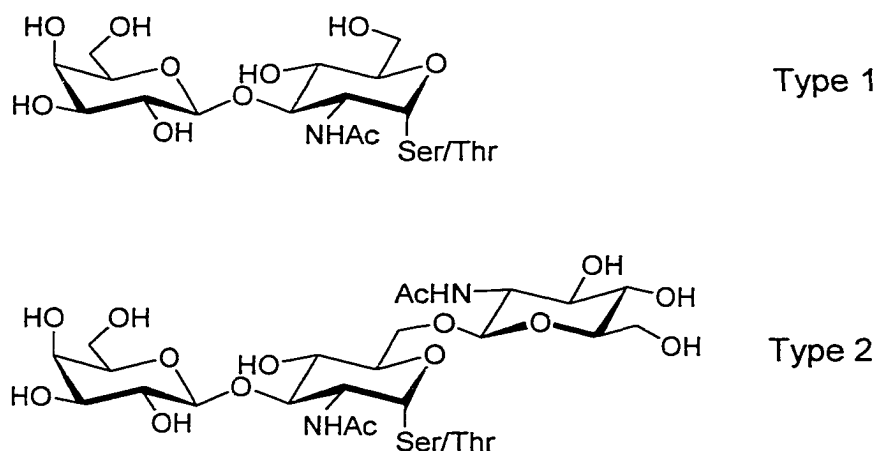


Figure 1.3: Type 1 and type 2 core structures of cell surface mucins.

1.4.2: Glycolipids

Glycosphingolipids are comprised of an oligosaccharide attached to a lipid part, the ceramide, which is formed from a sphingosine base to which fatty acids of various lengths are linked with amide bonds (Figure 1.4A).⁴⁰ Glucose is always β -linked to the primary hydroxyl group of the lipid.

Glycolipids are membrane constituents thought to be mainly located in the outer leaflet of the plasma membrane.

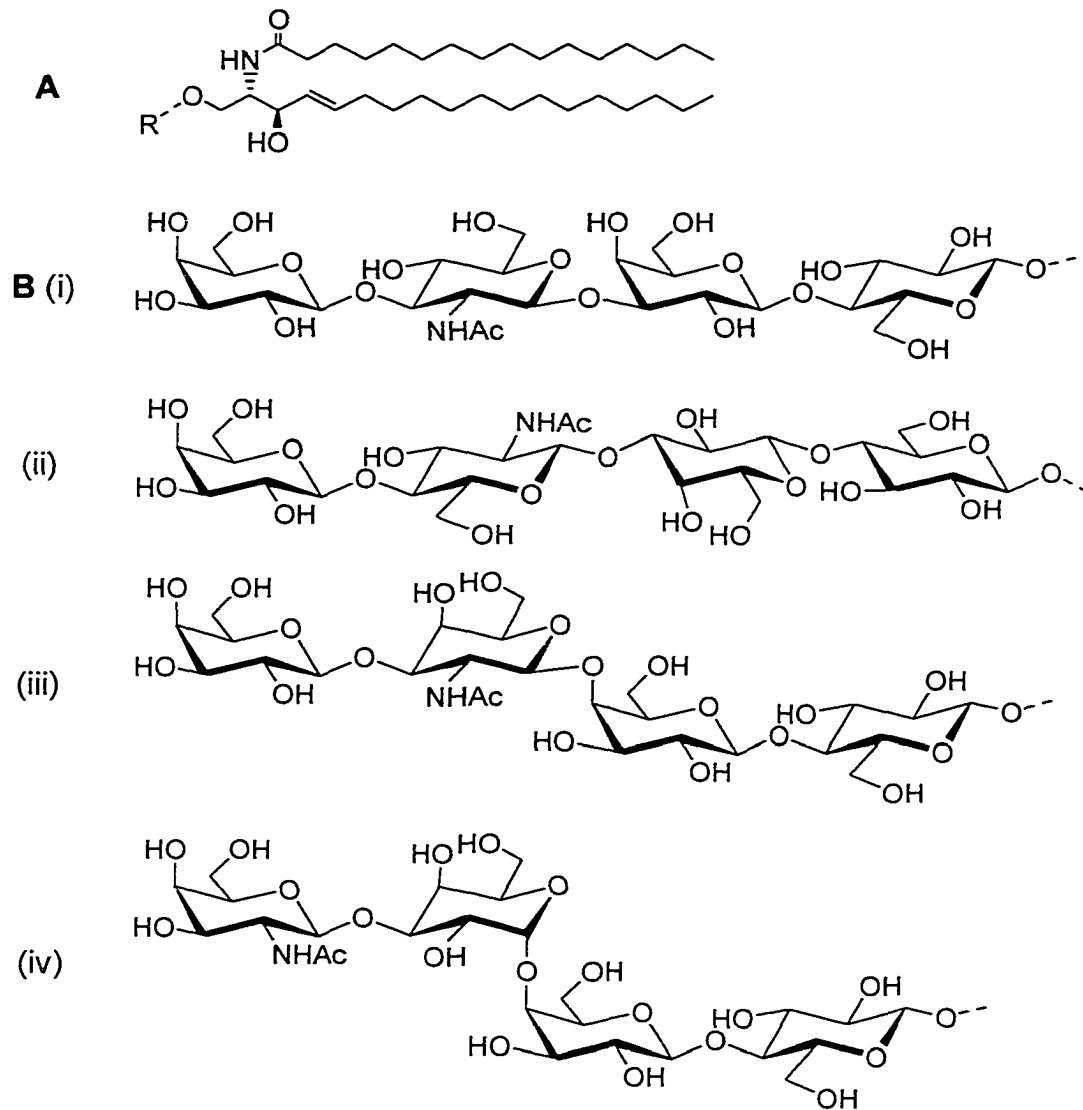


Figure 1.4: Structures of glycosphingolipids: **(A)** ceramide portion of glycosphingolipids; **(B)** tetrasaccharide core sequences (R group attached to the ceramide) found in glycosphingolipids (i) lactotetraosylceramide, (ii) neolactotetraosylceramide, (iii) gangliotetraosylceramide, and (iv) globotetraosylceramide.

The lipid portion of the glycolipid is anchored in the membrane and the carbohydrate part is exposed to the cell environment, as a polar head group.^{40,41}

The base and fatty acid in the glycolipid may vary in degree of hydroxylation, saturation, and chain length.⁴¹ These variations influence the physicochemical properties of the membrane,⁴¹ and the orientation and accessibility of the carbohydrate group on the glycolipid.⁴²⁻⁴⁵ The oligosaccharide portion of the glycolipid is assembled by specific glycosyltransferases on the luminal side of the Golgi apparatus.^{46,47}

Glycosphingolipids are grouped into several structural series, which are characterized by four different core tetrasaccharide elements from which most glycosphingolipids are derived by elaboration or truncation (Figure 1.4B). Gangliosides are a special class of globo-glycolipids that contain one or more *N*-acetylneuraminic acid residues,⁴⁸ which are found to be important in several pathogenic processes.⁴⁹

1.4.3: Human Blood Group ABO(H) Antigens

The human blood group antigens (Table 1.1) are carried on red cell membranes linked to the type 2 oligosaccharide core structures present in glycolipids.⁵⁰ Lewis antigens are incorporated into the red cell membrane from serum and have the type 1 oligosaccharide core.⁵¹⁻⁵³ Type 1 and 2 glycan chains differ in the position of the β -D-Gal to β -D-GlcNAc linkage (Figure 1.5).

The terminal structures that define the AB(H) determinants may be attached to type 1 or type 2 chains (Figure 1.5A & B).⁵⁰ In contrast, the Lewis-a and Lewis-b antigens can only occur on type 1 chains since in the type 2 chains the site of the galactose linkage to the 4 position of GlcNAc prevents the formation of Lewis structures (Figure 1.5C).

Table 1.1: Structures of the human blood group ABH and Lewis antigenic determinants.

Antigen	Structure
Lewis a	β -D-Galp(1→3) β -D-GlcpNAc 4 ↑ 1 α -L-Fucp
Lewis b	β -D-Galp(1→3) β -D-GlcpNAc 2 4 ↑ ↑ 1 1 α -L-Fucp α -L-Fucp
Lewis x	β -D-Galp(1→4) β -D-GlcpNAc 3 ↑ 1 α -L-Fucp
H-type 1	α -L-Fucp(1→2)- β -D-Galp(1→3) β -D-GlcpNAc
H-type 2	α -L-Fucp(1→2)- β -D-Galp(1→4) β -D-GlcpNAc
B ^a	α -D-Galp(1→3)- β -D-Galp(1→3/4) β -D-GlcpNAc 2 ↑ 1 α -D-Fucp
A ^a	α -D-GalpNAc(1→3)- β -D-Galp(1→3/4) β -D-GlcpNAc 2 ↑ 1 α -L-Fucp

^aEpitope may be attached to a type 1 or a type 2 core structure.

The Lewis-x structure, associated with inflammatory responses, is derived from the addition of α -L-fucose to the O-3 atom of the β -D-GlcpNAc residue of a type 2 chain by an $\alpha(1\rightarrow3)$ fucosyl transferase (Figure 1.5D).^{52,54,55} Blood group antigens may also be linked to the globo core structure (type 4 chain),⁵⁶⁻⁵⁹ but this combination is relatively rare on erythrocytes.

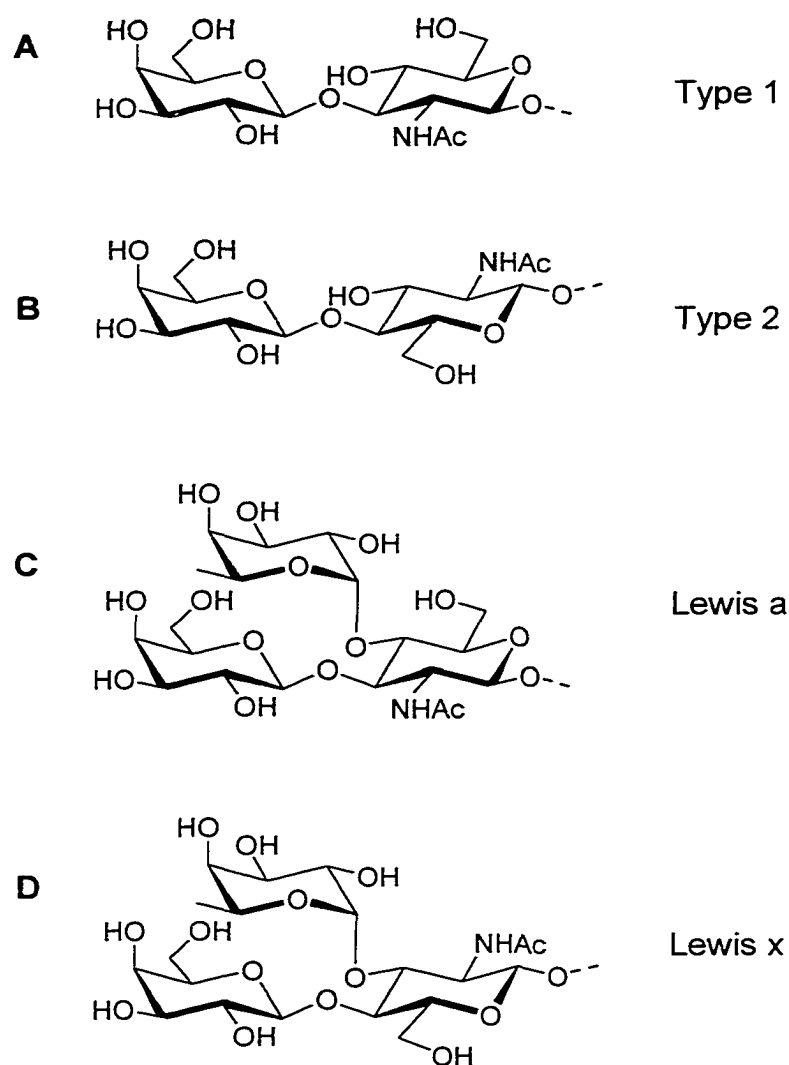


Figure 1.5: Terminal structures of the AB(O) blood group determinants.

1.4.4: Basis of the A, B, O Histo-Blood Groups

The biosynthetic basis for the variations in the blood groups are known to be a result of individual expression or lack of expression of a given glycosyl transferase activity.⁵³ The cloning of the ABO genes gave the first insight into the molecular genetics of the carbohydrate-defined blood group polymorphism.⁶⁰ In comparing the cDNA of the A and B alleles, it was observed that the differences were limited to four amino acid substitutions, of which two were involved in the difference of enzyme specificity.⁶¹ In Group O

individuals, it was found that the deletion of a single nucleotide at position 258 changed the reading frame and led to a truncated protein, if any, that was enzymatically inactive.⁶¹ This results in a histo-blood group without the terminal α GalNAc (A blood group) or the terminal α Gal residue (B blood group). The term O-blood group arose from a serological definition. "O"-stands for Ohne, German for without (without A or B blood group activity). The antigen that results from the activity of a fucose transferase on type 1 or type 2 oligosaccharide chains is called the H-antigen.

1.5: Lectins

Lectins are a class of carbohydrate-specific proteins of non-immune origin which are commonly detected by their ability to agglutinate erythrocytes. The richest source of these proteins is plants, where high levels are found in seeds. For example, the well-known lectins *Concanavalin A*, soybean agglutinin, pea lectin, and favin comprise 1-8% of the seed protein. Higher levels of lectins may be found in other plant tissues and organs. Several hundred plant lectins have been purified by affinity chromatography on immobilized carbohydrates in 10-100 mg quantities and many have been thoroughly characterized. Lectins, their biological roles, structures, applications and their interactions with carbohydrates have been extensively reviewed.^{31,62-68}

Of the four H specific lectins, *Ulex europaeus I* is a membrane bound legume lectin which is isolated from the *Ulex europaeus* seeds.²⁷ *Psophocarpus tetragonolobus II* is also a legume lectin known as the winged bean lectin.²⁸ *Galactia tenuiflora*²⁹ is a legume lectin from a tropical plant only found on an island of Mauritius. The legume lectin *Erythrinia corallodendron* is isolated from the coral tree.³⁰

1.5.1: Lectins and their Function

The two main properties of lectins are binding specificity for carbohydrates and bi- or polyvalency. In addition to plants, lectins are found

in animals, viruses, and microorganisms. They are most often located at the cell surface (integral membrane lectins) but may also occur outside the cell as extracellular protein (soluble lectins).

Soluble lectins are thought to be involved in the organization of the extracellular matrix and possibly, to play a role in cell migration and adhesion.⁶⁹ The major function of integral membrane lectins appears to be cell recognition.

The recognition event is based on the molecular fit between the pair of complementary structures found on the surface of interacting cells, or between those found on the surface of a cell and on a molecule in solution. Recognition occurring between carbohydrates and proteins can be regarded as an extension of the lock-and-key hypothesis introduced by Emil Fischer for the interactions between enzymes and their substrates.⁷⁰

1.5.2: General Structure of Legume Lectins

Lectins are classified based on common structural features. Although some borderline cases exist, most lectins fall into one of the following three classes: simple, mosaic (or multidomain), and macromolecular assemblies. Within each class, lectins may be subdivided into distinct families with similar sequences and structural properties. *Ulex europaeus* I, *Psophocarpus tetragonolobus* II, *Galactia tenuiflora* and *Erythrinia corallodendron* lectins are classified as simple lectins belonging to the legume family. Legume lectins typically are composed of two or four identical subunits (or protomers) of 25-30 kDa, each with a single carbohydrate binding site with the same specificity. Both a tightly bound Ca^{2+} and a transition metal, usually Mn^{2+} , are found in each subunit. These ions, Ca^{2+} and Mn^{2+} , are situated 4.25 Å apart and are found close to the carbohydrate binding site (9-13 Å). The two metal ions have a structural role, helping to position the amino acids that form contacts with the carbohydrate. These metal ions associate with four amino acid residues found on the lectin, and two of these residues, which are aspartic acids, are shared by both ions. In all legume lectins, there are four water

molecules in each subunit, which participate, directly or indirectly, in metal binding.

The three-dimensional structures of eleven legume lectins have been elucidated by high-resolution X-ray crystallography.⁶² Despite the different specificities of the proteins, the structures were found to be nearly superimposable and exhibit remarkable sequence homologies.⁶² The subunits are usually said to be primarily composed of two antiparallel β -sheets, one of six strands and the other of seven, and have an overall dome shape. However, Banerjee and co-workers³¹ have pointed out that the subunits are actually composed of three β -sheets: the 6-stranded sheet, the 7-stranded sheet and a small 5-stranded sheet. The small 5-stranded sheet plays a major role in holding the two larger sheets together. The *Ulex europaeus* I lectin is found to exhibit all the above structural characteristics of a legume lectin (Figure 1.6). The β -sheet, which contains six strands, is mostly flat, whereas the 7-stranded sheet is concave. The metal ions and the binding site of the carbohydrate are located within the concave seven-stranded sheet. This concave surface, which is found at the top of each protomer (identical or almost identical subunits making up lectins), provides a shallow binding site easily accessible to monosaccharides, as well as oligosaccharides and polysaccharides.

Despite their different specificity, legume lectins bind their respective sugar ligands through the side chains of three unchanging residues, an aspartic acid, an asparagine, and an aromatic amino acid⁷² or leucine.⁷³ Though the main amino acids involved in the binding of the carbohydrate ligands are highly conserved and have identical spatial disposition, the lectins in the legume family can discriminate between similar carbohydrates because the carbohydrates are oriented differently in the different binding sites. Since the amino acids in the binding site are identical, it is thought that the specificity relies on the small number of variable parts of the lectin that surround the binding site which would consequently affect the polar contacts.^{31,62}

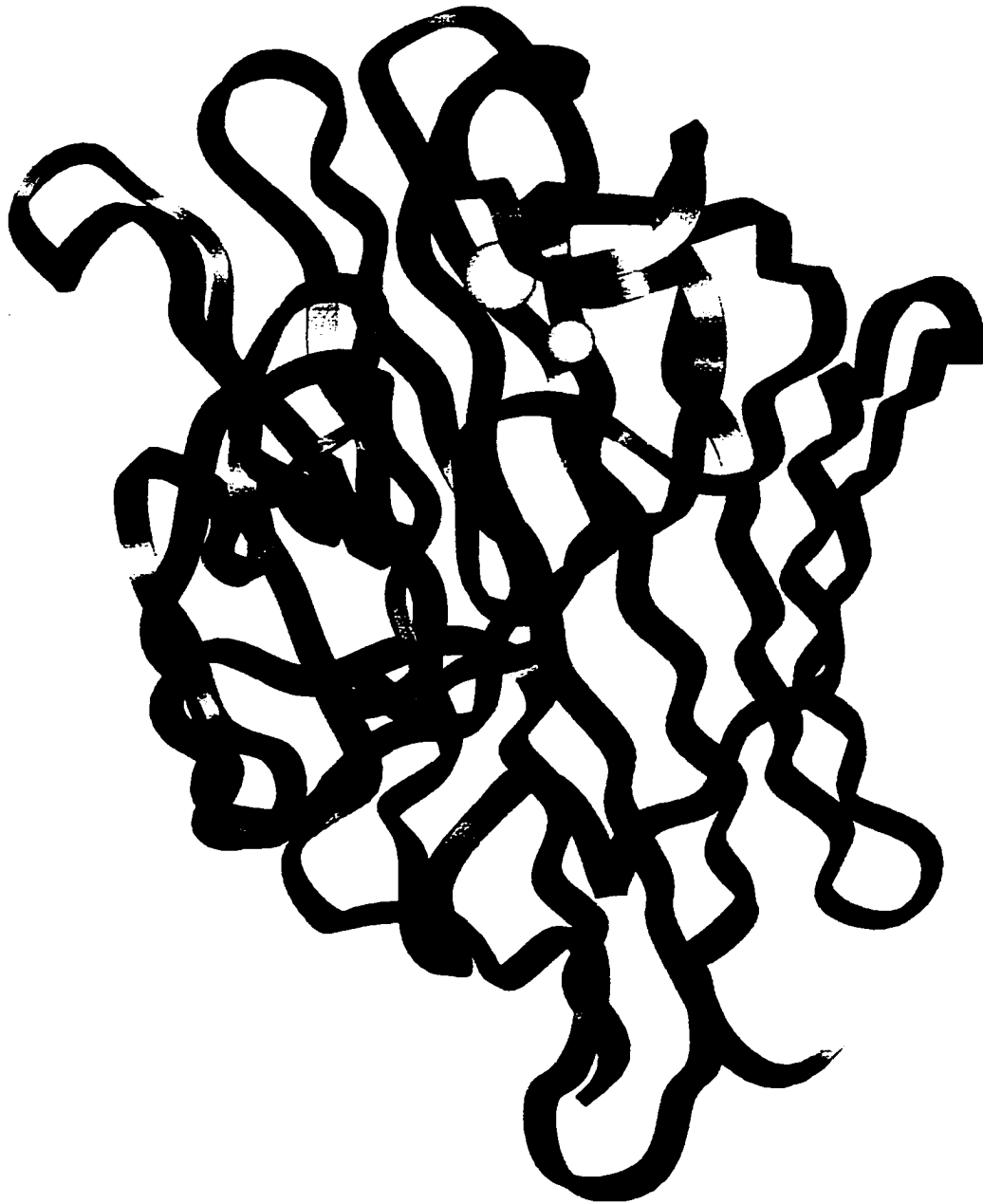


Figure 1.6: Structure of the *Ulex europaeus* I lectin in ribbon representation.⁷¹ Large sphere represents Ca²⁺ and small sphere depicts Mn²⁺.

Most known legume lectins dimerize into a structure called the 'canonical legume lectin dimer' (Figure 1.7).³¹ A large 12-stranded β -sheet characterizes the structure of this dimer. It is formed by the association of the

two 6-stranded β -sheets. Lectins from the coral tree (*Erythrina corallodendron*) and lectin IV from *Griffonia simplicifolia* do not form the canonical legume lectin dimer. It is suggested that this is due to steric hindrance and electrostatic incompatibility.³¹ For the lectins that form tetramers (Figure 1.8), this quaternary structure arises from the association of two dimers. In the cases of *Concanavalin A*, soybean agglutinin and the leuco-agglutinin from *Phaseolus vulgaris*, the tetramers are formed from two canonical dimers, whereas peanut lectin forms a tetramer, which does not include a canonical dimer. The *Ulex europaeus* I lectin has been crystallized and has been found to form a canonical dimer, though no structure has yet been published.⁷¹



Figure 1.7: Two views of a canonical legume lectin dimer.

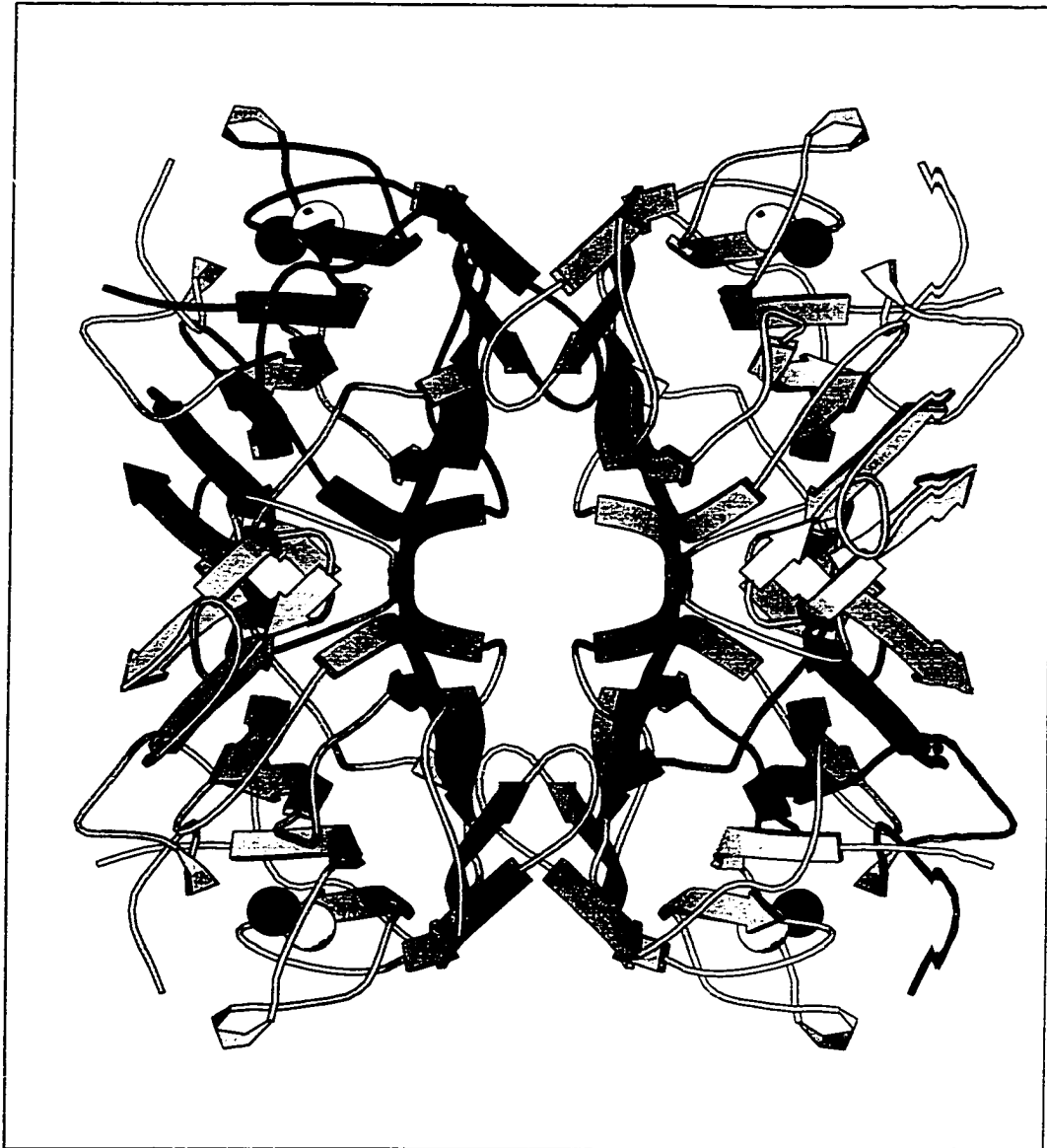


Figure 1.8: Tetramers formed from two canonical dimers of *Concanavalin A*. Spheres represent cations Ca^{2+} and Mn^{2+} .

1.5.3: Lectin Specificity

Lectins can also be classified into five groups, according to the monosaccharide for which they have the highest affinity: D-mannose, D-galactose/ D-N-acetylgalactosamine, D-N-acetylglucosamine, L-fucose, and D-N-acetylneuraminic acid. The affinity of the lectins for monosaccharides is

usually weak, with association constants in the millimolar range. Lectins also bind di-, tri-, and tetrasaccharides with association constants up to 1000-fold higher than that of the monosaccharide.⁶² Some lectins only bind oligosaccharides, these include *Griffonia simplicifolia* IV and *Phaseolus vulgaris*. *Ulex europaeus* I, *Psophocarpus tetragonolobus* II, and *Galactia tenuiflora*, belong to the group of L-fucose binding lectins. However, they bind their corresponding oligosaccharides much more tightly. The *Ulex* lectin binds the H-type 2 trisaccharide 900 fold tighter than L-fucose,⁶² which indicates a protein-oligosaccharide contact surface that extends beyond the fucose residue. *Erythrina corallodendron* is classified as a D-galactose/D-N-acetylgalactosamine lectin, although it binds more tightly with the disaccharide β -D-Galp(1 \rightarrow 4) β -D-GlcpNAc \rightarrow OR, and the H-type 2 trisaccharide (1).

1.5.4: Ligand Multivalency

Despite the low affinity and the relaxed specificity for monosaccharides, lectins exhibit very high affinity and specificity for oligosaccharides of cell surface glycoproteins and glycolipids. Univalent interactions are weak, it has been suggested that the multiple protein-carbohydrate interactions cooperate to give the required affinity and specificity for the recognition event.⁶² This may arise via either: 1) ligand multivalency; or 2) clustering of several binding sites through the formation of lectin oligomers.⁶²

Polyvalent interactions are characterized by the simultaneous binding of multiple ligands on one biological entity (a molecule, a surface) to multiple receptors on another (Figure 1.9). These interactions occur throughout biology,⁷⁴ and have a number of characteristics that monovalent interactions do not possess. Particularly, polyvalent interactions can be collectively much stronger than corresponding monovalent interactions.

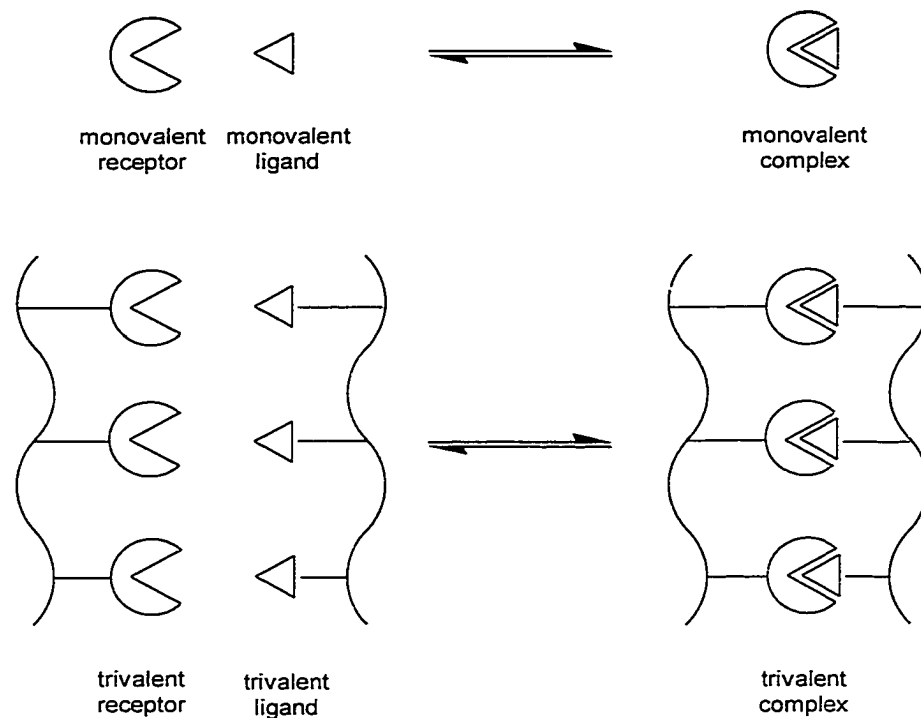


Figure 1.9: Monovalency versus polyvalency.

Studies have shown that ligand multivalency increases the avidity. The number of carbohydrate residues, as well as spacing and orientation, are important for adequate interaction.^{62,75} Lectins with more than two binding sites have been found to crosslink, forming homogeneous lattices and precipitating with divalent oligosaccharides.^{31,76-78} The multimeric nature of lectins partially explains the formation of these three-dimensional lattices as well as the increase in avidity with multivalent ligands.

1.5.5: Lectins and Medicine

The interactions of lectins with the sugars coating cells is exploited for biomedical purposes.⁷⁹⁻⁸⁷ Although these applications are predominantly based on precipitation and agglutination reactions, lectins are also used for the separation of cells.⁸⁸⁻⁹⁰ A clinical application of the cell separation ability of lectins is in the 'purification' of bone marrow cells.^{91,92}

Another clinical application of lectins is in blood typing.⁹³ Since each blood type is characterized by a specific immunodeterminant, an oligosaccharide, different lectins may be used to identify different human blood types. The lectin I of *Ulex europaeus* is found to agglutinate human red blood cells of group O, and therefore is used for the identification of individuals of the O blood group and for the identification of secretors or non-secretors by detection of H substance in saliva.^{94,95} Table 1.2 summarizes the different blood group determinants of each blood type as well as the lectin used in its classification.

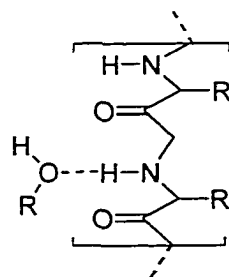
Table 1.2: Lectins used for blood typing.

Blood type	Determinant	Lectin
A	α -D-GalNAc	<i>Helix pomatia</i> , <i>Dolichos biflorus</i>
B	α -D-Gal	<i>Griffonia simplicifolia</i> IB ₄
O	α -L-Fuc	<i>Lotus tetragonolobus</i> , <i>Ulex europaeus</i> I
T	β -D-Galp(1→4)-D-GalpNAc	Peanut
Tn	α -D-GalpNAcSer	<i>Salvia sclarea</i>

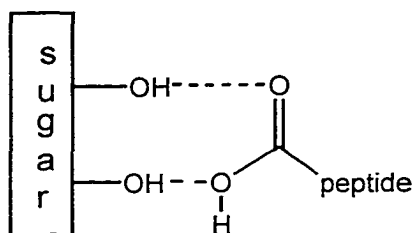
1.6: Lectin-Carbohydrate Interactions

Carbohydrates and lectins combine with each other through a network of hydrogen bonds, van der Waals interactions, hydrophobic interactions, and, in the case of legume and C-type lectins, coordination with metal. Of these interactions, hydrogen bonding is crucial in carbohydrate-protein association, in which water also plays a part. Sugars are highly polar molecules and are highly solvated in an aqueous environment. Upon binding, the carbohydrates exchange their solvation shell of water for the hydrogen bonds offered by the polar residues found in the protein's binding site, and most water molecules hydrogen-bonded to the polar residues in the binding site are displaced. The displaced water molecules reorganize themselves, forming new hydrogen bonds. Not only simple hydrogen bonds occur

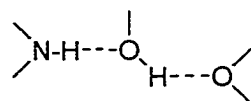
between the sugar and protein; bidentate and cooperative hydrogen bonding have also been observed⁹⁶ (Figure 1.10).



Simple (one donor and one acceptor)



Bidentate (two donors and one acceptor)



Cooperative (a hydroxyl groups acts as both acceptor and donor)

Figure 1.10: Examples of sugar-protein hydrogen bond types.

Numerous van der Waals contacts also provide additional stability to the carbohydrate-protein complex. Though individual van der Waals forces are weak, often only a fraction of 1 kcal/mol for each pair of atoms,⁶² the collectivity of their effect may make a significant contribution to the binding. Despite their distinctive polarity, carbohydrates also contain hydrophobic patches on their surfaces, due to the steric disposition of hydroxyl groups.

These patches form contacts with the hydrophobic zones in the protein's binding site, which generally involve aromatic, as well as non-polar amino acids. There are, of course, other factors such as polarization and induced dipoles that may contribute to the binding.

The dominant type of interactions on which a given protein-carbohydrate complex relies varies.⁹⁷ In lectin-carbohydrate complexes, hydrogen bonds between the protein and sugar, and those mediated by water play a large role. In the case of C-lectins, the calcium ion is required for the binding of the carbohydrate, though no direct contact between the ion and sugar are made.

Studies have shown that in lectin-carbohydrate complexes, the carbohydrate generally adopts a conformation close to the global energy minimum as calculated by potential energy calculations, such as the hard-sphere *exo-anomeric* (HSEA) force field. Although a similar situation is seen for antibody-carbohydrate complexes, significant deviation from the solution conformation can occur for residues that flank the principal epitope.^{98,99} However, further studies are required before broad generalizations may be made.

Water is also found to play a significant role in protein-carbohydrate interactions. It was found that hydrogen bonds mediated by water are as strong as those without the intervening water bridges.³ This finding reinforces the concept of structural water as an extension of the protein surface. As well, the displacement of a large number of water molecules from the protein binding site upon complexation has been observed. This is calculated to contribute favorably to the enthalpy and the free energy of complexation.¹⁰⁰

1.6.1: Thermodynamics

In order to attain a more thorough understanding of the process of recognition between carbohydrate and protein, a complete thermodynamic profile and high-resolution X-ray diffraction measurements are essential. Changes of free energy, ΔG , enthalpy (heat of binding), ΔH , entropy of

binding, ΔS , and heat capacity, ΔC_p , are the thermodynamic parameters required. These provide an appraisal of the relative contributions of the different interactions (hydrogen bonding, van de Waals forces, etc.) involved in the protein-carbohydrate association. Monitoring the changes in the thermodynamic parameters, as the structure of the carbohydrate is changed, provides a way to determine the contribution of certain portions of the oligosaccharide to the overall binding.

Interpretation of the thermodynamic data at the molecular level is complex, since the differences in energy measured may be due not only to the structural changes of the carbohydrate, but also to differential contributions, such as protein and solvent effects.¹⁰¹ Since in an aqueous environment, both the protein and the carbohydrate are normally hydrogen bonded to water, they must break their bonds to water in order to associate with each other. Therefore, the ligand-water and protein-water hydrogen bonds are replaced by protein-ligand bonds, and the released water returns to bulk solvent. Hence, the net binding energy is represented by the energy difference between the hydrogen bond energies of the protein and of the sugar with water (solute-solvent interactions) and those of the protein and sugar with each other (solute-solute interactions) and new water interactions with the complex.

The thermodynamic data⁹⁷ for several protein-carbohydrate interactions determined by calorimetry exhibit several trends. First, for association in aqueous solution, the enthalpy of binding is more negative than or equal to the free energy of binding.

Second, examination of the thermodynamics of carbohydrate binding has revealed the phenomenon of "entropy/enthalpy compensation".¹⁰²⁻¹⁰⁴ If the data are collected and a "compensation plot" is made, where $-\Delta H$ is plotted against $-T\Delta S$, a linear relationship is observed (slope ~ 1). This demonstrates the strong linear enthalpy-entropy compensation found in protein-carbohydrate interactions, and as a consequence, the free energy of binding varies little. This compensation has been interpreted both in terms of

changes in rotational degrees of freedom as glycosidic torsional angles are frozen,¹⁰² or in terms of the solvent reorganization which accompanies binding.^{5,105,106} An understanding of the molecular basis for compensation is important for the design of high-affinity, small-molecule inhibitors of carbohydrate/protein recognition such as, for example, anti-inflammatory drugs.

Third, the heat capacity change (ΔC_p) generally obtained for lectin-carbohydrate interactions ranges from -60 to -110 cal mol⁻¹ degree⁻¹. Calorimetric evaluation of the thermodynamics of association of several binding systems carried out by Chervenak and Toone, determined that ΔC_p is primarily a measure of solvent reorganization comprising 25-100% of the observed enthalpy of binding.^{105,108}

Oligosaccharides are quite flexible molecules due to their ability to rotate about the glycosidic linkage. However, lectins bind the sugars in a single conformation, which is not necessarily the most populated one in solution. Upon binding, the rotational freedom of the ligand becomes restricted, resulting in an unfavorable loss in entropy. Studies have suggested that this energetically unfavorable event is compensated by an advantageous change in enthalpy due to the removal of ligated water.⁶²

1.7: Constrained Oligosaccharides

The intrinsic affinity of oligosaccharide binding by proteins, such as antibodies and lectins, is generally characterized by association constants within the range $10^3 - 10^6 \text{ M}^{-1}$ frequently by a strong enthalpic contribution, offset by unfavourable entropy.^{5,62,97,104,109} It has been suggested that the conformational flexibility of oligosaccharides (which arises from motion about each glycosidic bond) may account for most of the unfavourable entropy.¹⁰² Theoretical estimates place the entropic loss per immobilized rotamer as high as 0.6 to 2.0 kcal/mol.^{102,110,111} Attempts to verify this hypothesis by synthesizing oligosaccharides that are constrained in a conformation pre-

organized for binding, have failed to show significantly higher free energy of binding.^{4,112-117}

Galabiose **2**, α -D-Galp(1 \rightarrow 4)Galp, is part of several biologically important glycolipids of the *globo* series, which function as adhesion receptors for bacterial surface proteins and toxins. Magnusson *et al.*¹¹² have assembled two tethered galabiose analogues, **3** and **4**, in order to stabilize the intersaccharide glycosidic bond, as to create water soluble inhibitors of bacterial adhesion (Figure 1.11). The crystal structures of a large number of galabiose-containing di- to pentasaccharides show that the HO-6 and HO-2' are situated close together. The presence of an intramolecular hydrogen bond between these two hydroxyls was determined by NMR.

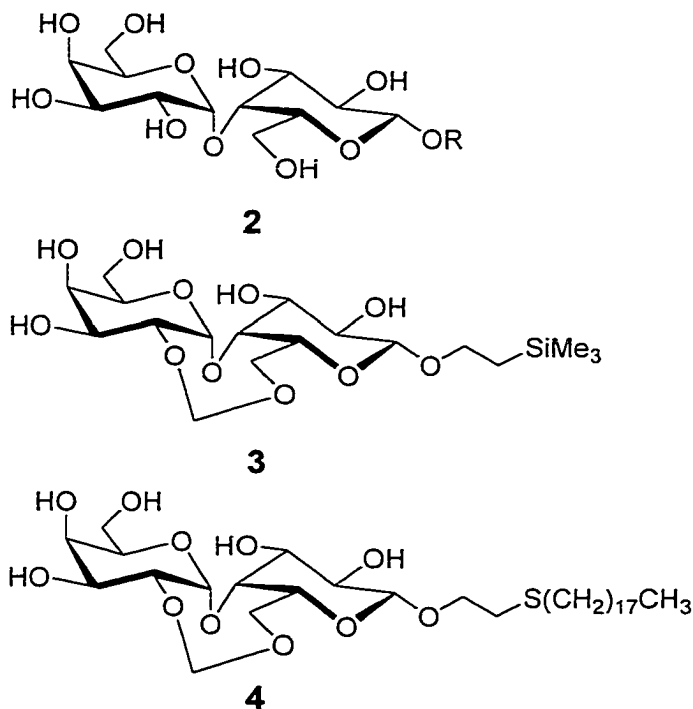


Figure 1.11: Galabiose **2** and the tethered galabiose analogues **3** and **4** prepared by Magnusson *et al.*¹¹²

The methylene-tether was introduced as a substitute to the hydrogen bond between OH-6 and OH-2', based on the assumption that it would

maintain the overall bioactive conformation of the ligands. Results from NMR experiments and computer modeling, have shown that the overall conformation of the tethered analogues and that of the native disaccharide were, indeed, very similar. A comparative binding study of the two constrained disaccharides and the native galabiose disaccharide was performed using three bacterial proteins. The proteins - the *Escherichia coli* pilus protein, PapG complexed with its chaperon PapD, Verotoxin, which is produced by enterotoxic *E. coli*, and the *Streptococcus suis* bacterium - are known to use galabiose-containing glycolipids as attachment points for the infectious process. Inhibition of the PapG/PapD protein complex and Verotoxin by the constrained sugar failed, as expected, since both require the presence of hydroxyls HO-6 and HO-2' that are blocked by the tether. The *Streptococcus suis* bacteria, for which the constrained carbohydrates were designed, were inhibited by the tethered galabiose analogues, however, the binding was weaker than that of the native disaccharide. It is thought that small, fine differences in the hydroxyl placements, seen in the computer modeling results, are responsible for the reduced binding strength.

In attempts to overcome the entropic penalties to binding and provide enhanced affinity, Bundle *et al.* have assembled a series of tethered analogues **6** to **11** of the trisaccharide α -D-Galp(1 \rightarrow 2)[α -L-Abep(1 \rightarrow 3) α -D-Manp1 \rightarrow OMe], **5**, that preorganize the ligand in its bound conformation (Figure 1.12).^{113,114} The design of the target molecules was based on the Se-155.4 monoclonal antibody-trisaccharide complex for which several protein crystal structures are available.^{113,114} These revealed the solvent exposed portions of the ligand, therefore indicating the sites for tethering.

The biological activity of the tethered structures were initially determined by EIA and these data showed that while their inhibitory activity was comparable to that of the native trisaccharide **5**, it was nevertheless slightly smaller ($\Delta\Delta G \approx +0.2-0.3$ kcal/mol). Precise thermodynamic data was obtained by titration calorimetry, which showed that the free energy difference is $\Delta\Delta G \approx +0.1$ kcal/mol.

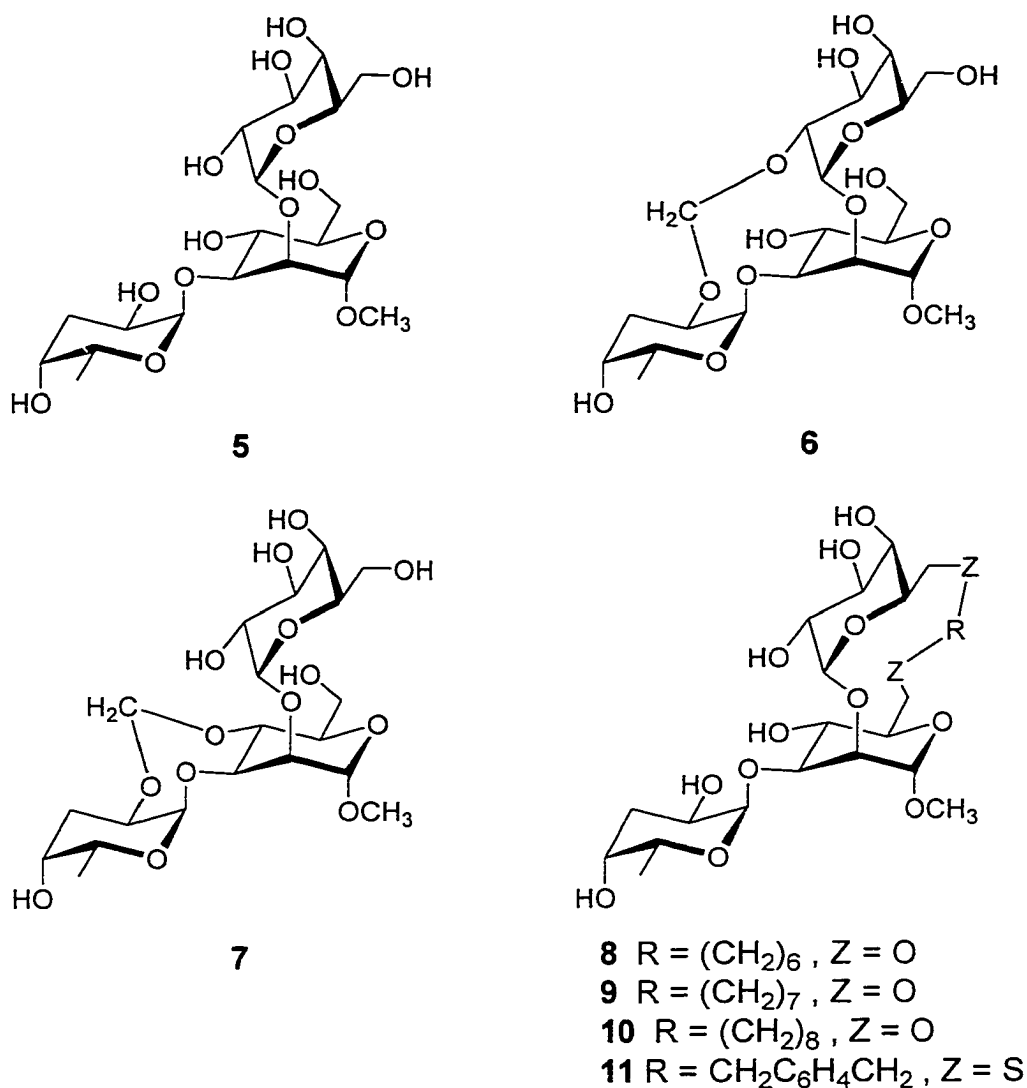


Figure 1.12: Native trisaccharide **5**, and structures of the tethered ligands **6** to **11**.

In this study, decreasing the flexibility of the ligand did not enhance the binding to antibody, though, it was observed that the nature of the tether did affect the binding.¹¹⁴ This is exemplified in the constrained ligands with the aryl tether versus those with oligomethylene ether tethers. The constrained carbohydrate with the aryl tether exhibited better binding than the other tethered molecules and the native trisaccharide.

The x-ray crystal structure of a biantennary octasaccharide-lectin *Lathyrus ochrus* complex, NMR data, and computer modeling were the basis for the design of the tethered trisaccharides of native β -D-GlcNAc(1 \rightarrow 2)- α -D-Manp(1 \rightarrow 3)- α -D-Manp1 \rightarrow OMe (**12**) prepared by Navarre *et al.* (Figure 1.13).^{115,116} The same trisaccharide is also bound by *Concanavalin A* (ConA) where an intramolecular hydrogen bond between HO-2 and HO-6'' is present in one of the possible docking modes with ConA. In a second proposed docking mode with ConA, it was determined that there was an intramolecular hydrogen bond between HO-4 and HO-6''. Two tethered trisaccharides **13** and **14** were designed in which a methylene-tether was used to replace the intramolecular hydrogen bonds and reduce the flexibility of the trisaccharide while retaining the bioactive conformation of the epitope. Therefore, tethered trisaccharides **13** and **14** were designed to mimic the two possible conformations that the carbohydrate may adopt when bound to ConA. The computer modeling showed that although the conformational space of the tethered trisaccharides was significantly reduced, they could still adopt the conformation of the parent trisaccharide.

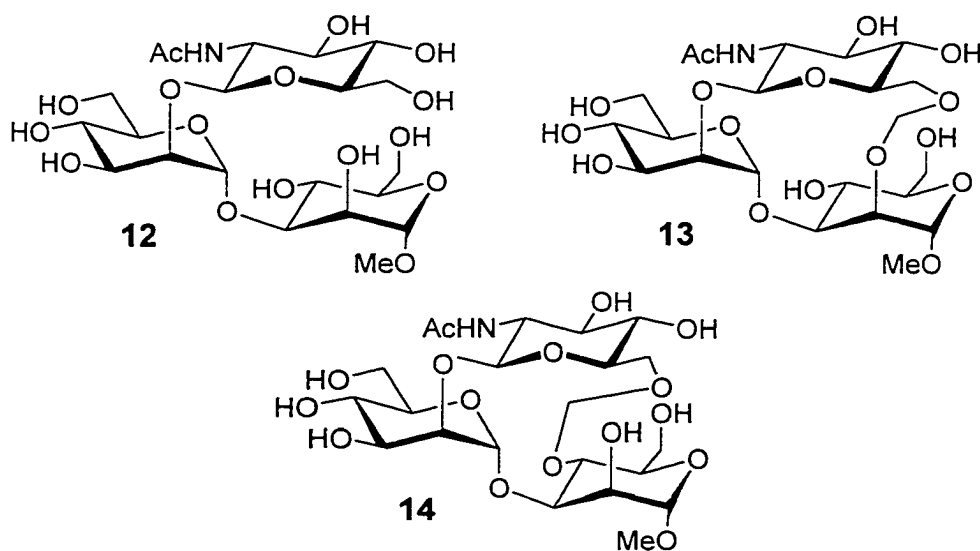


Figure 1.13: Native β -D-GlcNAc(1 \rightarrow 2)- α -D-Man(1 \rightarrow 3)-D-Man (**12**) and its tethered analogues (**13** and **14**).

However, the binding of the tethered trisaccharides **13** and **14** with the lectin relative to the native ligand did not improve.¹¹⁶ Calorimetry data¹¹⁶ for tethered trisaccharide **14** has recently been reported and shows that the complexation of **14** with ConA has a more favorable entropy term but that this term is offset by a smaller enthalpy contribution. Molecular modeling studies could not explain the loss of enthalpy since it seemed that both **13** and **14** have similar interactions with the protein.

Kolb has also published work in this area,¹¹⁷ concerning the design of E-selectin antagonists, as possible treatments for inflammatory and respiratory diseases. Based on previous work that revealed the receptor's tolerance to modifications at specific sites on the epitope, and NMR studies of SLe^X bound to E-selectin, a macrocyclic SLe^X analogue (**15**) was designed (Figure 1.14).¹¹⁷

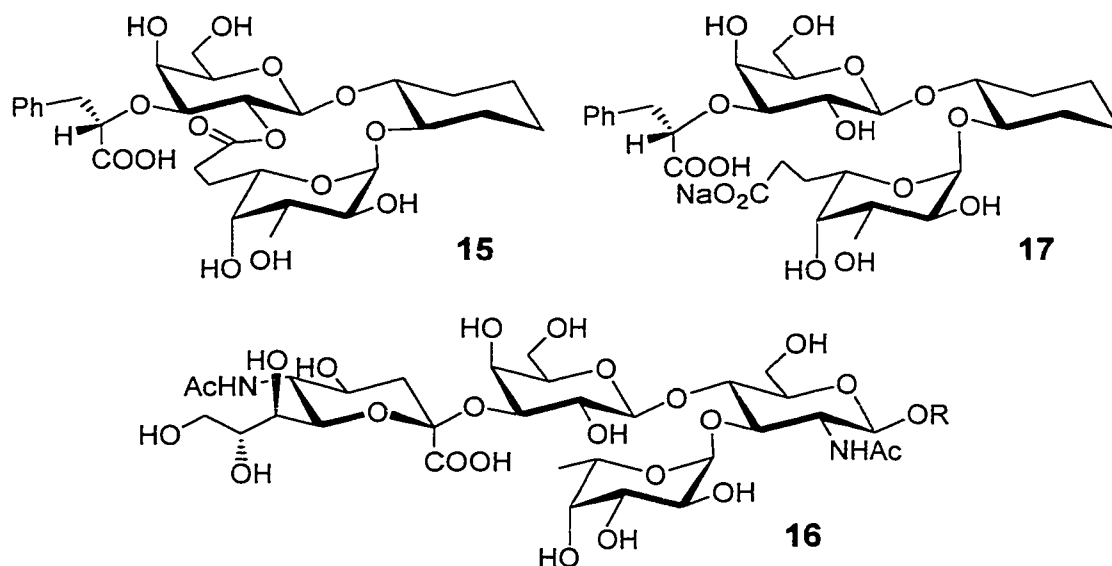


Figure 1.14: Sialyl Lewis X **16** and SLe^X analogues **15** and **17**.¹¹⁷

The substitution of both the *N*-acetylglucosamine and neuraminic acid residues were based on positive results from previous studies.^{118,119} Computer modeling of SLe^X **16** and the SLe^X analogue **15** shows that the conformational space adopted by the two molecules are very similar. It was

also determined that the probability distribution is narrower for **15**, implying that the analogue is structurally similar to the parent tetrasaccharide, but the core is more rigid. The binding of the constrained SLe^x analogue **15** to E-selectins was found to be 2.8 times weaker than **16**. Since an open chain analogue **17** was found to be a better inhibitor than the macrocyclic analogue **15**, it was suggested that the lower affinity of **15** may be due to a slight distortion of the acid orientation from the optimum position.

One of the earliest studies on constrained analogues was the trisaccharide β -D-GlcpNAc(1→2)- α -D-Manp(1→6)- β -D-Glcp1→O(CH₂)₇CH₃ (**18**), an acceptor substrate for the enzyme *N*-acetylglucosaminyltransferase V which adds a β GlcNAc residue to the 6-position of the central α Man unit (Figure 1.15). The Man(1→6) bond in oligosaccharides such as **18**, is known to be conformationally labile. In order to establish whether the transferase preferentially binds the gg or gt rotamer of the trisaccharide, constrained trisaccharides **19** and **20** were synthesized (Figure 1.15).⁴ The analogues **19** and **20** were designed to restrict the rotation about the C5-C6 bond of the β Glc residue, representing conformationally restrained models for the gt and gg conformations respectively. The kinetic data obtained by enzyme reactions revealed that the gg rotamer was the preferred acceptor substrate, reacting with the enzyme at a rate similar to that of the native trisaccharide **18**. The gt rotamer **19** showed very little activity. This result seems to indicate that the gg rotamer **20** represents the preferred conformation accepted by the β GlcNAc transferase, although restricted rotation about the C5-C6 bond of the β Glc residue does not seem to improve binding. Unfortunately, because these are enzymatic reactions, discriminating between enthalpy and entropy contributions is difficult.

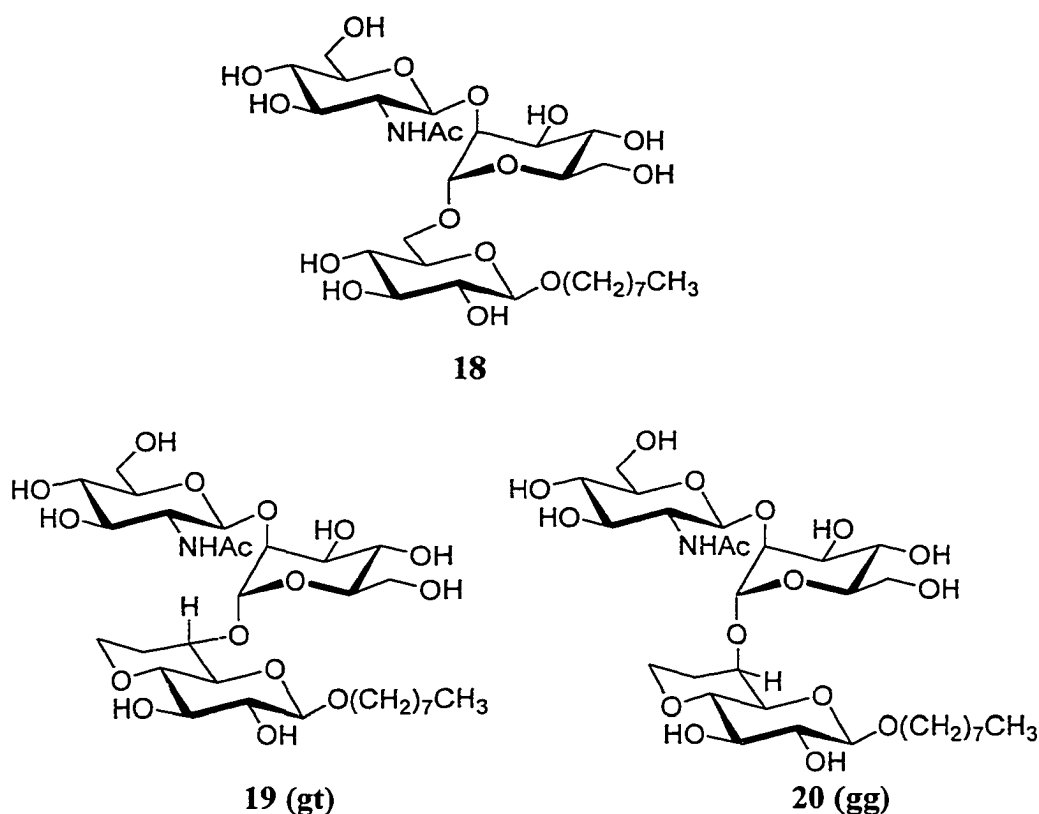


Figure 1.15: Parent substrate for GlcNAc transferase-V **18** and analogue substrates **19** and **20**.⁴

1.7.1: Overview on Constrained Oligosaccharides

In some of the above examples, long flexible tethers were employed to restrain the ligand. This incorporates another ‘flexibility factor’ into the system. Though it may aid in decreasing the flexibility about the glycosidic linkages, it may also contribute unfavorably to the entropy.

The nature of the tether is also an important element. As shown by Bundle *et al.*,¹¹⁴ the tether can create additional interactions with the protein or surrounding water, which may favor or disfavor binding. This is an interesting point when one is searching for an efficient inhibitor, but in studying the entropic penalty arising from ligand flexibility, the effect from the interaction of the tether may mask the effect from the decrease in flexibility.

This aspect must be considered when analyzing the data in this type of investigation.

As seen in most of these studies, the constrained oligosaccharides do not show increased binding. Though they were determined to have very similar solution conformations as their native counterparts, it has been suggested that the structural fidelity with the bound state may still be lacking.¹¹² Since the attempts to constrain oligosaccharide epitopes in a conformation pre-organized for binding have failed to show significantly higher free energy of binding, it seems that some of the concepts still need refinement.

Design of Constrained H-type 2 Derivatives

2.1: Pre-Organization of the H-type 2 Trisaccharide

Pre-organization of an oligosaccharide epitope in its bound conformation poses several difficulties, especially in relation to the ability of the tether to constrain the oligosaccharide in a bioactive conformation. By selecting an oligosaccharide such as the human blood group H-type 2 epitope for such studies, it is possible to access a range of distinct lectin binding sites, and increase the potential for identifying a recognition system in which entropic gains may be significant. Furthermore, the crystal structures of two H-antigen specific lectins have been solved^{71,120} and with the exception of *Erythrina corallodendron* lectin,³⁰ all the lectin sites have been extensively mapped by epitope congeners,^{103,121-125} thereby facilitating the design of tethered oligosaccharides.

Ulex europaeus I,²⁷ the primary lectin target of this synthetic study, binds to the H-type 2 human blood group determinant α -L-Fucp(1→2)- β -D-Galp(1→4)- β -D-GlcpNAc1→OR (1). The crystal structure of the H-type 2 oligosaccharide specific lectin from *Ulex europaeus* I without bound saccharide has been solved.⁷¹ Thermodynamic data obtained from van't Hoff plots for the binding of H-type 2 trisaccharide by *Ulex* lectin show large favorable enthalpy opposed by large unfavorable entropy ($\Delta G^{\circ} = -8$ kcal/mol, $\Delta H^{\circ} = -29$ kcal/mol, $T\Delta S^{\circ} = -21$ kcal/mol).¹⁰³ The size of the entropic penalty suggests that a conformational change may accompany the binding of the sugar.^{102,126-130}

We have therefore set out to design and synthesize tethered H-type 2 trisaccharides. Our design of the tethered H-type 2 trisaccharides are based on a crystal structure of the *Ulex* lectin⁷¹ and published studies of congener binding to three lectins, *Ulex europaeus* I, *Galactia tenuiflora* and *Psophocarpus tetragonobolus* II.^{103,121-125} Although there is currently no published x-ray structure for the complex with oligosaccharide, the *Ulex* lectin co-crystallizes with a molecule of 2-methyl-2,4-pentanediol, a precipitant used

for protein crystallization, and this complex provided a reference point for saccharide docking.

2.2: Mapping Study of the H-type 2 Trisaccharide

Detailed studies have been performed to map the H-type 2 epitope in order to determine the sites which are involved in the binding to the *Ulex europaeus* I lectin, as well as to the *Galactia tenuiflora* and *Psophocarpus tetragonolobus* II lectins.^{103,121-125} In order to determine which functional groups of the H-type 2 trisaccharide **1** were essential in the binding to these three lectins, a series of mono-deoxy, mono-methyl and mono-deoxyfluoro analogues of the H-type 2 trisaccharide were synthesized. The IC₅₀s of the analogues were determined by radioimmunoassays and consequently indicated which functional group changes most disrupted the binding to the lectins, and hence which functional groups were most important to the binding.

In the case of the *Ulex europaeus* I lectin, the mono-deoxy derivatives of H-type 2 trisaccharide **1** which sequentially omitted the hydroxyl groups at positions O-2, O-3, O-4 of fucose and O-3 of galactose lost most to all of their activity relative to that of the native H-type 2 trisaccharide. This indicates that these hydroxyl groups are necessary for binding to *Ulex*.

The mono-methyl and mono-deoxyfluoro derivatives replacing the hydroxyl groups at positions O-2, O-3, O-4 of fucose and O-3 of galactose illustrated that: 1) the hydroxyl groups on fucose are involved in hydrogen bonding to the protein and that they are hydrogen bond donors; 2) the hydroxyl groups on fucose must be buried within the binding site of *Ulex*; and 3) the hydroxyl group at the O-3 position of galactose is hydrogen bonded to the lectin at the periphery on the combining site.

A pentose congener of the H-type 2 trisaccharide in which the methyl group of fucose was replaced by a hydrogen was also found to have a significant decrease in activity, indicating that the methyl group fulfills an important hydrophobic interaction with the lectin.¹⁰³

The results of congener binding with the three H-type 2 trisaccharide specific lectins, *Ulex europaeus* I, *Galactia tenuiflora* and *Psophocarpus tetragonolobus* II are summarized in Figure 2.1 which identifies the key functional groups involved in binding.^{103,121-124}

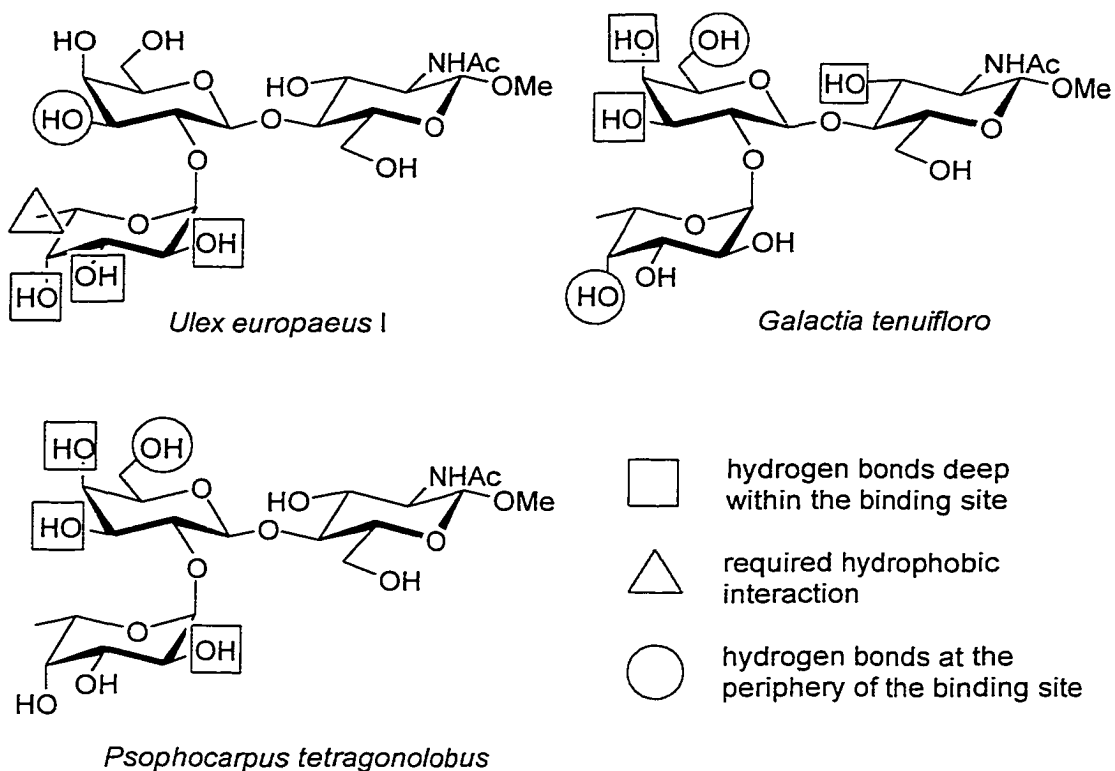


Figure 2.1: Congener mapping of the H-type 2 epitope.

2.2.1: Tethering Sites on the H-type 2 Trisaccharide

In order to design tethered derivatives of H-type 2 trisaccharide pre-organized in its bound conformation, the following criteria had to be fulfilled:

- the tether should not be attached to key polar groups that are involved in protein-carbohydrate interactions,
- the conformation of the bioactive epitope should be well approximated by tethering, and
- when bound, the tether should not interfere sterically with the surface of the protein.

In order to ensure that the tether met the first requirement, reference was made to the epitope mapping studies^{103,121-124} summarized in Figure 2.1.

Since the principle lectin of interest is the *Ulex* lectin, the binding topography of its H-type 2 epitope was examined. It indicated that the O-3 and O-6 position of glucosamine and the O-4 and O-6 position of galactose would be suitable sites for tethering. The methyl group of fucose, as long as that site remains hydrophobic, might also be an acceptable site for tethering. Tethers at some of these positions might not be suited for binding to winged bean lectin and very probably would cause problems for *Galactia*, which requires O-3 of GlcNAc for a buried hydrogen bond. From this information and excluding the possibilities that would result in the buckling of the trisaccharide, three possible tethered molecules were envisioned (Figure 2.2).

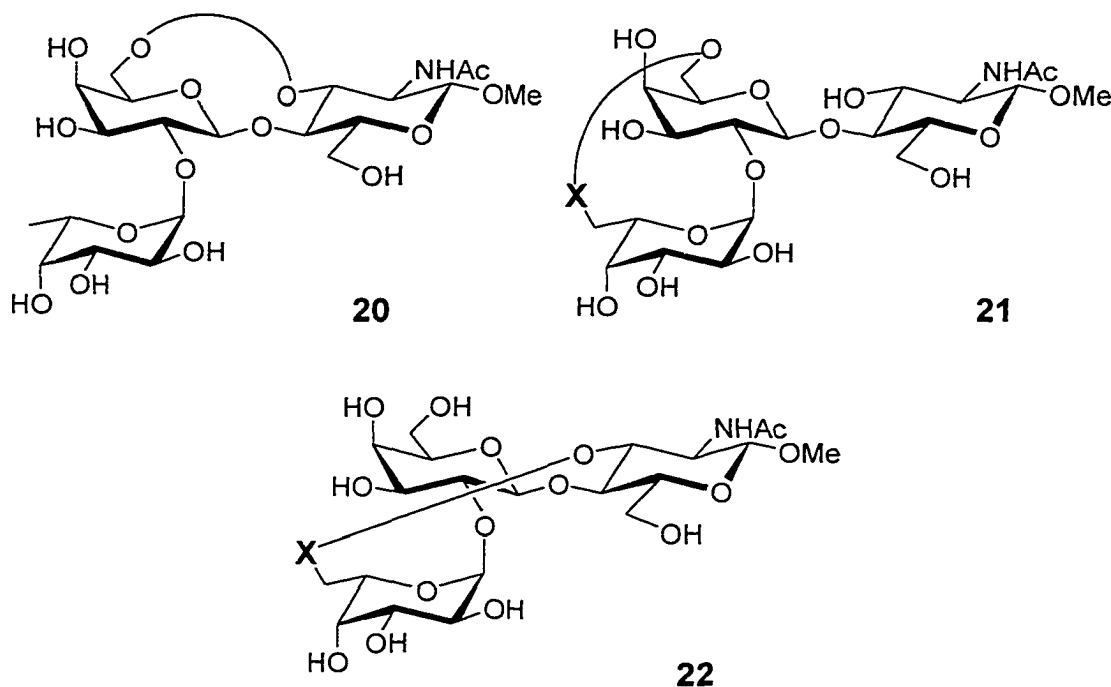


Figure 2.2: Possible tethered trisaccharides predicted from Lemieux's work.^{103,121-124}

2.3: Computer Modeling

The model of the tethered H-type 2 trisaccharide *Ulex* complex was developed in several stages. The co-ordinates for the *Ulex* structure with bound 2-methyl-2,4-pentanediol⁷¹ provided the starting point for positioning the ligand in the lectin site. Following an unpublished procedure of Lemieux,¹³¹ co-ordinates for α -L-fucopyranose were used to dock fucose in a manner such that the O-3 and O-4 atoms of α -L-fucopyranose were overlaid on the two hydroxyl groups of the pentanediol. Since epitope mapping of the H-type 2 ligand established that O-3 and O-4 of fucose are essential to binding¹²² and possess a synclinal relationship, this mode of docking seemed most consistent with the binding motifs of several published saccharide-lectin complexes.⁶² Having docked the monosaccharide residue, the coordinates of this sugar provided a key residue onto which the more complex trisaccharide **1** and **20-22** could be overlaid.

The conformation of trisaccharide **1** was modeled using the GEGOP forcefield¹³² and the global minimum energy conformation was selected. Since most oligosaccharide-protein complexes reveal bound oligosaccharides in conformations close to their energy minima, the fucose residue of trisaccharide **1** in its global energy conformer was overlaid on the fucose residue that was docked in the pentanediol binding site. This gave a model of trisaccharide **1** docked with lectin (Figure 2.3, 2.4 and 2.5). The approach was subsequently justified since transferred NOE studies¹³³ are consistent with a bound H-type 2 trisaccharide epitope in this low energy conformation (see Chapter 6).

Trisaccharide **1** in its low energy conformation was studied for tethering. Different tethered saccharides of compounds **20** and **21** with varying lengths of tethers were generated. Energy minimizations for the different tethered saccharides **20** and **21** were performed with the CVFF forcefield¹³⁵ of the *Discover*[®] software. The structures that puckered the sugar, or changed the overall shape of the native ligand were removed from

the list of possible targets. The tethered structures that remained, retained sufficient flexibility to adopt several low energy conformations that are similar to those of bound trisaccharide 1.

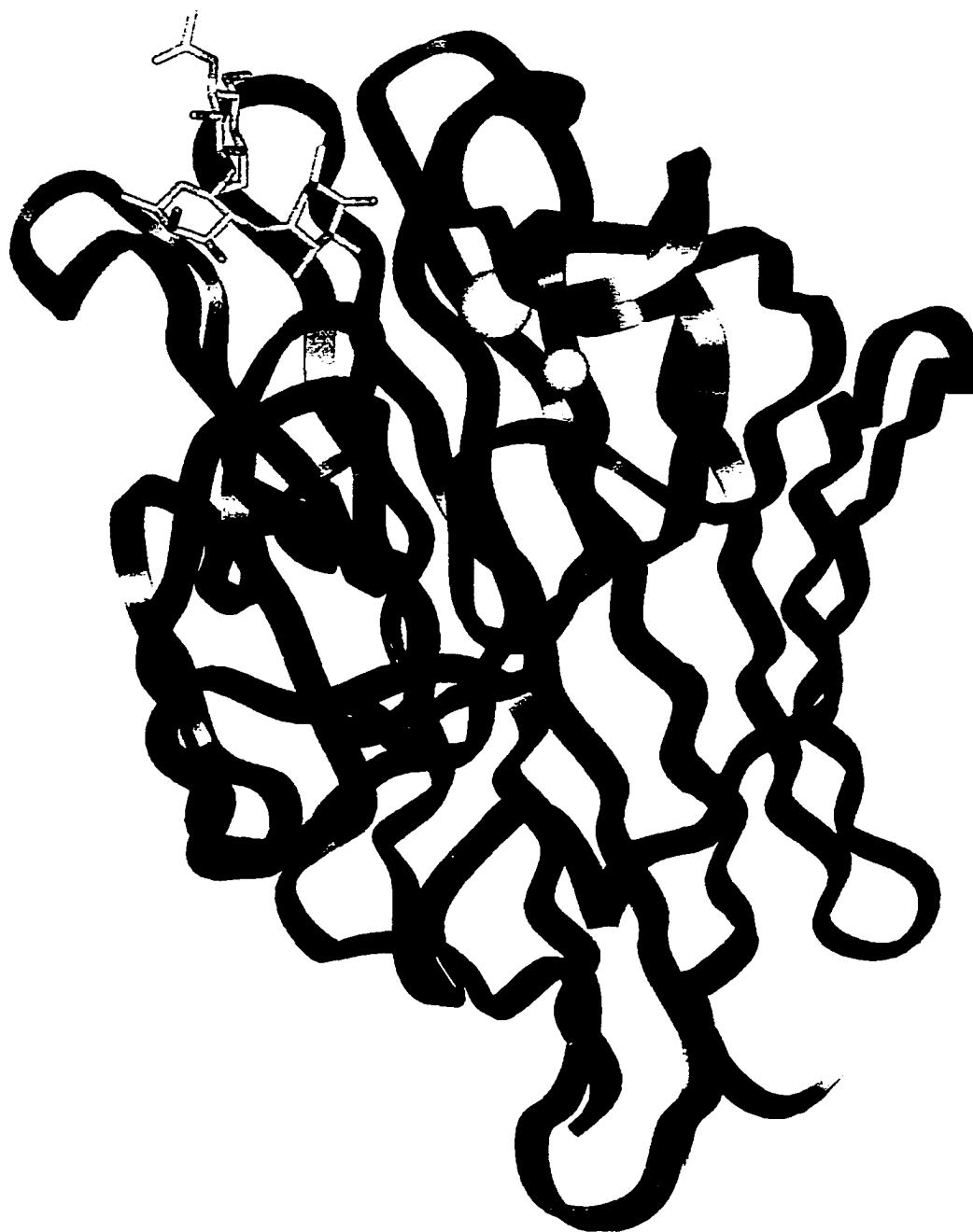


Figure 2.3: Ribbon representation of the *Ulex europaeus* I lectin with docked H-type 2 trisaccharide.^{71,131,134} Spheres represent cations Ca^{2+} and Mn^{2+} .

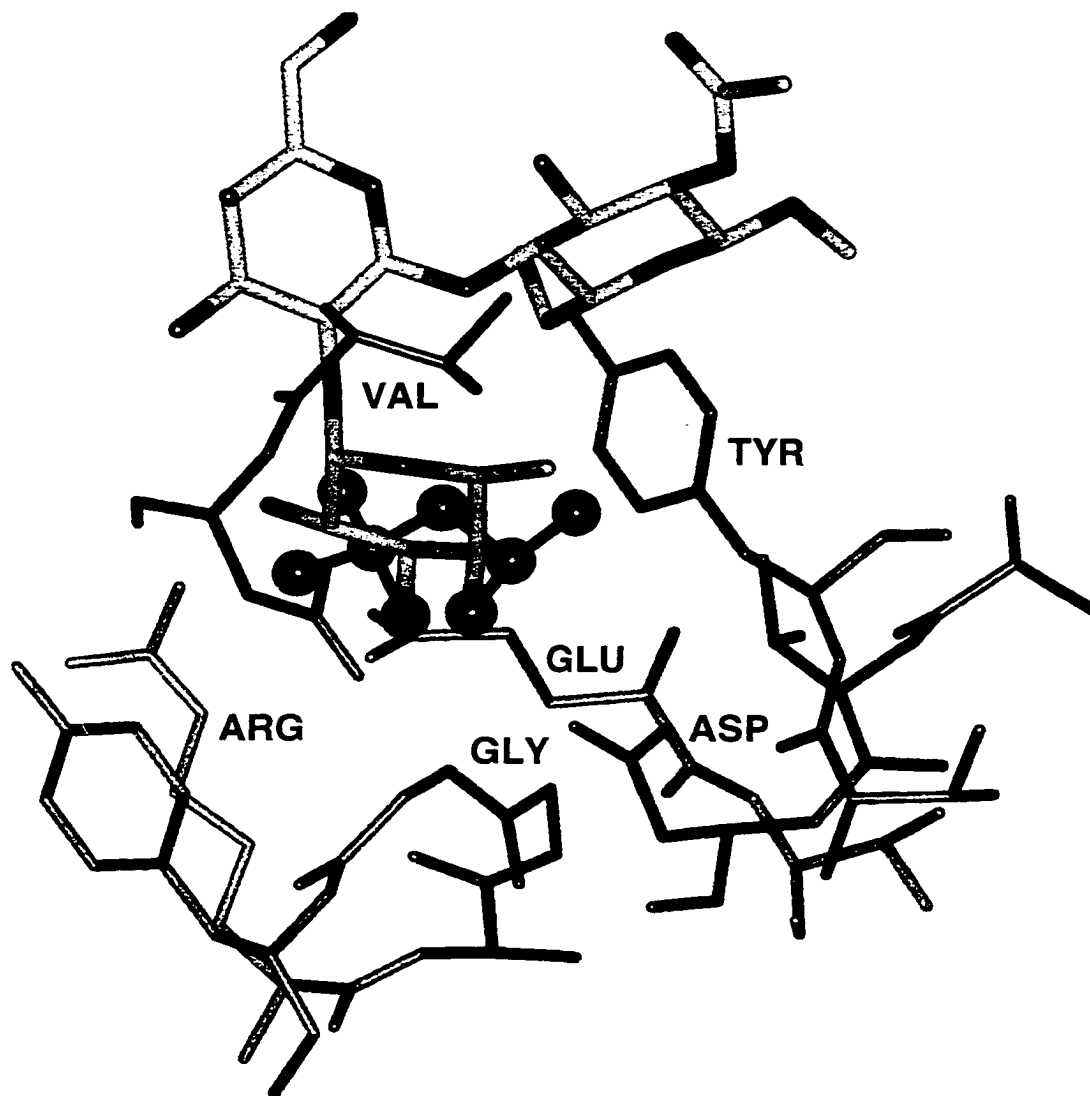


Figure 2.4: Computer modeling: binding site amino acids of the *Ulex* lectin co-crystallized with a molecule of (R)-2,4-dihydroxy-2-methylpentane and superimposed H-type 2 trisaccharide.¹³⁴

To confirm that the bound form of the tethered H-trisaccharides could adopt realistic conformations while avoiding tether-protein contacts, the energy minimized conformations were docked to give lectin-trisaccharide complexes. The docked complex was created by overlaying each of the tethered trisaccharides on the bound form of the H type 2 trisaccharide **1**. From the molecular modeling and docking of the carbohydrates, the following bridged trisaccharides remained as possible targets (Figure 2.6).

Tethered trisaccharides **24** and **25** aimed to restrict the rotation around one glycosidic bond, whereas tethered trisaccharides **26** would restrict the rotation around two glycosidic bonds. The heteroatoms involved in the tethering were varied as a second method of modifying the length of the tether. For example, in the case of the proposed tethered trisaccharides **24** (Y=O, n=0; Y=S, n=0; Y=O, n=1), the length between the C-6 of galactose and the O-3 of glucosamine varies between 4.77 Å, 5.04 Å and 5.21 Å.

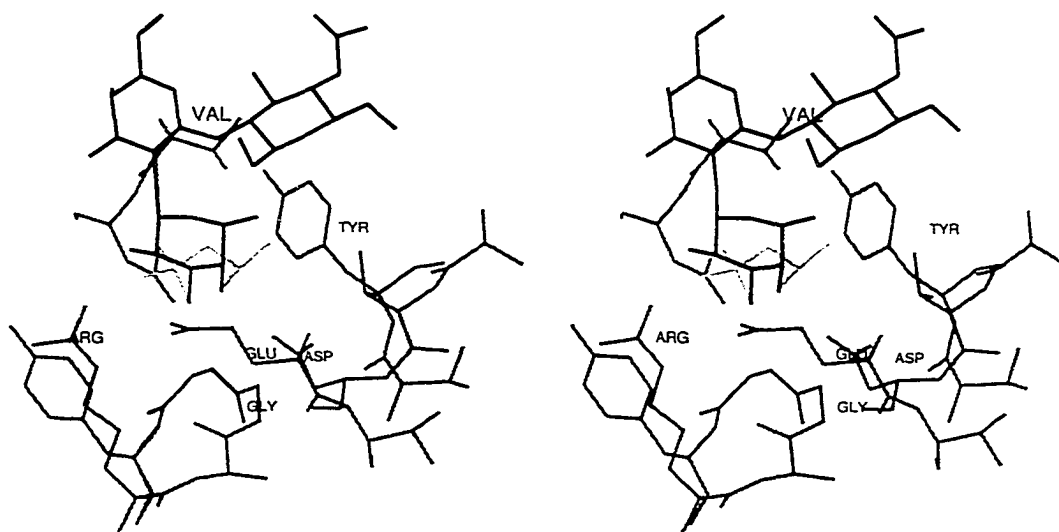


Figure 2.5: Computer modeling: a stereo plot of the binding site amino acids (mid grey lines) of the *Ulex europaeus* I lectin co-crystallized with a molecule of 2,4-dihydroxy-2-methylpentane (light gray lines) and superimposed H-type 2 trisaccharide (black lines).¹³⁴

Therefore, the sulfur offers a way of obtaining an intermediate length for the linkers differing in length by one carbon.

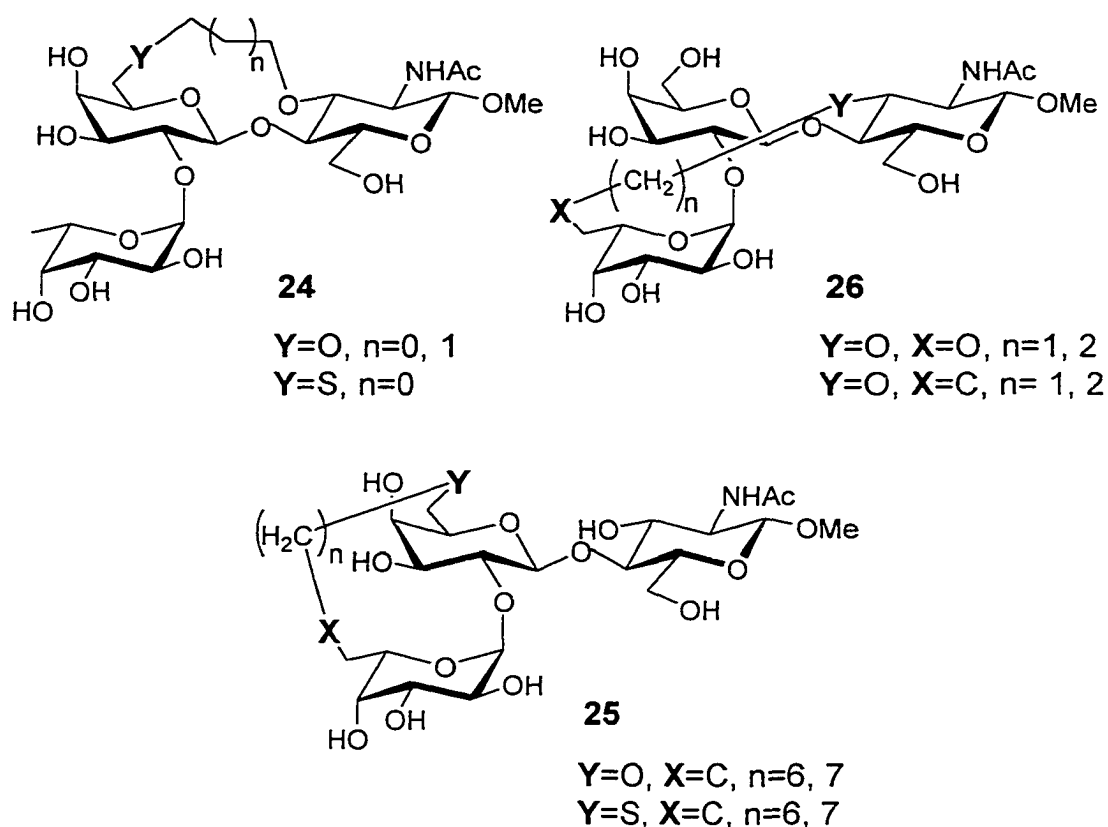


Figure 2.6: Potential tethered trisaccharides suggested by computer modeling.

The rationale for assuming that the pentanediol, as seen in the X-ray crystallography experiments, occupied the saccharide binding site of the *Ulex* lectin, is based on several factors. As mentioned earlier, several crystal structures of legume lectins and their substrates show large sequence homologies that include certain invariant amino acids.⁶² Some of these amino acids are known to participate in hydrogen bonding and hydrophobic interactions in the binding site, while others are involved in the coordination of the calcium and manganese ions.^{5,62,109,136} From the crystal structure of the *Ulex* lectin, it has been found that the amino acids usually involved in

coordinating the metal ions, asparagine and aspartic acid, are present and are in close vicinity to the ions.⁷¹ The pentanediol binding site contains the amino acids, asparagine, aspartic acid and tyrosine, that are often involved in buried carbohydrate-lectin hydrogen bonding and hydrophobic interactions. In this context, *Ulex europaeus* I fits the general binding site motif of legume lectins.^{62,136} In comparing the X-ray structure of *Ulex* with that of other legume lectins, the location of the 5-, 6-, and 7-stranded β -sheets, and the metal ions are superimposable. In addition, the binding site of 2-methyl-2,4-pentanediol is found to overlap with the binding site of the carbohydrate substrates.

The tethered H-type structures **24**, **25**, and **26** are effectively constrained to a narrow range of conformers similar to those of the bound state, while retaining sufficient flexibility to adopt several low energy conformations that are similar to those of bound native trisaccharide **1**.

In order to reduce the number of constrained H-type 2 trisaccharides to be synthesized, it was decided to attempt the synthesis of the tethered molecule **26** which would restrict rotation about two glycosidic bonds, and only one of the remaining tethered trisaccharides, either **24** or **25**, that restrict rotation about one glycosidic linkage. Trisaccharide **24** was selected over trisaccharide **25** because it involved a shorter tether. A shorter tether is thought to better restrain the flexibility of the oligosaccharide.

The structure of the target molecules allows us to explore several possible routes for their assembly. Since the tethering of preassembled oligosaccharides and the formation of large rings are low yielding processes,^{111,112} intramolecular glycosylation appeared to offer certain advantages for the assembly of the target molecules.

Synthesis of Constrained Trisaccharides via Intramolecular Glycosylation

3.1: Introduction

In order to study the conformational entropy penalty associated with immobilizing the glycoside linkages in the bound state, we have synthesized analogues of the H-type 2 trisaccharide. The tethers bridge the galactose and glucosamine monosaccharides, and the fucose and glucosamine residues of the trisaccharide. As well, tethered analogues of lactosamine have been synthesized. Although these tethered saccharides have been designed primarily for binding to the *Ulex europaeus* I²⁷ lectin, their bioactivity is determined for other H-type 2 specific lectins such as *Psophocarpus tetragonolobus* II lectin (winged bean lectin),²⁸ and *Erythrinia corallodendron*³⁰ lectins. The bioactivity of the H-type 2 trisaccharide and the tethered lactosamine derivatives is determined for the *Erythrinia corallodendron*³⁰ lectin.

3.1.1: Glycoside Synthesis – General Concepts

The most commonly employed method of synthesizing glycosides is based on the generation of an anomeric glycosyl cation from a glycosyl donor (Figure 3.1).¹³⁷ Once the leaving group of the glycosyl donor has departed, the carbocation formed is subsequently attacked by a nucleophile, such as a sugar alcohol, called a glycosyl acceptor. However, the mechanism does not always proceed via a S_N1 route. Glycosylation may also proceed via a S_N2 mechanism. This is the case when a glycosyl fluoride is used as the glycosyl donor. Despite considerable progress in the field of glycoside synthesis over the last 20 years, the words of Hans Paulsen¹³⁷ seventeen years ago still hold true: "...each oligosaccharide synthesis remains an independent problem, whose solution requires considerable systematic research and a good deal of know-how. There are no universal reaction conditions for oligosaccharide

syntheses.” The two main problems which are encountered in glycoside synthesis are regiochemical and stereochemical control of the reaction.¹³⁸

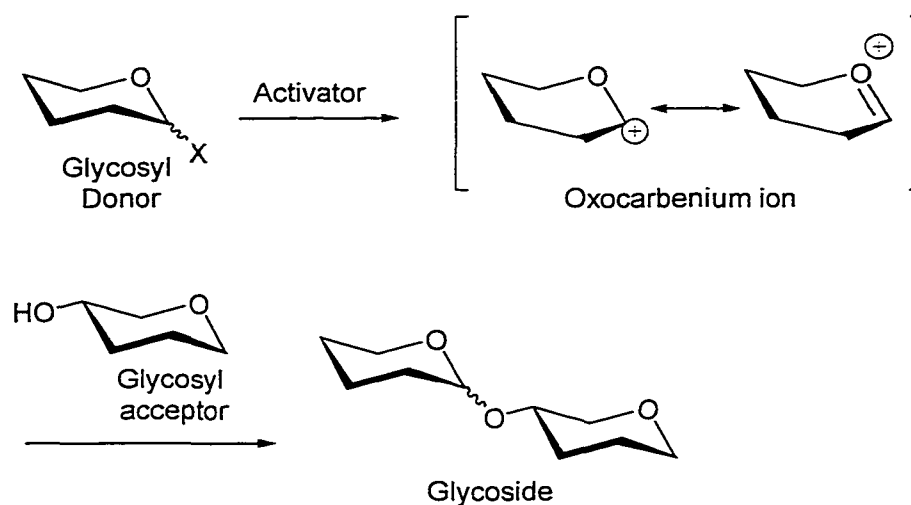


Figure 3.1: Glycosylation reaction.

The regioselectivity problem is most often solved by laborious selective protection and deprotection of the hydroxyl groups. Consequently, the development of protective group chemistry is of great importance in the synthesis of oligosaccharides.¹³⁹⁻¹⁴¹ Stereoselectivity is achieved in many different ways because the solutions are dependent on the nature of the desired product, i.e. whether it is a 1,2-*cis* or 1,2-*trans* glycoside. Some of the solutions have taken advantage of neighbouring group participation,^{142,143} solvent effects such as the 'nitrile effect',¹⁴⁴⁻¹⁴⁶ and the anomeric effect.¹⁴⁷⁻¹⁴⁹

3.1.2: Review of Intramolecular O-Glycosylation

A relatively new approach to the synthesis of stereocontrolled O-glycosidic linkages has been pursued by several groups. This method has been called intramolecular glycosylation,¹⁵⁰⁻¹⁵⁵ intramolecular aglycon delivery,¹⁵⁶⁻¹⁵⁸ or cyclo-glycosylation,^{159,160} and aims to control the delivery of the acceptor in order to obtain the desired stereochemistry at the new glycosidic linkage.

Stereocontrolled formation of glycosidic linkages is of great importance in carbohydrate chemistry. The most persistent difficulty has been the efficient synthesis of β -D-mannopyranosides. The β -linkage in D-mannosides is found in *N*-linked oligosaccharides as part of the core pentasaccharide of glycopeptides. Here, the problem of stereoselectivity is amplified in the case of the selective chemical preparation of β -D-mannosides (and β -L-rhamnosides) due to steric and stereoelectronic effects, which strongly favor the formation of α -glycosides. Several approaches aimed at the synthesis of these difficult 1,2-*cis*- β -linkages have been developed.¹⁶¹⁻¹⁷⁵ The most direct methods involve the use of non-participating group protected glycosyl halides and insoluble silver catalysts.¹⁶¹⁻¹⁷⁵ However, these methods suffer from the lack of reproducibility and the production of the α -glycoside as a side product leading to a difficult separation of anomers. The desire to improve the synthesis of these difficult β -linkages was the point of origin for the intramolecular glycosylation method.

Intramolecular glycosylations may be separated into two main categories. The first category involves a glycosyl donor and a glycosyl acceptor connected by a temporary, labile tether, which is cleaved during the formation of the glycosidic bond. In the second category, the glycosyl donor and glycosyl acceptor are connected by a stable, persistent tether and a ring is formed during the glycosylation step.

Our synthetic route to making tethered trisaccharides involves intramolecular glycosylations using a permanent tether. Hence, a brief review of intramolecular glycosylations will give the appropriate background information on what has already been accomplished by this method of glycosylation.

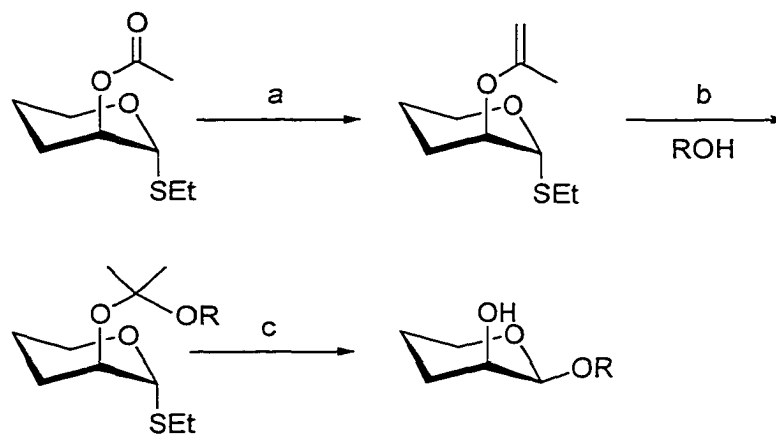
3.1.2a: Category 1 - Temporary Tethers

The approach to the synthesis of 1,2-*cis*- β -glycosidic linkages introduced by Hindsgaul and Barresi for β -D-mannopyranosides involves the initial covalent attachment of the glycosyl donor and the glycosyl acceptor via

mixed acetal formation. Intramolecular aglycon delivery occurs when the donor residue is activated (Scheme 3.1).¹⁵⁶⁻¹⁵⁸ The acetal-tether is removed immediately after the formation of the glycosidic bond, once the reaction is quenched with water.

The general procedure used to obtain the tethered glycosyl donor and acceptor involves the formation of the vinyl ether at the O-2 position of the mannose-donor by treating the 2-O-acetate with Tebbe's reagent (Scheme 3.1).¹⁷⁶ The mixed acetal is formed under acidic conditions by treatment with an equimolar amount of the glycosyl acceptor. The reaction time is crucial, no longer than 10 minutes, or the yield decreases drastically due to the formation of symmetrical dimerization product.¹⁵⁸

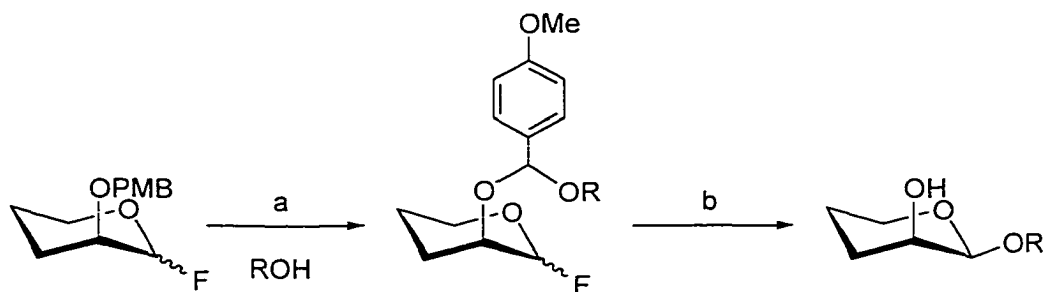
The best conditions for performing the intramolecular aglycon delivery step uses 5 equiv. of *N*-iodosuccinimide (NIS) and 5 equiv. of di-*t*-butyl-4-methylpyridine (DTBMP) in dry CH₂Cl₂, starting the reaction at 0°C and allowing it to warm to room temperature overnight.¹⁵⁸ The reaction time varied, depending on the steric hindrance involved in the glycosylation.



Scheme 3.1: a) Tebbe's reagent, THF-toluene-pyr, -40°C→15°C;
 b) *p*TsOH, CH₂Cl₂, -40°C, 10 min; c) 5 eq. NIS, 5 eq.
 DTBMP, CH₂Cl₂, 0°C→rt.

This approach leads solely to β -mannosides, without any chromatographic evidence for the formation of the α -anomer. It therefore eliminates the difficult separation step that is normally involved in the synthesis of β -mannosides. It is effective in syntheses involving glycosyl acceptors with primary hydroxyls; those with secondary hydroxyls tend to suffer from steric hindrance, resulting in lower yields. The methodology seems to be limited to the synthesis of disaccharides. Extending this process to trisaccharides has led to significantly lower yields.

Ogawa *et al.* have also explored the use of mixed acetals to accomplish the intramolecular delivery of the acceptor to yield the desired β -mannosides.¹⁷⁷⁻¹⁸¹ In this procedure, the *p*-methoxybenzyl (PMB) ether is used as the stereocontrolling element. The mannosyl donor carries the PMB group at the C2 position, and after treatment with the aglycon in the presence of 2,3-dichloro-5,6-dicyano-*p*-benzoquinone (DDQ) under anhydrous conditions, the mixed acetal is formed (Scheme 3.2). The glycosylation step is performed on the unpurified mixed acetal.



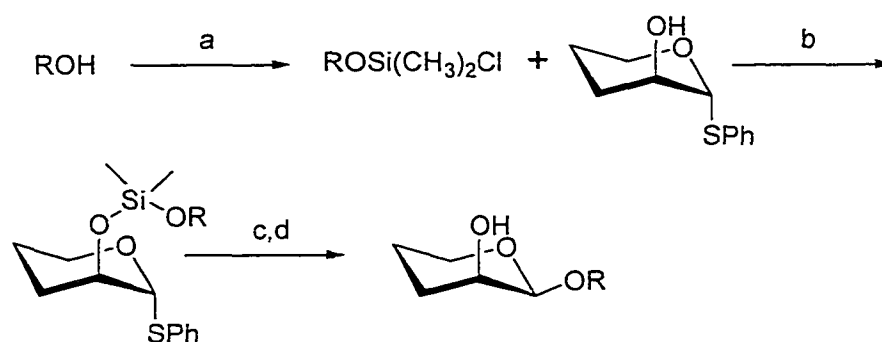
Scheme 3.2: a) DDQ, CH₂Cl₂; b) AgOTf, SnCl₂, DTBMP

The initial studies on this intramolecular glycosylation reaction involved mannosyl fluorides as donors.¹⁷⁷ These glycosylation reactions were promoted with silver triflate (AgOTf), SnCl₂, and DTBMP. The reactions were performed in various solvents (CH₂Cl₂, Et₂O, MeCN) though the solvent effect seemed minimal except in the case of toluene which resulted in a very

sluggish reaction and an intractable mixture of products. In later examples, methyl thioglycosides were used as donors¹⁷⁸⁻¹⁸¹ and the thioglycosides were activated by methyl triflate (MeOTf) in CH₂Cl₂ using DTBMP as an acid scavenger. Yields varied between 40 to 74% and only β-glycosides were observed.

This approach has also been adapted for use on a polyethylene glycol monomethyl ether polymer support.¹⁸² A thiomannoside is attached to the polymer support through a PMB-like linker at the C2 position. The mixed acetal is formed on the polymer support, allowing the unreacted aglycon to be washed away. Intramolecular glycosylation is achieved using MeOTf as the promoter. The desired product is then liberated into solution, leaving any side-products, such as hydrolysis or 1,2-elimination products, attached to the polymer support.

Stork *et al.* having utilized silanes for the intramolecular synthesis of C-glycosides,¹⁸³ applied this idea to the synthesis of β-mannosides.^{184,185} Preparation of the silicon-tethered glycosyl donor and acceptor involved the formation of the chlorodimethylsilyl ether of the acceptor by treatment of the acceptor with n-butyl lithium and dichlorodimethylsilane. This was followed by reaction of chlorosilane with the glycosyl donor and imidazole, which led to the attachment of the donor (Scheme 3.3).

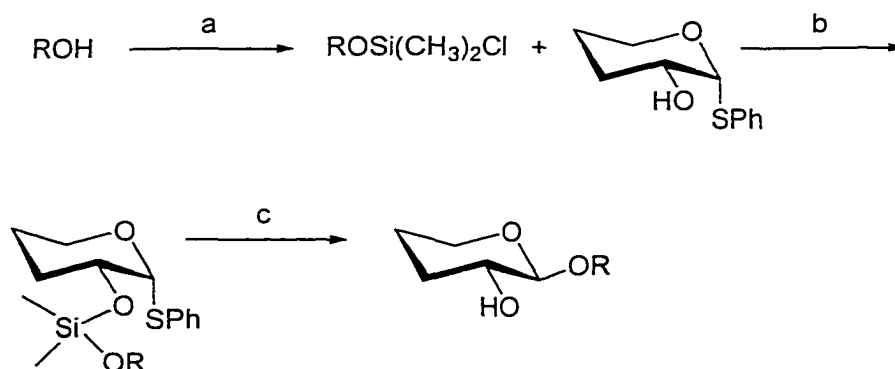


Scheme 3.3: a) n-BuLi, (CH₃)₂SiCl₂; b) imidazole; c) MCPBA, d) Tf₂O, DTBMP in CH₂Cl₂ -78°C→rt.

In the examples that used phenyl thiomannoside, the glycosylation method of choice was activation by the sulfoxide method introduced by Kahne.¹⁸⁶ The sulfoxide was prepared by treating a phenylthio glycoside with *m*-chloroperbenzoic acid (MCPBA), and this was then activated with triflic anhydride.

The intramolecular glycosylation resulted in the desired β -anomers, free of their α -counterparts. The yields generally were acceptable. In some cases, debenzoylation occurred at the O-6 position resulting in the formation of (1 \rightarrow 6) disaccharides as the main product.¹⁸⁵ No attempts were made to form tri- or tetrasaccharides.

Another approach to silicon-tethered mediated intramolecular glycosylations was developed by Bols (Scheme 3.4).¹⁸⁷⁻¹⁹² The work concentrated on the investigation of stereocontrolled synthesis of α -glucopyranosides and α -galactopyranosides.¹⁸⁷⁻¹⁹² The method of assembling the silyl acetal thioglycosides was very similar to that of Stork,^{184,185} and glycosylations were initially performed with NIS and triflic acid (TfOH).¹⁸⁷ When the method was extended to the synthesis of disaccharides, NIS and TfOH gave low yields, and therefore, the conditions were changed to NIS in refluxing nitromethane.¹⁹²

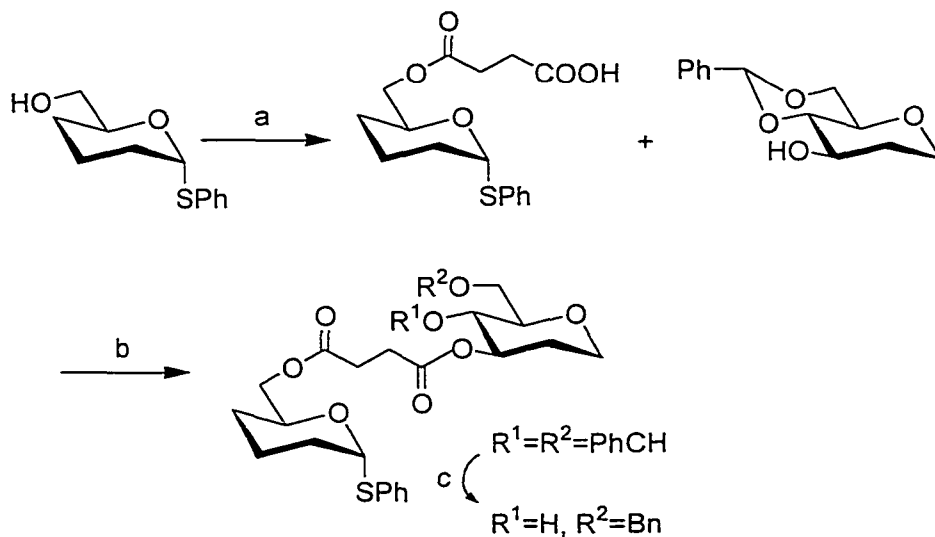


Scheme 3.4: a) (CH₃)₂SiCl₂, NEt₃, Et₂O; b) pyridine, THF;
c) NIS, TfOH in CH₂Cl₂ at 25°C.

Bols has succeeded in performing stereocontrolled glycosylations favoring α -glycosides without forming any of the β -anomers, but as yet no examples are given in the preparation of tri- or tetrasaccharides.

3.1.2b: Category 2 - Permanent Tethers

The approach to intramolecular glycosylation adopted by Ziegler *et al.*¹⁵⁰⁻¹⁵⁵ involves the connection of the glycosyl donor and acceptor by a stable bridge attached to a hydroxyl on each residue with one hydroxyl group of the acceptor residue left free for glycosylation. The general procedure used to obtain the tethered glycosyl residues involved treating the glycosyl donor with succinic anhydride, followed by DCC mediated condensation with the acceptor residue (Scheme 3.5). In most cases, a benzylidene protecting group was used on the acceptor moiety which via reductive ring-opening allows easy access to the O-4 position of the acceptor. It must be noted that although the succinic tether remains part of the molecule after the glycosylation, it is a removable tether.

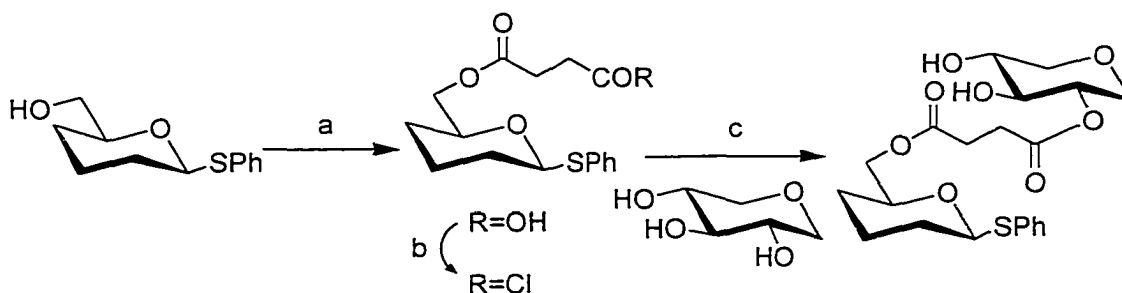


Scheme 3.5: a) 8 eq. succinic anhydride, cat. DMAP, pyridine;
 b) DCC, cat. DMAP, CH₂Cl₂ c) NaCNBH₃, HCl in Et₂O, THF.

The conditions used to execute the intramolecular glycosylations always involved activation by NIS and trimethylsilyltriflate (TMSOTf), though temperature and reaction time varied.¹⁵⁰⁻¹⁵⁵

The α/β ratios and yields obtained are not easily predictable. They seem to be governed by a combination of different effects, such as: linker position, anomeric effect, and orientation of the free hydroxyl on the acceptor residue. Ziegler *et al.* have also shown that the type of protecting groups used have little effect on the stereoselectivity of the reaction. The intramolecular glycosylation seems to be entropically favored over intermolecular glycosylation, since no other product but the intramolecularly tethered disaccharide was reported, although the reactions were performed under dilute conditions. In most cases the linker's neighbouring group participation ability does not seem to have any effect on the stereochemical outcome of the reaction.

Valverde *et al.*^{159,160} have reported a method similar to that of Ziegler, though in their studies, they report regioselective and stereoselective control in the glycosylation reactions with di-hydroxyl acceptors, therefore having two possible sites of glycosylation. The procedure used (Scheme 3.6) to obtain the similarly bridged glycosyl residues also involved treating the glycosyl donor with succinic anhydride or phthalic anhydride, but then followed by activation with thionyl chloride and coupling of the glycosyl residues by use of dibutylstannylidene acetals under microwave irradiation.

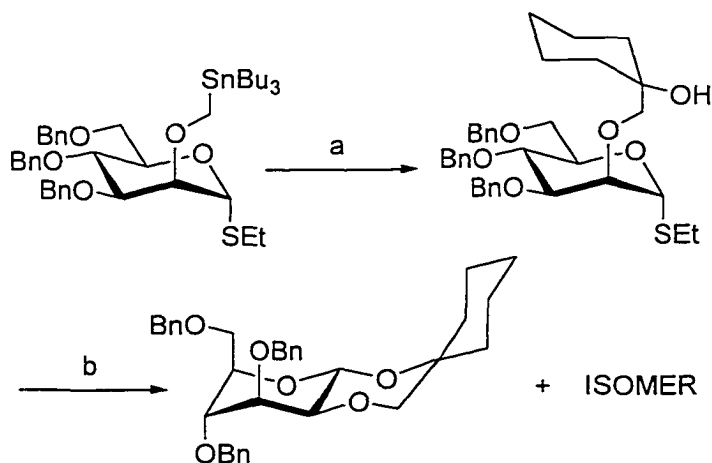


Scheme 3.6: a) Succinic or phthalic anhydride, NEt_3 ; b) SOCl_2 ;
c) Bu_2SnO , microwave irradiation.

In each of the cases, the coupling left two free hydroxyls as potential sites for glycosylation.

The conditions used to carry out the intramolecular glycosylations always involved activation by NIS and triflic acid, and reaction times of 10 minutes, at different temperatures. Very good stereocontrol and regiocontrol was achieved and yields varied between 65 to 80%. Temperature was found to influence the stereoselectivity of the intramolecular glycosylation – colder temperatures leading to higher selectivity. The nature of the tether (phthalic versus succinic esters) also did not seem to effect stereoselectivity, although it must be pointed out that the tether lengths are very much the same. When applying this method to the synthesis of β -mannosides, it was found that the stereoelectronic effects outweighed the influence of the tether, since only α -mannosides were obtained.

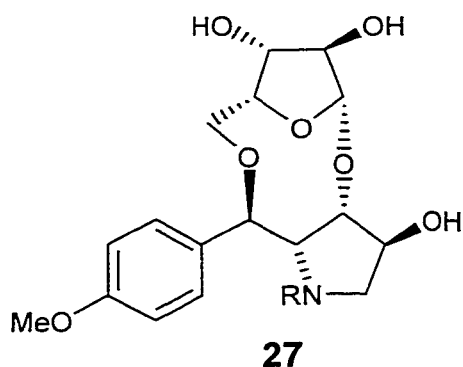
Another example of an intramolecular glycosylation which falls into the second category is by Hindsgaul and Bols¹⁹³ and it involves the synthesis of a tributyltinmethylated sugar, followed by treatment with *n*-BuLi and reaction with cyclohexanone. The resulting hemiacetal was activated with NIS and the α -anomer was the major product, even though this means that the ring has to adopt the unfavorable 1C_4 conformation (Scheme 3.7).



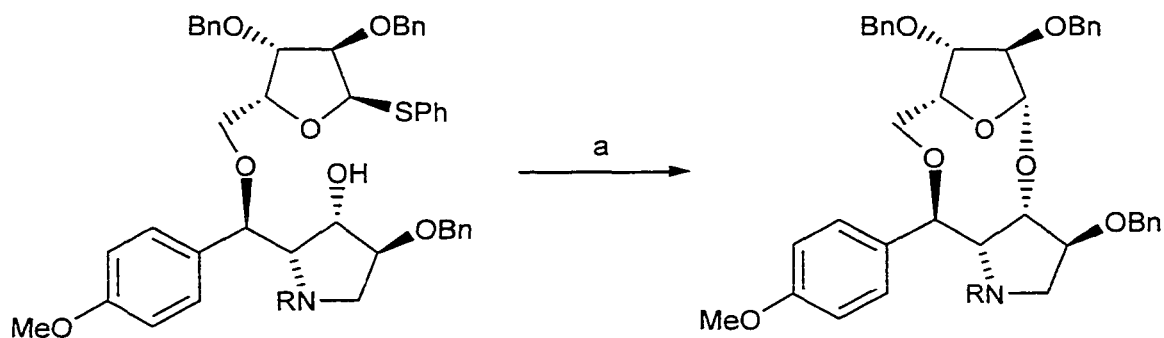
Scheme 3.7: a) *n*-BuLi, cyclohexanone (51%); b) NIS, CH₃NO₂(57%).

This example shows that an intramolecular glycosylation with a 6-membered transition state would be unfavorable for β -mannoside synthesis unlike the 5-membered transition state of the acetal tethers.^{156-158,177-182,184,185,187-192} This must be taken into consideration when designing an intramolecular glycosylation in β -mannoside synthesis.

Intramolecular glycosylation has also been used in the total synthesis of AB3217-A (**27**), a novel anti-mite substance.^{194,195} This target molecule,

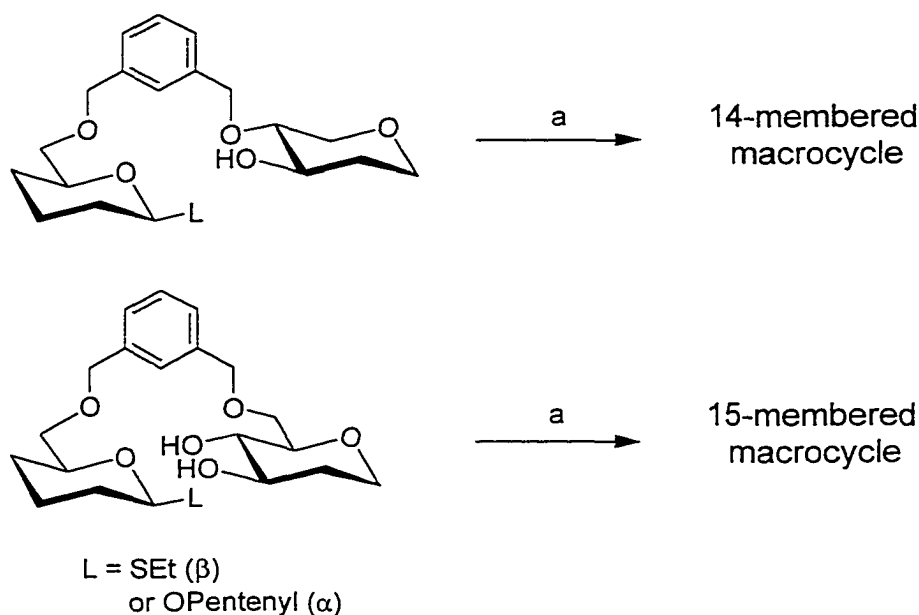


which contains a nine-membered ring, was assembled via intermolecular etherification and intramolecular glycosylation. The intramolecular glycosylation of the α -phenyl thiofuranoside was best accomplished by *N*-bromosuccinimide in toluene at 90°C yielding the β -anomer (Scheme 3.8). Other solvents or temperature gave much poorer yields.



Scheme 3.8: a) *N*-bromosuccinimide, toluene, 90°C, 24 hours (64%).

Schmidt *et al.* have designed an efficient intramolecular glycosylation supported by a rigid spacer (Scheme 3.9).^{196,197} A detailed study showed that the intramolecular glycosylations which generated 14-membered rings were generally stereoselective, favoring the β -anomer, and high yielding (77-93%), whereas, when 15-membered macrocycles were generated, the reactions though stereoselective, gave lower yields (65-72%). These lower yields were attributed to the competing reaction of the intermolecular oligomer formation. Running the reactions under more dilute conditions increased the yields of the target molecule.



Scheme 3.9: a) NIS, TMSOTf, CH₂Cl₂ at room temperature.

It was also observed that the attachment of the acceptor affected the stereochemical outcome of the reaction.¹⁹⁷ The D- and L-threo- and L-erythro-attachment of the acceptor gave exclusively the β -linkage, whereas the D-erythro-attachment favored the α -linkage (Figure 3.2).

In one example where an α/β mixture was obtained when using the *m*-xylylene spacer, the authors increased the stereoselectivity by limiting the

conformational space of the donor and acceptor moieties by using a bulkier spacer (Scheme 3.10).¹⁹⁷

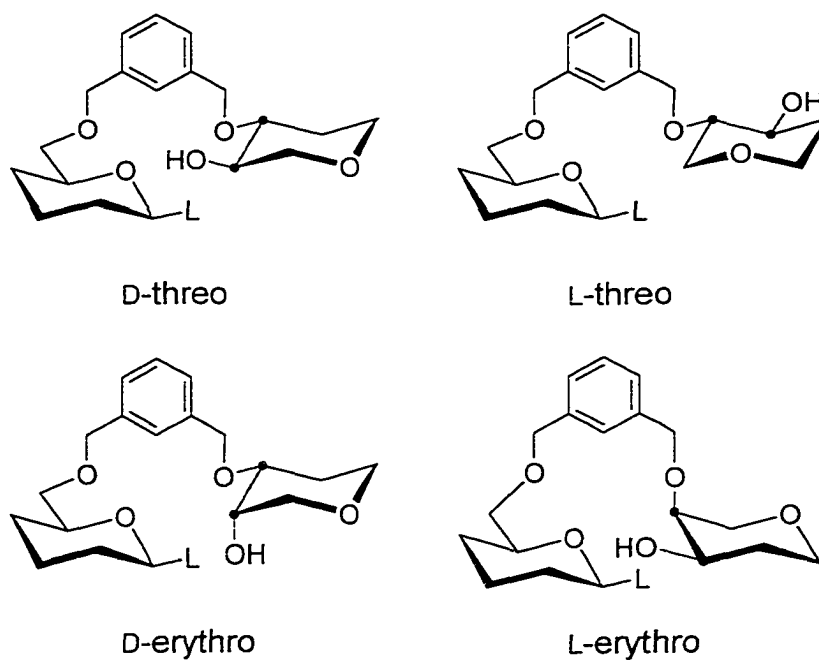
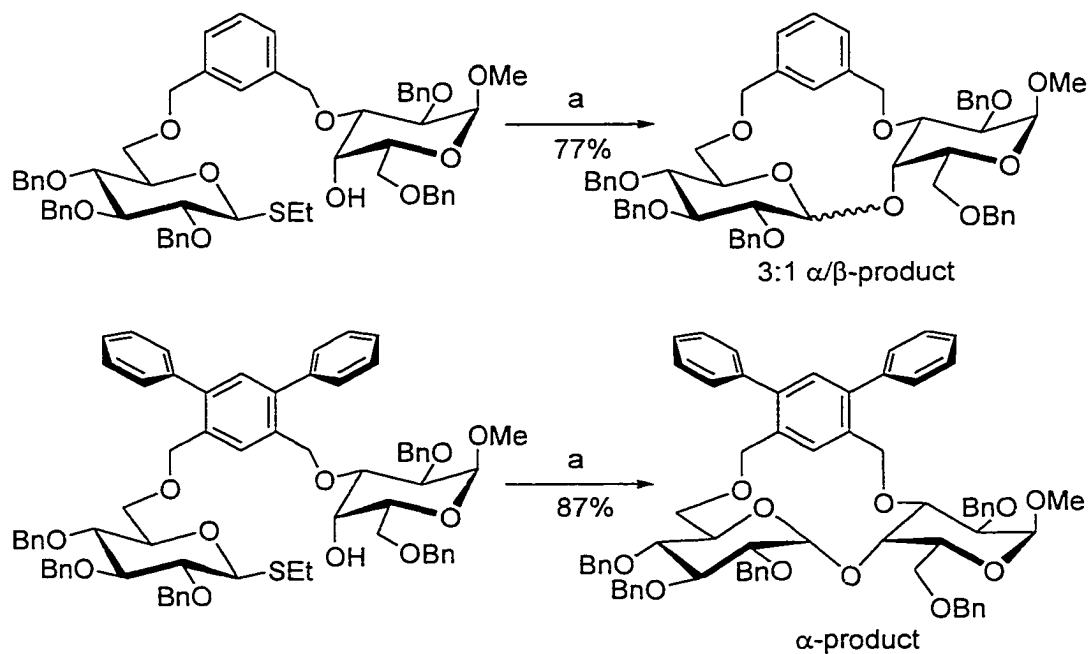
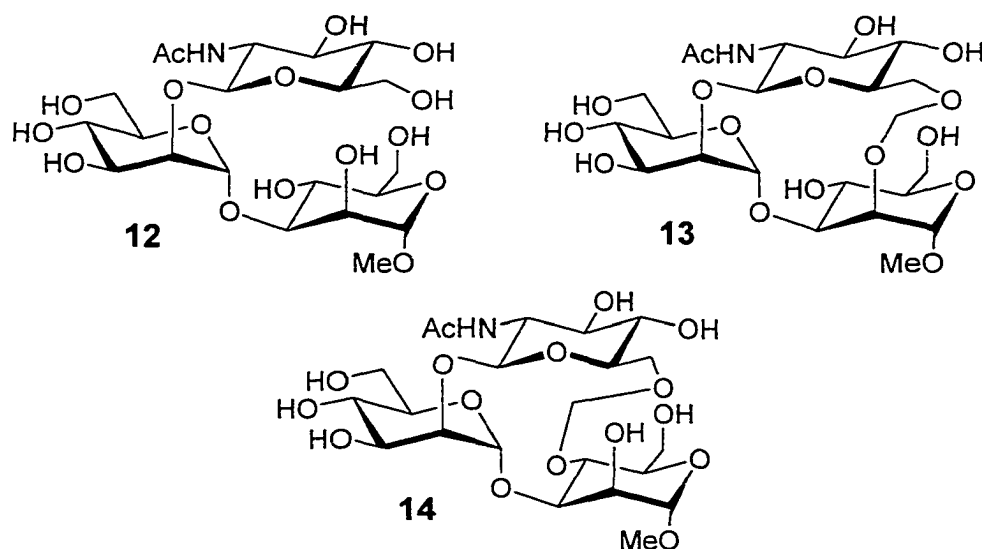


Figure 3.2: Various attachments of the acceptor.

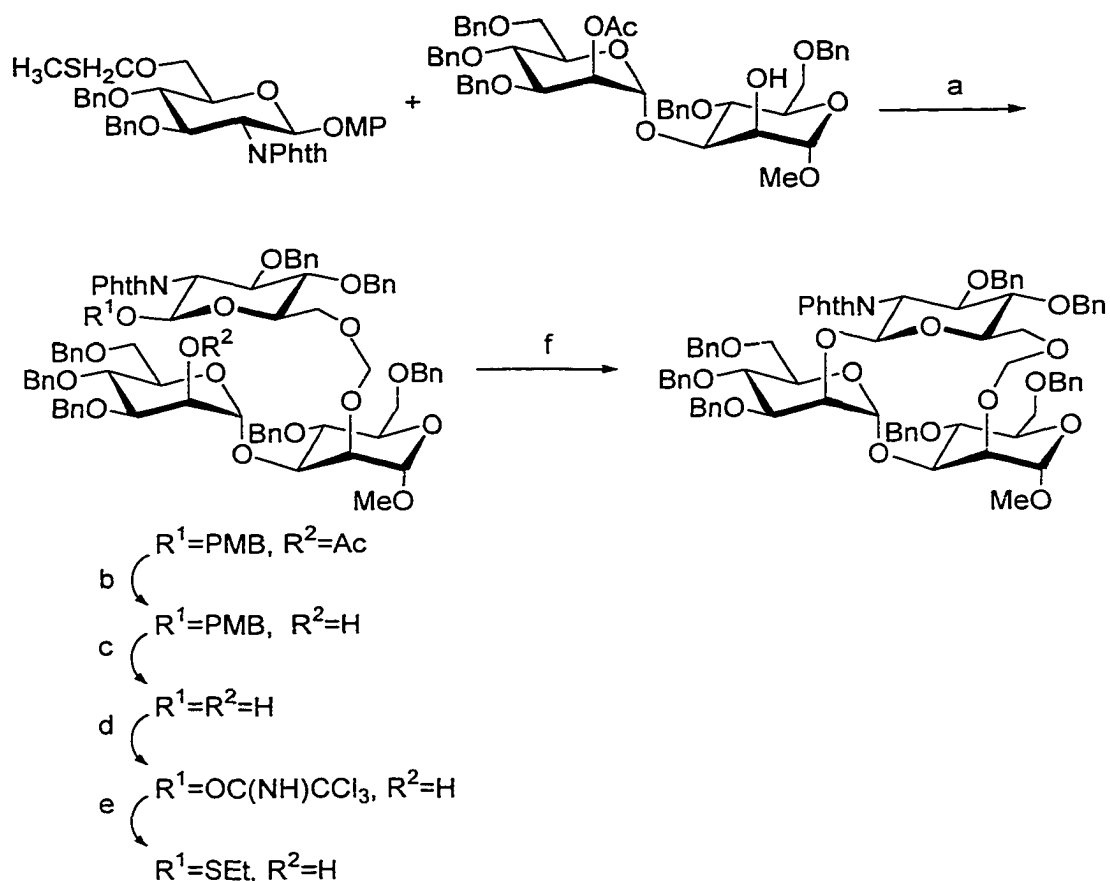


Scheme 3.10: a) NIS, TMSOTf, CH_2Cl_2 at room temperature.

The trisaccharide β -D-GlcpNAc(1 \rightarrow 2)- α -D-Manp(1 \rightarrow 3)-D-Manp (**12**) is known to bind to *Concanavalin A*. The tethered trisaccharides **13** and **14** were designed by Boons *et al.*^{115,116} to mimic the two possible conformations that the carbohydrate may adopt when bound to ConA. The methylene-tether was used to reproduce the conformation stabilized by an intramolecular hydrogen bond and reduce the flexibility of the trisaccharide while retaining the bioactive conformation of the epitope. Both tethered trisaccharides **13** and **14** were assembled via intramolecular glycosylation (Scheme 3.11). The tether used in these examples is not removable as in most of the other cases cited thus far. Here the tether is intended to remain in the final structure and was incorporated in the design of the target molecules.



The methylene-tether was introduced by coupling the two sugar residues in the presence of NIS and TfOH. After further protecting group manipulations, the linked sugars underwent an intramolecular glycosylation promoted by NIS and TMSOTf (34% yield). This yielded solely the α -anomer. A very similar reaction scheme was followed in order to obtain the tethered trisaccharide **14**.



Scheme 3.11: a) NIS, TfOH; b) KO^tBu, MeOH; c) CAN; d) Cl₃CCN, DBU; e) BF₃Et₂O, EtSH; f) NIS, TMSOTf.

3.1.2c: Overview of Intramolecular O-Glycosylation

At the present, the application of intramolecular glycosylation has been limited to di- and trisaccharides. As summarized here, these approaches include successful methods to control the stereo- and regioselectivity of glycosidic bond formation via pre-arranged glycosides. Important factors which affect the stereoselectivity and regioselectivity of the intramolecular glycosylations are the position of the tether, type of tether (silyl vs. mixed acetal vs. succinic/phthalic), temperature, and the size of ring formed. Thus far, no significant effect on the stereoselectivity of the intramolecular glycosylation reaction has been observed due to protecting groups. Though

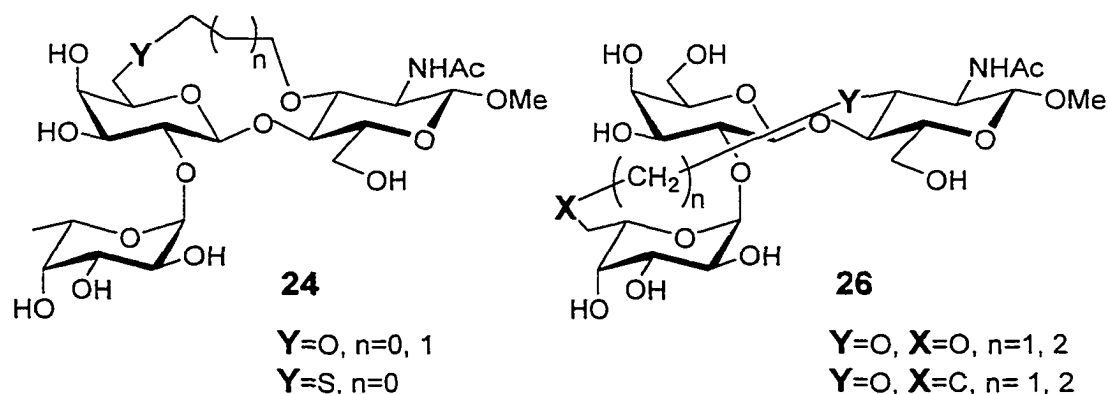
as yet, the protecting groups utilized do not include groups that lock the pyranose ring of the donor residue in a specific conformation.

In making the β -1,2-*cis* glycosides, the approaches involving the temporary tethers of Hindsgaul,¹⁵⁶⁻¹⁵⁸ Stork,^{184,185} Bols,¹⁸⁷⁻¹⁹² and Ogawa¹⁷⁷⁻¹⁸¹ are the most successful. The approaches involving the permanent tethers either give solely the undesired α -anomer or a mixture of anomers. This is most likely due to the longer length of the permanent tethers, relative to the temporary tethers, which are not as effective in restraining the residues as the temporary tethers that yield only the β -product. In the examples reported by Ziegler¹⁵⁰⁻¹⁵⁵ and Valverde,^{159,160} it might be advantageous to explore tethers of smaller lengths in order to increase stereoselectivity and perhaps have a better chance of an efficient approach to β -mannoside synthesis.

An important observation is that the reactions cited in this review were run at concentrations of 0.07M to as low as 0.003M for more complex glycosylations.¹⁵⁷ As was demonstrated by Schmidt *et al.*,¹⁹⁷ these dilute conditions favor the intramolecular reaction.

3.2: Synthesis of Constrained H-type 2 Trisaccharides

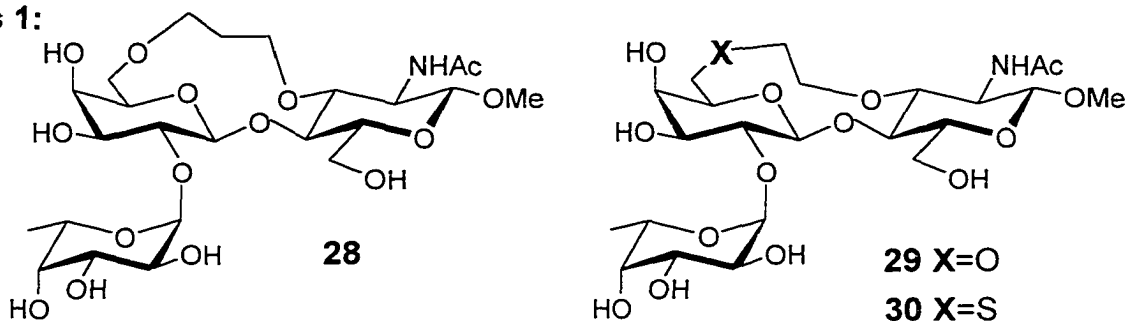
The accumulated literature on the development and application of intramolecular O-glycosylation encouraged us to consider the method for the synthesis of the tethered target trisaccharides **24** and **26**.



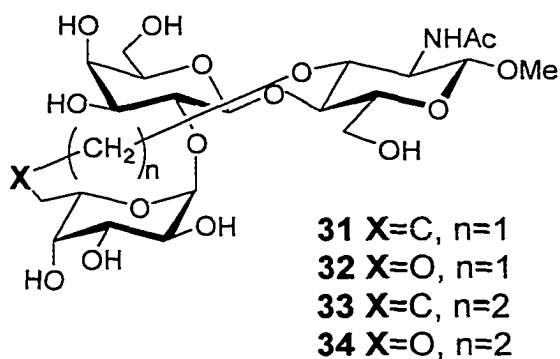
Since the tethers required to restrain the H-type 2 epitope are short (2 to 3 carbons long) it was plausible that these tethers could also aid in establishing the desired stereochemistry of the glycosidic bonds.

From molecular modeling, it was determined that there were three possible versions of molecule **24** which mimic the predicted bound conformation of the native H-type 2 trisaccharide: tethered trisaccharides **28**, **29**, and **30**. It was also found from the molecular modeling that there are four possible versions of molecule **26**, which are suitable pre-organized H-type 2 derivatives: tethered trisaccharides **31**, **32**, **33**, and **34**. Of these constrained H-type 2 derivatives, it was decided to undertake the synthesis of molecules **28**, **29**, and **31**.

Series 1:



Series 2:



Although the tethered trisaccharides from series 2 are very interesting target molecules since they restrain the rotation about two glycosidic bonds, enzyme immunoassay (EIA) results on model compounds (discussed later)

established that tethered trisaccharides **31** and **33** had the most potential to bind to *Ulex europaeus* I. However, the synthesis of these compounds would require chain elongation at the C6 position of fucose and the preliminary EIA results indicated that substitution at this position could cause problems. Therefore the target structures **28** and **29** were given the highest priority.

3.2.1: Synthesis of Constrained H-type 2 Trisaccharide 28

3.2.1a: Strategy

Retrosynthetic analysis of constrained trisaccharide **28** (Figure 3.3) suggested tethering the ethyl thiogalactoside **35** and the 2-acetamido-2-deoxy-glycopyranoside **36** via a 1,3-propanediol (**37**). The order of assembly of these three components may vary. Glycosylation of the two sugars followed by tethering of the disaccharide may be envisioned. A second route to the tethered disaccharide **38**, would involve initial tethering of the two sugars with the 1,3-propanediol linker, followed by an intramolecular glycosylation. The latter was the method of choice, since it has been demonstrated that intramolecular glycosylations generally proceed in high yield,^{150-160,177-185,187-197} whereas, tethering of preassembled oligosaccharides, and formation of large rings, are low yielding processes.¹¹³ In the course of our investigation, a similar strategy for the assembly of different tethered trisaccharides appeared in the literature.^{115,116}

Preliminary computer modeling suggested that even without neighbouring group participation a tethered structure such as **39** would favor the delivery of the galactopyranosyl group from the β -face leading to a β -glycoside. This facial selectivity was initially attributed to a combination of ring strain and a steric mismatch between the 6-O-benzyl and 2'-O-*p*-methoxybenzyl groups. Other groups^{115,116,153} have reported that 'prearranged' molecules favor the formation of one glycosidic form depending on the relative configuration of the tethered donor and acceptor.

protecting group manipulations. Therefore, a thioglycoside was the donor of choice for the glycosylation reactions.

A number of strategies were considered for tethering two monosaccharides prior to intramolecular glycosylation (Figure 3.4). Routes **1a** and **1b** employ monosaccharide 3-hydroxypropyl ethers to displace sulphonate esters from the second monosaccharide residue. Alternatively, route **2** accomplishes the tethering of the two monosaccharides by sequential substitution reactions using a monosaccharide alkoxide as the nucleophile, with the sulphonate leaving group attached to the less hindered tether moiety of the monosaccharide 3-hydroxypropyl ether.

Subsequent steps involving the selective deprotection of the O-2 position of galactose, followed by glycosylation with fucopyranosyl donor **40** and deprotection, would then lead to the desired tethered trisaccharide **28**.

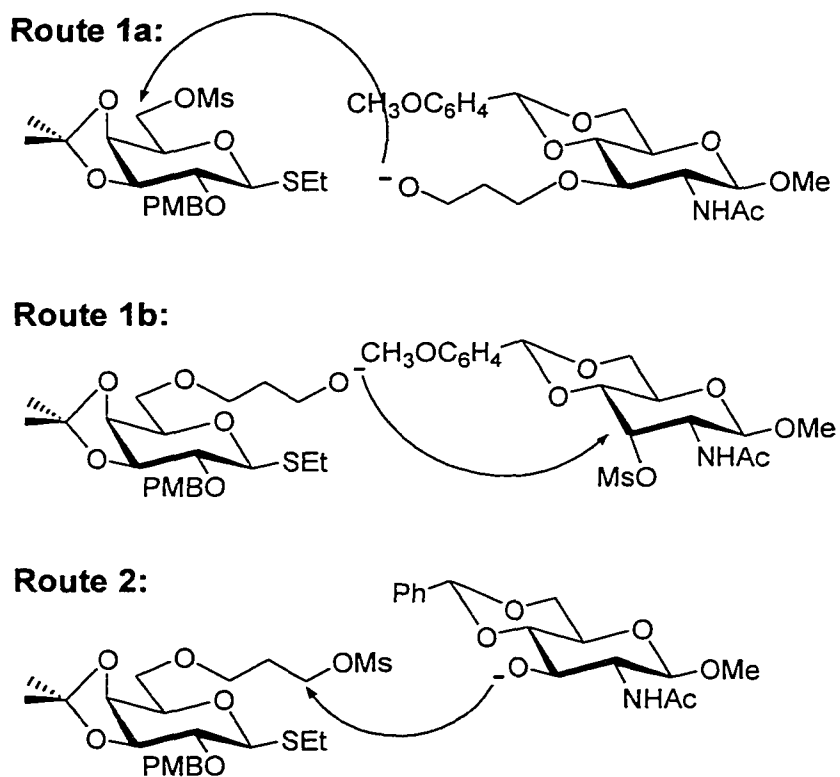
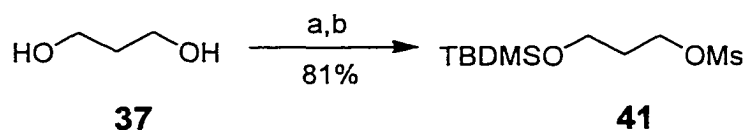


Figure 3.4: Potential strategies for tethering two monosaccharides.

3.2.1b: Preparation of the Linker

The linker synthon **37** was prepared in a one pot synthesis. Treatment of 1,3-propanediol with one equivalent of sodium hydride in THF (Scheme 3.12) followed by addition of *t*-butyldiphenylsilyl chloride¹⁹⁹ gave the corresponding silyl ether which was not isolated. Methanesulphonyl chloride and triethylamine were then added to the desired linker **41** in 81 % yield. Preparation of the linker in two distinct steps leads to lower overall yield, probably due to losses in the purification steps.



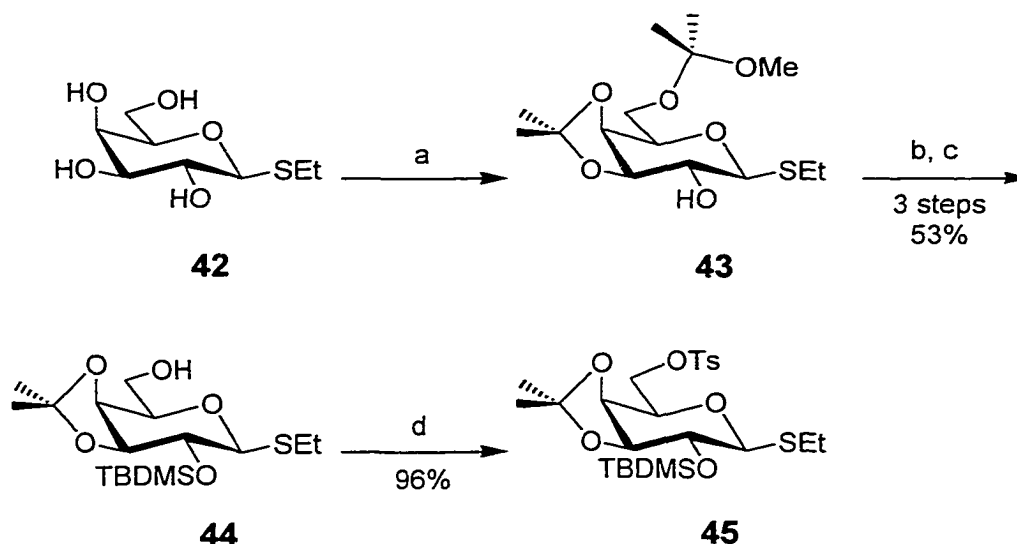
Scheme 3.12: a) NaH, THF, TBDMSCl; b) Et₃N, MsCl.

3.2.1c: Tethering the Monosaccharide Synthons

a) Route 1a

This route involves synthesis of the alkoxide of a 3-hydroxypropyl β-D-*N*-acetylglucosamine ether, which would be employed to displace the sulphonate ester from the galactose monosaccharide residue (see Figure 3.4).

In order to synthesize a galactose donor with two different groups at the O-2 and O-6 position, mixed acetal **43**²⁰⁰ was prepared from thioglycoside **42**²⁰⁰ (Scheme 3.13). This mixed acetal allowed protection of the O-2 position of galactose with the *t*-butyldimethylsilyl group, and then selective removal of the mixed acetal under mild hydrolytic conditions gave monosaccharide **44** in 53% yield.²⁰¹ The toluenesulphonate **45** was then prepared by treating **44** with toluenesulphonyl chloride in dry pyridine.

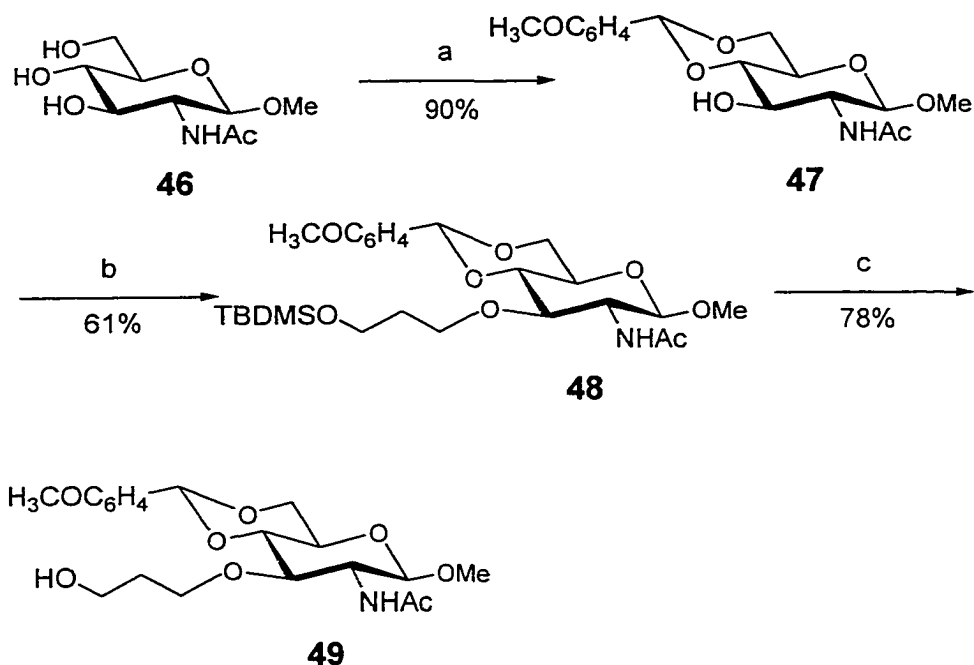


Scheme 3.13: a) $(\text{CH}_3)_2\text{C}(\text{OCH}_3)_2$, TsOH; b) TBDMSCl, NaH, THF; c) H^+ ; d) TsCl, dry pyridine.

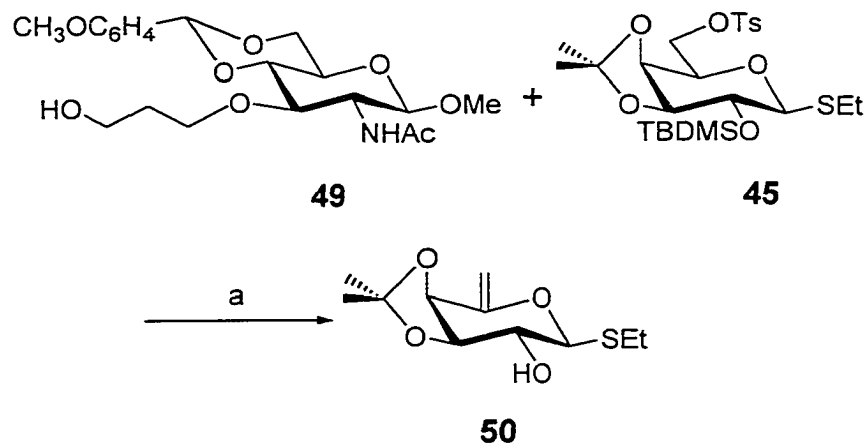
A convenient way to prepare the β -D-N-acetylglucosamine monosaccharide **47** (Scheme 3.14) was found to involve preparing a suspension of **46**^{202,203} (sonication may be needed) in dry acetonitrile, followed by treatment with anisaldehyde dimethyl acetal and a catalytic amount of TsOH. The mixture was stirred overnight, filtered, and washed with acetonitrile, yielding benzylidene acetal **47** (90%).

Reaction of the monosaccharide alkoxide generated from **47** with the linker **41** gave **48** from which the TBDMS protecting group was removed with TBAF in THF (Scheme 3.14).

The linkage of the two monosaccharides was then attempted (Scheme 3.15). Alcohol **49** was treated with NaH in dry DMF, and the toluenesulphonate **45** was added to the mixture. Only elimination product **50** was isolated and no displacement product was observed. As discussed later, this type of result has literature precedent.²⁰⁴



Scheme 3.14: a) $p(\text{CH}_3\text{O})\text{C}_6\text{H}_4\text{CH}(\text{OCH}_3)_2$, TsOH, CH_3CN ;
 b) **41**, NaH, dry DMSO; c) TBAF in THF.



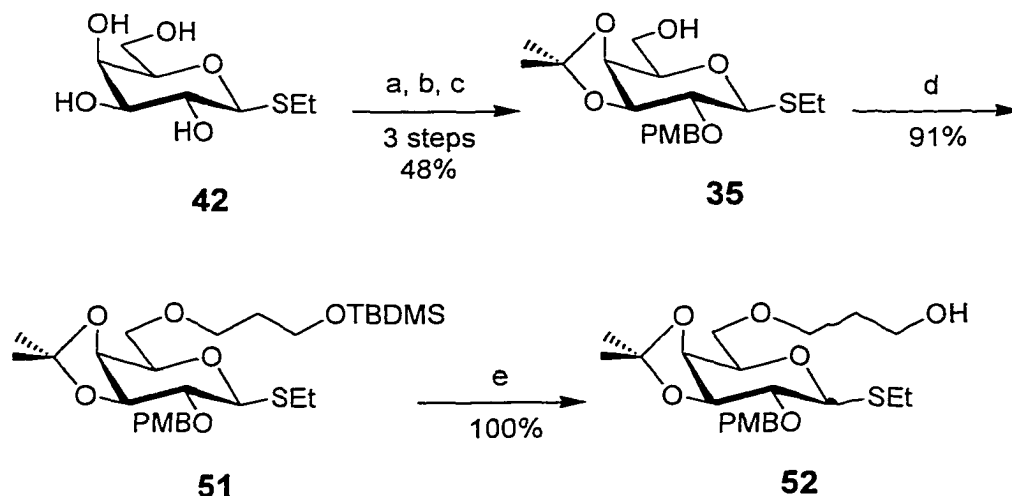
Scheme 3.15: a) NaH, dry DMF.

b) Route 1b

The linkage of the monosaccharides following this route was attempted again, this time by generating the alkoxide of a β -galactopyranoside

monosaccharide 3-hydroxypropyl ether, which would then be employed to displace the sulphonate ester from the *N*-acetylglucosamine residue.

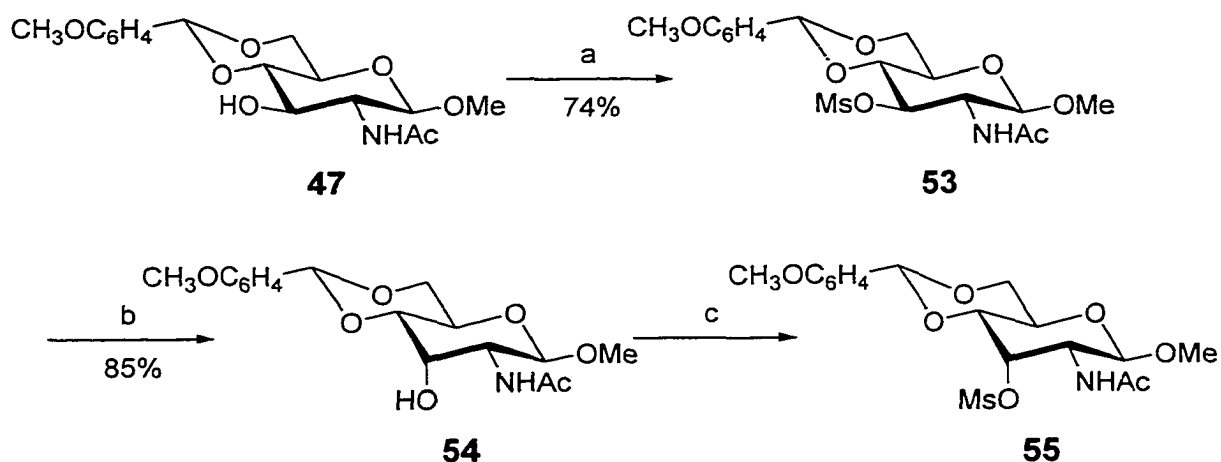
Since a galactose donor with two different groups at the O-2 and O-6 position was still required, the β -galactopyranoside monosaccharide 3-hydroxypropyl ether was also prepared from the mixed acetal **43** described earlier (Scheme 3.16).²⁰⁰ The mixed acetal allowed protection of the O-2 position of galactose with the *p*-methoxybenzyl group, and then selective removal of the mixed acetal under mild conditions of hydrolysis to give monosaccharide **35**.²⁰¹ Reaction of the monosaccharide alkoxide generated from **35** with the linker **41** gave **51** from which the TBDMS protecting group was removed with TBAF in THF.



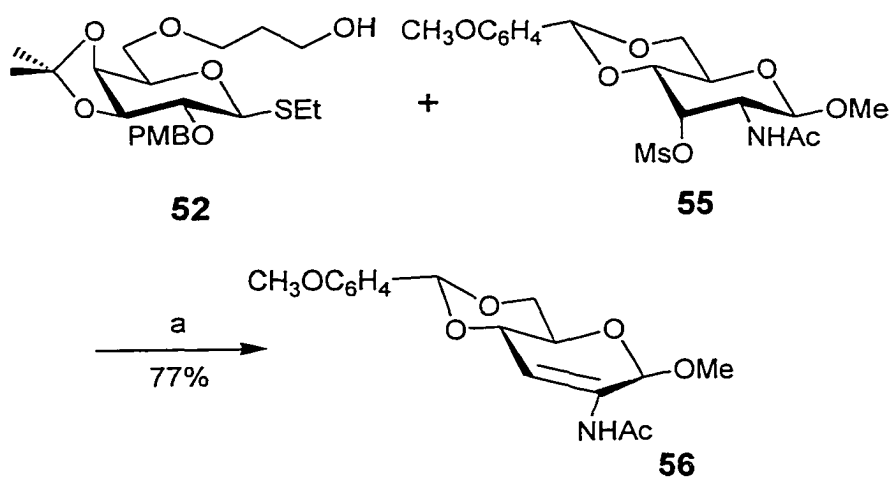
Scheme 3.16: a) $(\text{CH}_3)_2\text{C}(\text{OCH}_3)_2$, TsOH; b) PMBCl, NaH, DMF; c) H^+ ; d) NaH, TBDMSO $(\text{CH}_2)_3\text{OTs}$, THF; e) TBAF, THF.

Since the displacement on the "*N*-acetylglucosamine" residue involves a secondary position, inversion of configuration would occur at C3. In order to obtain the *N*-acetylglucosamine structure after the $\text{S}_{\text{N}}2$ reaction, the sulphonate ester of the *N*-acetylglucosamine residue was used (Scheme 3.17). The benzylidene acetal **47** was sulphonated,²⁰⁵ and then treated with NaOAc

and water in 2-methoxyethanol by following the procedure reported by Jeanloz²⁰⁶ for the synthesis of the corresponding methyl 2-acetamido-2-deoxy-4,6-O-*p*-methoxybenzylidene- β -D-allopyranoside. The product **54** was then sulphonated to give the sulphonate ester **55**.²⁰⁶



Scheme 3.17: a) MsCl, NEt₃, CH₂Cl₂; b) NaOAc, H₂O, CH₃OCH₂CH₂OH, 118°C; c) MsCl, NEt₃, CH₂Cl₂.



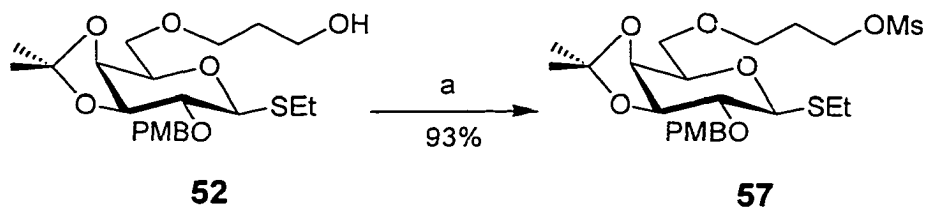
Scheme 3.18: a) NaH, dry DMF.

The linkage of the monosaccharides was attempted again by treating **52** with NaH in DMF, to generate the alkoxide, and adding the sulphonate **55**. Again, only the elimination product was observed (Scheme 3.18).

c) Route 2

As described above, route **1** (**1a** and **1b**) led to elimination products. In route **1a**, it was seen that even primary sulphonates of galactose are notoriously resistant to nucleophilic displacements. This has been discussed in the literature,²⁰⁵ and has been attributed to unfavorable interaction between the incoming nucleophile and the axial substituent at C4, which sterically and/or electronically hinders attack at the C6 position. In route **1b**, linkage was unsuccessful, since a S_N2 reaction was attempted on a secondary ring carbon, on which displacement is even more disfavored and complicated by inversion of configuration. Consequently, the tethered molecule **39** (Figure 3.3) was approached by a sequence of nucleophilic substitution reactions using a monosaccharide alkoxide as the nucleophile, with the sulphonate leaving group attached to the tether moiety.

The first nucleophilic substitution reaction occurs in the synthesis of galactose donor **51** (Scheme 3.16) which, after conversion into sulphonate **57** (Scheme 3.19), is followed by a second nucleophilic substitution reaction to give the target linked monosaccharides **39** (Scheme 3.20).

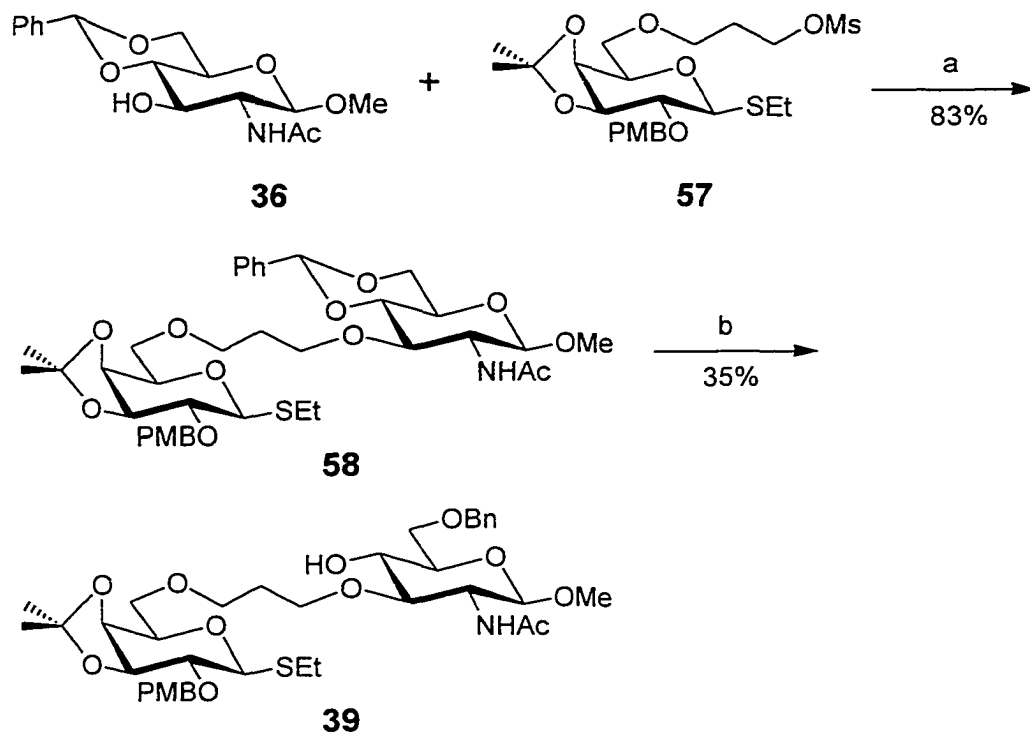


Scheme 3.19: a) MsCl, NEt₃, CH₂Cl₂.

The coupling of the sugars was executed in dry THF. Once the alkoxide of **36**²⁰⁷ was formed, and after the addition of sulphonate **57**, a few

drops of DMSO were added. The tethered compound **58** was obtained in 83% yield (Scheme 3.20). DMSO facilitates a faster reaction presumably by dissociation of the sodium alkoxide ion pair of **36**.

In practical terms, this was the route which provided the only feasible means by which the two monosaccharide synthons could be tethered via an S_N2 reaction prior to intramolecular glycosylation.



Scheme 3.20: a) NaH, THF, DMSO; b) NaCNBH₃, HCl in ether, 3 Å MS, THF.

Reductive opening of the benzylidene acetal with sodium cyanoborohydride and hydrochloric acid in ether and THF gave compound **59** in poor yield (36%) presumably due to the acid sensitivity of the PMB group and the ability of the acetamide to undergo reductive ring opening. Intermediate **39**, possessing both a donor site and an acceptor site, is set up to undergo intramolecular glycosylation.

The structure of **39**, as well as its acetylated derivative (**39-OAc**), was verified by one dimensional $^1\text{H-NMR}$, two dimensional GCOSY and HMQC experiments. The acetylated derivative showed the predicted downfield shift of the resonance for the H4' of *N*-acetylglucosamine (Figure 3.5). [It should be noted that due to the naming protocol for compounds **58** and **39**, the formal reducing residue (GlcNAc) is designated by *prime*. This is the reverse of the normal convention of oligosaccharides, where the non-reducing sugar residue is primed. This convention is followed for all tethered monosaccharides.]

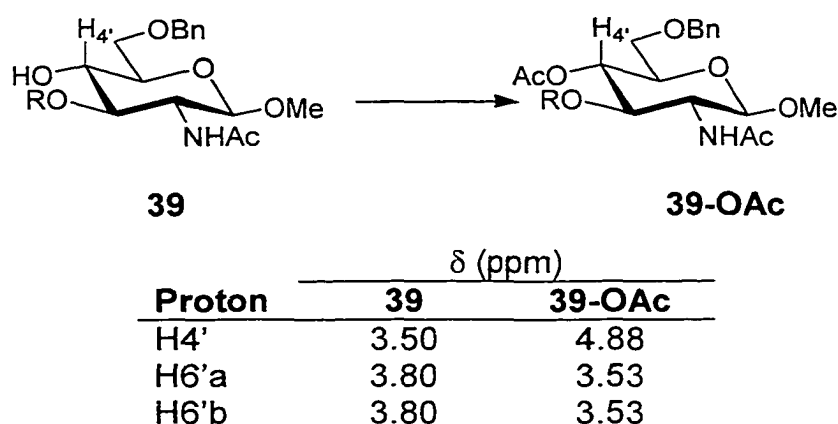
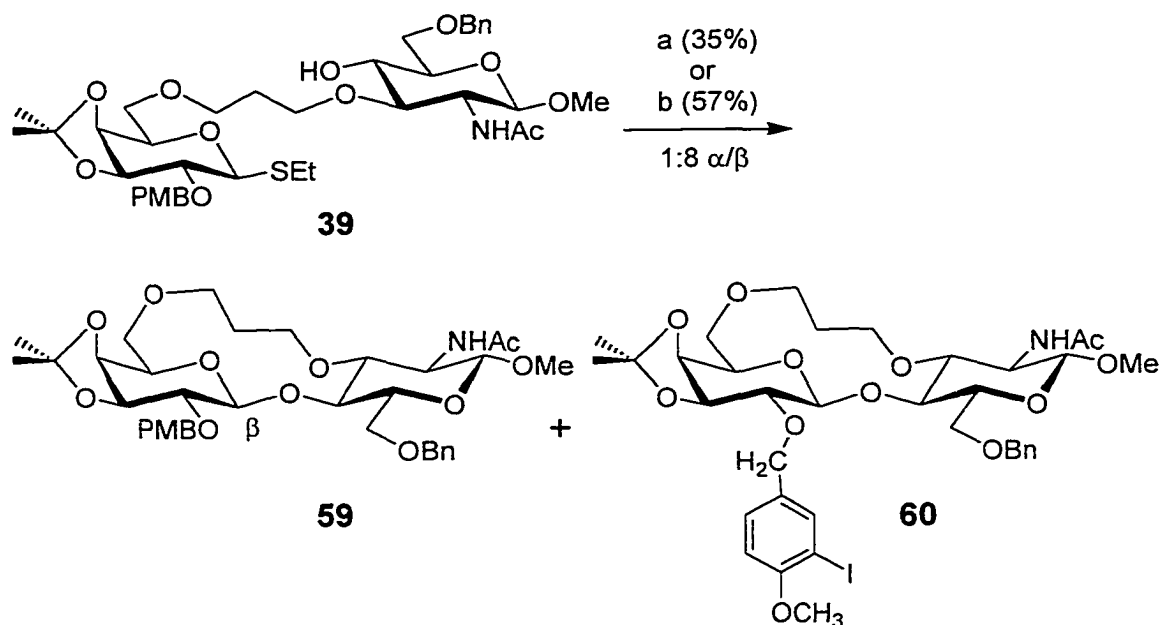


Figure 3.5: Confirmation of the regioselectivity of the benzylidene acetal reductive ring opening.

3.2.1d: Intramolecular Glycosylation

Two methods of activation were investigated for the intramolecular glycosylation of **39** (Scheme 3.21). The first method, which uses NIS and silver triflate, gave a glycosylation product **59** in low yield (35%). However, this was accompanied by partial iodination of the *p*-methoxybenzyl group (**60**), a fatal side reaction since the iodinated PMB group was found to be stable to DDQ oxidation. The second method of glycosylation using MeOTf and DTBMP resulted in a higher yield, 57%, and an α/β ratio of 1:8 was observed.

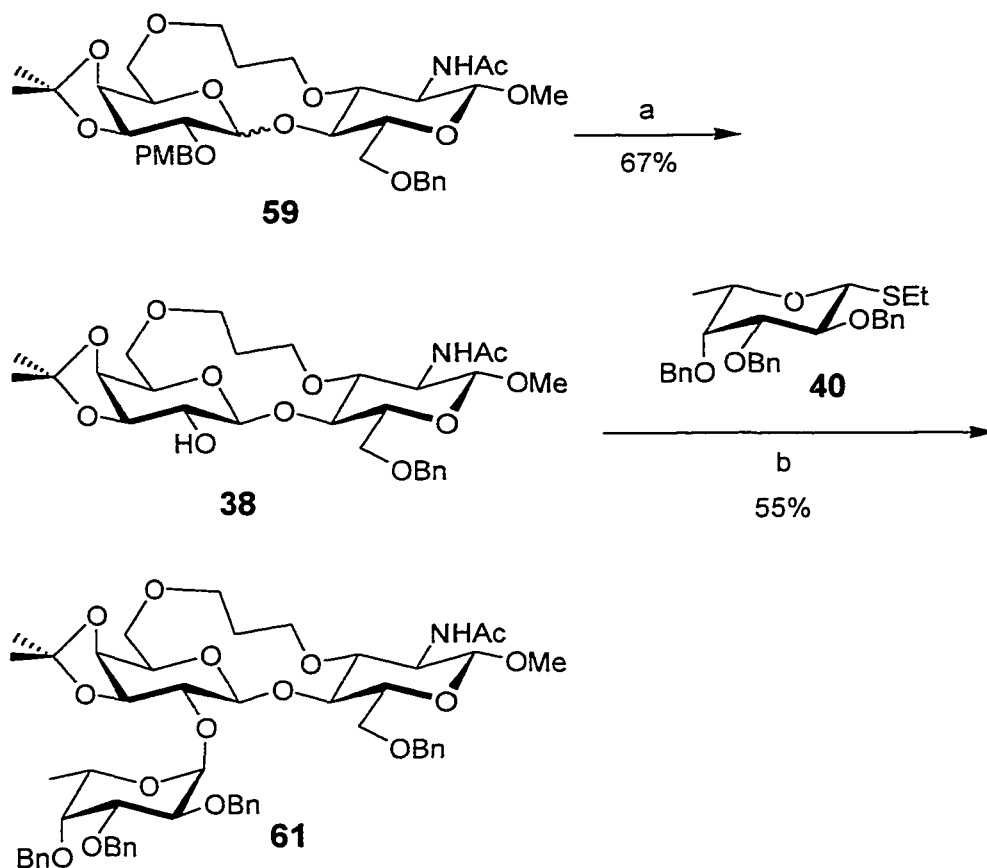


Scheme 3.21: a) AgOTf, NIS, 4 Å MS, CH₂Cl₂;
 b) MeOTf, 4 Å MS, DTBMP, CH₂Cl₂.

The structure of the desired β -product **59**, though not completely free of the α -anomer, was verified by one dimensional ¹H-NMR, two dimensional GCOSY and HMQC experiments. The proton ³J_{1',2'} (8.4 Hz) and ¹J_{C1',H1'} (158.7 Hz) coupling constants of H1' of galactose and the C1' chemical shift ($\delta_{C1'} = 104.3$ ppm) are all indicative of the β -product. T-ROESY and HMBC experiments verified that the desired 1'→4 bond had been formed.

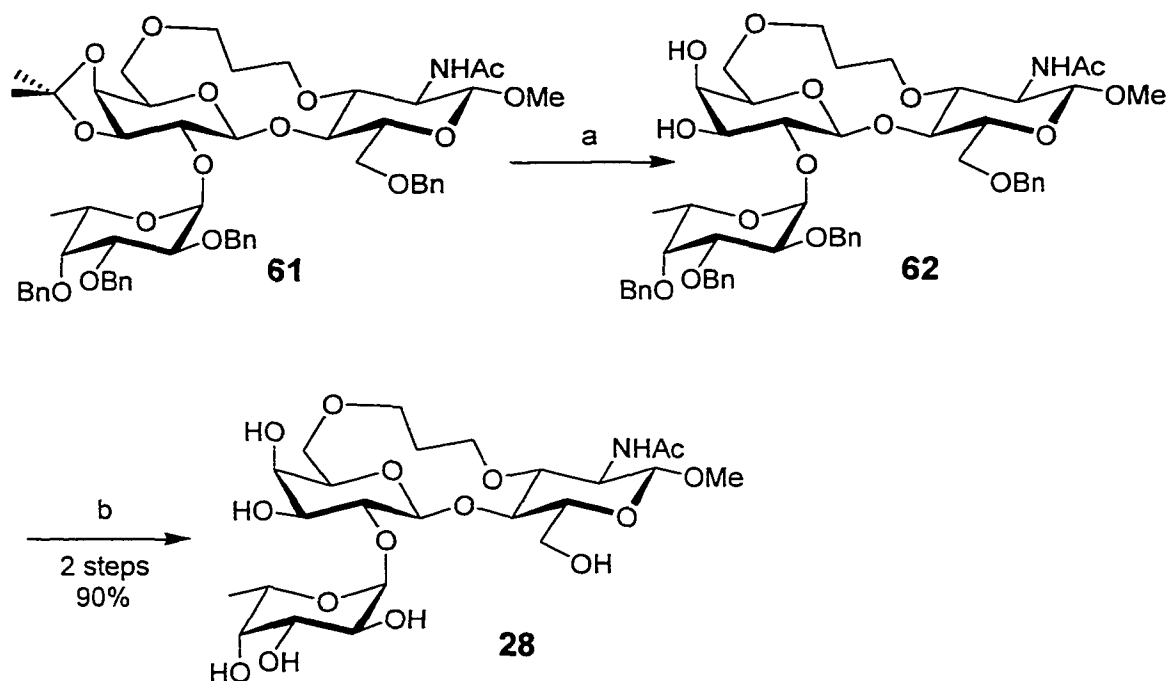
3.2.1e: Assembly and Deprotection of the Tethered Trisaccharide

The α/β mixture of tethered disaccharide **59** was subjected to selective deprotection with DDQ to give **38** in 67% yield (Scheme 3.22), accompanied by partial loss of the isopropylidene acetal. At this stage, the successful separation of the α/β -mixture of **38** was achieved. The disaccharide acceptor **38** was glycosylated by the fucose thioglycoside **40**²⁰⁸ which was activated by dimethyl(methylthio)sulfonium triflate (DMTST). This gave the tethered trisaccharide **61** in 55 % yield.



Scheme 3.22: a) DDQ, CH₂Cl₂, H₂O; b) DMTST, 4 Å MS, DTBMP, CH₂Cl₂.

The protected tethered trisaccharide **61** was then deprotected by hydrolysis of the acetal, followed by hydrogenolysis of the benzyl groups to give the tethered H-type 2 trisaccharide **28** in 90% yield over two steps (Scheme 3.23).



Scheme 3.23: a) 90% AcOH 65°C; b) H₂, Pd(OH)₂/C, EtOH.

3.2.2: Synthesis of Constrained H-type 2 Trisaccharide 29

The synthesis of tethered trisaccharide **29** was achieved by means of a sequence similar to that described for compound **28**, involving sequential substitution reactions using a monosaccharide alkoxide as the nucleophile, with the sulphonate leaving group attached to the tether moiety of the monosaccharide ether.

In the synthesis of **28**, several problems were encountered in the reductive opening of the benzylidene ring using sodium cyanoborohydride and HCl in dry ether. In that instance, a PMB protecting group was found to be too acid labile for the reaction conditions and, at times, ring opening of the isopropylidene was also observed.

In an attempt to circumvent these problems, the galactose donor was modified (Figure 3.6) by replacing the offending PMB group by the acid stable allyl group and the isopropylidene group by two benzyl groups. This modified

galactose donor was later used in the synthesis of the three-carbon tethered trisaccharide **28**.

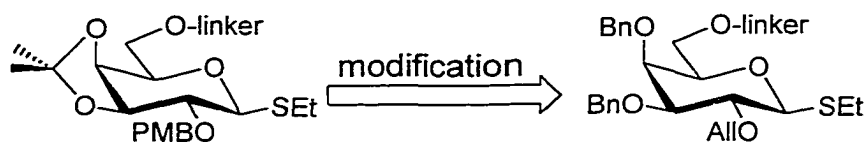
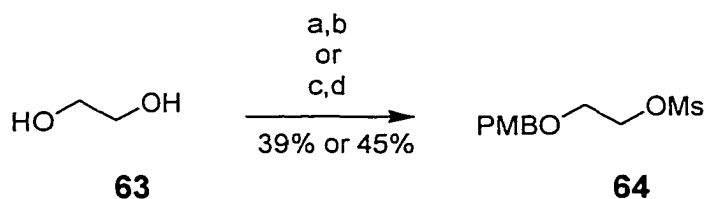


Figure 3.6: Modified galactose donor.

3.2.2a: Preparation of the Linker

Starting from ethylene glycol (**63**), two one pot syntheses of linker **64** were explored (Scheme 3.24). The first involved treatment of 1,2-ethanediol with one equivalent of sodium hydride in THF followed by addition of *p*-methoxybenzyl chloride (cf. synthesis of **41**). Methanesulphonyl chloride and triethylamine were then added to the reaction mixture, which gave the desired linker **64** in 39 % yield. In retrospect, since it is known that the monosilylation of **63** is a high yield reaction (82%)¹⁹⁹ and that ethylene glycol tends to have a very high water content, the reason for the low yield of linker **64**, compared to that of linker **41**, is most likely due to the fact that no steps were taken to dry the ethylene glycol.



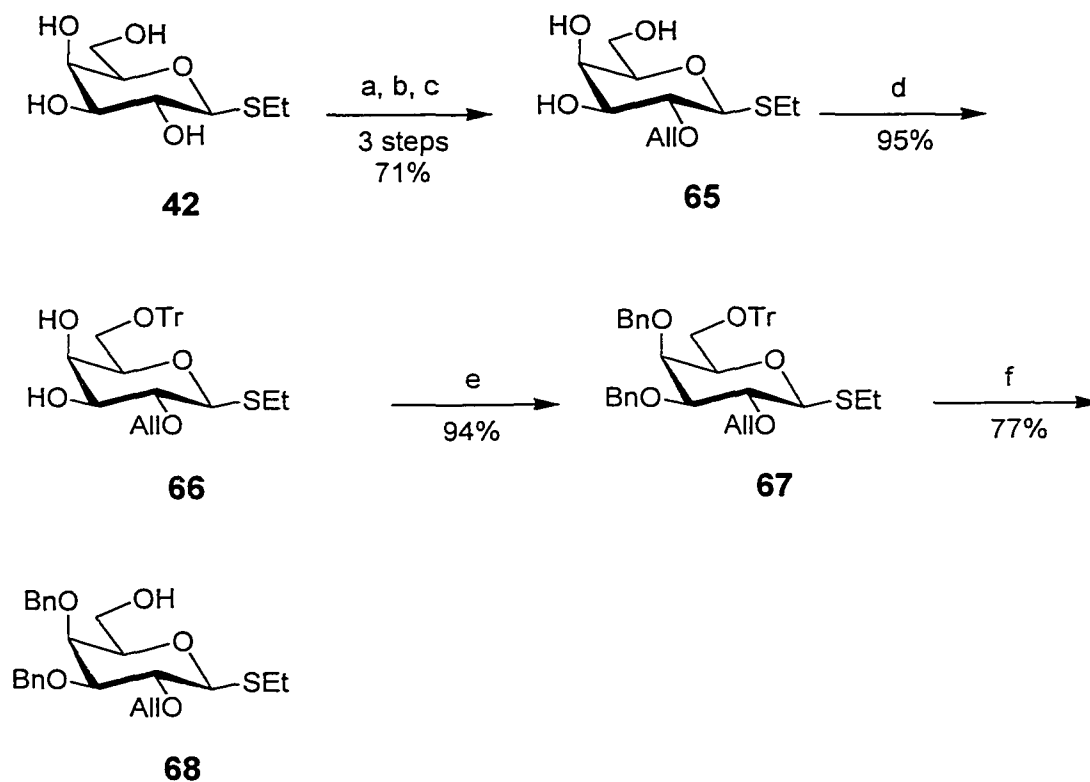
Scheme 3.24: a) NaH, PMBCl in THF; b) NEt₃, MsCl;
 c) Bu₂SnO, PMBCl, Bu₄NI in toluene;
 d) NEt₃, MsCl in CH₂Cl₂.

The second method involved refluxing a suspension of **63** and dibutyltin oxide in toluene, with removal of water (Dean Stark trap) until the

solution becomes clear.²⁰⁹ The solution was concentrated, and the resulting stannylene was treated with *p*-methoxybenzyl chloride, tetrabutylammonium iodide and refluxed overnight. After removal of solvent, the resulting alcohol was sulphonated to give **64** in 45% overall yield. Again, since the actual amount of diol **63** used in the reaction is unknown, due to water content, the above yield may actually be higher.

3.2.2b: Preparation of the Galactose Donor

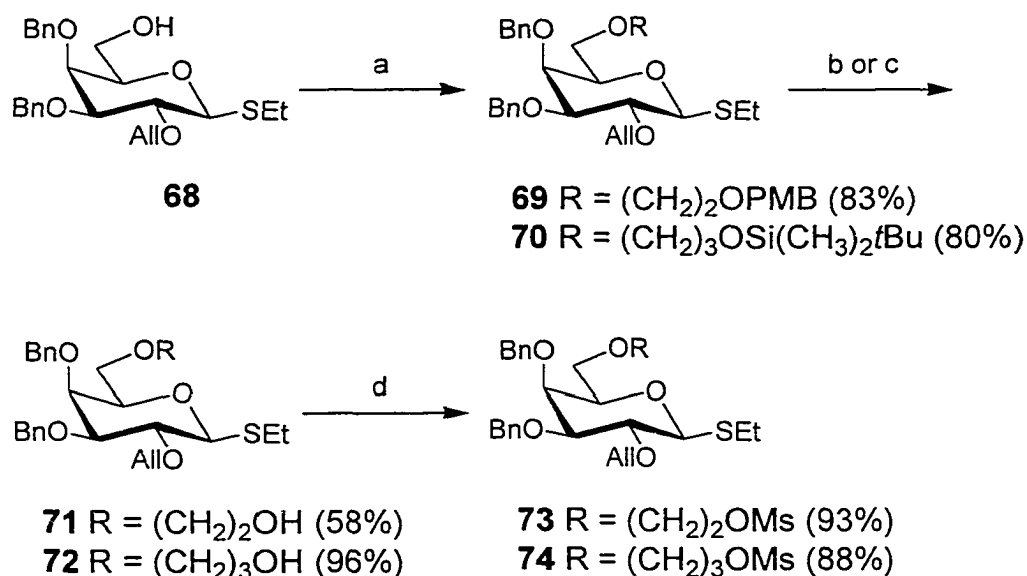
Allylation of the O-2 position of galactose was achieved by selective protection of positions O-3, O-4, and O-6 (mixed acetal **43**,²⁰⁰ Scheme 3.13) followed by treatment with NaH and allyl bromide (Scheme 3.25).



Scheme 3.25: a) $(\text{CH}_3)_2\text{C}(\text{OCH}_3)_2$, TsOH; b) NaH, AlIBr, THF; c) H^+ ; d) TrCl, dry pyridine; e) NaH, BnBr, DMF; f) H^+ .

Hydrolysis of the acetals gave thioglycoside **65**²⁰⁰ in 71% yield from starting material **42**. The primary hydroxyl was then selectively protected with a trityl group, followed by benzylation of the remaining hydroxyl groups. The removal of the trityl group under conditions of hydrolysis liberated the C6 position for tethering.

Reaction of the monosaccharide alkoxide generated from **68** with linker **64** gave the *p*-methoxybenzyl ether **69**, and with linker **41** gave silyl ether **70** (Scheme 3.26). Compounds **69** and **70** were then deprotected, yielding alcohols **71** and **72**, respectively. These alcohols were converted into the corresponding sulphonates by treatment with methanesulphonyl chloride to yield **73** and **74**.



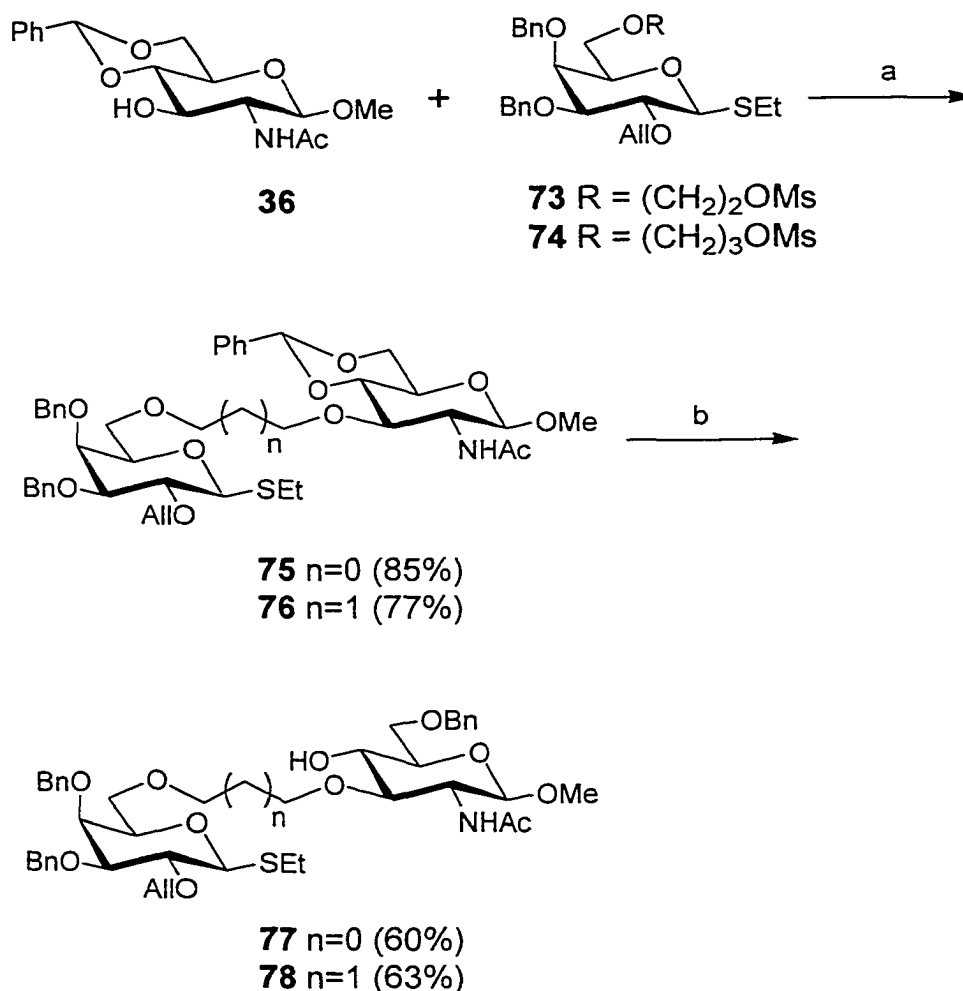
Scheme 3.26: a) NaH, THF, **64** or **41**; b) DDQ, H₂O in CH₂Cl₂;
 c) TBAF in THF; d) NEt₃, MsCl in CH₂Cl₂.

3.2.2c: Tethering the Monosaccharide Synthons

Coupling of the monosaccharides was executed as described earlier (cf. section 3.2.1d – route **2**). Methanesulphonate **73** was added to the alkoxide of **36**, in the presence of DMSO, yielding tethered product **75** (85%)

(Scheme 3.27). Reductive opening of the benzylidene acetal with sodium cyanoborohydride and hydrochloric acid in ether and THF gave compound **77** in 60% yield, an improvement over that obtained previously (cf. Scheme 3.20). These steps were repeated for methanesulphonate **74**, with a similar improvement in yield (65%).

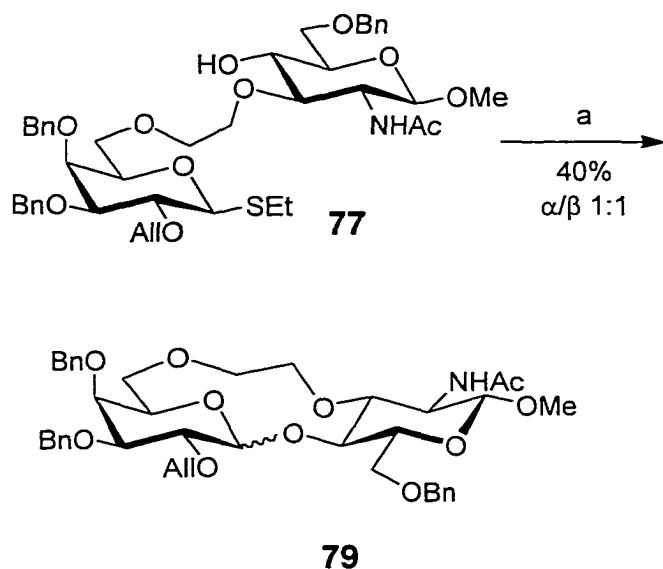
Intermediates **77** and **78**, both possessing a donor site (thioglycoside moiety) and an acceptor site (free hydroxyl), are setup to undergo an intramolecular glycosylation. Their structures, as well as that of their acetylated derivatives were verified by one dimensional $^1\text{H-NMR}$, two dimensional GCOSY and HMQC experiments (cf. Figure 3.5).



Scheme 3.27: a) NaH, DMSO; b) NaCNBH₃, HCl in Et₂O, 3 Å MS.

3.2.2d: Intramolecular glycosylations

Different methods of activation were tried for the intramolecular glycosylation of **77** (Scheme 3.28), and are summarized in Table 3.1. Although a reasonable yield could be obtained by activation with NIS (entry 4), the reaction proceeded with no selectivity and the α,β anomers were inseparable by chromatography. These results will be discussed in section 3.3.3.



Scheme 3.28: a) NIS, AgOTf and 4 Å MS in CH₂Cl₂.

Table 3.1: Summary of the different activation methods used in the glycosylation of compound **77**.

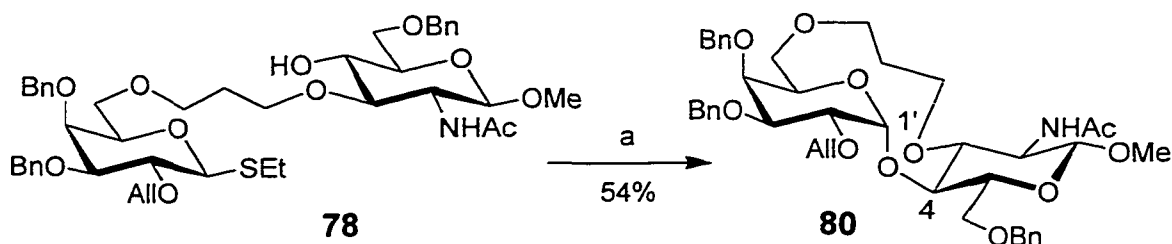
Entry #	Activator	Yield (%)	% β^a
1	MeOTf	14	>98
2	DMTST	22	>98
3	NIS, AgOTf, rt	19	>98
4	NIS, AgOTf, 0°C	40	50

^aPercent β were determined by NMR.

The structure of the tethered β -glycoside **79**, though not completely free of the α -anomer, was verified by one dimensional ¹H-NMR, two dimensional GCOSY and HMQC experiments. The homonuclear ³J_{1,2} (7.8

Hz) and heteronuclear $^1J_{C1',H1'}$ (158.6 Hz) coupling constants of H1' of galactose and the C1' chemical shift ($\delta_{C1'} = 104.3$ ppm) confirmed the structure of the β -product **79**. A T-ROESY experiment verified the position of the glycosidic linkage.

The intramolecular glycosylation of the three carbon tethered molecule **78** was performed using methyltriflate and 2,6-di-*t*-butyl-4-methylpyridine and resulted in a higher yield, 54%, but surprisingly, only the α -disaccharide was obtained (Scheme 3.29).

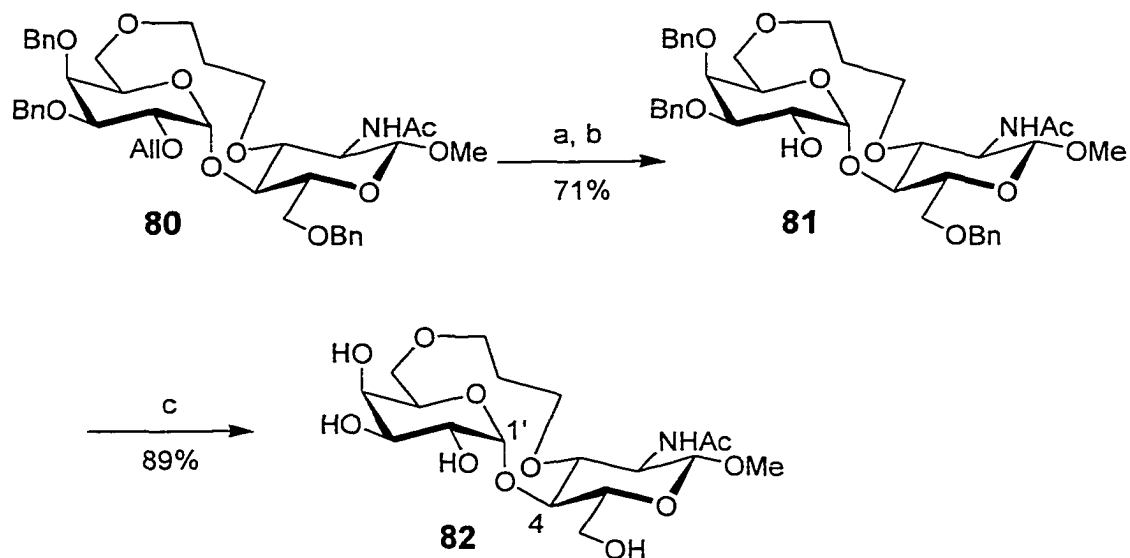


Scheme 3.29: a) MeOTf, DTBMP and 4 Å MS in CH_2Cl_2 .

The structure of the tethered glycoside **80** was verified by one dimensional 1H -NMR, two dimensional GCOSY and HMQC experiments (cf. Table 3.1). The homonuclear $^3J_{1',2'}$ coupling constant was not obtained due to peak overlap. The $^1J_{C1',H1'}$ coupling constant (165.3 Hz) of galactose and the C1' chemical shift ($\delta_{C1'} = 92.8$ ppm) gave results suggesting the α -anomer was obtained. In order to further confirm this finding, the O-2' position of tethered disaccharide **80** was deprotected (Scheme 3.30) by first treating with potassium *t*-butoxide in dimethylsulphoxide to isomerize the allyl group, followed by hydrolysis of the vinyl ether to obtain intermediate **81**. Characterization of product **81** showed $^3J_{1',2'} = 3.8$ Hz, $^1J_{C1',H1'} = 166.0$ Hz, and $\delta_{C1'} = 93.8$ ppm thus confirming that the α -product was indeed obtained.

Further deprotection by hydrogenation over 20% palladium hydroxide on charcoal gave tethered disaccharide **82** (Scheme 3.30). The $^3J_{1',2'}$ (3.1 Hz) and $^1J_{C1',H1'}$ (165.5 Hz) coupling constants and C1' chemical shift ($\delta_C = 94.6$

ppm) obtained from 1D $^1\text{H-NMR}$ and HMQC experiments for **82** were again consistent with the presence of the α -anomer. During interpretation of the T-ROESY and HMBC spectra (in CD_3OD) to establish that the $1' \rightarrow 4$ linkage had been formed, it was noted that the expected H1'/H4 NOE was significantly reduced. This implied that the glycosidic bond had adopted the anti-conformation. Further discussion of this result will be made in Chapter 5.



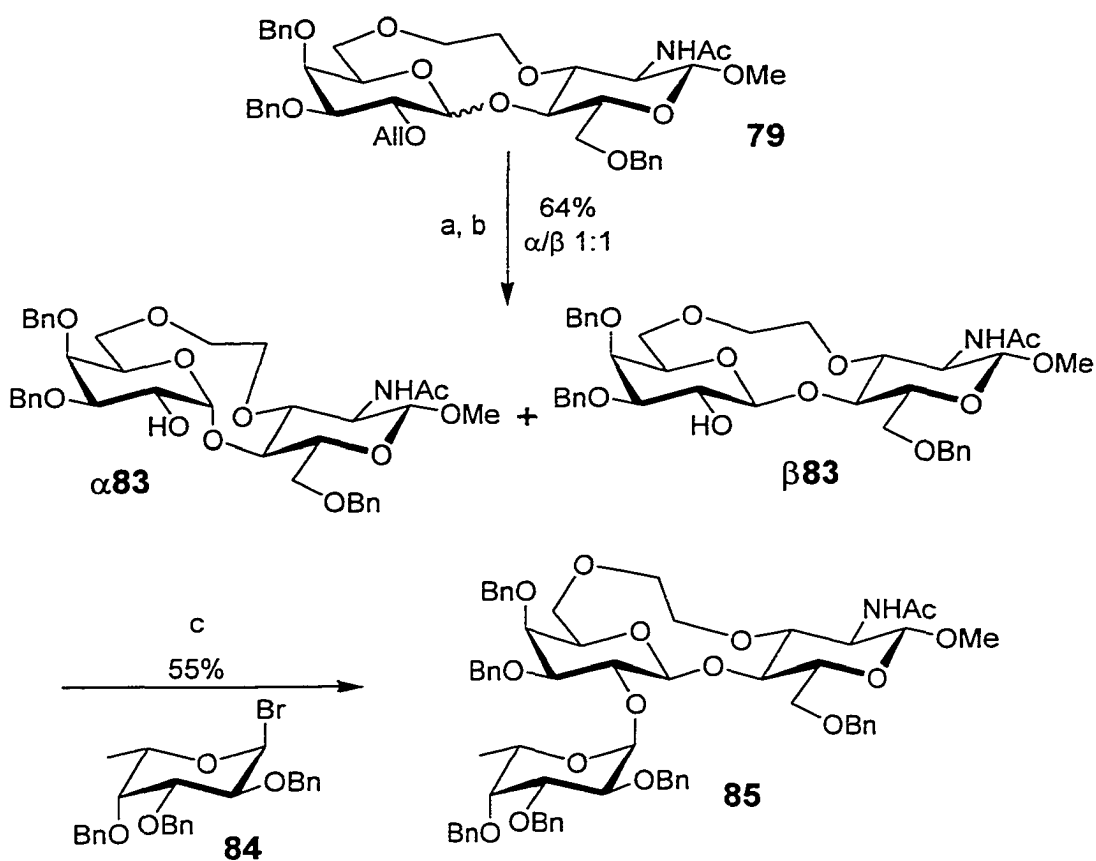
Scheme 3.30: a) $t\text{-BuOK}$, DMSO; b) H^+ ; c) H_2 , $\text{Pd}(\text{OH})_2/\text{C}$, EtOH.

3.2.2e: Assembly and Deprotection of the Tethered Trisaccharide

The α/β mixture of tethered disaccharide **79** was subjected to selective deprotection by base isomerization of the allyl ether ($t\text{-BuOK}$ in DMSO), followed by hydrolysis of the vinyl ether to obtain disaccharide **83** in 64% yield (Scheme 3.31). At this point the α/β mixture could be separated by chromatography.

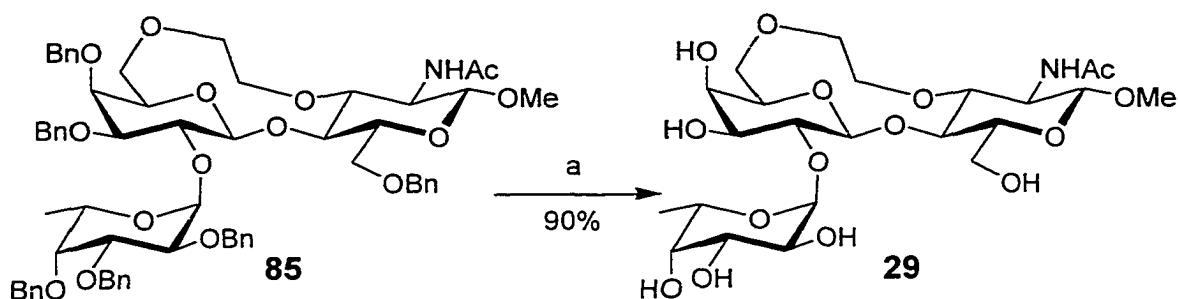
The disaccharide acceptor β **83** was glycosylated by the fucopyranosyl bromide **84** using halide-ion catalyzed glycosylation.¹⁴⁸ At typical reaction concentrations, the glycosylation was extremely slow and would not go to completion. Upon concentration, the reaction rate noticeably increased,

giving tethered trisaccharide **85** in 55 % yield with complete consumption of the acceptor.



Scheme 3.31: a) *t*-BuOK, DMSO; b) H^+ ; c) Bu_4NBr , DTBMP, DMF and 4 Å MS in CH_2Cl_2 .

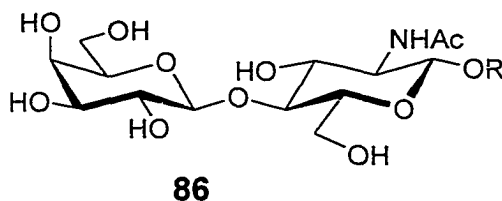
The protected tethered trisaccharide **85** was then deprotected by hydrogenolysis of the benzyl groups to give the tethered H-type 2 trisaccharide **29** in 90% yield (Scheme 3.32).



Scheme 3.32: a) H₂, Pd(OH)₂/C, EtOH.

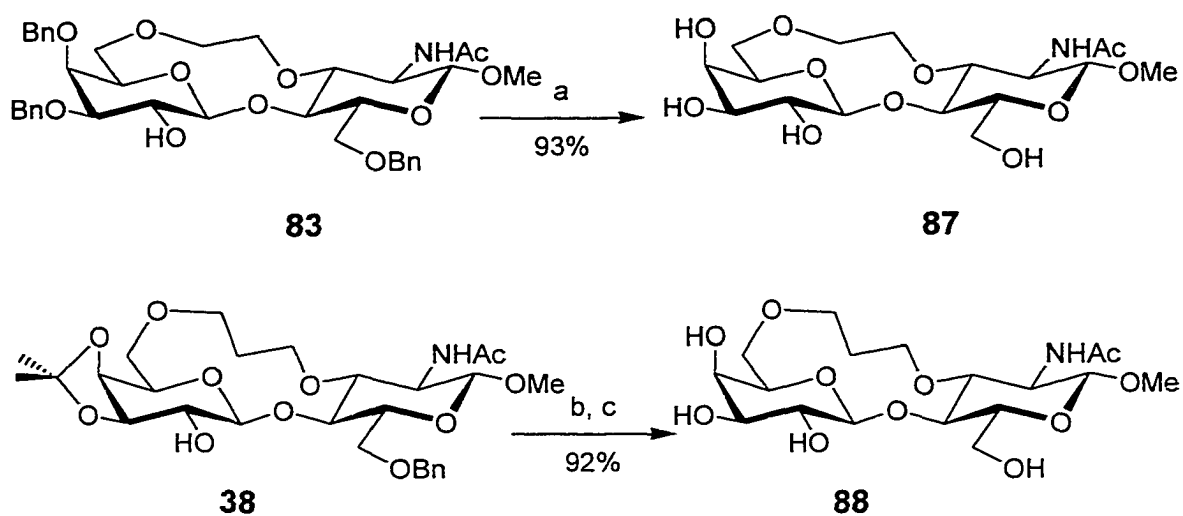
3.2.3: Synthesis of Lactosamine Derivatives

Erythrina corallodendron lectin is found to have an affinity for lactosamine **86**, therefore the tethered derivatives **87** and **88** were prepared.

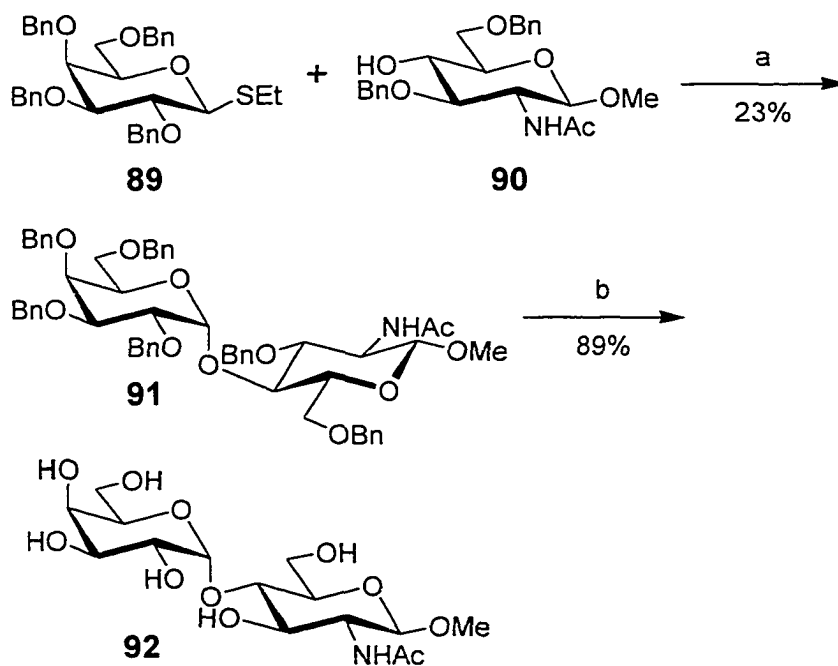


Tethered disaccharides **87** and **88** were obtained, respectively, by hydrogenation of **83**, or hydrolysis and hydrogenation of intermediates **38** (Scheme 3.33). The constrained disaccharides **87** and **88** were to be tested for activity with *Erythrina corallodendron* lectin.³⁰

α -Lactosamine was synthesized for use in NMR studies of tethered α -disaccharide **82**. Thioglycoside **89**,²¹⁰ activated with NIS and silver triflate, was glycosylated with *N*-acetylglucosamine **90**²¹¹ to give α -disaccharide **91** (Scheme 3.34). After deprotection by hydrogenation, α -lactosamine **92** was obtained in an overall yield of 20%.



Scheme 3.33: a) H_2 , $\text{Pd}(\text{OH})_2/\text{C}$, EtOH; b) H^+ ; c) H_2 , $\text{Pd}(\text{OH})_2/\text{C}$, EtOH.

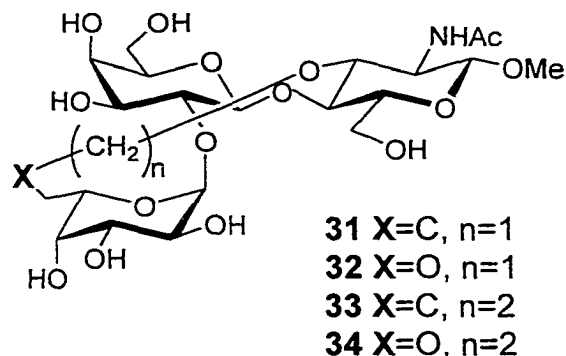


Scheme 3.34: a) NIS, AgOTf in CH_2Cl_2 ; b) H_2 , $\text{Pd}(\text{OH})_2/\text{C}$, EtOH.

3.2.4: Influence of Substituents at C6 of Fucose on Binding to *Ulex*

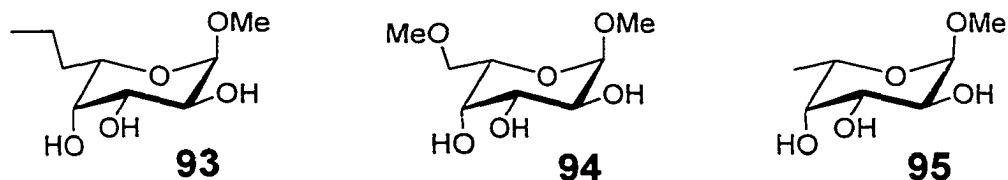
Computer modeling confirmed that tethered trisaccharides **31** to **34** were possible mimics of native H-type 2 trisaccharide.

Series 2:



From Lemieux's mapping studies of H-type 2 trisaccharide,^{103,121,125} it was found that there is a required hydrophobic interaction between the *Ulex* lectin²⁷ and C6 of fucose. It was therefore uncertain what would be the effect of having an ether linkage or an extended carbon chain emanating from the C6 position of fucose. To the best of our knowledge, there are no studies on the effects of substituents at that position on the binding of H-type 2 trisaccharide to the *Ulex* lectin.

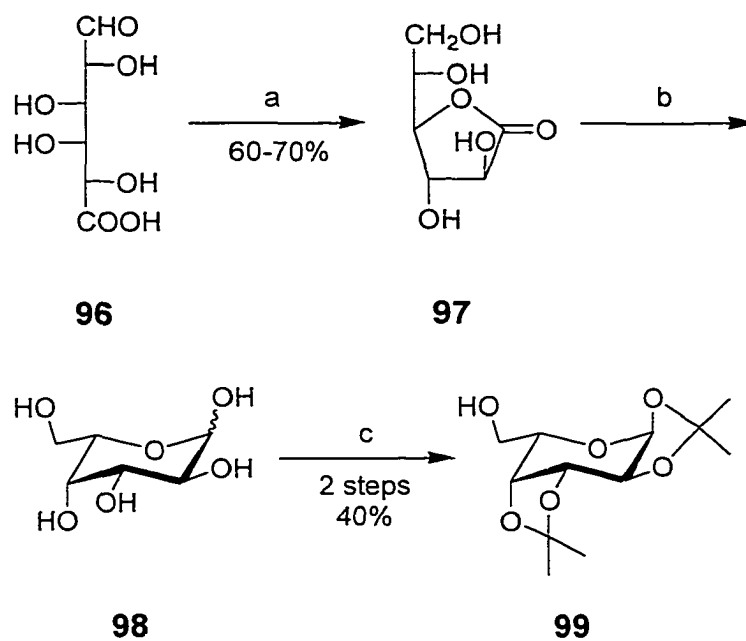
The following model study was then performed: fucose analogues were synthesized in order to determine if any of these modifications at C6 would hinder the binding with *Ulex*. Fucose derivatives **93** and **94** were synthesized and their biological activities relative to methyl- α -L-fucopyranoside (**95**) were determined by solid phase immunoassay with the *Ulex europaeus* I lectin.²⁷



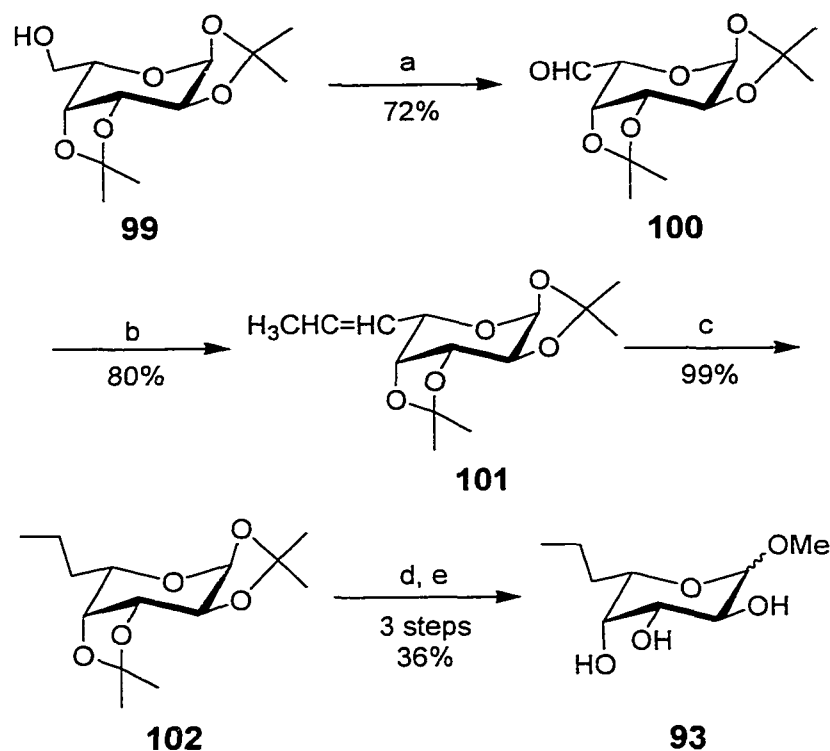
3.2.4a: Preparation of Fucose Derivative 93

The synthesis of fucose derivative **93** commences with galacturonic acid (**96**) (Scheme 3.35), which was converted into L-galactose (**98**) by following literature procedures²¹² involving two consecutive reductions with sodium borohydride (NaBH_4). The first NaBH_4 treatment reduces the aldehyde (C1), while the second reduces the lactone **97** to the corresponding lactol **98**. The hydroxyl at C6 was then differentiated from the others by conversion to the 1,2,3,4-di-O-isopropylidene- α -L-galactose **99**.²¹³

Alcohol **99** was oxidized to aldehyde **100** via Swern oxidation²¹⁴ (Scheme 3.36), followed by carbon homologation by a Wittig reaction,^{215,216} and hydrogenation.



Scheme 3.35: a) NaBH_4 , H_2O , $\text{pH}=7.0$; b) NaBH_4 , amberlite-IR-120(H^+), $\text{pH}\leq 6.0$; c) $(\text{CH}_3)_2\text{CO}$, H^+ , anhyd CuSO_4 .

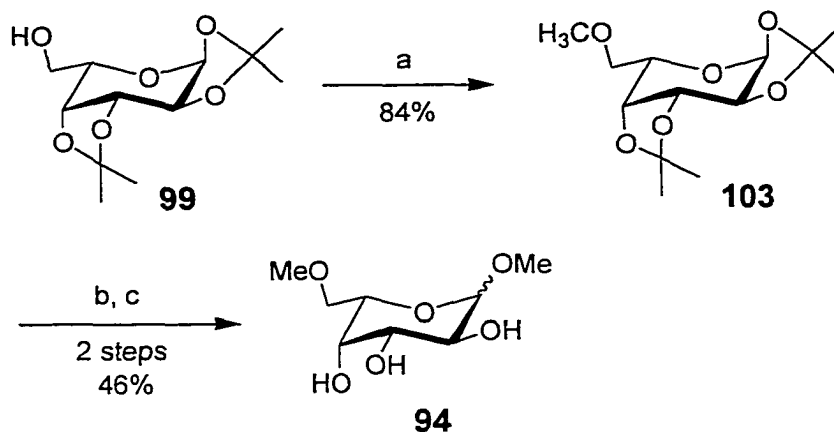


Scheme 3.36: a) Swern oxidation; b) $\text{Ph}_3\text{PCH}_2\text{CH}_3\text{Br}$,²¹⁷ NaH , TDA-1 in THF; c) H_2 , Pd/C; d) H_2O , H^+ at 80°C ; e) MeOH , H^+ .

A phase transfer catalyst, tris[2-(2-methoxyethoxy)ethyl]amine (TDA-1), was used to improve the yield of the Wittig reaction by increasing the solubility of the phosphonium salt in THF²¹⁶ (a 30% yield improvement was observed). Though the stereochemical outcome of the Wittig reaction held no persistent consequences, only the Z-isomer was isolated. Hydrolysis of the acetonides followed by Fischer glycosylation with methanol, led to the fucose derivative **93**.

3.2.4b: Preparation of Fucose Derivative 94

Fucose derivative **94** was synthesized via the common intermediate **99** (cf. Scheme 3.35). Methylation of the free hydroxyl, hydrolysis of the isopropylidene acetals, and Fisher glycosylation with methanol, gave fucose derivative **94** (Scheme 3.37).



Scheme 3.37: a) NaH, CH₃I in THF; b) H₂O, H⁺ at 80°C;
c) MeOH, H⁺.

3.2.4c: Biological Activity

In order to establish whether extension of the carbon skeleton at C6 of fucose compromises binding, the inhibitor activity of **93** and **94** were measured relative to that of the methyl- α -L-fucopyranoside (**95**) by competition enzyme immunosorbent assay. The results (Figure 3_7) showed that the fucose derivative **93** is a more active inhibitor of the *Ulex* lectin than **94**. Despite the unusual shape of the curve for **93**, it was concluded that a hydrophobic extension at C6 could be incorporated in an active trisaccharide. Guided by these results, our attention was directed to the constrained trisaccharide tethered at the C6 position of fucose via a C-C bond and not an ether bond. Hence, the tethered trisaccharides **32** and **34** were removed from our list of target molecules.

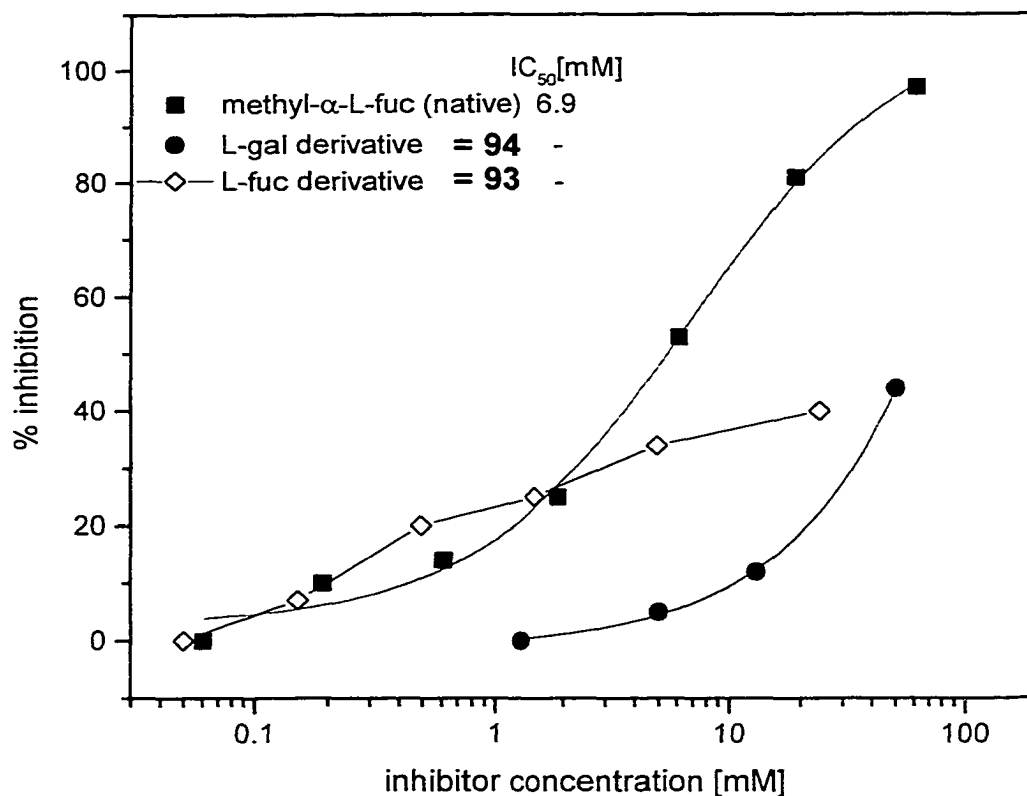


Figure 3.7: Inhibitor activities of fucose derivatives **93** and **94** relative to methyl α -L-fucopyranoside (**95**) obtained by competition EIA.

3.2.5: Synthesis of Constrained H-type 2 Trisaccharide 31

3.2.5a: Strategy

From the retrosynthetic analysis of constrained trisaccharide **31** (Figure 3.8), it was apparent that the assembly of the target molecule could begin with the tethering of ethyl thiofucopyranoside **104** and the 2-acetamido-2-deoxy-glucopyranoside **36**. After some manipulation, this would lead to tethered monosaccharides **105**, which would then undergo an intermolecular glycosylation with a galactose donor such as **106**. After further protecting

group manipulation, intermediate **107** would undergo an intramolecular glycosylation to produce the tethered trisaccharide **31**.

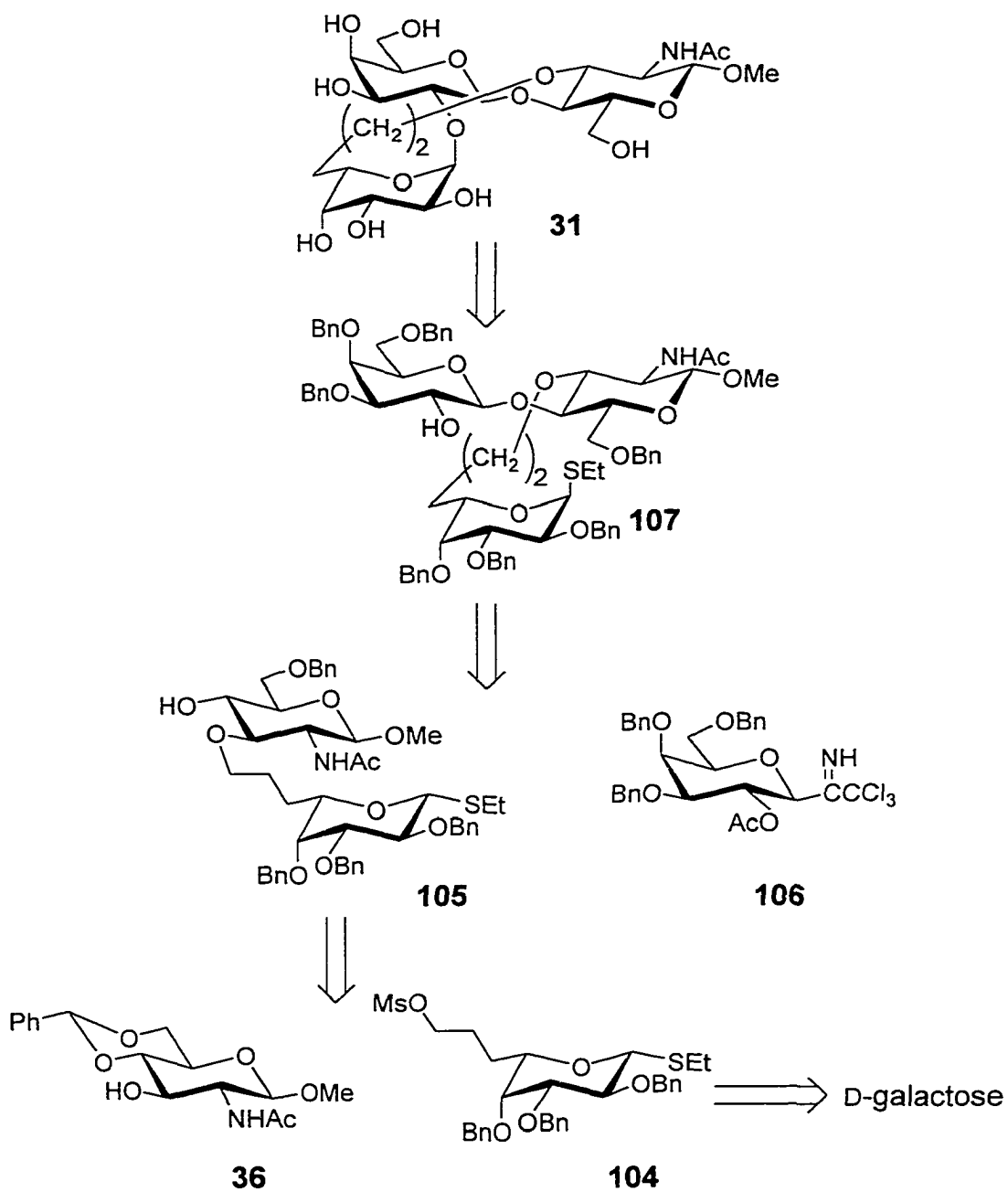


Figure 3.8: Retrosynthesis of the tethered H-type 2 trisaccharide **31**.

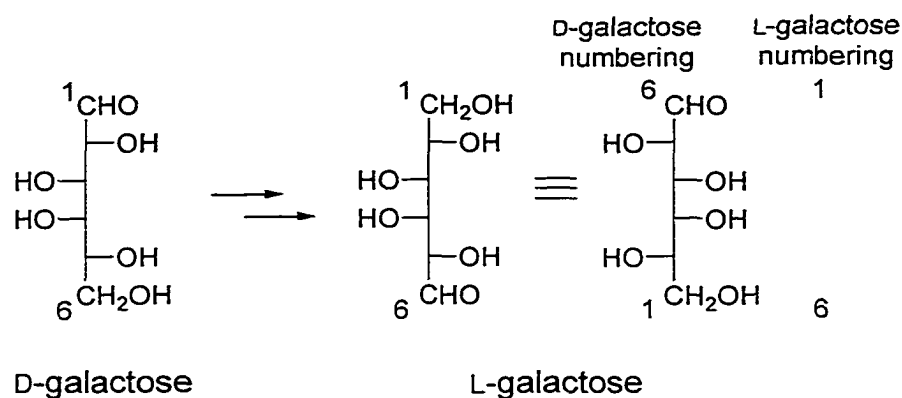
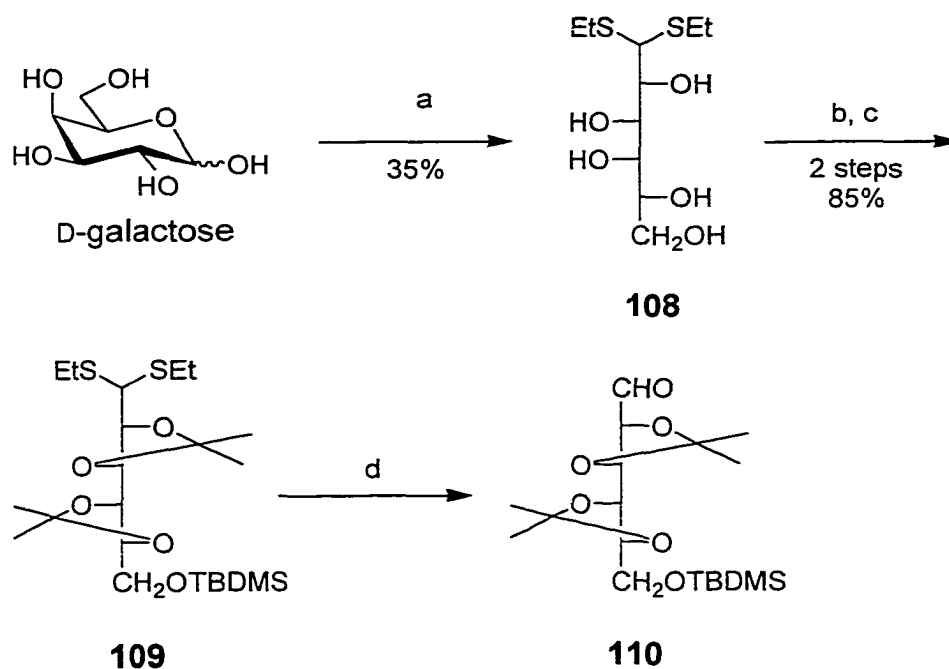


Figure 3.10: Conversion of D-galactose to L-galactose.

The synthesis started with commercially available D-galactose which was converted into the corresponding dithioacetal by treatment with ethanethiol (EtSH) and concentrated hydrochloric acid (Scheme 3.38).²¹⁸⁻²²⁰ In order to differentiate the primary hydroxyl, the 1,2,3,4-di-O-isopropylidene derivative was made, followed by treatment with TBDMSCl, affording the silyl ether **109**. The dithioacetal moiety was then oxidized to the aldehyde **110**, by means of a mixture of mercuric salts.^{219,221}

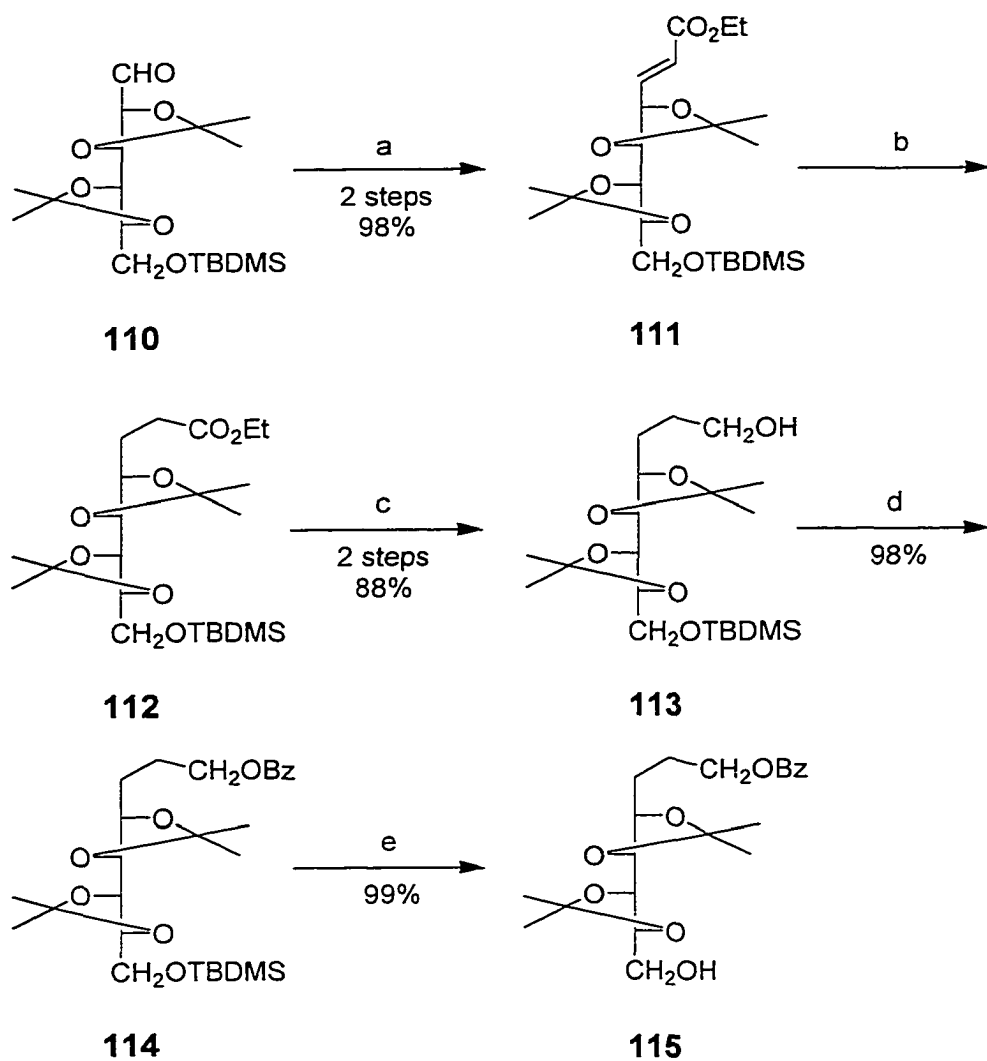
The planned chain elongation was achieved by a Horner-Emmons reaction²²² on compound **110**, yielding the corresponding α,β -unsaturated ester **111** (Scheme 3.39) in a 98% yield from thioacetal **109**. With sodium borohydride and bismuth(III) chloride²²³ reduction of the conjugated double bond followed by reduction of the ethyl ester with LAH yielded derivative **113**. Alcohol **113** was then benzoylated and the silyl ether was deprotected with TBAF to give alcohol **115**.

The primary alcohol **115** was then oxidized via the Swern method (Scheme 3.40).²¹⁴ It was determined by ¹H-NMR of the crude aldehyde **116** that complete conversion to the aldehyde was not obtained. The acetonide groups of compound **116** were hydrolyzed and then benzoylated with benzoyl chloride in the presence of DMAP in pyridine to give a mixture of α - and β -compounds **117** in a 57% yield from the alcohol **115**.

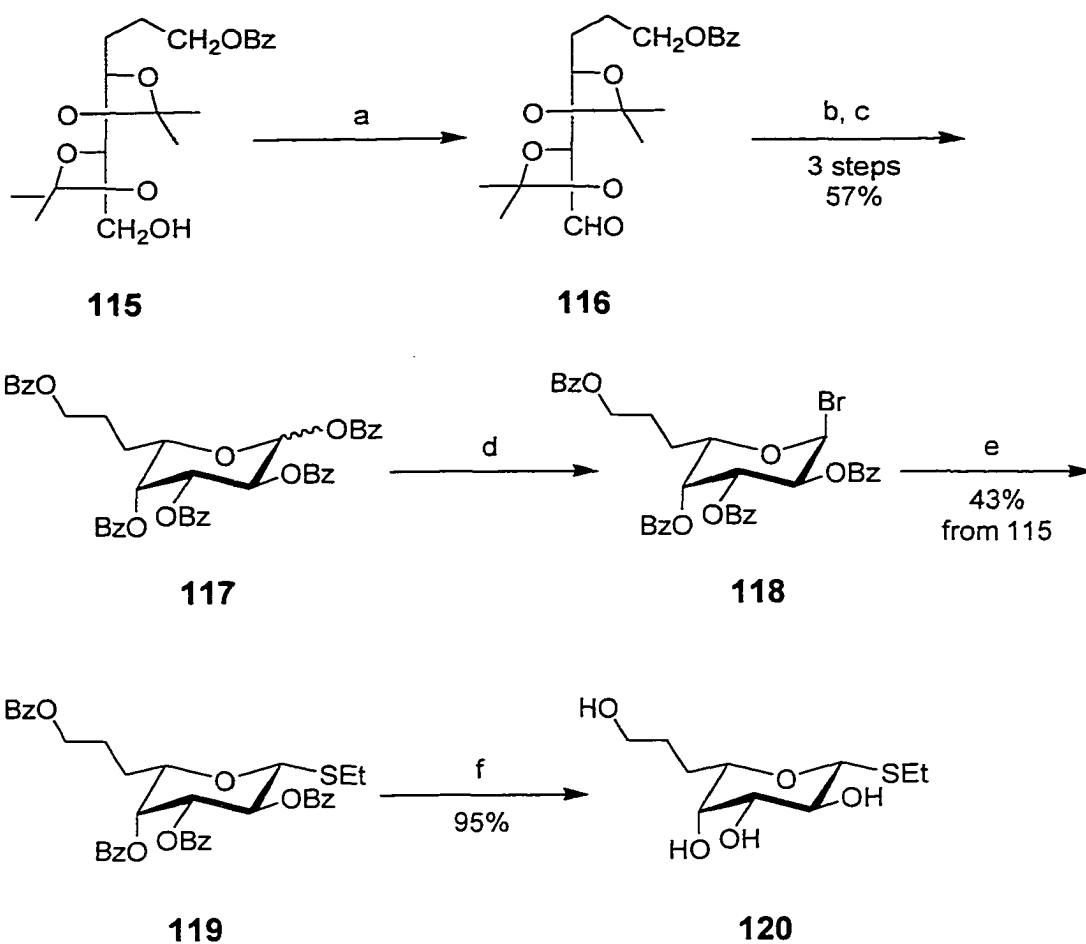


Scheme 3.38: a) EtSH, conc. HCl; b) $(\text{CH}_3\text{O})_2\text{C}(\text{CH}_3)_2$, acetone, conc. H_2SO_4 ; c) TBDMSCl, pyridine; d) HgO, HgCl₂, $(\text{CH}_3)_2\text{CO}$, H₂O.

Compound **117** (mixture of α - and β -anomers) was then treated with HBr in acetic acid, giving the glycosyl bromide **118**.²¹⁹ The crude bromide **118** was treated with EtSH and NaH in DMF to yield thiofucopyranoside **119** in 43% yield over two steps. The stereochemistry of bromide **118** was not verified by analytical methods, but was assumed to be α based on considerations of the anomeric effect.¹⁴⁷⁻¹⁴⁹ In addition isolation of **119** exclusively as the β -anomer from a nucleophilic displacement reaction further supports this assignment. Debenzoylation of thioglycoside **119** was achieved by treatment with freshly prepared NaOMe in MeOH. Interestingly, if the debenzoylation was run at room temperature, only the three secondary benzoyl groups were removed, while the primary benzoyl group remained intact. In order to have complete debenzoylation, refluxing was necessary.

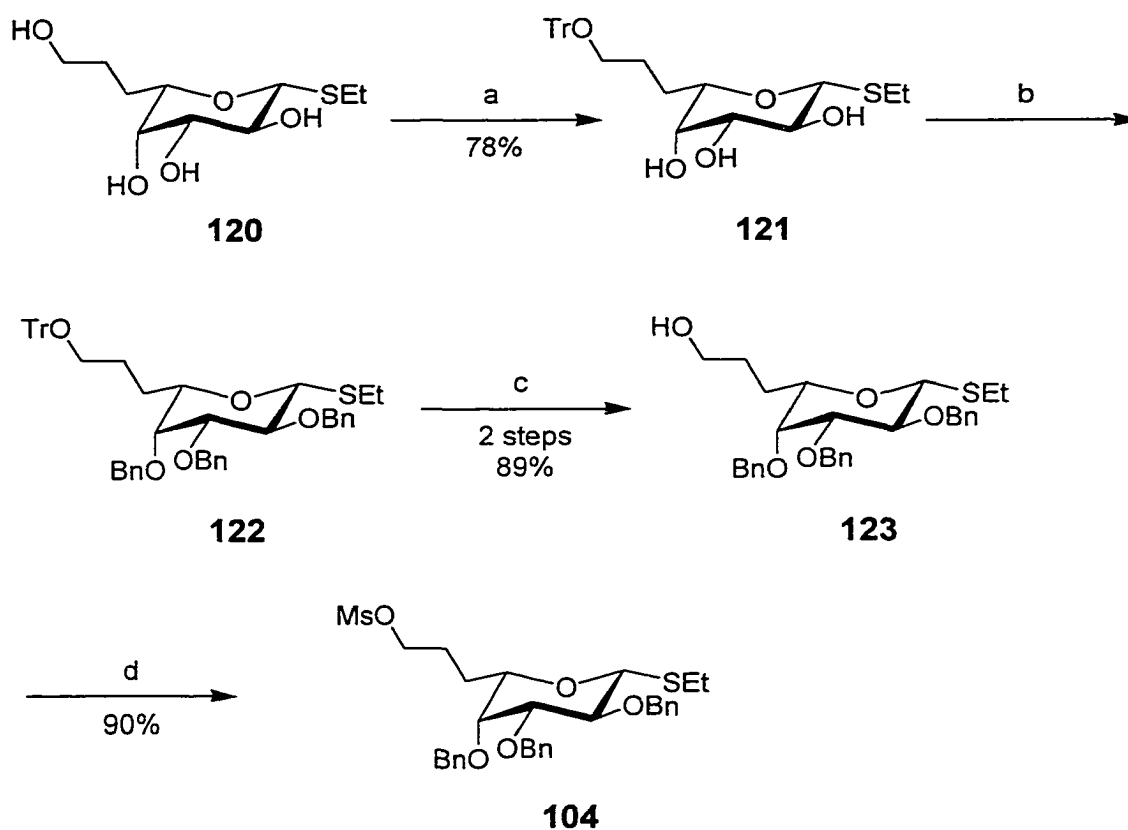


Scheme 3.39: a) $(\text{EtO})_2\text{POCH}_2\text{CO}_2\text{Et}$, NaH in THF;
 b) NaBH_4 , BiCl_3 in 95% EtOH; c) LAH in ether;
 d) BzCl , pyridine; e) TBAF in THF.



Scheme 3.40: a) Swern oxidation; b) 80% AcOH at 80°C; c) BzCl, DMAP in pyridine; d) HBr in AcOH, CH₂Cl₂; e) NaH, EtSH in DMF; f) NaOMe in MeOH, reflux.

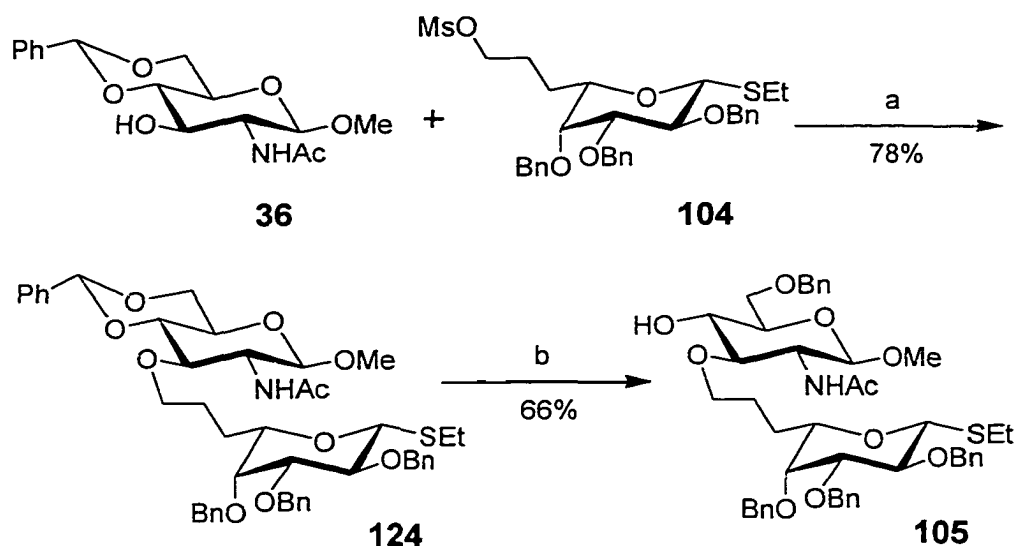
Selective protection of the primary alcohol of thioglycoside **120** with a trityl group, followed by benzylation gave intermediate **122** (Scheme 3.41). Hydrolysis of the trityl group followed by treatment with methanesulphonyl chloride and triethylamine in CH₂Cl₂ gave compound **104**.



Scheme 3.41: a) TrCl in pyridine; b) NaH, BnBr in DMF;
 c) cat. TsOH, 9:1 MeOH/EtOAc; d) NEt₃,
 MsCl in CH₂Cl₂.

3.2.5c: Tethering the Monosaccharide Synthons

Tether coupling of the sugars was carried out in the usual way, giving linked product **124** in 78% yield (Scheme 3.42). Reductive opening of the benzylidene ring with sodium cyanoborohydride and hydrochloric acid in ether and THF yielded alcohol **105** (66%).



Scheme 3.42: a) NaH, DMSO in THF; b) NaCNBH₃, HCl in ether, 3 Å MS, THF.

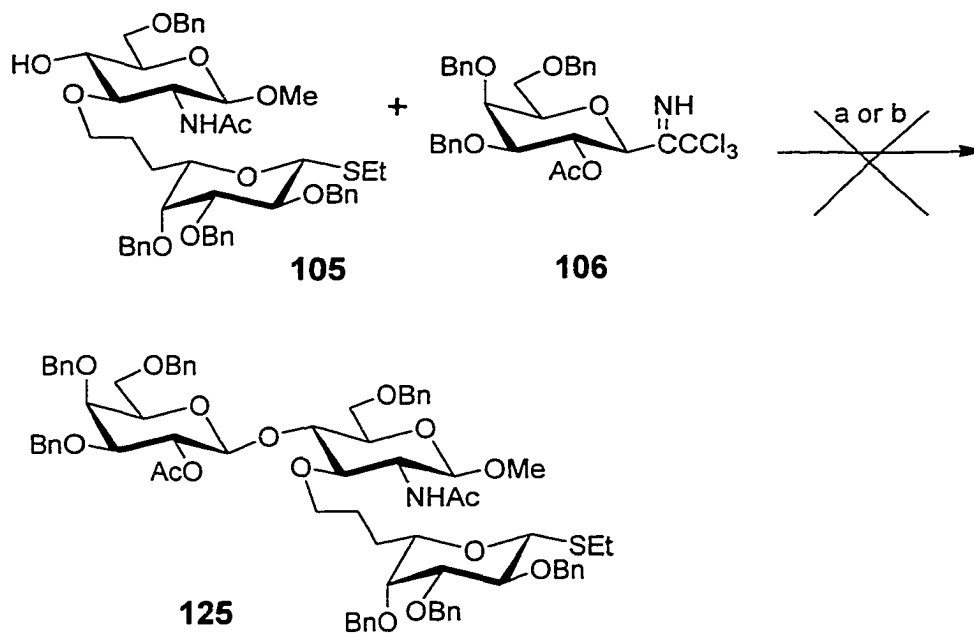
3.2.5d: Glycosylation

A few attempts were made to glycosylate the O-4 position of the *N*-acetylglucosamine residue of **105** with galactose donors. The two first methods involved the trichloroacetimidate donor **106** (Scheme 3.43). Selective activation of the imidate **106** in the presence of the thioglycoside **105** was attempted with TMSOTf. The reaction gave a complex mixture (tlc analysis) of products. Interestingly, the only product isolated was the thioglycoside of **106**, formed presumably from the activation of thioglycoside **105** and transglycosylation of ethanethiol. Attempts to selectively activate imidate **106** with boron trifluoride etherate also failed.

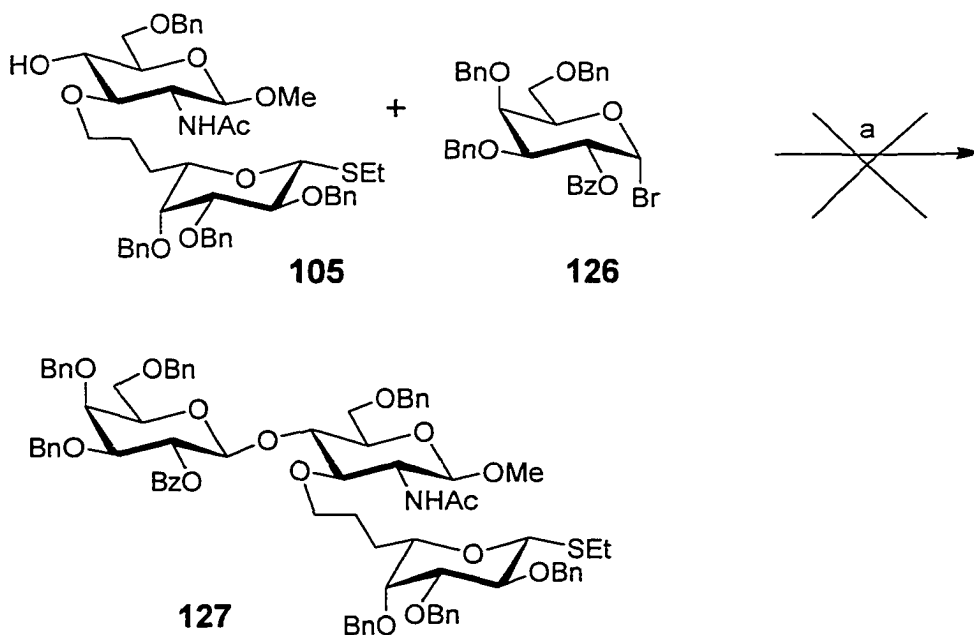
A third attempt was made using galactosyl bromide **126** as the donor (Scheme 3.44) activated by silver triflate.²²⁴ This attempt also failed.

This was recognized to be the most difficult target due to the required chain elongation and the number of steps involved. Difficulty with the intermolecular glycosylation step precluded the successful completion of this approach in this thesis. However, it is proposed that the target constrained trisaccharide **31** could be attained if orthogonally protected lactosamine was

first synthesized and then coupled with the fucose derivative **104** (Figure 3.11).



Scheme 3.43: a) TMSOTf, 4 Å MS, CH_2Cl_2 ; b) BF_3OEt_2 , 4 Å MS, CH_2Cl_2 .



Scheme 3.44: a) AgOTf , 4 Å MS, CH_2Cl_2 .

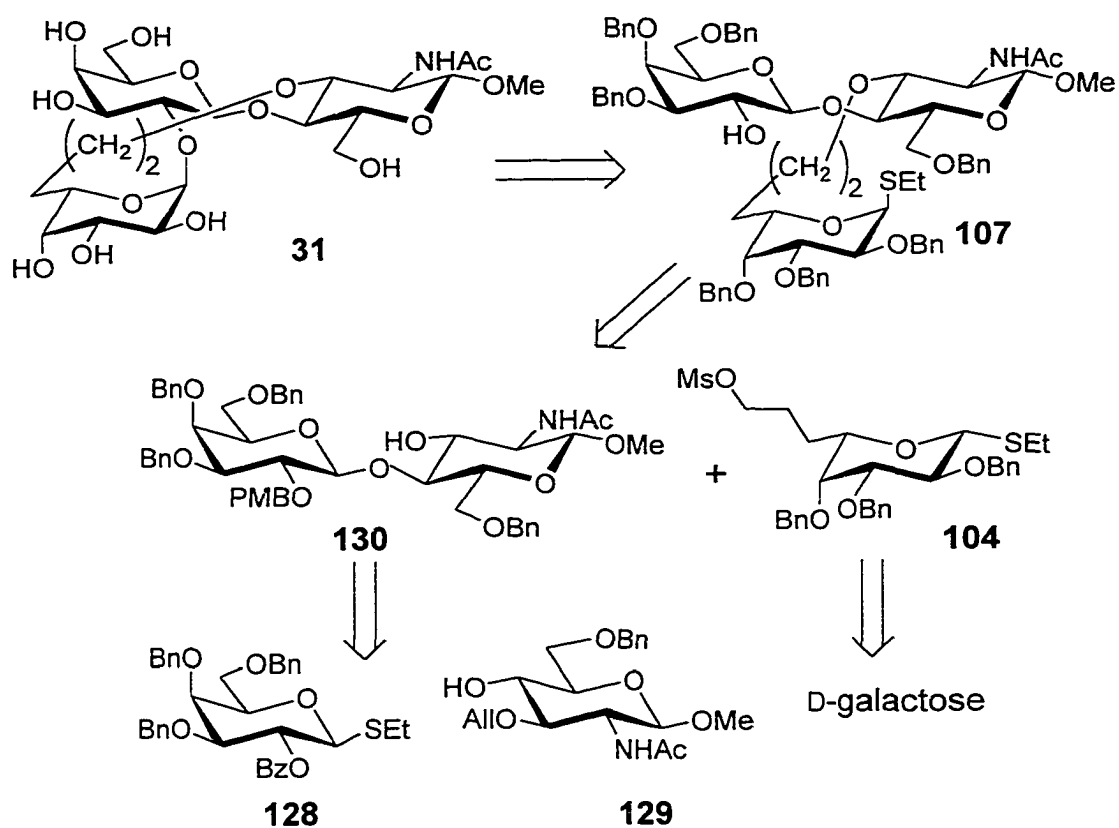


Figure 3.11: Proposed route to constrained trisaccharide **31**.

3.3: Investigation of the Intramolecular Glycosylation

In section 3.2.1d and 3.2.2d, it was observed that changes in the protecting groups on the donor moiety of the tethered monosaccharides, caused drastic changes in the stereochemical outcome of the intramolecular glycosylation. The following is an investigation of the intramolecular glycosylation to determine which factors control the stereoselectivity of these reactions.

3.3.1: Observation

In the two different intramolecular glycosylations involving the three carbon linker, the stereochemical outcome of the reactions exhibited an almost complete reversal (Figure 3.12).

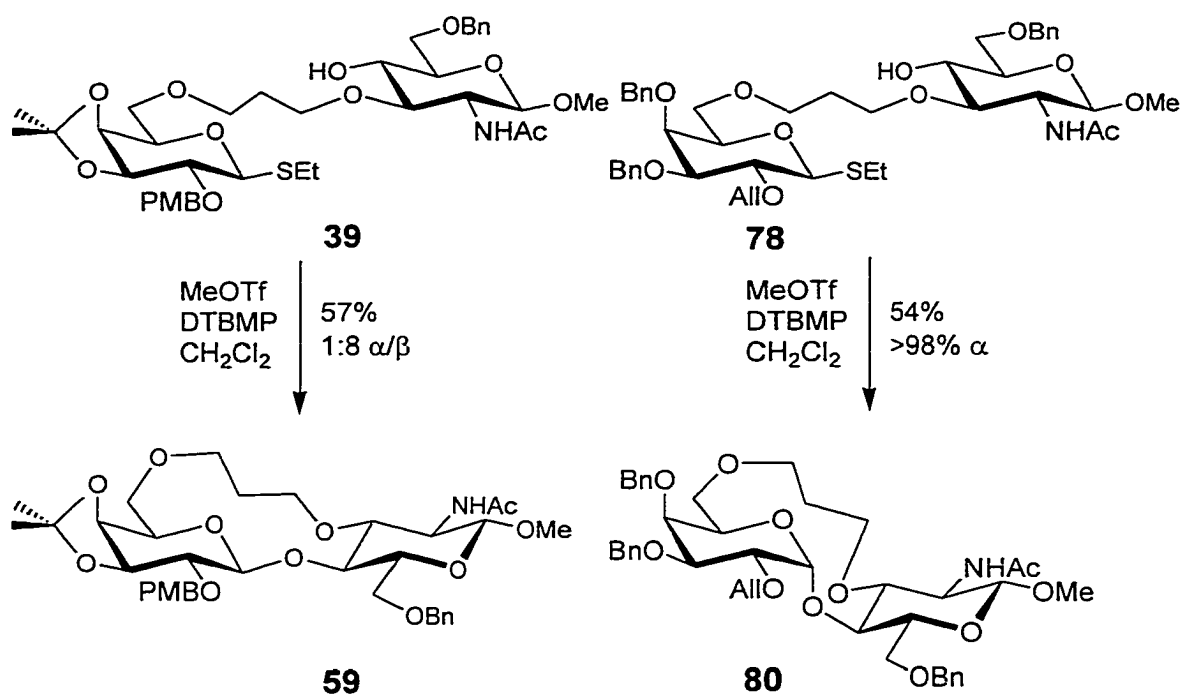
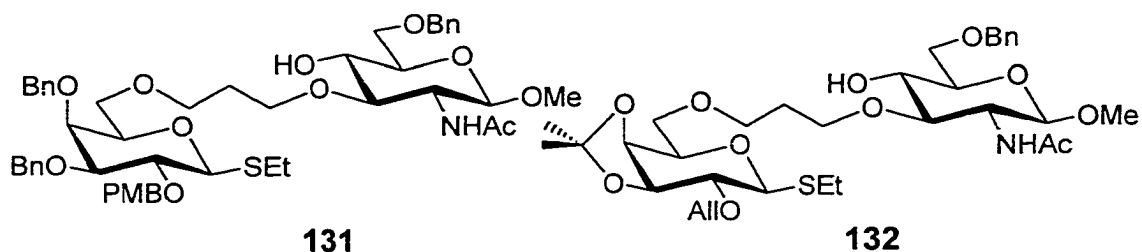


Figure 3.12: Intramolecular glycosylations involving the three carbon linker.

Initially, the stereoselectivity observed, favoring the β -anomer, in the intramolecular glycosylation of **39** was attributed to a combination of ring strain and a steric mismatch between 6-O-benzyl and 2'-O-*p*-methoxybenzyl groups. Other researchers^{115,116,153} have reported that 'prearranged' molecules favor the formation of one glycosidic form depending on the relative configuration of the tethered donor and acceptor. When the opposite stereoselectivity was observed for prearranged compound **78** (the α -anomer was obtained exclusively), it was apparent that both ring strain and the relative configuration of the tethered donor and acceptor were not the sole factors influencing selectivity. Since ring strain was ruled out as a contributing factor (both processes involved formation of rings of the same size), we were left with either a steric mismatch between 6-O-benzyl and 2'-O-*p*-methoxybenzyl groups, or reactivity differences resulting from the constrained chair conformation imposed by the isopropylidene acetal on O'-3

and O'-4 of galactose. In order to investigate the possible origin for the change in the stereoselectivity of these intramolecular glycosylations, the acetonide of **39** was replaced by benzyl ether groups (compound **131**), while an acetonide was used to replace two benzyl groups on the galactose residue of **78** (compound **132**).

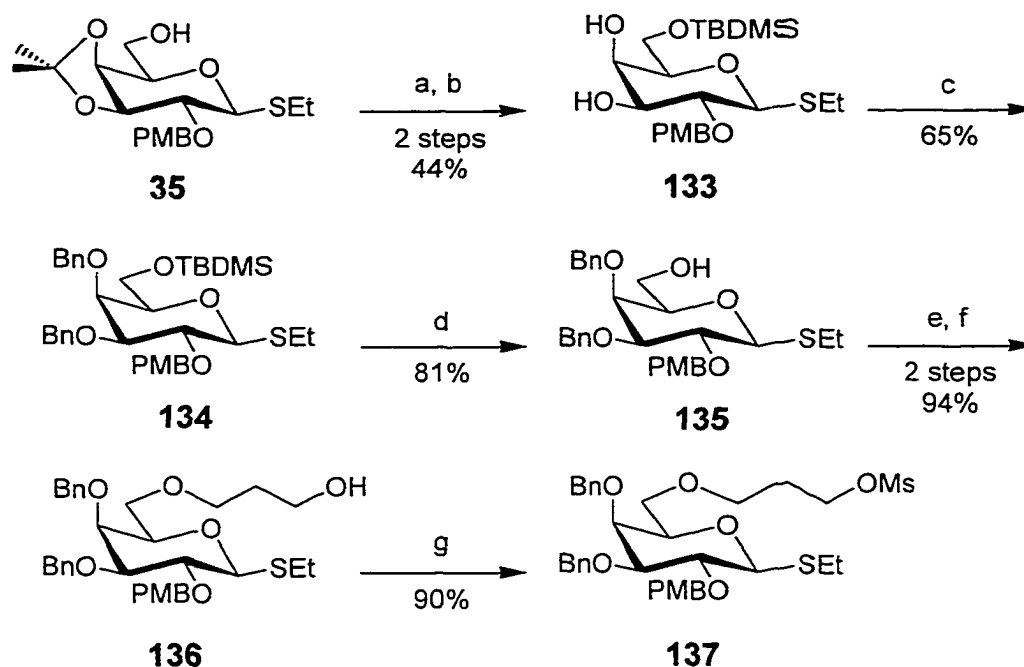


Compound **131** was synthesized in order to determine how the PMB group affected the stereochemical outcome of the intramolecular glycosylation. Compound **132** was assembled to ascertain the effect of the acetonide on the stereoselectivity of the intramolecular glycosylation.

3.3.2: Synthesis of the Intramolecular Glycosylation Precursors

The intramolecular glycosylation precursor **131** was made starting from the acetonide **35** (Scheme 3.45). The isopropylidene acetal was hydrolyzed selectively in the presence of the *p*-methoxybenzyl group by a mild acidic treatment with tetrafluoroboric acid in methanol at 0°C. The primary hydroxyl group was selectively protected as its *t*-butyldimethylsilyl ether **133**, which was followed by benzylation of the secondary alcohols to give intermediate **134**. The low yield obtained in the benzylation was due to significant desilylation of the benzylated-product, which became benzylated at the primary position.

After removal of the silyl ether, the resulting alcohol was treated with NaH and the linker **41**, followed treatment with TBAF to give compound **136**. The thioglycoside **136** was then converted to methanesulphonate **137**.

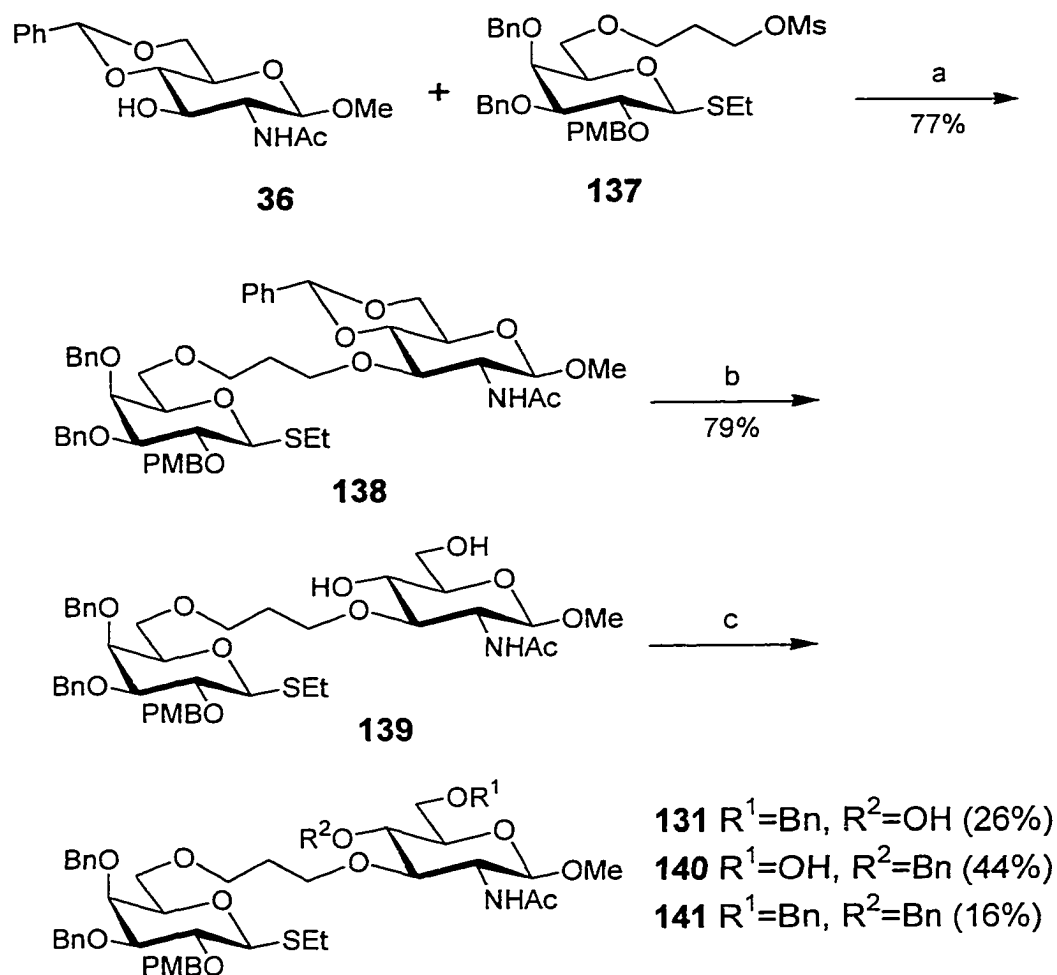


Scheme 3.45: a) HBF_4 in MeOH; b) TBDMSCl, imidazole in DMF; c) NaH, BnBr in DMF; d) 1M TBAF in THF; e) NaH, **41**, THF; f) 1M TBAF in THF; g) NEt_3 , MsCl in CH_2Cl_2 .

The sulphonate **137** was coupled to *N*-acetylglucosamine **36** to produce the tethered derivative **138** (Scheme 3.46). The benzylidene acetal was hydrolyzed with tetrafluoroboric acid in methanol yielding diol **139** in 79%. Selective benzylation of diol **139** at the primary position was attempted by performing the reaction at 0°C ,²²⁵ but all possible benzylated products were observed (**131**, **140**, and **141**). The desired product **131** was isolated in 26% yield.

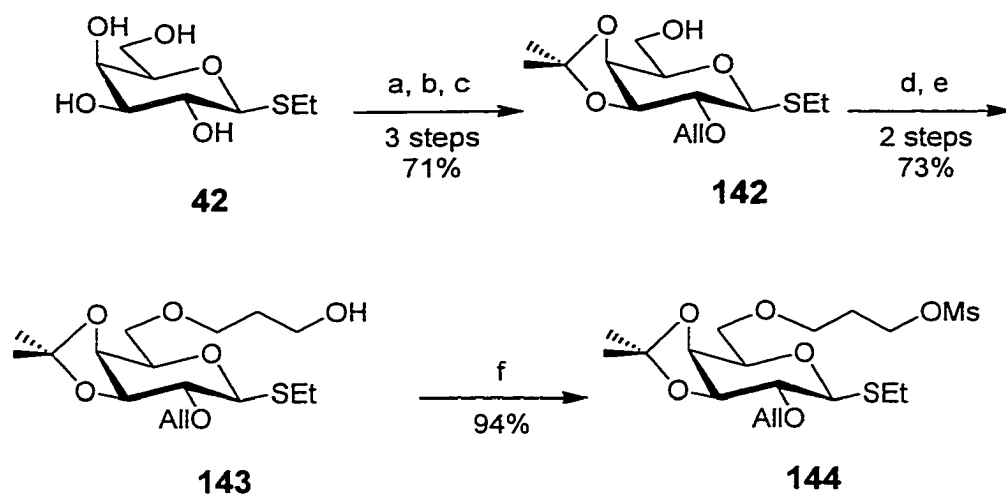
Compound **132** was made following the route used to synthesize tethered trisaccharide **28** (cf. section 3.2.1d – route **2**). The mixed acetal protection of galactose allows selective protection of the O-2 position with the allyl group, while permitting subsequent selective removal of the protecting group of O-6 under mild hydrolysis resulting in monosaccharide **142** in 71% yield (Scheme 3.47). Reaction of the monosaccharide alkoxide generated

from **142** with the linker **41**, followed by removal of the TBDMS protecting group with TBAF in THF gave intermediate **143**.

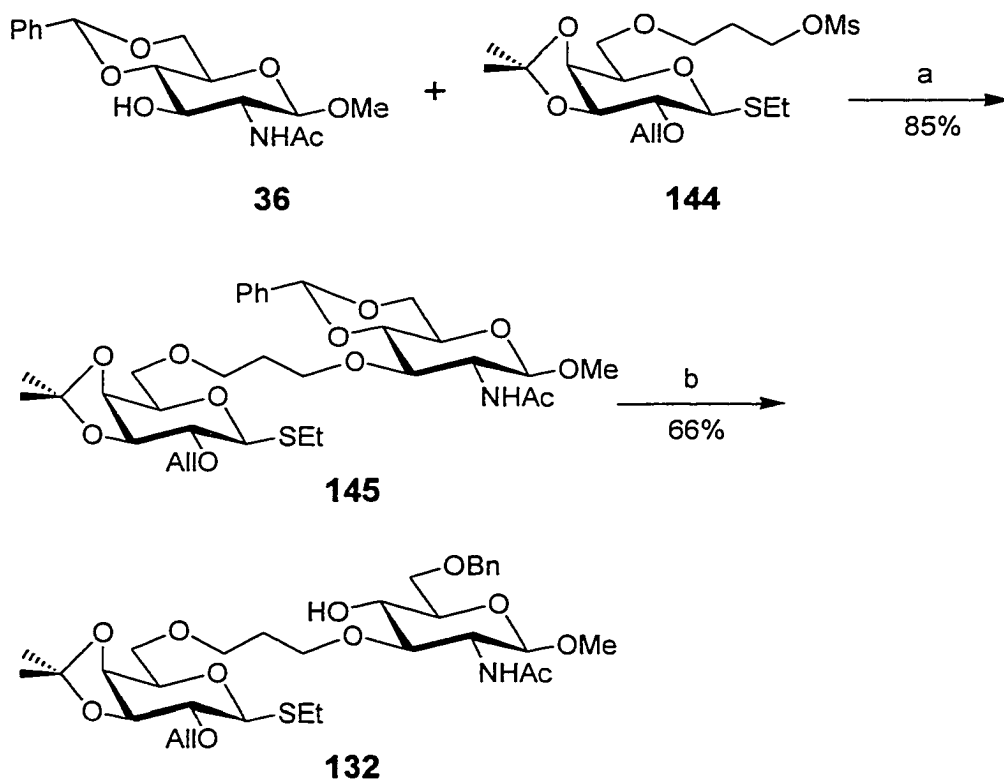


Scheme 3.46: a) NaH, DMSO in THF; b) HBF₄ in MeOH;
c) NaH, BnBr in DMF at 0°C.

After converting alcohol **143** into sulphonate **144** (Scheme 3.47), *N*-acetylglucosamine **36** and sulphonate **144** were reacted to yield the tethered monosaccharides **145** (Scheme 3.48). Reductive opening of the benzylidene ring of **145** with sodium cyanoborohydride and hydrochloric acid in ether and THF gave compound **132**.



Scheme 3.47: a) $(\text{CH}_3)_2\text{C}(\text{OCH}_3)_2$, TsOH; b) AlIBr , NaH, DMF; c) H^+ ; d) NaH, **41**, THF; e) TBAF, THF; f) NEt_3 , MsCl in CH_2Cl_2 .



Scheme 3.48: a) NaH, THF, DMSO; b) NaCNBH_3 , HCl in ether, 3 Å MS, THF.

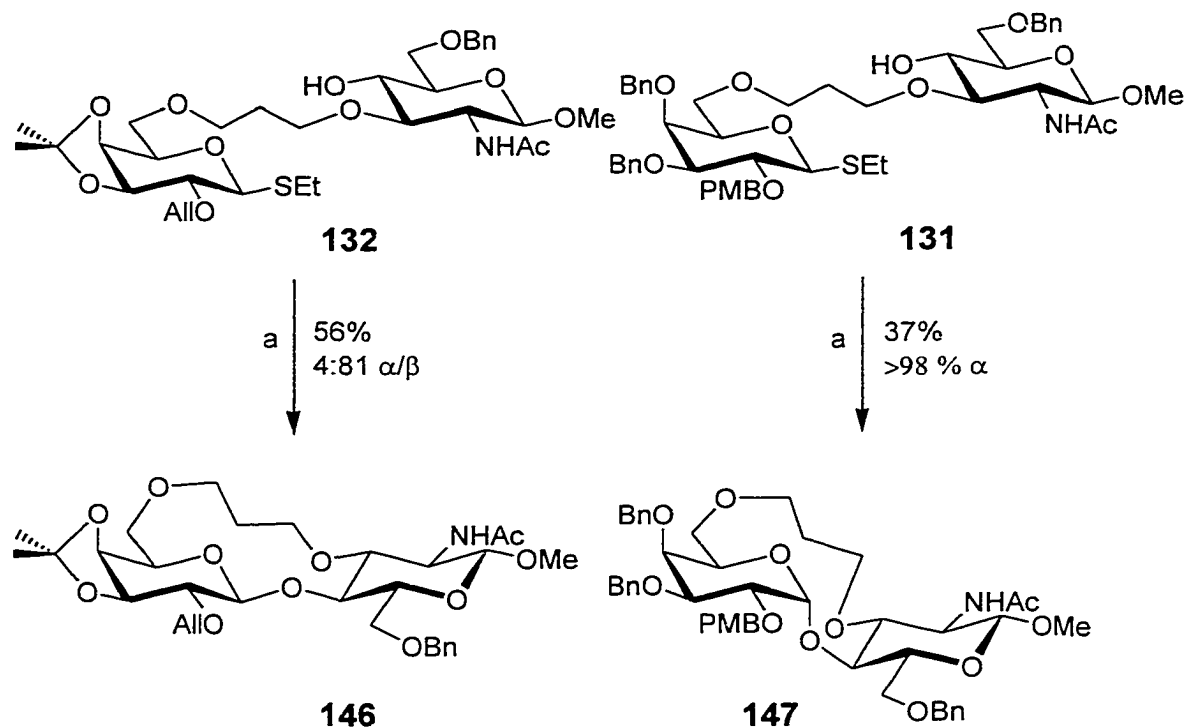
3.3.3: Intramolecular Glycosylation

The conditions used for activation of the thioglycosides **132** and **131** were identical to those previously used for thioglycosides **39** and **78**. Activation of **132** led to the β -anomer, whereas the intramolecular glycosylation of **131**, favored the α -anomer, just as was found for compound **78** (Scheme 3.49). This indicates that the stereoselectivity of the intramolecular glycosylation of compounds **132** and **39** is not governed by the steric mismatch between the 6-O-benzyl and 2'-O-*p*-methoxybenzyl groups but rather is attributable to the isopropylidene group at O'-3 and O'-4 of galactose. It is presumed that the acetonide must constrain the pyranose ring in such a way that the incoming acceptor is preferably delivered to the β -face.

The idea that a protecting group can control the stereochemical outcome of a glycosylation reaction has been demonstrated before through anchimeric assistance (neighbouring group participation),^{142,143} and control of the reactivity of the glycosyl donor.²²⁶⁻²³⁰ Ley *et al.* have reported, and used to their advantage, the torsional deactivation effect of a cyclohexane-1,2-diacetal.²³¹⁻²³² This deactivating effect arises from the rigidity imposed by the fused cyclic acetals which consequently resist the conformational changes required for glycosylation (formation of the half-chair oxocarbenium ion – cf. Figure 3.1), hence the reactivity of the sugar decreases. A similar event occurs in our intramolecular glycosylation. The rigidity of the acetonide maintains the chair conformation of the donor, hence the most direct route for approach of the tethered-acceptor is via the β -face.

When the acetonide is replaced by the benzyl groups, the galactosyl donor is free to undergo the conformational changes (successively boat and half-chair conformation) for glycosylation, and the incoming acceptor may arrive at either the α - or β -face. This was observed in the intramolecular glycosylation of compounds **78** and **131**, the stereochemistry must be governed by the non-participating group and the anomeric effect. The anomeric effect, which is believed to mainly arise from the interaction

between the axial lone pairs of electrons on the ring oxygen atom and the antibonding σ^* -orbitals of the C-OR bond, contributes importantly to the compositions of isomeric mixtures at equilibrium favoring the α -anomers over the β -anomers.

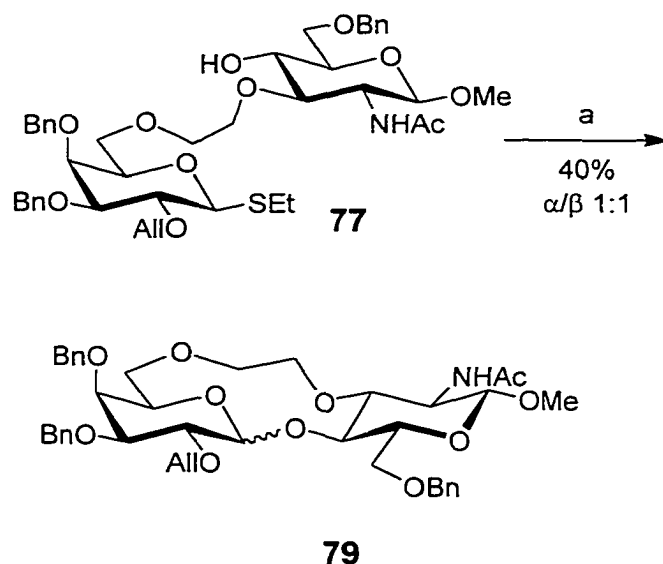


Scheme 3.49: a) MeOTf, DTBMP, 4 Å MS in CH_2Cl_2 .

The structures of the tethered glycosides **146** and **147**, were verified by one dimensional $^1\text{H-NMR}$, two dimensional GCOSY and HMQC experiments. The $^3J_{1',2'}$ (**146**: 8.4 Hz; **147**: 2.8 Hz) and $^1J_{\text{C}1',\text{H}1'}$ (**146**: 158.7 Hz; **147**: 165.6 Hz) coupling constants of H1' of galactose and the C1' chemical shift (**146**: $\delta = 104.3$ ppm; **147**: $\delta = 93.1$ ppm) all indicate that the β -anomer **146** was the major product and the α -anomer **147** was the only product obtained. T-ROESY experiments also confirmed the 1,4 position of the glycosidic bond.

In an earlier example the intramolecular glycosylation of compound **77** resulted in an α/β ratio of 1:1 (Scheme 3.50). The loss of the α -selectivity that

would be predicted by the model glycosylations of **131** and **132**, is attributed to the macrocyclic ring strain caused by the shorter tether.



Scheme 3.50: a) MeOTf, DTBMP, 4 Å MS in CH₂Cl₂.

The stereochemical outcome of the intramolecular glycosylations reported here demonstrate the importance of the O-3:O-4 acetonide in controlling the conformation of the pyranose ring, on which the oxocarbenium ion is developed. As we show, this effect can be modulated by the length of the tether.

Biological Activity of the Constrained Carbohydrates

4.1: Introduction

Solid phase immunoassays offer a convenient format to measure relative inhibitory power and serve here to provide the first estimates of our attempts to achieve affinity gains by pre-organization of the H-type 2 oligosaccharide epitopes. To determine whether the constrained H-type 2 and lactosamine epitopes synthesized increased affinity for any of the four lectins, *Ulex europaeus* I,²⁷ *Psophocarpus tetragonolobus* II lectin (winged bean lectin),²⁸ *Galactia tenuiflora*²⁹ and *Erythrinia corallodendron*,³⁰ enzyme-immunosorbent assays (EIA) were conducted.

4.2: Solid-Phase Immunoassay

Enzyme immunoassays require only small amounts of protein and relatively little sugar inhibitor. Besides economical use of valuable protein and inhibitor, their principal advantages are of speed and convenience.

4.2.1: Basic Principles of EIA

EIA methods were first developed for antibody receptors. EIA is based on primary interactions, meaning it measures the direct binding of the protein to its antigen. Depending on the objective, this type of assay may measure the amount and specificity of antibodies, the amount of antigen or inhibitor activity. Their convenience and environmentally friendly nature (cf. radioisotopes) have lead to frequent applications in immunology, biology, and medicine.²³³

In an EIA, the unlabeled component (either antibody or antigen) is adsorbed to a polystyrene surface, such as the wells of a microtiter plate. This allows the use of small volumes and gives EIA the potential of rapidly handling high numbers of samples. The adsorption of the unlabeled component to the polymeric support is due to intermolecular forces of

attraction (van der Waals forces). In the most common format, antigen is attached to the plate surface and binding of labeled antibody is assayed (Figure 4.1). The label consists of an enzyme, which is used later in quantifying the binding phenomenon by catalyzing a reaction that produces a color change.

The specific steps involve absorption of the antigen to the EIA plate, blocking any remaining reactive sites on the EIA plate by addition of protein (BSA, or casein from milk). Labeled antibody is then allowed to bind to the unlabeled antigen, and unbound antibody and other proteins are removed by multiple washing steps. Since one of the reactants in the EIA is attached to a solid-phase, the separation of bound and free reagents is easily made by such washing procedures. Antibody binding is detected by a reaction that converts a colorless substrate into a colored reaction product. The color change, which can be observed by eye, is read quantitatively in the microtiter plate well by specially designed 96-channel spectrophotometers.

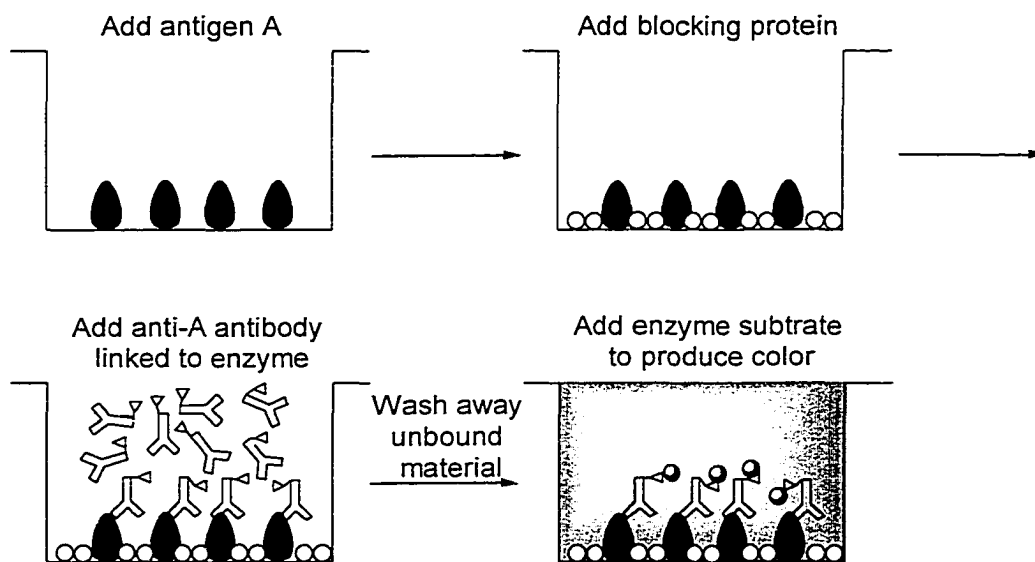


Figure 4.1: The enzyme immunosorbent assay (EIA).

4.2.2: Competition EIA

The use of passive adsorption onto the polymeric support allows a great deal of flexibility in assay design. EIAs may be classified into four groups: direct, indirect, sandwich, and competition. In order to determine the IC_{50} 's of our tethered carbohydrates with the different lectins proposed, a direct competition EIA was performed.

In this type of assay, a fixed amount of unlabeled antibody is absorbed to the wells in a microtiter plate. A standardized quantity of labeled antigen is allowed to bind to the absorbed protein in the presence and absence of varying amounts of inhibitor. After washing away any bound antigen and inhibitor, the displacement of the labeled antigen is quantified. Characteristic inhibition curves are generated and the IC_{50} of the test samples are determined.

4.2.3: Protocol

The EIA was performed in duplicate using a variant of previously described methods.^{234,235} Our assay sequence consisted of (Figure 4.2):

- attachment of affinity purified lectin to the wells of a microtiter plate (96-well format);
- washing to remove unadsorbed lectin;
- addition 2% BSA as a blocking protein;
- washing to remove excess BSA;
- labeled antigen, a biotin labeled BSA H-type 2 oligosaccharide conjugate,²³⁶ is added to inhibitor free wells to provide the reference signal;
- preparation of a series of mixtures containing a fixed concentration of the biotin-labeled H-type 2 glycoconjugate and serial dilutions of the inhibitor (synthesized tethered molecules);
- incubation of these mixtures with plate bound lectin to allow the competitive binding to occur.
- washing to remove any labeled or unlabeled material which is

- unbound;
- addition of horseradish peroxidase (HRP) labeled streptavidin to the wells. Streptavidin binds to biotin at any site where the H-type 2 trisaccharide hasn't been displaced by the carbohydrate inhibitor;
- addition of HRP substrate, 3,3',5,5'-tetramethylbenzidine (TMB), and peroxide to the wells leads to immediate formation of a blue color, that is proportional to the amount of H-type 2 still attached to solid phase lectin;
- analysis of the resulting color is performed using a multichannel spectrophotometer at 450 nm (yellow color is stable for 1 hour);
- generation of an inhibition curves which will give the IC_{50} of the tethered molecules.

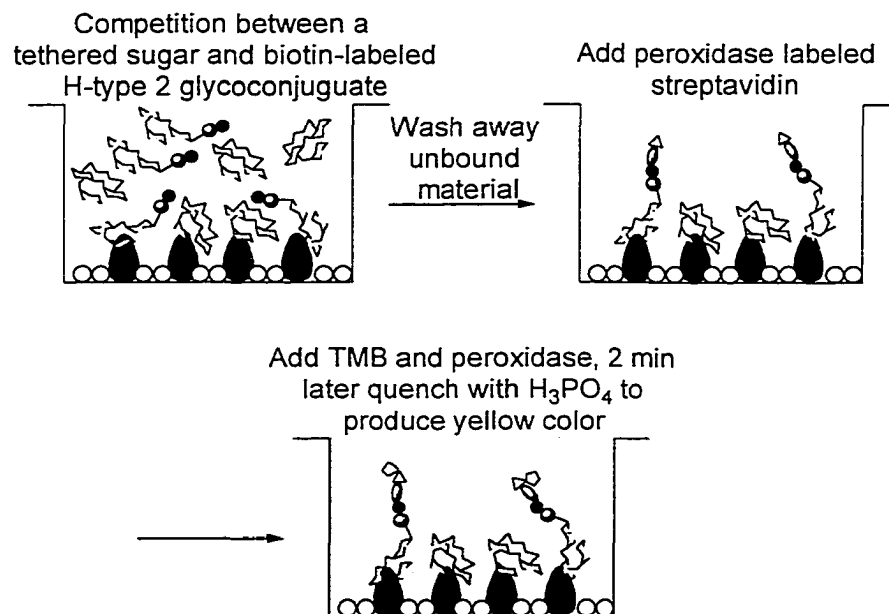


Figure 4.2: Direct competition assay format to determine IC_{50} values.

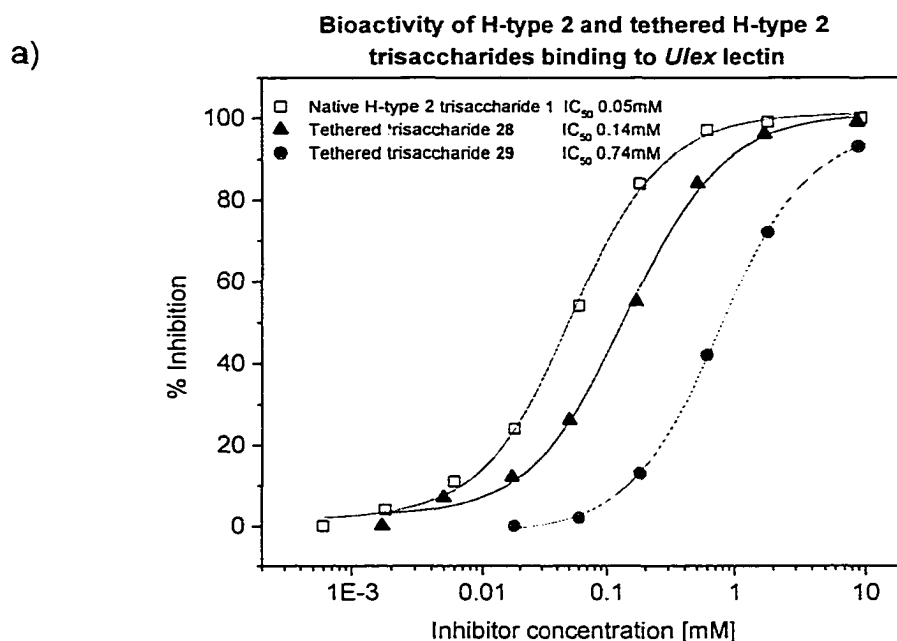
Provided that certain conditions are fulfilled, it has been shown that EIA can yield a direct estimate of K_a , the equilibrium constant.²³⁴ Even when these conditions are not met, comparison of IC_{50} values relative to a standard, here the untethered H-type 2 trisaccharide **1**, allows the calculation of $\Delta(\Delta G)$ for inhibitors. This provides a reliable estimate of binding strength. The error in the estimation of IC_{50} between successive experiments is approximately $\pm 5\%$. This translates into $\Delta(\Delta G)$ differences no larger than $0.2 \text{ kcal mol}^{-1}$ when the binding strength of analogues are compared.

4.3: Results

4.3.1: Binding Studies of the Constrained Trisaccharides

28 and 29 with *Ulex europaeus* I and Winged Bean

The biological activity of the tethered trisaccharides **28** and **29** with *Ulex europaeus* I²⁷ and *Psophocarpus tetragonolobus* II²⁸ lectins were determined. The tethered trisaccharides **28** and **29** were good inhibitors of glycoconjugate binding to the *Ulex* lectin, however, the untethered H-type 2



b)

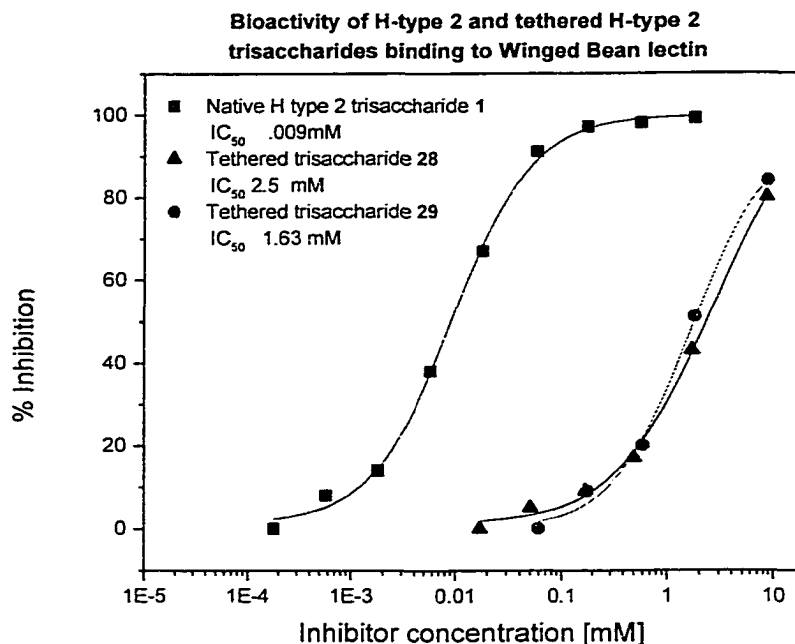


Figure 4.3: Biological activity of the tethered **28** and **29** relative to native trisaccharide **1** assayed with the *Ulex europaeus* I and WBA lectins.

ligand **1** exhibited binding that was 3 times higher than **28** and 15 times stronger than **29** (Figure 4.3a). In sharp contrast, trisaccharide **1** was 250 times more active than **28**, and 163 more active than **29** when each was assayed for binding to *Psophocarpus tetragonolobus* lectin (Figure 4.3b).

4.3.2: Binding Studies of the Constrained

Di- and Trisaccharides with *Erythrinia corallodendron*³⁰

The IC_{50} of the native H-type 2 trisaccharide **1** was determined to be 0.022 mM, and 0.17 mM for β -lactosamine **148** (gift from R. U. Lemieux). None of the tethered trisaccharides (**28** and **29**) or tethered disaccharides (**87** and **88**) showed activity with *Erythrinia corallodendron*.

epitope. NMR and computational studies are required to understand this difference in biological activity.

The dramatic reduction of inhibitory power for **28** and **29** with the *Psophocarpus tetragonolobus* lectin ($\Delta(\Delta G^\circ) = + 3.3 \text{ kcal mol}^{-1}$ and $\Delta(\Delta G^\circ) = + 3.0 \text{ kcal mol}^{-1}$) points to substantial destabilization of the ligand-protein complex. Lemieux's model for topology of the binding surface of the native H-type 2 trisaccharide **1** with the lectin proposed that O-6 of galactose is involved in hydrogen bonding at the periphery of the binding site.¹²² Nevertheless, it should be noted that epitope mapping established that substitution of a 6-O-methyl galactose residue for galactose resulted in a $\Delta(\Delta G^\circ) = +0.1 \text{ kcal mol}^{-1}$. This would suggest that there are no immediate steric or electronic problems in alkylation of this hydroxyl group. Introduction of the tether may result in several changes that could account for the loss of binding energy. These would include changes in the rotamer distribution of the hydroxymethyl group, adverse affects on an extended network of hydrogen bonds that involve structured water molecules or a simple steric clash between the tether and protein.

Since there have been no mapping studies done on the native H-type 2 trisaccharide with *Erythrinia corallodendron*, we did not know beforehand whether the tether attached to O-6' and O-3 would interfere with binding. The severe decrease in binding affinity observed for tethered trisaccharides **28** and **29**, and the tethered disaccharides **87** and **88** relative to the native trisaccharide **1** and the β -lactosamine **148**, leads us to believe that either: 1) the tether is attached to key polar groups that are involved in protein-carbohydrate interactions, 2) the conformation of the bioactive epitope has been distorted by tethering, or 3) the tether interferes sterically with the surface of the protein. Shaanan *et al.* have reported the crystal structure of the lactose-*Erythrinia corallodendron* complex.¹²⁰ It was determined that lactose is held by seven hydrogen bonds involving HO-6', HO-4' and HO-3' of galactose. If the H-type 2 trisaccharide **1** did have a similar binding topography to lactose, the lack of activity of the tethered di- and

trisaccharides could be explained by attachment of the tether at O-6' resulting in a loss of a hydrogen bond.

Lemieux's mapping studies¹²² of the native H-type 2 trisaccharide **1** with *Galactia tenuiflora*²⁹ have shown that both the hydroxyl groups at O-6' and O-3 are involved in the binding interaction with the lectin. Consequently, this lectin is unlikely to be active with tethered trisaccharides **28** and **29**. Furthermore, none of this lectin is currently available for testing.

These data highlight the difficulty in designing a tether that can effectively constrain an oligosaccharide in a bioactive conformation whilst avoiding unfavourable protein contacts. Apparently, even modification of hydroxyl groups that are thought to lie at the periphery of the wing bean lectin binding site and which should be involved in relatively weak hydrogen bonds may cause sufficiently unfavourable interactions to destabilize the complex by approximately +3 kcal mol⁻¹.

NMR and Modeling Studies of the Free Conformations of H-Type 2 Trisaccharide and Constrained Derivatives

5.1: Introduction

The role of oligosaccharides in biochemical processes largely depends on mutual molecular recognition between carbohydrates and proteins. The knowledge of their conformations in solution and their flexibility has become important in understanding the molecular mechanism of oligosaccharide-protein interactions and, in particular, the maintenance of its specificity.

The inherent flexibility of many oligosaccharides in solution gives rise to structures that are generally best described as ensembles of distinct conformers. A combination of different structural and electronic contributions are responsible for this effect.²³⁷ In order to determine solution conformation, the interplay between theory and experiment is essential in the conformational analysis of oligosaccharides.

5.1.1: Conformational Parameters of Oligosaccharides

Nearly all hexoses with the D-configuration adopt stable 4C_1 chair conformations in solution and in the solid state (Figure 5.1). Fucose, the only common 6-deoxy-hexose to occur in mammalian carbohydrate antigens, has the L-configuration and exists as a stable 1C_4 chair conformation. In modeling oligosaccharides composed of these common monosaccharide units, it is implicitly assumed that these conformations are adopted by the individual monosaccharides. In dynamic simulations, this restriction may be relaxed.

When two monosaccharides are glycosidically linked, their spatial dispositions are defined by the two torsion angles ϕ (phi) and ψ (psi) about the glycosidic linkage, or, in the case of 1,6 glycosidic linkages, also by a third torsion angle ω (omega) (Figure 5.2). IUPAC convention defines ϕ by the heavy atoms O5'-C1'-O1-Cx, ψ by C1'-O1-Cx-Cx+1 and ω by O5-C5-C6-O6. In crystallographic studies this IUPAC convention is always followed.

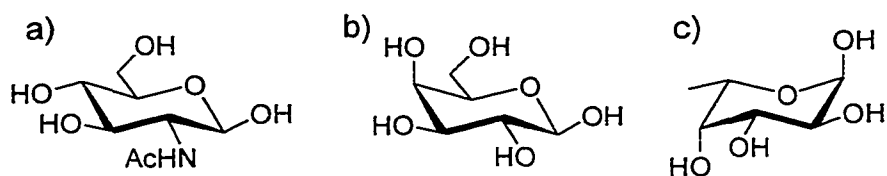


Figure 5.1: Absolute configuration of monosaccharides found in the H-type 2 trisaccharide: a) β -D-N-acetylglucosamine; b) β -D-galactopyranose; c) α -L-fucopyranose.

However, solution NMR data records the relative positions of hydrogen atoms, and ϕ_H and ψ_H are defined using the anomeric and aglyconic hydrogens; $\phi_H = H1'-C1'-O1-Cx$, $\psi_H = C1'-O1-Cx-Hx$ ($C1'-O1-C6-H6$ in the case of 1 \rightarrow 6 linkages), and $\omega_H = H6-C6-C5-H5$ (Figure 5.2).

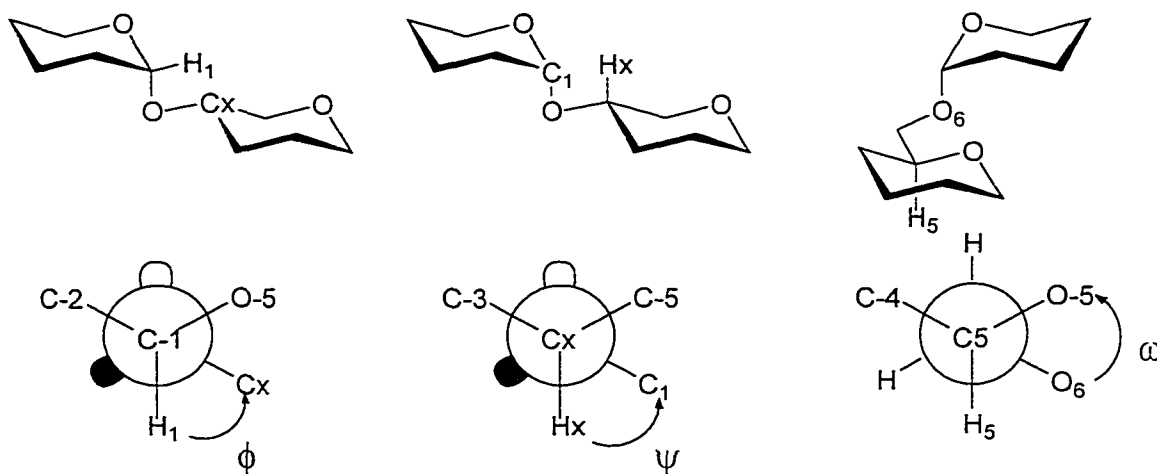


Figure 5.2: The torsion angles ϕ (phi) and ψ (psi) shown for a (1 \rightarrow 4) linked disaccharide; $\phi_H = H1'-C1'-O1-C4$; $\psi_H = C1'-O1-C4-H4$. The torsional angle ω (omega) is shown for a (1 \rightarrow 6) linked disaccharide; $\omega = O5-C5-C6-O6$.

5.1.2: Anomeric Effect

The anomeric effect, identified by Edward²³⁸ and particularly by Lemieux,¹⁴⁷⁻¹⁴⁹ is the tendency of an electronegative substituent to favour the axial orientation at C1 of pyranose sugars. This is often referred to as the *endo*-anomeric effect and mainly arises from the interaction between the axial lone pairs of electrons on the ring oxygen atoms and the antibonding σ^* -orbitals of the C-OR bonds (Figure 5.3). This leads to the shortening of the bond connecting the ring oxygen atom to the anomeric carbon and lengthening of the C-OR bond in anomers where the -OR group is axial. This means that the axial C1-O1 bond is longer than the equatorial C1-O1 bond.²³⁹ The *endo*-anomeric effect contributes importantly to the free energies of carbohydrates and hence to their preferred conformations and reactivities, and also to the compositions of isomeric mixtures at equilibrium.

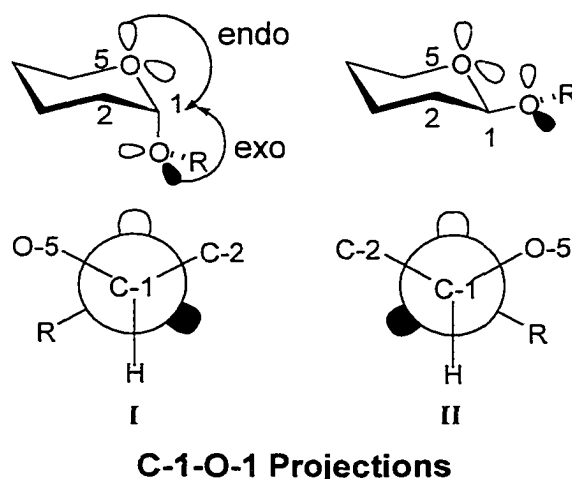
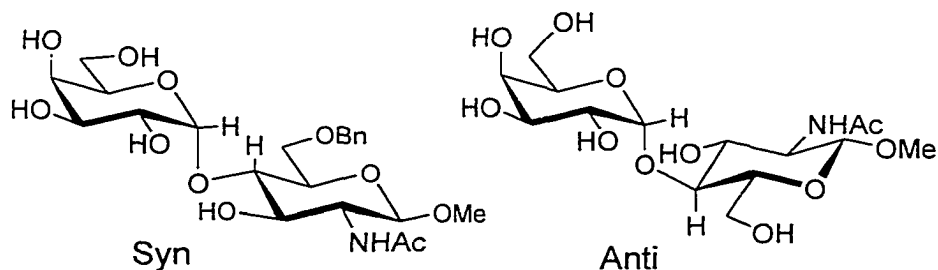


Figure 5.3: Rotamer states preferred by glycosides with axial and equatorial groups due to the *exo*-anomeric effect.

The orientation of groups bonded to the anomeric oxygen atom of pyranosides are subject to the anomeric effect^{147,240} which represents a barrier to interconversion about the exocyclic C-O bonds at the anomeric centre of glycosidic linkages. The anomeric effect that influences the

conformation of glycosidic linkages is termed the *exo-anomeric effect*. This arises from $n \rightarrow \sigma^*$ delocalization of electrons from the exocyclic oxygen atom (anomeric oxygen) to the C1-O5 bond. When the lone pairs of the exocyclic oxygen are *anti*-periplanar to C1-O5, this delocalization is most effective. This stereoelectronic effect causes glycosides with axial and equatorial substituents at the anomeric centre to prefer the rotamer states shown in Figure 5.3.

Due to the contribution of both the *exo-anomeric effect* and the *endo-anomeric effect*, most rotamers place the O1-C_x bond *anti*-periplanar to the C1-C2 bond. This results in a *syn* relationship between the anomeric and aglyconic protons.²⁴¹⁻²⁴⁴ The *anti*-conformation, where the anomeric and aglyconic protons are in a *anti* relationship, has only been observed as a minor component of the populated conformers in D₂O solution.²⁴⁵⁻²⁴⁹



It is necessary to evaluate the angles ϕ and ψ to determine the orientation of one sugar residue with respect to a bonded neighbouring sugar (or other aglycon). The ϕ torsion angle is restricted by the *exo-anomeric effect*, while the ψ angle is also found to be significantly limited by non-bonded interactions.²⁵⁰ Therefore, many oligosaccharides are thought to have well defined conformations and this knowledge is directly relevant to understanding their role in biochemical processes. Recent work has shown that depending on the demands of sugar-protein interactions the glycosidic linkage may adopt the *anti*-conformer in the bound state.^{99,251,252}

5.1.3: Determination of the Solution Conformation of Oligosaccharides

5.1.3a: Nuclear Magnetic Resonance

NMR is the only technique which can yield high resolution structural data of oligosaccharides in solution. Two NMR parameters provide information about three dimensional structure: spin-spin coupling and dipolar coupling also known as the nuclear Overhauser effect (NOE).

Homonuclear spin-spin coupling, quantified in terms of coupling constants (J), is dependent on the dihedral angle between vicinal protons. The ring conformation of a monosaccharide can be determined from the $^3J_{H,H}$ values obtained from 1H NMR data. These values give information on the relationships of pairs of vicinal protons.

As mentioned in section 5.1.1, the conformation of oligosaccharides is described by the ring conformations of the sugar residues and the torsion angles ϕ and ψ (Figure 5.2). These torsional angles define the rotamer states about each of the two C-O bonds in the glycosidic linkage. The ϕ and ψ angles can be derived from a Karplus relationship using the heteronuclear $^3J_{C,H}$ values between the anomeric proton and the aglyconic carbon, and the anomeric carbon and the aglyconic proton.

The NOE is a through-space effect which is manifested by a change in intensity of a given proton resonance when the resonance of a nearby proton ($< 5\text{\AA}$) is perturbed.²⁵³ The NOE is proportional to the inverse sixth power of the distance between the protons in question. Hence, NOE acts as a sensitive 'molecular ruler'.

5.1.3b: Theoretical Predictions

Due to the time scale of NMR techniques, averaged inter-proton distances and angular information are obtained from the NOEs and J values.¹²⁷ Experimentally obtained $^3J_{C,H}$ coupling constants may be employed to further define the conformations of the glycosidic linkages (Figure 5.4). Since the number of distances or torsional angle constraints are limited, NMR data are generally supported by molecular modeling calculations in order to

refine the results. The two approaches are complementary since NMR measurements are useful in determining the possible conformations, and energy calculations are useful in determining which conformations are accessible.

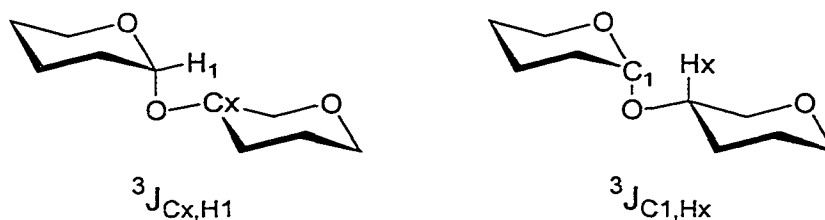


Figure 5.4: $^3J_{C,H}$ coupling constants about the glycosidic linkage.

One of the earliest conformational energy calculations on oligosaccharides was developed by Lemieux *et al.*^{241,250,254} At about the same time Rees also used a related approach to describe polysaccharide conformation.²⁵⁵ Lemieux used a simple forcefield (mathematical expression) which considers the non-bonded interactions (Kitaygorodsky function)²⁵⁶ between the sugar residues, the *exo*-anomeric effect and a rigid monosaccharide chair geometry to calculate the relative energies of oligosaccharides. The forcefield was named “Hard Sphere *Exo*-Anomeric Effect” (HSEA).^{241,254} HSEA calculations were found to give results which correlated well with those obtained by NMR experiments.²⁵⁷

The NMR-based conformational analysis of oligosaccharides generally has one of two goals: either to determine the solution conformation for its own sake, or to determine the effects of binding to a protein in that conformation. In the first case, the traditional approach has been to use distance-mapping procedures to determine the sterically allowed and NOE-consistent conformations, often using the HSEA forcefield^{241,254} and more recently including ensemble averaging of conformational states.²⁵²

Unlike proteins for which there are large numbers of intra-residue NOEs, oligosaccharides almost invariably provide insufficient NOE or

coupling constant data to define unique conformations. Consequently, conformational studies of oligosaccharides employ a combination of theoretical calculations and experimental NMR data. Initially, NOE derived inter-proton distances were compared with those predicted by potential energy calculations that assumed (at least for the purpose of the calculation) a single dominant conformation.^{241,254} Later approaches incorporated a Boltzman weighted distribution of conformers across the potential surface described by the forcefield selected for the potential energy calculations.²⁵⁸

With the increased capacity of computers, it has become possible to perform more elaborate calculations, such as molecular dynamics (MD) simulations over extended time intervals.²⁵⁹ These calculations provide a trajectory of oligosaccharide motions and permit the computation of time averaged inter-proton distances. The molecular models developed using MD approaches may even be used to back-calculate NOEs.²⁵² Similar information may also be generated by Monte Carlo (MC) minimization routines²⁵⁸ that can be applied to forcefields, such as HSEA or its successor GEGOP,¹³² that have proved successful in modeling carbohydrates.

Irrespective of the precise approach adopted (MD or MC), calculated inter-residue proton-proton distances are compared to experimentally determined values. The agreement between the calculated and experimentally derived data is taken as supporting the particular conformation(s).

In the last decade, the use of Monte Carlo sampling or molecular dynamics simulation has become more popular since they provide ensemble averages of conformations rather than a single conformation. The ensemble averages are often more representative of the properties of solvated oligosaccharides than any single conformation.²⁶¹

The solution conformation of trisaccharide **1** was determined using T-ROESY (homonuclear 2D transverse rotating-frame nuclear Overhauser effect)^{262,263} data to obtain distance restraints for molecular modeling.

5.2.1: Proton and Carbon Assignments for the H-type 2 Trisaccharide

Assignments were made for all ¹H and ¹³C resonances of **1** in D₂O at 300 K (Table 5.1) using 1D ¹H-NMR, GCOSY and HMQC data (Figure 5.5, 5.6 and 5.7). The coupling pattern for this trisaccharide was determined by the heavily overlapped GCOSY and decoupled HMQC data. HMQC experiments were used to assign the chemical shifts of overlapping protons in the crowded spectral envelope spanning 3.40 to 3.95 ppm.

Table 5.1: Proton and carbon assignments and coupling constants^a for H-type 2 trisaccharide **1** in D₂O at 300K.

Proton	βGlcNAc	βGal	αFuc
H1	4.45(8.3)	4.55(8.3)	5.31(2.9)
H2	3.76	3.68	3.82
H3	3.66	3.85(3.5)	3.82
H4	3.77(9.8)	3.89(0.6)	3.83
H5	3.47(2.1, 5.8)	3.71	4.23(6.7)
H6a	4.00(12.1)	3.82	1.23
H6b	3.82	3.75	
NHAc	2.04		
OCH ₃	3.51		
C1	102.8(162.0)	101.1(163.6)	100.2(175.0)
C2	56.0	77.2	72.5
C3	73.3	74.4	69.9
C4	77.0	70.2	70.5
C5	76.1	76.1	67.7
C6	61.0	61.9	16.1
NHAc	23.0		
OCH ₃	57.9		

^aNumbers in parentheses refer to ³J proton coupling constants, and for the carbon resonances, the number refers to the ¹J_{C,H} coupling constant.

The ¹J_{C,H} values of 162.0 Hz and 163.6 Hz obtained for H1 and H1' confirm the β-linkages, whereas the ¹J_{C,H} of 175.0 Hz for H1'' establishes the

α -linkage. Verification of the positions glycosidic linkages was made by means of an HMBC experiment (Figure 5.8).

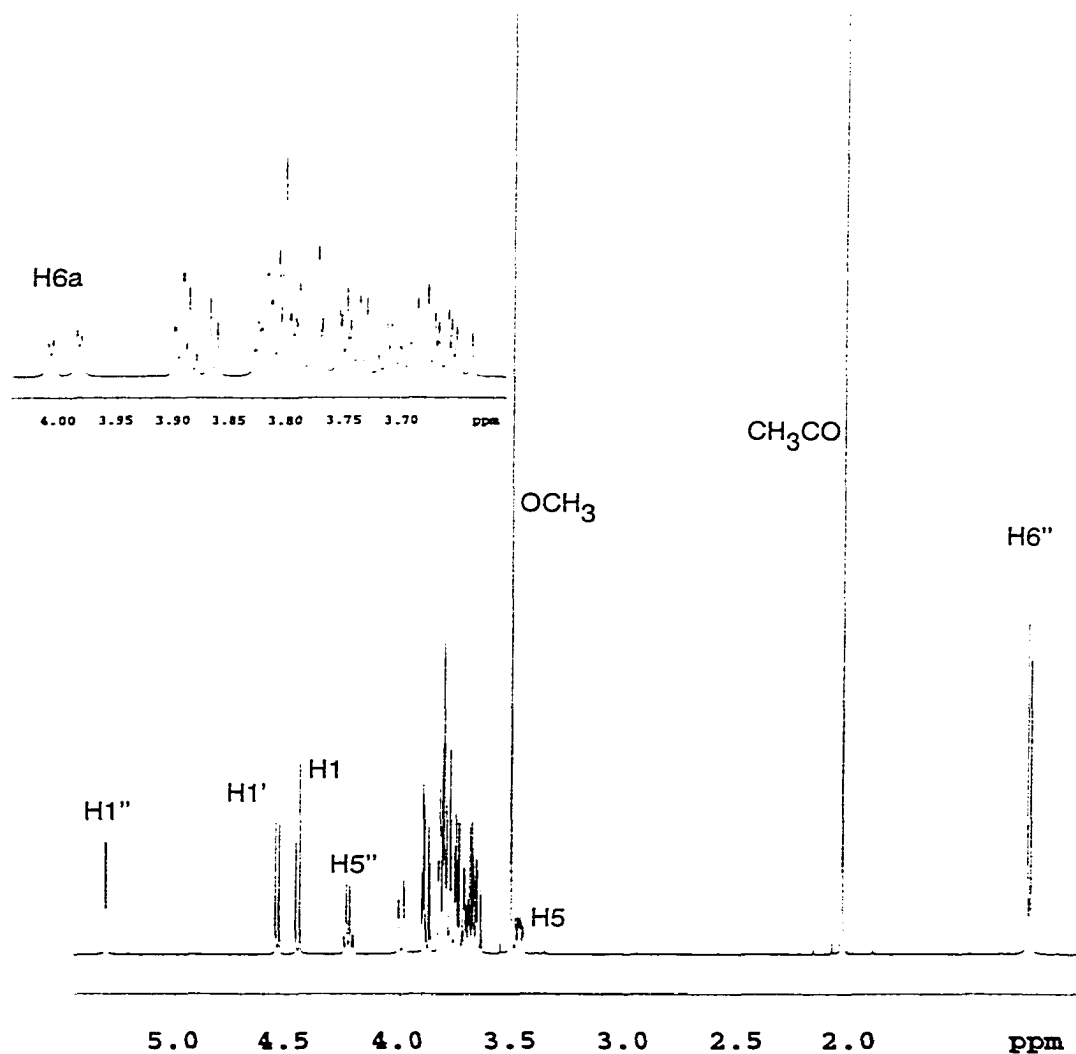


Figure 5.5: 1D ¹H-NMR spectrum of H-type 2 trisaccharide 1 in D₂O.

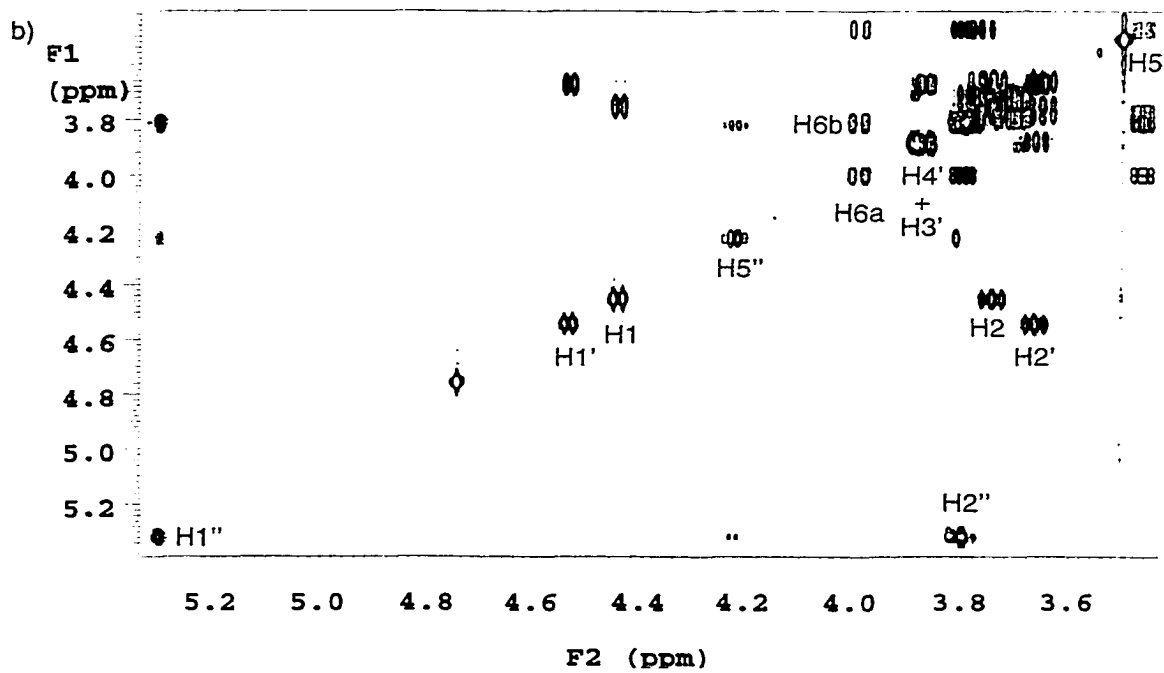
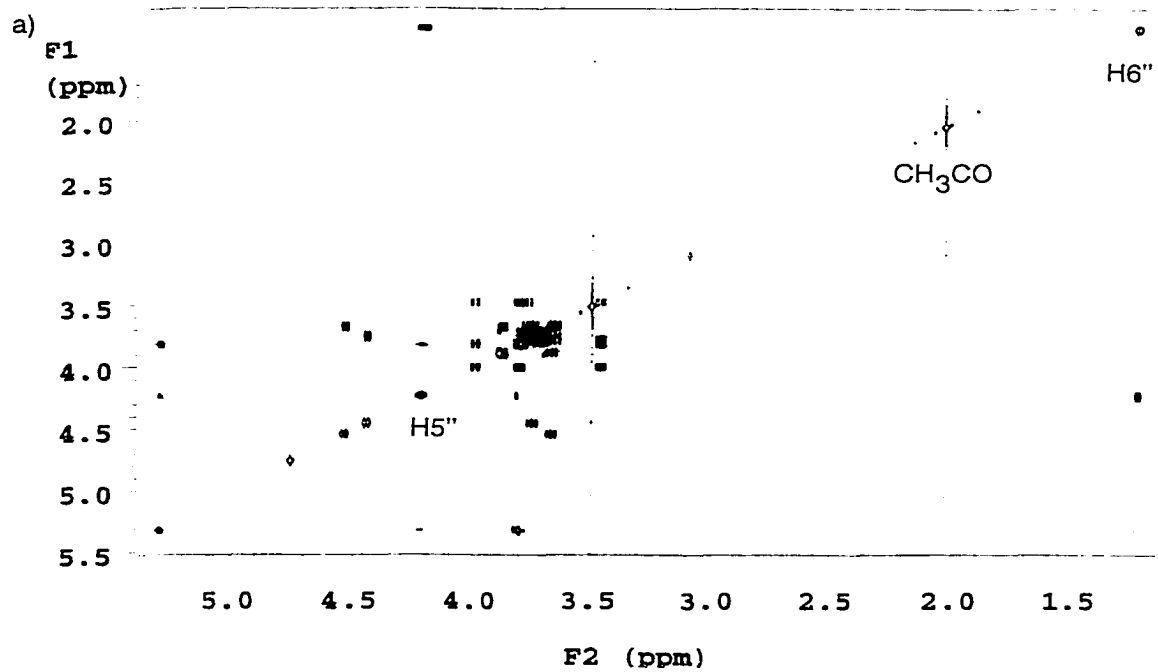


Figure 5.6: GCOSY spectrum of H-type 2 trisaccharide **1** in D₂O.

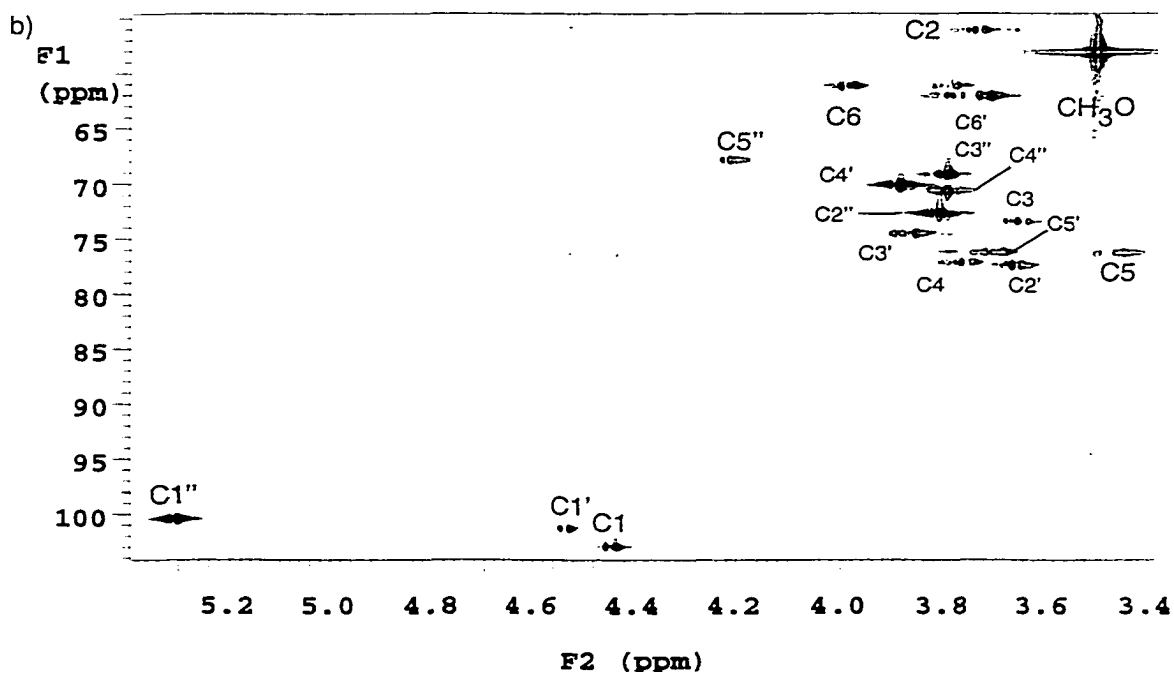
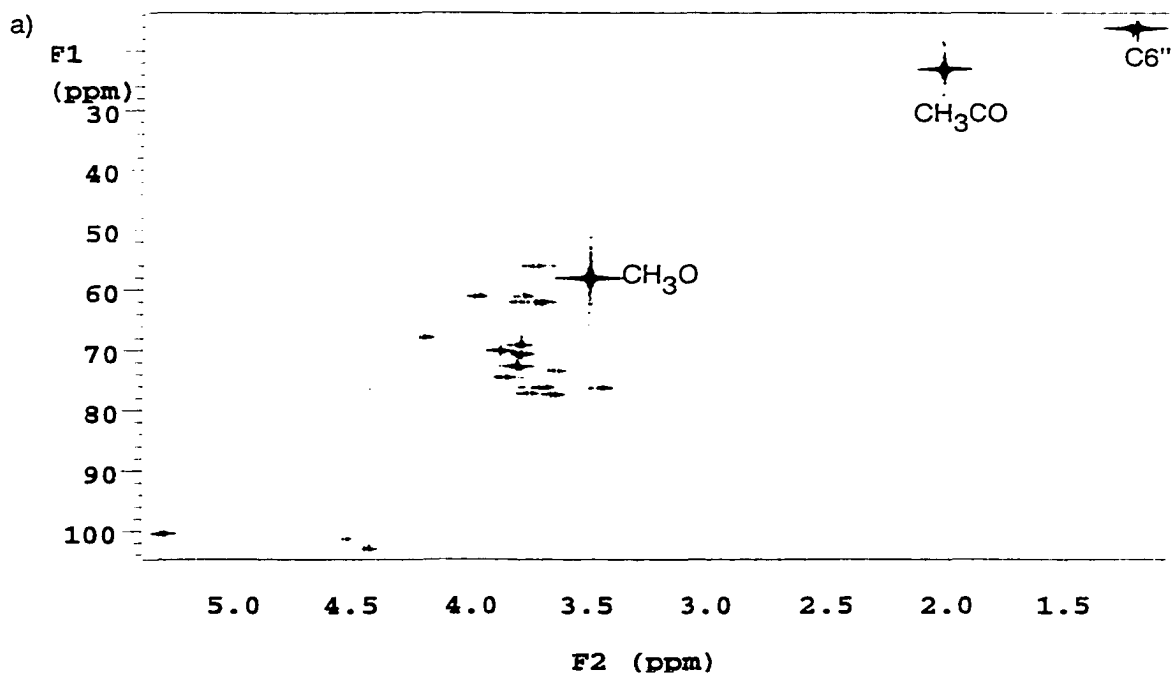


Figure 5.7: Decoupled HMQC spectrum of H-type 2 trisaccharide 1 in D₂O.

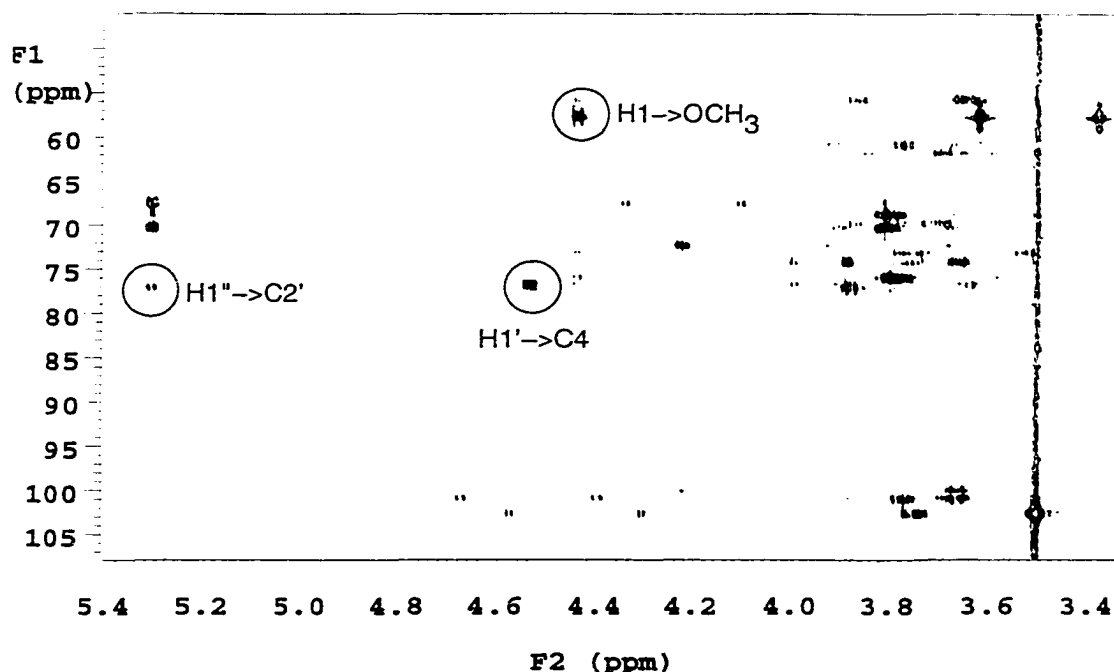


Figure 5.8: HMBC spectrum of H-type 2 trisaccharide **1** in D₂O.

5.2.2: T-ROESY Distance Measurements for the H-type 2 Trisaccharide 1

Distance constraints to be used in the molecular modeling of the free H-type 2 trisaccharide **1** were derived from a T-ROESY experiment (Figure 5.9). Integrated ROE volumes were converted to inter-residue proton-proton distances by comparison with the integrated volumes of a known intra-residue distance such as that in β -D-galactose H1-H5 (2.20 Å) or α -L-fucose H1''-H2'' (2.44 Å). A set of distances was derived for each internal reference and then averaged to give the NOE-derived proton-proton distances (Table 5.2).

As indicated in Table 5.2, NMR constraints were assigned to three restraint groups: strong, medium and weak. Each group was set to a minimum distance of 1.8 Å and a maximum distance of 2.7 Å for strong, 3.3 Å for medium, and 5.0 Å for weak. These restraints were used in the molecular modeling of the trisaccharide **1**. As indicated in Table 5.2, some restraints were weakened in the molecular modeling process in order to generate structures that did not violate the restraints.

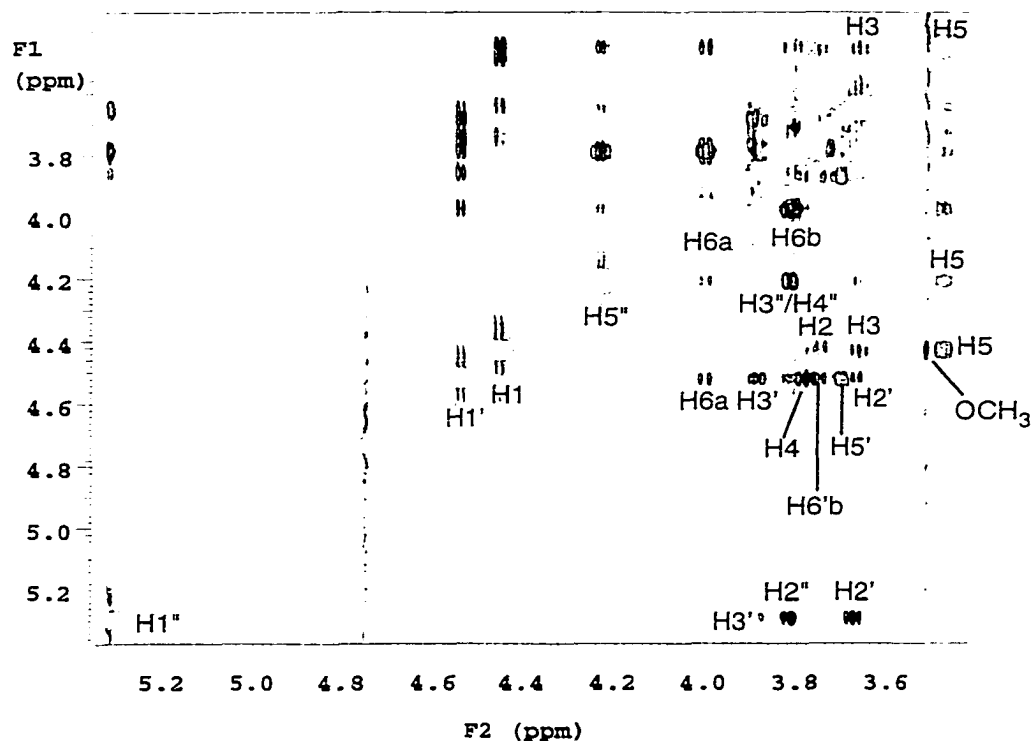


Figure 5.9: T-ROESY spectrum of H-type 2 trisaccharide 1 in D₂O.

Table 5.2: Experimental ROE values and distance restraints (Å) for modeling studies of H-type 2 trisaccharide 1.

Proton Pairs	Relative ROE	Distance (Å)	Restraint ^a
H1''/H2'	0.77	2.3	Strong
H1''/H3'	0.39	4.8	Weak
H1'/H6a	0.31	2.7	Medium ^a
H1'/H4	1.00	2.2	Strong
H5''/H6a	0.18	3.0	Medium
H5''/H5	0.27	2.8	Medium

^aRestraints were relaxed by one degree for molecular modeling.

From the T-ROESY correlations certain conclusions may be made about the position of the glycosidic linkage and conformation of the sugar. The strong correlation between H1' and H4 confirms the correct linkage of the galactose residue to that of *N*-acetylglucosamine. This strong correlation also indicates that the protons about that glycosidic linkage adopt the predicted *syn*-conformation.

The strong correlation between H1'' and H2' verifies the desired linkage between the fucose and galactose residues. As mentioned above, this strong correlation also indicates that the protons about this glycosidic linkage adopt the expected *syn*-conformation.

5.2.3: Solution Conformation of the Trisaccharide 1

To model the three dimensional shape of the trisaccharide **1**, the AMBER forcefield^{264,265} with additional parameters derived for carbohydrates^{266,267} was used for molecular mechanics and dynamics simulations. The generation of 10 pseudorandom starting structures by dynamic quenching, was followed by restrained simulated annealing and minimization to give families of minimized structures consistent with the ROE distance restraints shown in Table 5.2.

In the case of trisaccharide **1**, this minimized into a major family of structures (Figure 5.10a) about the $\beta\text{Galp}(1\rightarrow4)\text{GlcPNAc}$ ($\phi \approx 42^\circ$, $\psi \approx 4^\circ$) and $\alpha\text{Fucp}(1\rightarrow2)\text{Galp}$ ($\phi \approx 44^\circ$, $\psi \approx 14^\circ$) glycosidic linkages. The major family represents a group of structures in which the anomeric and aglyconic protons of the two glycosidic linkages have the usual *syn*-conformation. The minimization of **1** also gave a second minor family of structures (Figure 5.10b) about the $\beta\text{Galp}(1\rightarrow4)\text{GlcPNAc}$ ($\phi \approx 31^\circ$, $\psi \approx -153^\circ$) and $\alpha\text{Fucp}(1\rightarrow2)\text{Galp}$ ($\phi \approx 52^\circ$, $\psi \approx -1^\circ$) glycosidic linkages. The minor family represents structures in which the protons on the $\beta\text{Galp}(1\rightarrow4)\text{GlcPNAc}$ linkage are close to being in the *anti*-conformation. The lowest energy structure belonged to the major family of conformers (Figure 5.11).

It has been established that in a flexible molecule, such as an oligosaccharide, the proton-proton distances derived from NOESY or T-ROESY data do not represent a single or true solution conformer but a r^{-6} weighted average of all of the conformers present in solution.¹⁰⁴ In an attempt to simulate the dynamic behavior of the H-type 2 trisaccharide **1** in solution, restrained molecular dynamics (MD) simulations were performed.

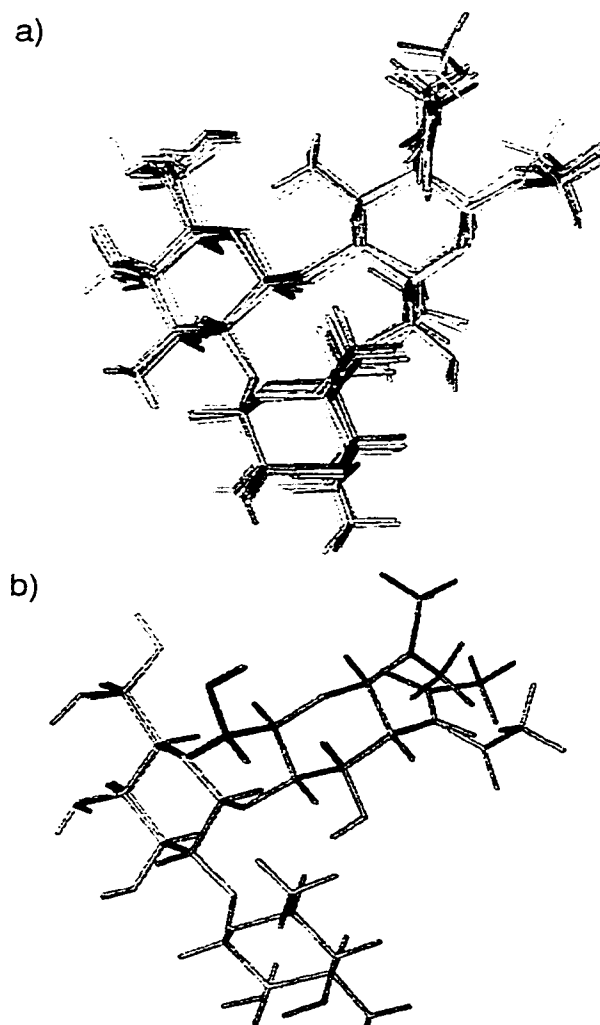


Figure 5.10: Energy minimization of trisaccharide 1 using ROE restraints produced a) a major family of structures, and b) a minor family of structures.

The lowest energy structure (Figure 5.11) was chosen from the minimized conformers as the starting point for a 5 ns dynamic simulation, using the same restraints as described in Table 5.2. From the MD data, the values of ϕ and ψ about both glycosidic linkages were plotted over the time course of a 5000 ps MD simulation at 300 K (Figure 5.11). The trajectory of a MD simulation illustrates the degree of motional freedom, or the area of conformation space available to the oligosaccharide.

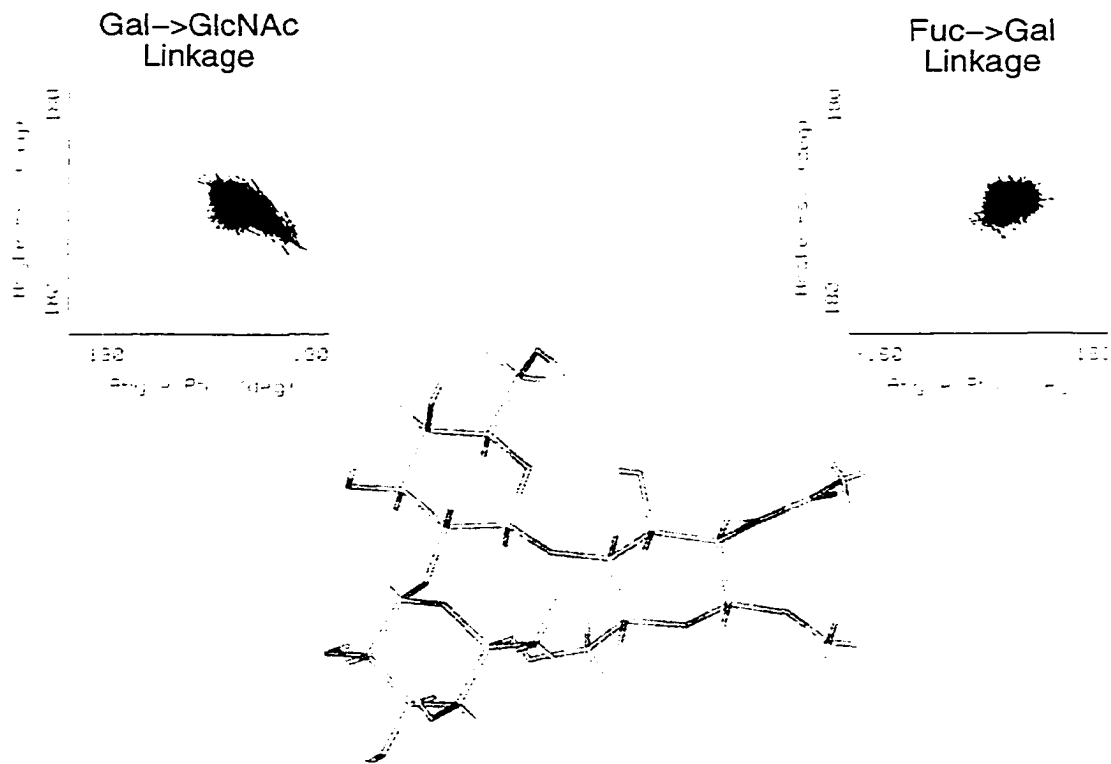


Figure 5.11: Lowest energy structure of **1** with graphs that depict the trajectory of a 5000 ps MD simulation about both glycosidic linkages.

Theoretical, back-calculated inter-proton distances were obtained from the restrained dynamics simulation using software provided by the Homans' group (MDPROCESS) using a r^{-6} formalism (Table 5.3). When comparing theoretical and experimental inter-proton distances, values that differ by 20% or less are considered to lie within experimental error.²⁶⁸ The results obtained from the dynamics simulation, with the exception of the H1''-H3' distance, were in reasonable agreement with the experimental inter-proton distances derived from T-ROESY correlations. Hence, the lowest energy conformer

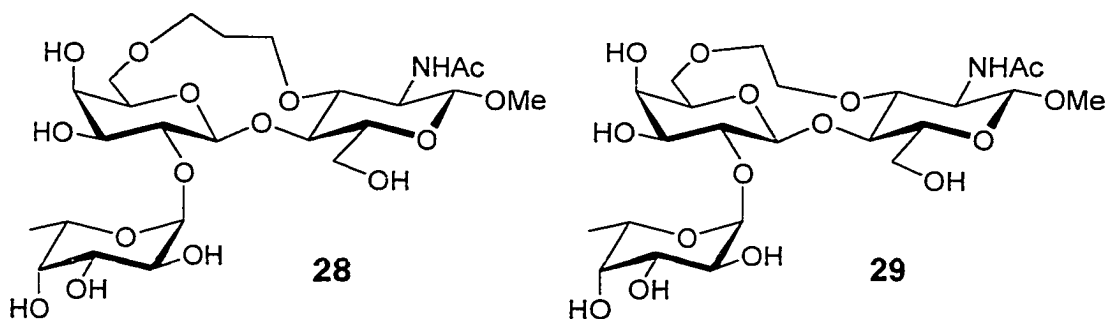
(Figure 5.11) is representative of the free solution conformation of H-type 2 trisaccharide.

Table 5.3: Calculated and experimental inter-proton distances for the H-type 2 trisaccharide.

Inter-residue Proton Pairs	Calculated distance (Å)	Experimental distance (Å)
H1''/H2'	2.3	2.3
H1''/H3'	3.8	4.8
H1'/H6a	2.4	2.7
H1'/H4	2.5	2.2
H5''/H6a	2.7	3.0
H5''/H5	2.5	2.8

5.3: The Solution Conformation of Constrained Trisaccharides 28 and 29

The solution conformation of the constrained H-type 2 derivatives **28** and **29** were determined to allow a comparison with that of the native H-type 2 trisaccharide (**1**). This comparison will aid in accounting for inhibition activity differences of **28** and **29** with the legume lectin, *Ulex europaeus* I. The solution conformation of constrained trisaccharide **28** and **29** was determined using T-ROESY data to obtain distance restraints for molecular modeling.



5.3.1: Proton and Carbon Assignments for Trisaccharides 28 and 29

Assignments for **28** and **29** are based on 1D $^1\text{H-NMR}$, GCOSY and HMQC data, as was done for the H-type 2 trisaccharide **1**, and summarized in Tables 5.4 and 5.5.

Table 5.4: Proton and carbon assignments with coupling constants^a for constrained trisaccharide **28** in D₂O at 300K.

Proton	βGlcNAc	βGal	αFuc	Tether
H1	4.45(8.2)	4.46(8.1)	5.39(2.0)	
H2	4.13(11.0)	3.71(9.5)	3.82 ^b	
H3	3.77(9.5)	3.86	3.81 ^b	
H4	4.09(9.5)	3.78	3.81 ^b	
H5	3.45(1.8)	3.79	4.18(6.8)	
H6a	4.07(11.7)	3.87	1.25	
H6b	3.85	3.79		
NHAc	2.04			
OCH ₃	3.52			
Gal-CH ₂				3.78, 3.65
GlcNAc-CH ₂				3.87, 3.44
CH ₂				1.72-1.79
C1	104.0(160.7)	103.0(161.7)	100.1(175.2)	
C2	51.2	76.1	72.6 ^b	
C3	79.0	75.0	69.0 ^b	
C4	74.4	69.9	70.4 ^b	
C5	76.4	75.6	67.7	
C6	61.2	69.4	16.1	
NHAc	22.9			
OCH ₃	58.1			
Gal-CH ₂				69.4
GlcNAc-CH ₂				57.7
CH ₂				29.5

^aNumbers in parentheses refer to 3J proton coupling constants, and for the carbon resonances, the number refers to the $^1J_{\text{C,H}}$ coupling constant.

^bAssignments established by comparing with assignments of **1**.

As in the case of H-type 2 trisaccharide **1**, the $^1J_{\text{C,H}}$ values obtained for H1 and H1' of the tethered trisaccharides **28** and **29** were consistent with β -glycosidic linkages, whereas the $^1J_{\text{C,H}}$ of H1'' for the two tethered

trisaccharides confirmed that the fucose residues were α -linked to galactose. As in the structure determination of **1**, verification of the position of glycosidic linkages was made from HMBC data.

Table 5.5: Proton and carbon assignments with coupling constants^a for constrained trisaccharide **29** in D₂O at 300K.

Proton	β GlcNAc	β Gal	α Fuc	Tether
H1	4.50(8.6)	4.44(7.7)	5.48(3.5)	
H2	3.79	3.75(9.3)	3.82 ^b	
H3	3.64	3.90(3.5)	3.82 ^b (3.5)	
H4	3.65	3.83	3.88 ^b (0.9)	
H5	3.56	3.53	4.19(6.6)	
H6a	3.93	3.94	1.25	
H6b	3.80	3.58		
NHAc	2.02			
OCH ₃	3.51			
Gal-CH ₂				3.92, 3.51
GlcNAc-CH ₂				4.13(1.8, 12.3), 3.56
C1	101.8(163.2)	103.3(161.7)	99.3(174.1)	
C2	55.9	75.6	70.3 ^b	
C3	82.6	75.2	69.0 ^b	
C4	74.9	72.5	70.1 ^b	
C5	80.7	76.1	67.6	
C6	62.5	69.9	16.1	
NHAc	22.8			
OCH ₃	57.8			
Gal-CH ₂				71.7
GlcNAc-CH ₂				71.1

^aNumbers in parentheses refer to ³J proton coupling constants, and for the carbon resonances, the number refers to the ¹J_{C,H} coupling constant.

^bAssignments established by comparison with assignments of **1**.

5.3.2: T-ROESY Distance Measurements for Constrained Trisaccharides 28 and 29

The ROEs between inter-residue proton pairs and their ROE ratios for constrained trisaccharides **28** and **29** were determined by T-ROESY and normalized as described for **1** (Table 5.6).

Strong correlations between H1' and H4 were observed, in both tethered trisaccharide **28** and **29**, confirming the correct linkage of the galactose residue to *N*-acetylglucosamine and the predicted *syn*-conformation. The same applies to the fucose-galactose linkage based on the H1''/H2' interaction.

Table 5.6: Interproton distances (Å) derived from experimental ROE values for constrained trisaccharides **28** and **29**.

Proton pairs	Tethered trisaccharide 28			Tethered trisaccharide 29		
	Relative ROE	Dist. (Å)	Restraint	Relative ROE	Dist. (Å)	Restraint
H1''/H2'	1.00	2.6	Strong	1.00	2.6	Strong
H1''/H3'	0.07 ^a	4.0 ^a	Weak	^a	3.7 ^a	Weak
H1'/H6a						
H1'/H4	2.57	2.3	Strong	^a	2.4 ^a	Strong
H5''/H6a	0.09	3.1	Medium	^a	^a	
H5''/H5	0.66	2.8	Strong ^b			Strong
H1/OCH ₃	0.93	2.8	Medium		2.6	

^aNot calculated due to overlapping resonances.

^bRestraint had to be weakened.

5.3.3: Solution Conformation of the Constrained Trisaccharides 28 and 29

Families of minimized structures consistent with the ROE distance restraints derived from T-ROESY data for the constrained trisaccharide **28** and **29** were obtained as described for the native H-type 2 trisaccharide **1**.

Constrained trisaccharide **28**, when minimized gave a major family of structures (Figure 5.12a) about the $\beta\text{Galp}(1\rightarrow4)\text{Glc pNAc}$ ($\phi \approx 34^\circ$, $\psi \approx 4^\circ$) and $\alpha\text{Fucp}(1\rightarrow2)\text{Galp}$ ($\phi \approx 49^\circ$, $\psi \approx 19^\circ$) glycosidic linkages, representing a group of structures in which the protons on the two glycosidic linkages have the usual *syn*-conformation. The minimization of H-type 2 trisaccharide **28** also gave a second minor family of structures (Figure 5.12b) about the $\beta\text{Galp}(1\rightarrow4)\text{Glc pNAc}$ ($\phi \approx 43^\circ$, $\psi \approx 5^\circ$) and $\alpha\text{Fucp}(1\rightarrow2)\text{Galp}$ ($\phi \approx -21^\circ$, $\psi \approx -25^\circ$) glycosidic linkages. The minor family represents structures in which the conformation about the $\beta\text{Galp}(1\rightarrow4)\text{Glc pNAc}$ glycosidic linkage is very

similar to the structures in the major family. The major difference lies in the $\alpha\text{Fucp}(1\rightarrow2)\text{Galp}$ glycosidic linkage, where the fucose residue has been rotated. The lowest energy structure belonged to the major family of conformers.

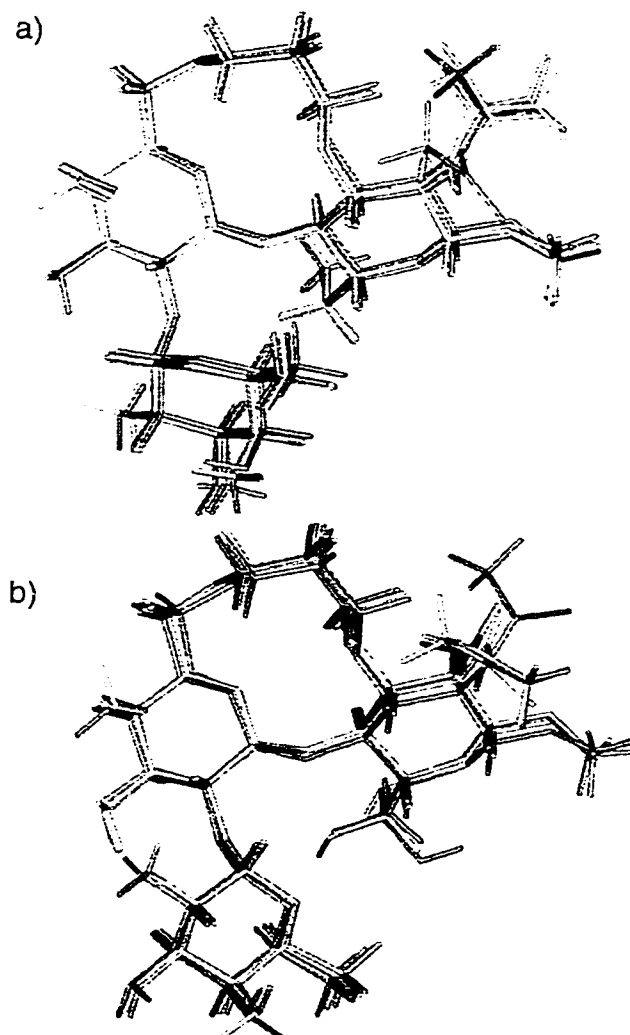


Figure 5.12: The minimization of constrained trisaccharide **28** using its ROE restraints produced a) a major, and b) a minor family of structures.

The constrained trisaccharide **29**, minimized into a major family of structures (Figure 5.13a) about the $\beta\text{Galp}(1\rightarrow4)\text{Glc}p\text{NAc}$ ($\phi \approx 41^\circ$, $\psi \approx -11^\circ$) and $\alpha\text{Fucp}(1\rightarrow2)\text{Galp}$ ($\phi \approx 49^\circ$, $\psi \approx 19^\circ$) glycosidic linkages. The major family represents a group of structures in which the protons on the two glycosidic linkages have the usual *syn*-conformation.

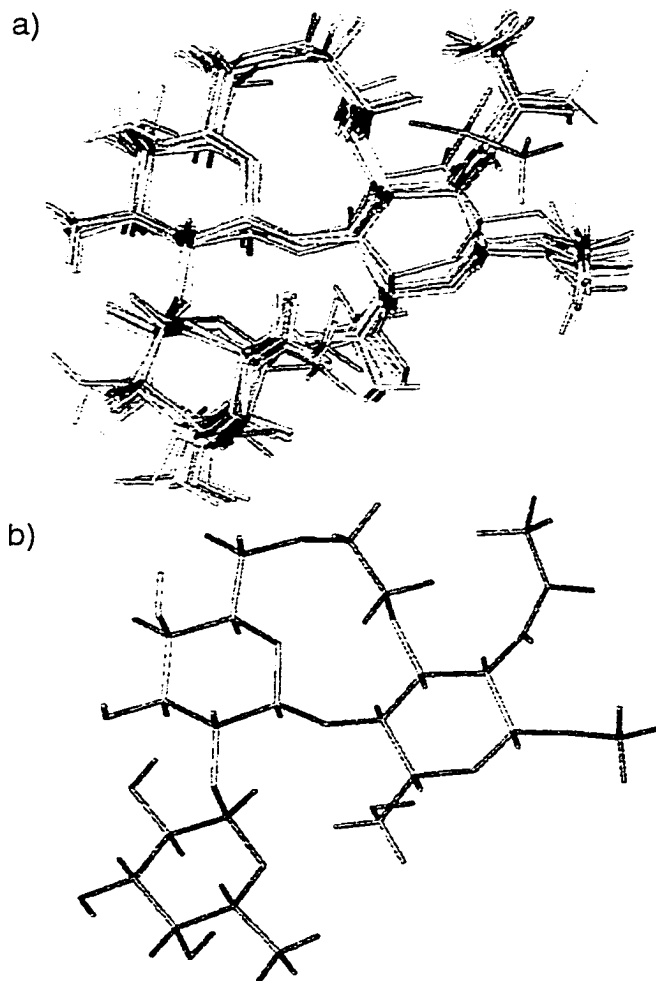


Figure 5.13: The minimization of constrained trisaccharide **29** using its ROE restraints produced a) a major, and b) a minor family of structures.

The minimization of trisaccharide **29** also gave a second minor family of structures (Figure 5.13b) about the $\beta\text{Galp}(1\rightarrow4)\text{Glc}p\text{NAc}$ ($\phi \approx 41^\circ$, $\psi \approx -11^\circ$) and $\alpha\text{Fucp}(1\rightarrow2)\text{Galp}$ ($\phi \approx -22^\circ$, $\psi \approx -19^\circ$) glycosidic linkages. In this case, as for compound **28**, the minor family represents structures in which the conformation about the $\beta\text{Galp}(1\rightarrow4)\text{Glc}p\text{NAc}$ glycosidic linkage is very similar to the structures in the major family, and the main difference involves the $\alpha\text{Fucp}(1\rightarrow2)\text{Galp}$ glycosidic linkage, where the fucose residue has been rotated. The lowest energy structure was determined to belong to the major family of conformers.

In order to simulate their dynamic behavior, restrained molecular dynamics (MD) simulations were performed for the tethered trisaccharides **28** and **29**. The starting point for 5 ns of restrained simulated annealing used the lowest energy structures of each molecule (Figure 5.14) obtained from the minimized conformers.

The same restraints as described in Table 5.6 were used for the MD simulation. From the MD data, the values of ϕ and ψ about both glycosidic linkages were plotted over the time course of a 5000 ps MD simulation at 300K (Figure 5.14). The trajectory of a MD simulation illustrates the degree of motional freedom, or the area of conformational space available to the oligosaccharide.

Theoretical, back-calculated inter-proton distances were obtained from the restrained dynamics simulation (Table 5.7). The results obtained from the dynamics simulation (calculated distances) were in reasonable agreement with the experimental inter-proton distances derived from T-ROESY correlations. Hence, the two lowest energy conformers (Figure 5.14) are representative of the free solution conformation of the constrained trisaccharides **28** and **29**.

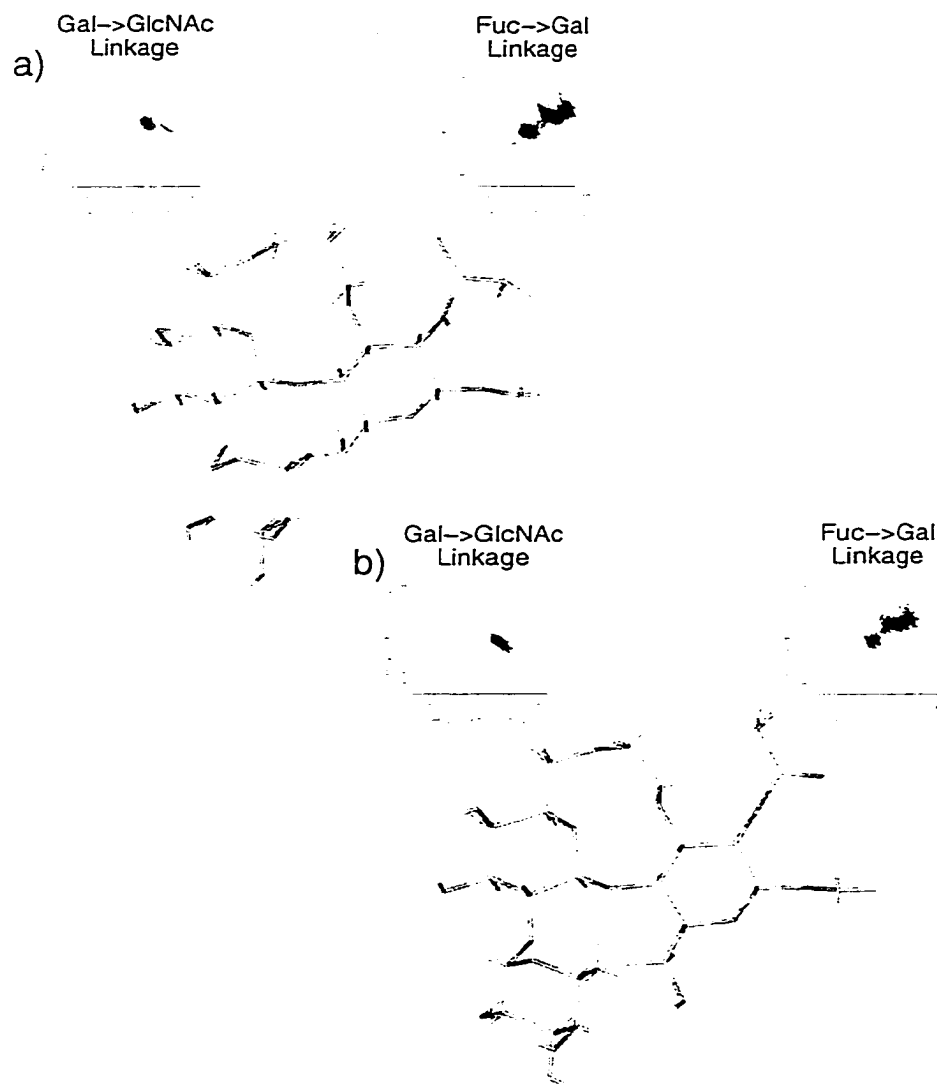


Figure 5.14: Lowest energy structure obtained from the minimization used as a starting point for the MD simulations of the constrained trisaccharides a) **28** and b) **29**. Graphs depict the trajectory of a 5000 ps MD simulation of the constrained trisaccharides about both glycosidic linkages.

Table 5.7: Calculated and experimental interproton distances (Å) obtained for constrained trisaccharides **28** and **29**.

Inter-residue Proton Pairs	Tethered Trisaccharide 28		Tethered Trisaccharide 29	
	Calculated Distance (Å)	Experimental Distance (Å)	Calculated Distance (Å)	Experimental Distance (Å)
H1''/H2'	2.3	2.6	2.4	2.6
H1''/H3'	3.8	4.0	3.5	3.7
H1'/H6a	2.1 & 2.6	^a	3.2 & 3.6	^a
H1'/H4	2.2	2.3	2.4	2.4
H5''/H6a	2.5	3.1	2.5	^a
H5''/H5	2.7	2.8	3.3	^a

^aNot calculated due to overlapping resonances.

5.4: Comparison of Solution Conformation of 1 and its Tethered Derivatives 28 and 29

In comparing the calculated and experimental results of the solution conformation of **1** with those of the trisaccharides **28**, and **29** (Table 5.8 and 5.9), it appears that the constrained H-type 2 derivatives maintain the overall shape of the epitope. This is evident when the lowest energy structures of H-type 2 trisaccharide are superimposed over that of the constrained derivatives **28** and **29** (Figure 5.15). Since the fucose residue contains the functional groups most important in the H-type 2 trisaccharide-*Ulex* interaction, the fucose residues of the trisaccharides in Figure 5.15 were overlapped.

Table 5.8: NOE distances obtained from NMR and theoretical investigation of the solution conformation of H-type 2 trisaccharide **1**, and constrained trisaccharides **28** and **29**.

Proton pairs	Native H-type 2 (1)		Tethered 28		Tethered 29	
	Calc. dist. (Å)	Exp't. dist. (Å)	Calc. Dist. (Å)	Exp't. dist. (Å)	Calc. dist. (Å)	Exp't. dist. (Å)
H1''/H2'	2.3	2.3	2.3	2.6	2.4	2.6
H1''/H3'	3.8	4.8	3.8	4.0	3.5	3.7
H1'/H6a	2.4	2.7	2.1 & 2.6	^a	3.2 & 3.6	^a
H1'/H4	2.5	2.2	2.2	2.3	2.4	2.4
H5''/H6a	2.7	3.0	2.5	3.1	2.5	^a
H5''/H5	2.5	2.8	2.7	2.8	3.3	^a

^aNot observed due to overlapping resonances.

Table 5.9: Torsional angles obtained from theoretical calculations for the solution conformation of trisaccharide **1**, tethered trisaccharides **28** and **29**.

Torsional angles	Native H-type 2		Tethered 28		Tethered 29	
	Major family	Minor family	Major family	Minor family	Major family	Minor family
$\phi_{\text{Gal}\rightarrow\text{GlcNAc}}$	42°	31°	34°	43°	41°	41°
$\psi_{\text{Gal}\rightarrow\text{GlcNAc}}$	4°	-153°	4°	5°	-11°	-11°
$\phi_{\text{Fuc}\rightarrow\text{Gal}}$	44°	52°	49°	-21°	49°	-22°
$\psi_{\text{Fuc}\rightarrow\text{Gal}}$	14°	-1°	19°	-25°	19°	-19°

In Figure 5.15, it can be seen that there has been some movement of the *N*-acetylglucosamine residue. Since it does not take part in any critical interaction with the *Ulex europaeus* I lectin, no important contacts will be lost, although it is possible that new steric clashes with the protein could arise.

The values of ϕ and ψ about both glycosidic linkages were plotted over the time course of the MD simulations for each of the trisaccharides. The trajectory of a MD simulation illustrates the degree of motional freedom, i.e. the conformational space available to the oligosaccharide. Comparing these trajectories (Figure 5.16), the most apparent observation is the extra flexibility in the $\alpha\text{Fucp}(1\rightarrow2)\text{Galp}$ linkage of both constrained trisaccharides. It seems that constraining one glycosidic linkage resulted in extra freedom of the second glycosidic linkage. Hence, the conformational entropy of the tethered molecules has been redistributed. Could this be a significant factor in their binding affinity with *Ulex* lectin? Another observation is the reduced flexibility of the $\beta\text{Galp}(1\rightarrow4)\text{GlcNAc}$ linkage, which was the aim of tethering these residues.

The family of geometries observed in the ϕ versus ψ graphs about the $\beta\text{Galp}(1\rightarrow4)\text{GlcNAc}$ linkages of both constrained trisaccharide are complementary. Together, they make up most of the family of geometries observed for the H-type 2 trisaccharide **1**.

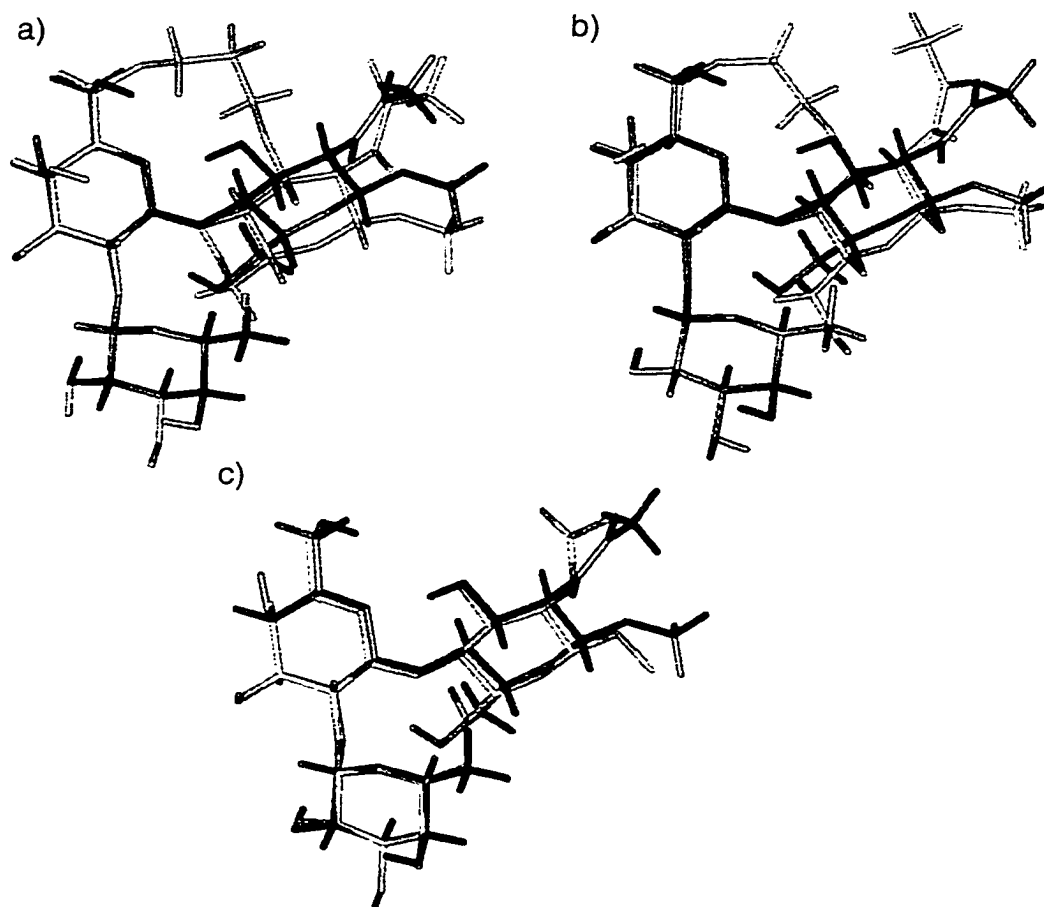


Figure 5.15: Superimpositions of the NMR derived lowest energy conformations of the native H-type 2 trisaccharide **1** (AMBER forcefield) with a) **28**, b) **29**, and c) the GEGOP global minimum for **1**.

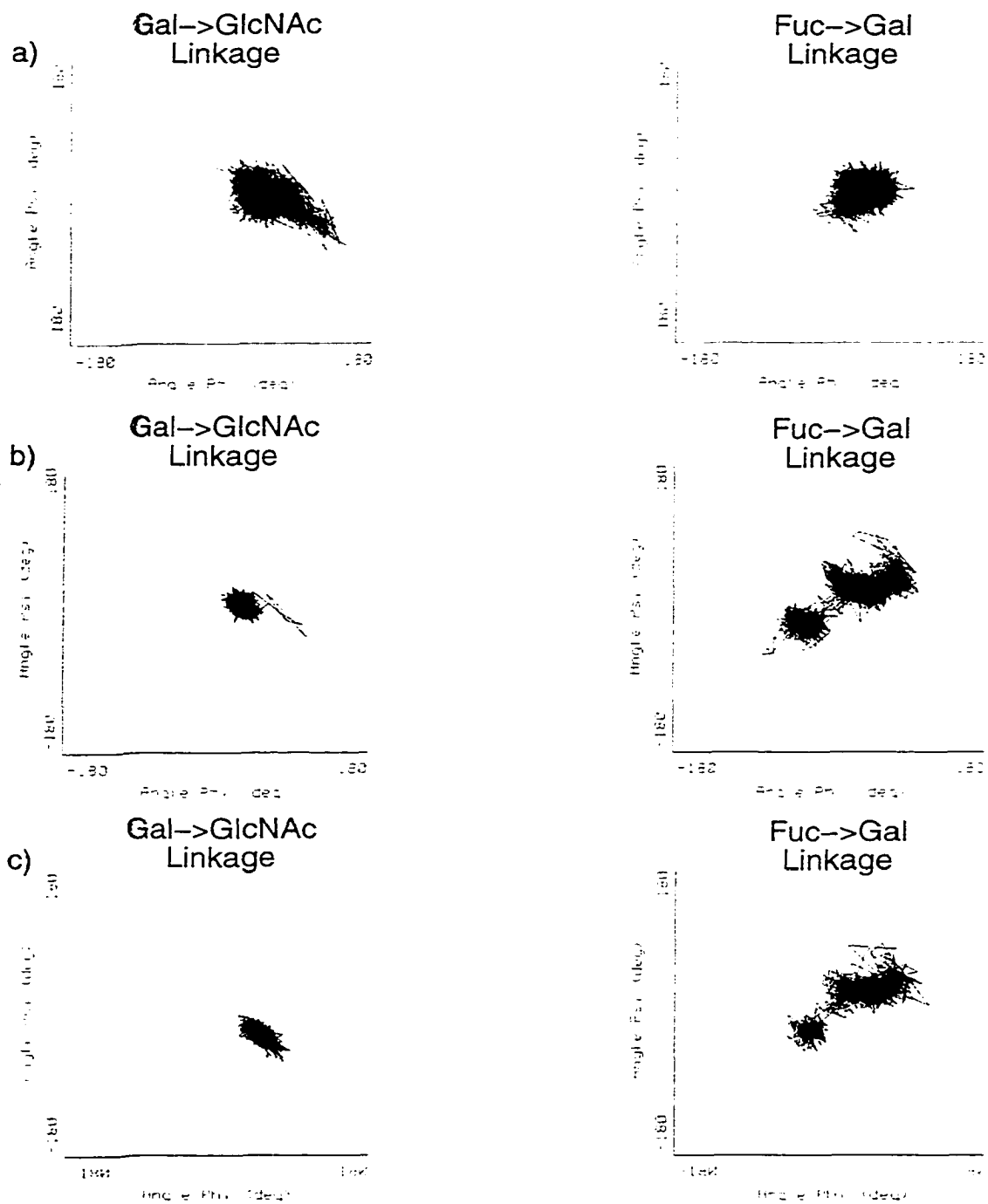


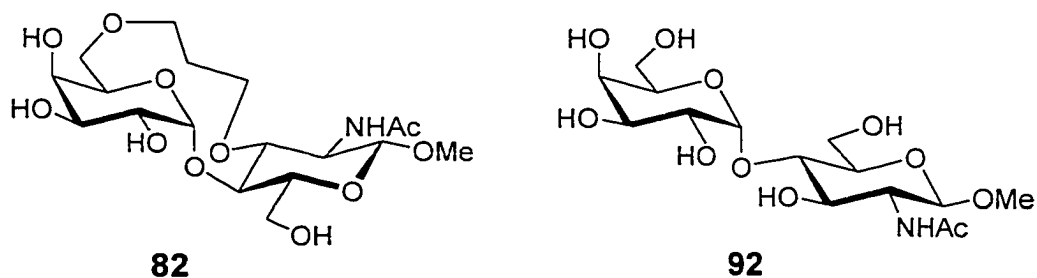
Figure 5.16: Graphs depicting the glycosidic linkage trajectory of the 5000 ps MD simulation of a) **1**, b) **28** and c) **29**.

Thus, tethering of the H-type 2 trisaccharide was successful in decreasing the flexibility of the molecule about the $\beta\text{Galp}(1\rightarrow4)\text{Glc}p\text{NAc}$ linkage while maintaining the conformation of the active epitope. Two points of concern are the apparent increase of flexibility about the $\alpha\text{Fucp}(1\rightarrow2)\text{Galp}$ linkage and the movement of the *N*-acetylglucosamine residue.

It should be pointed out that the *N*-acetyl group in the modeling of trisaccharides **1**, **28**, and **29** did not solely adopt the preferred *trans* conformation, even though AMBER^{264,265} was originally designed for the simulation of peptides. This demonstrates one limitation of the carbohydrate-modified AMBER forcefield.^{266,267}

5.5: Conformational Analysis of a $\alpha\text{Galp}(1\rightarrow4)\beta\text{Glc}p\text{NAc}\rightarrow\text{OCH}_3$ Disaccharide that Adopts the ANTI-Conformation

During the course of this investigation an unexpected synthetic product, disaccharide **82**, was produced. It was obtained from an intramolecular glycosylation that resulted solely in the α -disaccharide product. This section of the thesis describes attempts to probe its conformation and to compare it with the corresponding untethered $\alpha\text{Galp}(1\rightarrow4)\beta\text{Glc}p\text{NAc}\rightarrow\text{OCH}_3$ disaccharide **92**. The solution behaviour of tethered disaccharide **82** was determined using T-ROESY data to obtain distance restraints for molecular modeling. The importance of this work lies in the unique conformation of **82**, which permits the calibration of the heteronuclear three bond coupling constants in the *anti*-conformation.



5.5.1: Proton and Carbon Assignments for Tethered Disaccharide 82

Initial assignments were made for **82** in D₂O at 300 K (Table 5.10) using GCOSY and HMQC data as was done for the H-type 2 trisaccharide. The coupling pattern for disaccharide **82** is easily determined from the well resolved GCOSY spectrum (Table 5.10). Decoupled HMQC data were used to assign the chemical shifts of overlapping protons in the crowded spectral envelope spanning 3.92-3.67 ppm and to obtain coupling constants ³J_{H,H} which could not be determined from the ¹H-NMR data. The signals of C4 and C5 of βGlcNAc were assigned by HMBC.

Table 5.10: Proton and carbon assignments with ³J_{H,H} coupling constants for tethered disaccharide **82** in D₂O at 300K.

Proton	βGlcNAc	αGal	Tether
H1	4.45(8.5) ^a	5.31(3.1) ^a	
H2	3.79(10.2) ^b	3.86/3.89	
H3	3.97 ^c	3.89/3.86	
H4	3.74(3.8) ^b	3.89	
H5	3.73	4.55(2.1, 11.1) ^a	
H6a	4.14(11.3) ^a	3.88	
H6b	3.89	3.58(2.6, 13.0) ^a	
NHAc	2.03		
Gal-CH ₂			3.73(12.9) ^b , 3.46 ^c
GlcNAc-CH ₂			3.69(12.3) ^b , 3.91 ^c
CH ₂			1.65-1.80
C1	101.1(161.1) ^d	94.6(165.5) ^d	
C2	56.7	69.1/69.4	
C3	78.0	69.4/69.1	
C4	75.8	68.2	
C5	73.2	65.1	
C6	61.59	67.5	
NHAc	22.6		
Gal-CH ₂			60.5
GlcNAc-CH ₂			67.0
CH ₂			29.3

^aCoupling constants determined from ¹H-NMR.

^bCoupling constants determined from coupled HMQC data.

^cCoupling constants not obtained due to higher order signal.

^dCoupling constants (¹J_{C,H}) determined by coupled HMQC data.

Since H4 and H5 of β GlcNAc had degenerate chemical shifts in D₂O, it was not possible to determine the conformation of the tethered disaccharide **82** by a T-ROESY experiment in this solvent. Therefore, the NMR experiments were repeated in CD₃OD, where the H3, H4 and H5 resonances are resolved.

Assignments were made for **82** in CD₃OD at 300 K (Table 5.11) using GCOSY and HMQC data. The chemical shifts and $^3J_{H,H}$ coupling constants of **82** were obtained in the same manner as in D₂O (Table 5.10). The $^3J_{H,H}$ values measured for **82** are consistent with the 4C_1 chair conformation of both pyranose rings.²⁶⁹

Table 5.11: Proton and carbon assignments with $^3J_{H,H}$ coupling constants for tethered disaccharide **82** in CD₃OD at 300K.

Proton	β GlcNAc	α Gal	Tether
H1	4.31(8.4) ^a	5.16(3.7) ^a	
H2	3.72(8.8) ^b	3.80(10.4) ^b	
H3	3.92(9.2) ^b	3.75(3.3) ^a	
H4	3.74(12.4) ^b	3.67(1.8) ^a	
H5	3.55(4.6) ^a	4.52(11.2) ^a	
H6a	4.01(2.9, 11.7) ^a	3.93(12.7) ^b	
H6b	3.94	3.43(3.0) ^b	
NHAc	1.94		
Gal-CH ₂			3.79(12.7, 3.6) ^b , 3.32 ^c
GlcNAc-CH ₂			3.83 ^c , 3.74 (10.3, 1.8) ^b
CH ₂			1.58-1.72 ^c
C1	102.4(159.6) ^d	95.6(164.6) ^d	
C2	58.1	69.8	
C3	79.0	71.2	
C4	77.4	70.6	
C5	74.5	65.9	
C6	63.2	69.0	
NHAc	22.9		
Gal-CH ₂			60.9
GlcNAc-CH ₂			67.2
CH ₂			30.9

^a Coupling constants determined from 1H -NMR. ^b Coupling constants determined from coupled HMQC data. ^c Coupling constants not obtained because the signal was a complex multiplet. ^d Coupled HMQC determined $^1J_{C,H}$.

5.5.2: Proton and Carbon Assignments for Untethered Disaccharide 92

For comparison, assignments for α -lactosamine methyl glycoside **92** were made in CD₃OD at 300 K (Table 5.12) using GCOSY and HMQC data as described for tethered disaccharide **82**. In comparing the $^3J_{H,H}$ values of **82** and **92**, it is apparent that they are consistent with the 4C_1 chair conformation.²⁶⁹

Table 5.12: Proton and carbon assignments with $^3J_{H,H}$ coupling constants for disaccharide **92** in CD₃OD at 300K.

Proton	β GlcNAc	α Gal
H1	4.32(7.9) ^a	5.21(3.8) ^a
H2	3.69(10.2) ^b	3.83(12.6) ^b
H3	3.70(11.4) ^b	3.70
H4	3.56(9.5) ^b	3.87
H5	3.36(2.2, 4.8) ^a	3.91
H6a	3.90(14.4) ^b	3.74(10.2) ^b
H6b	3.83	3.67
NHAc	1.96	
C1	103.1(162.0) ^d	102.73(174.0) ^d
C2	56.4	70.5
C3	75.4	71.1
C4	81.1	70.6
C5	76.4	73.1
C6	61.9	62.5
NHAc	22.4	

^a Coupling constants determined from 1H -NMR.

^b Coupling constants determined from coupled HMQC data.

^c Coupling constants not obtained because the signal was a complex multiplet.

^d Coupling constants ($^1J_{C,H}$) determined by coupled HMQC data.

5.5.3: T-ROESY Distance Measurements for Tethered Disaccharide 82

The T-ROESY experiment of tethered disaccharide **82** (Figure 5.17), gave the required distance constraints to be used in the molecular modeling. Integrated ROE volumes were converted to inter-residue proton-proton distances by comparison with the integrated volumes for a reliable intra-

residue distance, such as β -D-*N*-acetylglucosamine H1-H5 (2.53 Å) and α -D-galactose H1'-H2' (2.39 Å). A set of distances was derived for each internal reference and then were averaged to give the NOE-derived proton-proton distances (Table 5.13). As shown in Table 5.13, some restraints were not incorporated in the theoretical calculations in order to broaden the array of conformers to be sampled. Illustrated in Figure 5.18 are the reporter regions where all of the observed inter-residue ROE connectivities are found.

From these data, it was possible to establish the identification of the methylene group ether-linked to galactose and to *N*-acetylglucosamine (Table 5.11). The large correlations observed for proton pairs H1'-H3 and H1'-H5, and most notably the weak correlation between H1' and H4 are consistent with the unusual *anti*-conformation for compound **82**.

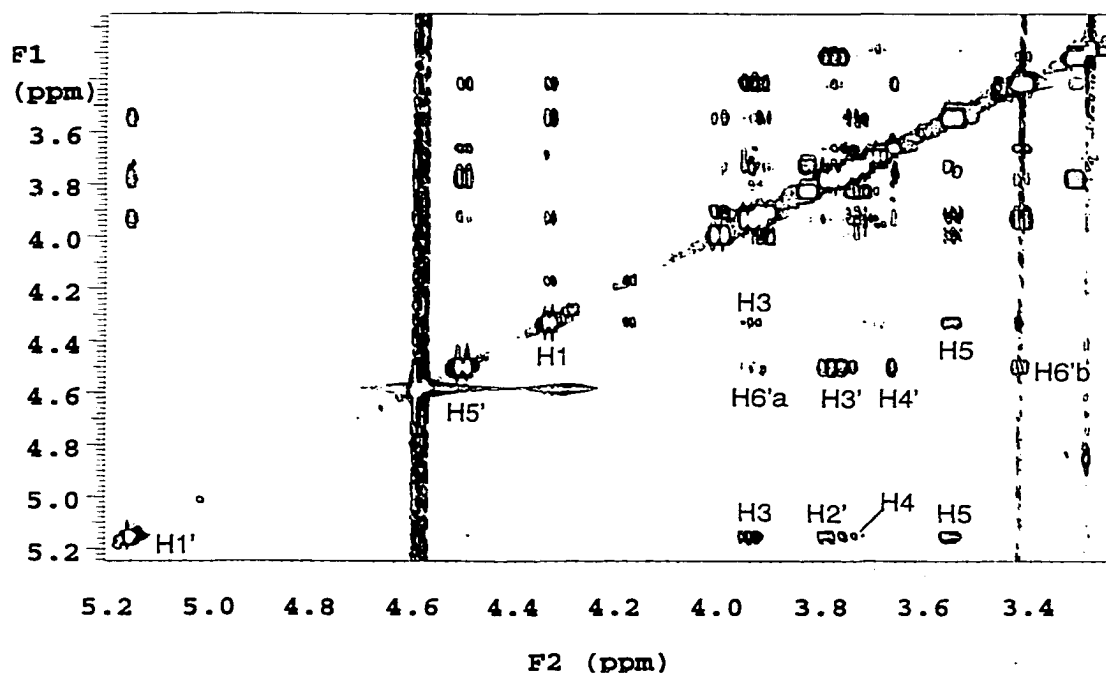


Figure 5.17: T-ROESY spectrum of tethered disaccharide **82** in CD₃OD.

Table 5.13: Experimental ROE values and distance restraints
(Å) for modeling studies of tethered disaccharide **82**.

Proton Pair	Relative ROE	Distance (Å)	Restraint
H1'/H3	1.00	2.3	Strong
H1'/H5	0.95	2.3	Strong
H1'/H4	0.06	3.6	Weak
H5'/H6'a	0.13	3.2	
H5'/H6'b	0.46	2.6	

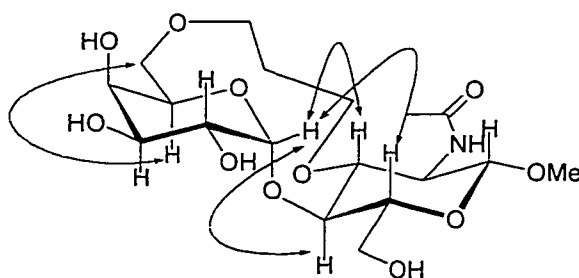


Figure 5.18: Diagnostic inter- and intra-residue ROE connectivities of compound **82**.

5.5.4: T-ROESY Distance Measurements for Untethered Disaccharide 92

Table 5.14 lists the ROEs between carbon-linked protons and their ROE ratios for α -lactosamine **92**, which have been normalized as described for **82**.

Table 5.14: Experimental ROE values and inter-proton distances
(Å) for untethered α -disaccharide **92**.

Proton Pair	Relative ROE	Distance (Å)
H1'/H3	0.09	3.4
H1'/H5	^a	
H1'/H4	1.00	2.3

^a No correlation observed.

A T-ROESY experiment for untethered **92** (Figure 5.19) showed strong correlations between H1' and H4, a very weak correlation between H1' and H3, and no correlation between H1' and H5. This indicates that **92** adopts the stereoelectronically preferred *syn*-conformation. Illustrated in Figure 5.20 are the reporter regions where all of the observed inter-residue ROE connectivities are found for **92**.

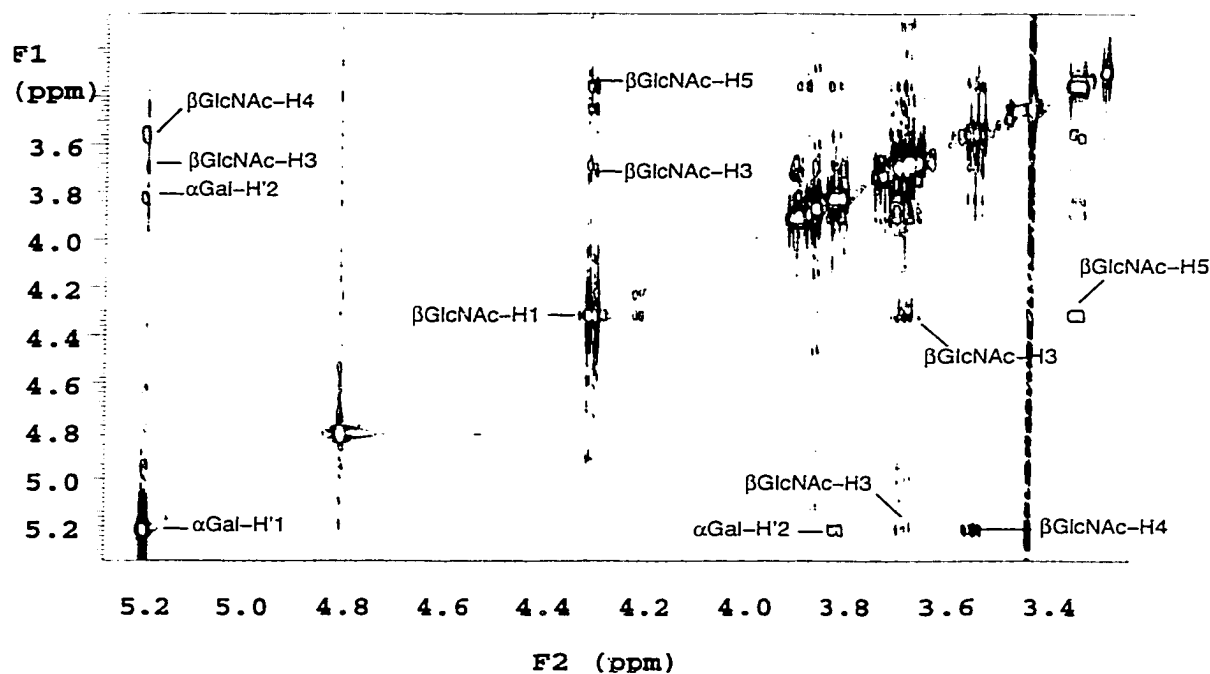


Figure 5.19: T-ROESY spectrum of untethered disaccharide **92** in CD₃OD:

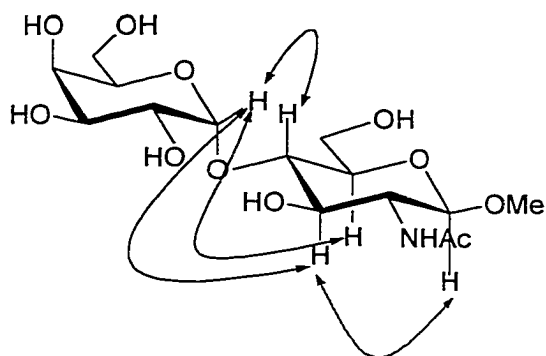


Figure 5.20: Inter- and intra-residue ROE connectivities observed in disaccharide **92**.

5.5.5: EXSIDE Experiments

In order to describe the three-dimensional structure of the tethered disaccharide **82**, the torsion angles ϕ and ψ should be determined. These angles are reflected by NMR-observable parameters, specifically the H1'-C1'-O1-C4 and C1'-O1-C4-H4 heteronuclear coupling constants. The Karplus-type curves for these small vicinal couplings have been experimentally established by Lemieux et al.,^{270,271} and since then refined by modeling and calculations.²⁷² HMBC experiments were run in attempts to obtain the $^3J_{C,H}$ coupling constants, but they were not successful in providing reliable values due to peak distortion by passive couplings. In order to experimentally determine the torsion angles ϕ and ψ , a two-dimensional EXSIDE²⁷³ spectrum was recorded. In this procedure, the heteronuclear long-range coupling is scaled in the indirectly detected ^{13}C dimension.

Using Q3 inversion pulses²⁷⁴ of 12.7 ms duration, the H1'-C1'-O1-C4 coupling constant was determined to be 4.4 Hz in CD₃OD. The torsional angle ϕ was derived from a Karplus-type relationship²⁷² (Eq. 5.1) using the $^3J_{C4,H1'}$ coupling constant (4.4 Hz) and by solving the quadratic equation for torsional angles ϕ of 28° or 141°.

$$^3J_{C,H} = 5.7 \cos^2\phi - 0.6 \cos\phi + 0.5 \quad (\text{Eq. 5.1})$$

Several attempts were made to determine the C1'-O1-C4-H4 coupling constant in CD₃OD. Since the H3 and H5 resonances were too close to the H4 resonance, and excitation of mutually coupled protons is detrimental to the success of the EXSIDE experiment, large pulse widths were required which prevented the experiment from being successful (T2 relaxation).

Therefore, 1D, GCOSY and HMQC experiments of compound **82** were recorded in other solvents to see if the H3, H4, and H5 resonances could be further separated. The solvent, which gave the best separation, was pyridine-d₅. The EXSIDE experiment was then repeated for **82** in pyridine-d₅ at 600 MHz. Although the experiment worked in principle, the sensitivity was very poor.

Therefore, the sample of **82** in pyridine-d₅ was run at 800 MHz (NANUC - University of Alberta National NMR Centre). Both EXSIDE experiments were successful, with good sensitivity (Figure 5.21). A $^3J_{C4,H1'}$ coupling constant of 4.2 Hz and $^3J_{C1',H4}$ of 7.0 Hz were obtained. The quadratic equation (Eq. 5.1) was solved for torsional angles ϕ of 31° or 139° and ψ of 180°. The fact that the ϕ torsional angle agrees well with that obtained in CD₃OD and that the inter-proton distances obtained in pyridine-d₅ are identical to those in CD₃OD, indicates that the conformation of the tethered disaccharide **82** is solvent independent.

The $^3J_{C1',H4}$ of 7.0 Hz obtained here is the largest $^3J_{C,H}$ coupling constant that one may obtain according to the Tvaroska *et al.* derived Karplus curve²⁷² and indicates that ψ is 180°. To the best of our knowledge, this makes the $^3J_{C1',H4}$ of tethered disaccharide **82** the largest measured across a glycosidic linkage.

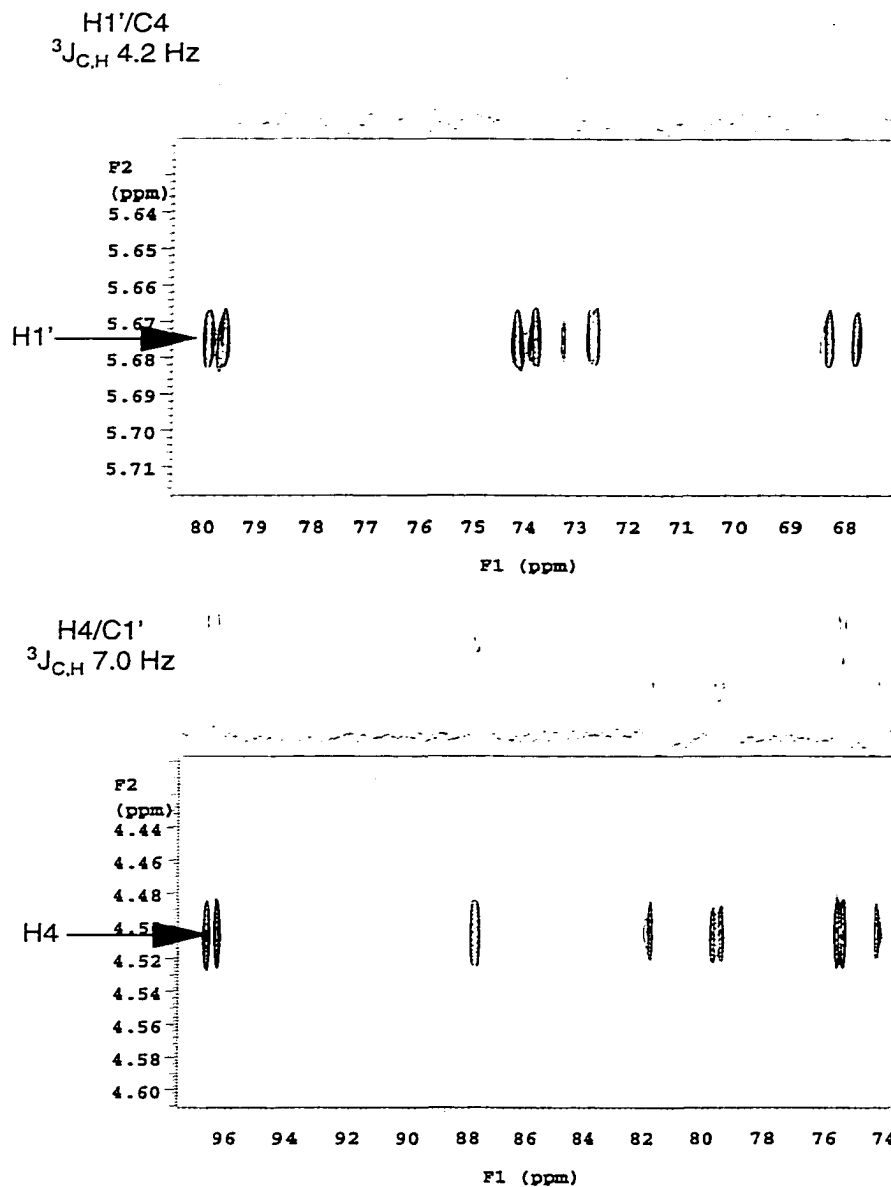


Figure 5.21: Two-dimensional EXSIDE²⁷³ spectra in pyridine-d₅ used to obtain the a) H1'-C1'-O1-C4 and b) C1'-O1-C4-H4 coupling constants.

5.5.6: Conformation of the Disaccharide 92

The AMBER forcefield^{264,265} with additional parameters derived for carbohydrates^{266,267} was used to model the three dimensional structure of the untethered $\alpha\text{Galp}(1\rightarrow4)\beta\text{GlcPNAc}\rightarrow\text{OCH}_3$ disaccharide **92**. The terms describing the *exo*-anomeric effect were set to zero, allowing us to sample a broad array of conformers.

The generation of 10 pseudorandom starting structures, followed by restrained simulated annealing and minimization to give a family(ies) of minimized structures, correlated with the ROE distance restraints derived from T-ROESY data obtained in CD₃OD for tethered disaccharide **82**. This was done to examine whether the factors that generally governs the favorable *syn*-conformation, would dominate over the restraints for *anti*-**82**. This minimized into one family (Figure 5.22a) about the $\alpha\text{Galp}(1\rightarrow4)\text{GlcPNAc}$ glycosidic linkage ($\phi \approx -32^\circ$, $\psi \approx -174^\circ$) corresponding to the *anti*-conformer.

The minimization was repeated a second time for the untethered disaccharide **92**, but no restraints were applied during the simulated annealing and minimization. This gave two families of minimized structures (Figure 5.22b); the largest family corresponding to the *syn*-conformation ($\phi \approx -15^\circ$, $\psi \approx -25^\circ$) and the smaller family to the *anti*-conformation ($\phi \approx -31^\circ$, $\psi \approx -173^\circ$).

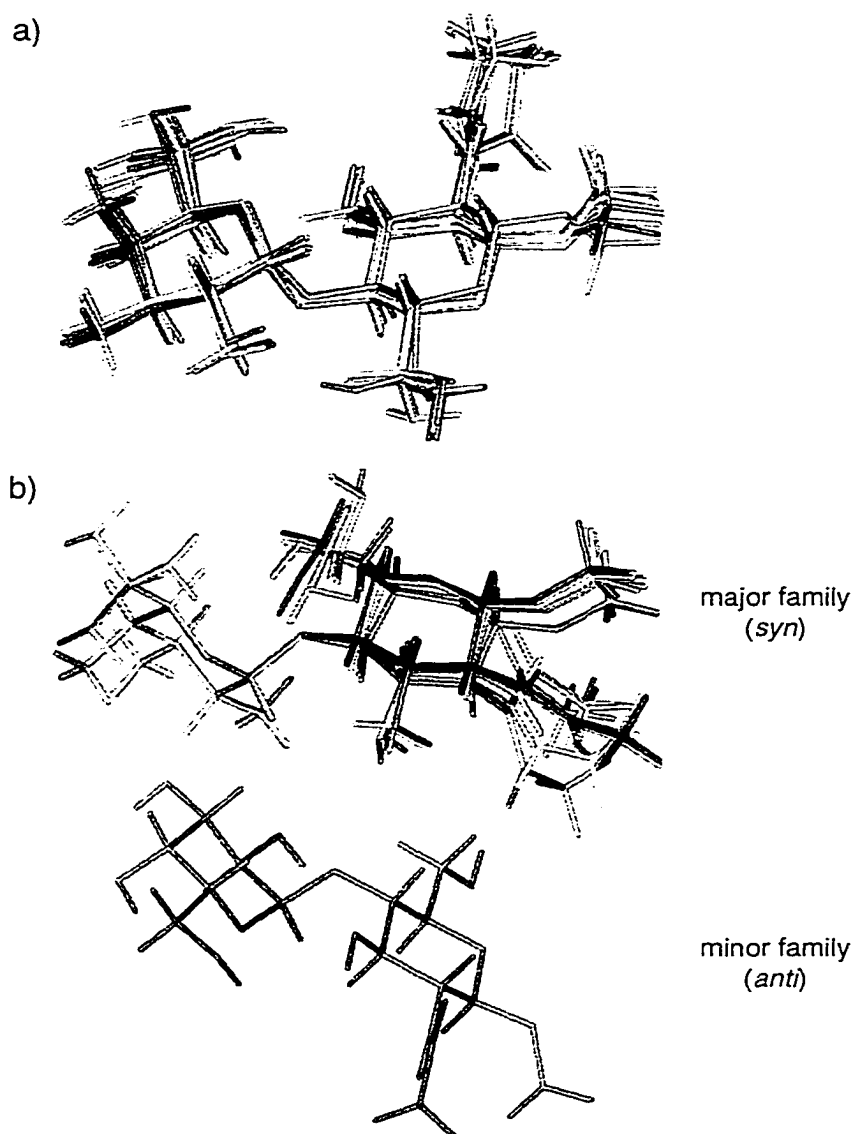


Figure 5.22: Structures resulting from the minimization of disaccharide **92**: a) using ROE restraints obtained from the tethered disaccharide **82**; b) without using any restraints.

5.5.7: Conformation of the Tethered Disaccharide 82

To avoid biasing the conclusions reached for the conformation of tethered α -lactosamine **82**, two computer models were assembled representing the *anti*- and *syn*-conformation, **82a** and **82b**.

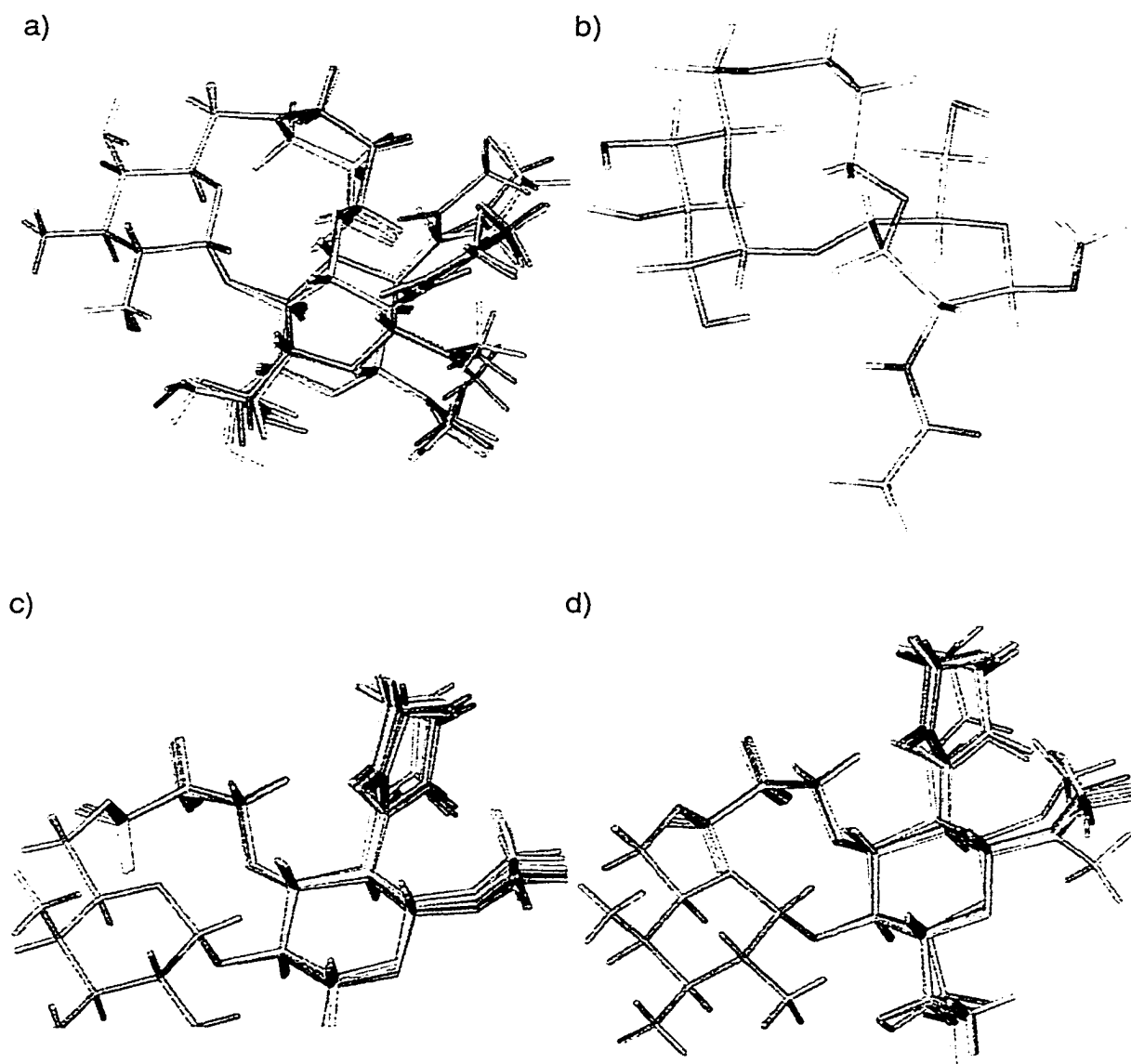


Figure 5.23: Structures resulting from the minimization of: a) *anti*-conformer **82a** using ROE restraints; b) minimized *syn*-conformer **82b**, which anneals to c) **82b** using ROE restraints and d) **82b** without using restraints.

Table 5.15: Summary of results from molecular modeling indicating the major and minor families of conformers found for each structure.

	α LacNAc (92)		<i>Anti</i> -tethered α LacNAc (82a)		<i>Syn</i> -tethered α LacNAc (82b)	
	Major	Minor	Major	Minor	Major	Minor
With ROE restraints of 82	<i>Anti</i> $\phi = -32^\circ$ $\psi = -174^\circ$	NA	<i>Anti</i> $\phi = -27^\circ$ $\psi = -162^\circ$	NA	<i>Anti</i> $\phi = -18^\circ$ $\psi = -170^\circ$	NA
No ROE Restraints	<i>Syn</i> $\phi = -15^\circ$ $\psi = -25^\circ$	<i>Anti</i> $\phi = -31^\circ$ $\psi = -174^\circ$	<i>Anti</i> $\phi = -32^\circ$ $\psi = -174^\circ$	NA	<i>Anti</i> $\phi = -19^\circ$ $\psi = -170^\circ$	NA

NA: Not applicable.

5.5.8: Solution Dynamics of Tethered Disaccharide **82**

It has been established that for a flexible molecule, such as an oligosaccharide, proton-proton distances derived from NOESY or T-ROESY data do not represent the single or true solution conformers but a r^{-6} weighted average of all of the conformers present in solution.¹⁰⁴ In attempts to simulate the dynamic behavior of the tethered disaccharide in solution, restrained molecular dynamics simulations were performed. The lowest energy conformer was chosen from the minimized structures as a starting structure for 5 ns of restrained simulated annealing or dynamic simulation. This resulted in one family about the minimum energy conformation about the α Galp(1 \rightarrow 4) β Glc pNAc linkage ($\phi \approx -27^\circ$, $\psi \approx -162^\circ$, Figure 5.24, Table 5.16). The restrained dynamics simulation produced ROEs that exhibited good agreement with experimental ROEs.

Table 5.16: Theoretical and experimental ROE values of tethered disaccharide **82**.

Proton Pairs	Calculated distance (Å)	Experimental distance (Å)
H1'/H3	2.1	2.3
H1'/H5	2.3	2.3
H1'/H4	3.6	3.6

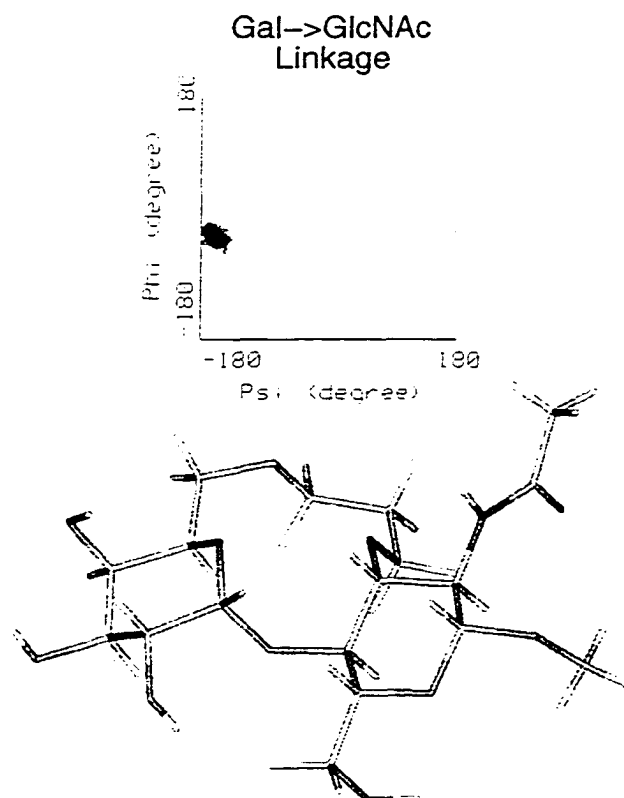


Figure 5.24: Lowest energy structure of **82** with graphs depict the trajectory of a 5000 ps MD simulation about both glycosidic linkages.

5.5.9: Conclusion

Due to the contributions of both the *exo*-anomeric effect and the *endo*-anomeric effect, the *syn*-conformation of the protons found in the glycosidic linkage would generally be predicted as the lowest energy conformation. This was shown to be the case in the T-ROESY data and modeling of untethered $\alpha\text{Galp}(1\rightarrow4)\beta\text{GlcNAc}\rightarrow\text{OCH}_3$, **92**.

The tethered $\alpha\text{Galp}(1\rightarrow4)\beta\text{GlcNAc}\rightarrow\text{OCH}_3$ disaccharide **82** was found to exist in the *anti*-conformation. Whether the NOE restraints obtained

from the T-ROESY data of the tethered disaccharide in CD₃OD are applied to the untethered α -disaccharide **92**, or to the *anti*-conformation **82a** or *syn*-conformation **82b**, the lowest energy structure obtained is always the *anti*-conformer. This is contrary to what is normally expected in a glycosidic linkage. In order to adopt the *syn*-conformer, the pyranose rings of **82** must distort into a skewed chair in order to avoid steric clashes. The ³J_{H,H} values of **82** indicate that the pyranose rings of the *anti*-structure remain in the chair form. As expected, the untethered disaccharide **92** minimizes (without ROE restraints) to the *syn*-conformer, which implies that the *anti*-conformation of tethered disaccharide **82** must result from the presence of the tether.

Tethered disaccharide **82** is the first example of a constrained deprotected disaccharide which is “frozen” in the normally sparsely populated high-energy *anti*-conformation. A constrained protected disaccharide that adopts the *anti*-conformation in CDCl₃ has been very recently reported by Geyer *et al.*²⁷⁵

NMR and Theoretical Studies of the Bound Conformations of H-Type 2 and its Constrained Derivatives

6.1: Introduction

The information existing in carbohydrate structures are decoded through the process of molecular recognition by protein receptors. These interactions mediate biological responses such as: host-parasite interactions, fertilization, autoimmune disorders, and cellular differentiation.^{62,63} Knowledge of the three dimensional structures of these biomolecules (carbohydrate, proteins, and complexes) can assist in the design of new carbohydrate-based therapeutics.

X-ray crystallography has allowed access to detailed information on the three dimensional structure of protein-carbohydrate complexes.⁶⁴ Postulates on the major factors involved in these interactions have been made based on these data coupled with those obtained from titration microcalorimetry.⁹⁷ Although X-ray crystallography has achieved many results in this field, quite often oligosaccharides are located on glycoproteins or on protein-carbohydrate complexes which are not suited for crystallography due to their intrinsic flexibility.

6.2: NMR Investigation of Protein-Carbohydrate Interactions

Recently, researchers have begun to study the molecular recognition process between oligosaccharides and proteins by NMR employing analyses at different levels of complexity.²⁷⁶ Since carbohydrates exhibit greater dynamic fluctuations than proteins, NMR measurements may reveal new information about the bound conformation of carbohydrate ligands.

6.2.1: Different NMR Protocols

Different types of information may be obtained from NMR studies of protein-oligosaccharide complexes in solution. These could be classified into three categories which may reveal a) structural information on the protein

residues involved in the molecular recognition event; b) information on the bound carbohydrate; and c) information on the protein-oligosaccharide complex.

6.2.2: Titration NMR Experiments

The specificity and affinity of binding, association constants and equilibrium thermodynamic parameters may be determined from titration NMR experiments.²⁷⁷⁻²⁸² Such experiments may provide a means to analyze sugar-induced perturbations of proteins and *vice versa*. Generally, the specific binding of carbohydrates to lectins is monitored by recording a series of ¹H NMR spectra at constant protein concentration with varying sugar concentrations, usually between six and eleven different concentrations. By running these titration experiments at different temperatures and following the van't Hoff type of analysis, the kinetic and thermodynamic parameters may also be determined.

6.2.3: Chemically Induced Dynamic Nuclear Polarization

The amino acids involved in the protein-carbohydrate interaction may also be deduced by titration, NOESY, and chemically induced dynamic nuclear polarization (CIDNP) experiments.²⁸³ In the case where sugar recognition involves the aromatic amino acid side chains, the photo CIDNP method may be used to monitor the effect of sugar binding on the receptor. After laser irradiation in the presence of a radical pair-generating dye, the aromatic amino acids are able to generate CIDNP signals. Since this method requires the accessibility of the aromatic residues by the light-absorbing dye, it is only suitable for monitoring the surface properties of a protein receptor, and the effect of the sugar binding on the protein, provided that aromatic amino acids are involved in the binding process. The shape and intensity of the CIDNP signals are determined in the absence and presence of the carbohydrate ligand.

6.2.4: NMR Relaxation Experiments

From relaxation experiments, it is possible to say something about the ligand exchange timescale and the size of the complex. NMR relaxation properties depend on the spectral density functions, which in turn are sensitive to molecular motion. Spectrometer frequency, molecular size, and inter-nuclear distances are also important parameters. Since the molecular motion of a carbohydrate changes following complexation to a protein, its relaxation properties will also be affected. Therefore, NMR relaxation measurements may be used to monitor the change of mobility of carbohydrates upon binding.^{284,285}

6.2.5: Transferred Nuclear Overhauser Enhancement Studies

The transferred NOE (TRNOE)²⁸⁶⁻²⁸⁸ is one of the few experiments that is capable of providing information on ligand conformation in the solution bound state. TRNOE is a particular example of the NOE in the presence of exchange, in this case the exchange of a ligand molecule between free solution and the bound state, where it is complexed to a large receptor molecule (e.g., a protein).^{98,289-294}

Figure 6.1 illustrates the dynamic exchange occurring between a protein-ligand complex with a large excess of free ligand. Protons in the free state may be too far apart for a measurable NOE to develop, but in the bound state, protons (H_a and H_b) may be close enough for an NOE to be measured. However, NOE measurements do not occur in the bound state. Rapid dissociation of the complex occurs and the free sugar maintains the information acquired in the bound state for a given period of time. The NOE measurements are made in the free state with magnetization transfer achieved through a combination of chemical exchange and cross-relaxation mechanisms. After this time, the ligand equilibrates back to its initial free state.

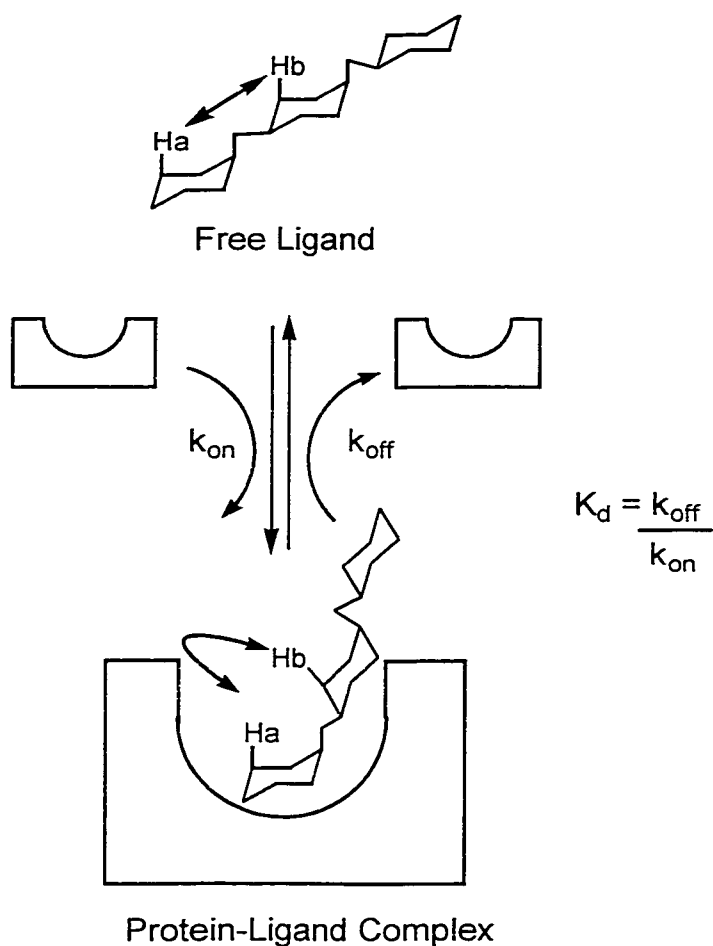


Figure 6.1: Representation of a protein-ligand complex in dynamic exchange with a large excess of the free ligand.

Since the exchange rate is fast on the NMR timescale, separate resonances are not observed for the free and bound ligand. A single resonance is observed at the weighted average of the chemical shifts. Since proteins are slow tumbling molecules, they have much broader linewidth and less intense signals than those of the carbohydrate. And since this protocol calls for a high oligosaccharide:protein ratio (10-50:1), there are no problems in differentiating the averaged carbohydrate resonances from background protein.

6.2.5a: Required Conditions for TRNOE

Several conditions must be satisfied in order to observe transferred NOEs and to permit their quantitative interpretation. The rate of dipole-dipole transitions that give rise to an NOE is governed by the cross-relaxation rate constant (σ). When the ligand is bound to protein it experiences a slower tumbling or molecular reorientation than it does in the unbound state, where it tumbles rapidly. This results in ligand cross relaxation rate constants $\sigma_{\text{bound}} \gg \sigma_{\text{unbound}}$. Therefore, provided exchange between free and bound states is rapid compared to the relaxation rate, the free ligand acts as a reservoir that effectively magnifies the intensity of the NOE of the bound state as the free ligand samples the bound state, many times during the period of cross relaxation. As some describe it “free ligand carries a memory of the NOE developed in the bound state”.

The conditions for a successful transferred NOE experiment may be summarized:

- ◆ large molecular weight protein receptor (the larger the protein the slower the overall tumbling rate and the larger σ_{bound}),
- ◆ an intermediate strength association constant ($K_a \approx 10^4$ - 10^6 M^{-1}),
- ◆ rapid exchange between free and bound states (dissociation rate constant k_{-1} off rate $\approx 10^2$ - 10^3 sec^{-1}),
- ◆ excess of ligand over receptor protein (typical ratios ligand:receptor 10-50:1).

6.2.5b: Observation of Transferred NOEs

A solution of the sample protein is exchanged with buffer in D_2O . The typical concentration of protein ranges from ≈ 100 to $500 \mu\text{M}$. Ligand is added in portions and a simple 1D NOE spectrum is recorded. Free ligand gives positive NOEs, while transferred NOEs appear as negative NOEs with some line broadening characteristic of large molecular weight species. The sign of the NOEs is dependent on tumbling ability, i.e. molecular weight of the molecule, therefore the ligand would give a negative NOE. Optimum negative

transferred NOE intensities are achieved by titrating more ligand and if necessary by raising the temperature to increase the exchange rate and to obtain narrower lines. If binding remains too tight to enter the rapid exchange regime a variety of techniques to weaken binding may be employed, for example changing pH. A complete transfer NOE investigation requires the examination of NOE build-up curves.

6.2.5c: Quantitative Interpretation of Transferred NOEs

In order to interpret transferred NOE in a quantitative manner it is not sufficient to observe a steady state NOE for the bound ligand undergoing rapid exchange with the free state. Instead, NOESY spectra are recorded at different mixing times generally in the range 50-400 ms. This provides for creation of build-up curves and extrapolation of distances to zero mixing time. Build-up curves also allow the identification of NOEs that arise through indirect effects, such as ligand three spin effects.

A more difficult situation to treat is the problem of spin diffusion. This arises via magnetization transfer between ligand protons well separated in space. Their apparent NOE connections arise through the intermediacy of protons attached to the protein molecule, but also through ligand protons. In this way the two ligand protons appear to be closer to each other than would otherwise be predicted. In principle, it should be manifested in build up curves. The problem was encountered and undetected in one of the first disaccharide-antibody TRNOE studies.²⁹⁵ The best experimental solution to this problem was demonstrated by the same authors in a second publication.²⁹⁶ Transferred NOEs measured in the rotating frame (TR-ROESY) distinguish indirect effects from direct effects. Direct NOEs detected by the ROESY experiment appears as positive cross peaks and three spin effects or relayed effects appear as negative cross peaks.

Inter-proton distances are calculated in the same manner as described earlier. However, distances extracted for different mixing times are plotted

and extrapolated to zero mixing times. These are the final distances employed to infer the bound conformation.

6.3: Molecular Modeling of Carbohydrate-Protein Complexes

Many questions concerning protein-carbohydrate interactions are associated with conformational behavior. As is the case with free carbohydrate ligands, NOE distance constraints are frequently too few in number to permit the definition of a unique set of conformers. In the case of branched trisaccharides n to $n+2$ inter-residue NOEs are encountered and these distances make a significant reduction in the range of possible conformations sampled.⁹⁸ However, for disaccharides the number of NOEs will always be such that computational methods will be required to complement the experimental data.

Calculations can be made at several levels of sophistication with respect to the mathematical treatment and also with respect to the model of the complex.^{290,297} In our studies, only a semi-quantitative analysis has been pursued.

Treatment of transferred NOEs may be performed while essentially ignoring the protons of the protein binding site. In this way the modeling is done essentially as described for the free ligand with the exception of the larger correlation time of the bound state. It is generally presumed that a single conformer is bound, which therefore simplifies the treatment of the bound conformation when it is used to back calculate the expected NOEs.

Recently, programs have been introduced that permit a full relaxation matrix treatment of the ligand-protein complex. In this way the motion of the ligand in the complex, as well as the contribution of the protein protons to the relaxation of the ligand, are explicitly treated. For this a model of the complex is required with docked ligand. This approach lies beyond the scope of this thesis.

The above approaches represent the two extremes of quantitative interpretation of NOEs. Calculations that treat the complex encounter the

problem of a unified forcefield that is able to treat oligosaccharides as well as protein. As in the conformational analysis of oligosaccharides, there is no general forcefield presently in use for the conformational analysis of protein-carbohydrate interactions. A variety of forcefields has been shown to provide satisfactory agreement between experimental and modeled data.²⁶¹ Forcefields which have been specifically developed for carbohydrates are HSEA,^{241,254} PFOS,²⁹⁸ and GEGOP.¹³² CVFF is a general forcefield which has shown to be useful for deriving three dimensional structures of carbohydrates.¹³⁵ General molecular mechanics programs that have been adapted for carbohydrates are: MM3,²⁹⁹ CHARMM,^{300,301} GROMOS,³⁰² and Tripos.³⁰³ Amber (Assisted Model Building with Energy Refinement), which is used here, is a forcefield designed by Kollman for the simulation of peptides and nucleic acids,^{264,265,304} and which has been modified with additional parameters derived for carbohydrates.^{266,267}

6.4: Outline of Investigation

This investigation involves four major parts:

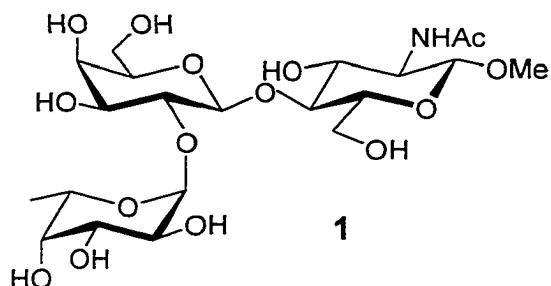
- ◆ The first, includes the determination of the bound conformation of the native H-type 2 trisaccharide (**1**) by NMR.
- ◆ The second part, involves the investigation of the bound conformation of tethered trisaccharide **28** by NMR.
- ◆ The third, includes modeling studies of the bound conformation of trisaccharide **1** and **28**.
- ◆ The last section summarizes the information learned from the investigation of the bound conformations of the trisaccharides **1**, and **28** with *Ulex europaeus* I.

6.5: Results and Discussion

6.5.1: Determination of the Bound Conformation of Trisaccharide 1

This current investigation centres on probing the bound conformation of the H-type 2 trisaccharide, α -L-Fucp(1→2)- β -D-Galp(1→4)- β -

D-Glc_pNAc→CH₃ (**1**), when bound to *Ulex europaeus* I lectin. Currently there is no published crystal structure of the *Ulex* lectin with bound sugar. The bound conformation of trisaccharide **1** was determined using TRNOESY data to obtain distance restraints for molecular modeling.



6.5.2: NMR Studies of the Bound Conformation of Trisaccharide 1

6.5.2a: Experimental Protocol

The following procedure was used by Dr. Mark Milton (postdoctoral fellow in Dr. Bundle's group) to perform TRNOE experiments. Final optimal conditions employed 0.44 mM of *Ulex europaeus* I dissolved in 10 mM PBS at pH 7.0 with an optimal concentration of H-type 2 trisaccharide **1** of 2.5 mM. The concentration of the protein was determined by UV absorbance ($A_{280} = 0.786$ for the sample diluted 1:20).²³⁵ TRNOEs were measured with a sugar:protein ratio of 6:1.

One-dimensional analogues of 2D- $T_{1\rho}$ -filtered TRNOESY spectra were acquired at a starting temperature of 27°C and the temperature was raised in 3 degree steps until a final temperature of 45°C was reached. An experimental temperature of 45°C was chosen as this resulted in superior TRNOE enhancements and an absence of NOESY enhancements due to free sugar.

A series of 2D $T_{1\rho}$ -TRNOESY spectra³⁰⁵ was then acquired with differing mixing times (100→500 msec). However, spectra acquired with mixing times greater than 0.3 s were of poor quality. It was also observed that the sample surprisingly resisted denaturation after several days of

heating at 45°C over a 3 months span. TRNOESY experiments were performed on samples containing a 6 fold excess of sugar and a mixing time of 300 ms was used. Build-up curves were not made.

6.5.2b: Results

Relative intensities obtained from $T_{1\rho}$ -TRNOESY spectra (Table 6.1) for the H-type 2 sugar in complex with *Ulex europaeus* I showed some differences to those measured for the H-type 2 trisaccharide sample (free in solution). The difference in the NOE values for free and bound form of **1** for interproton distances H1''/H4, suggests that a different rotamer about the glycosidic bond may be adopted when bound to *Ulex*, though when compared to the calculated value (cf. Table 5.3) this difference is not as significant. The difference in H1''-H3' NOE values is questionable, because the experimental distance for the bound H-type 2 trisaccharide **1** agrees with the back-calculated distance free **1** (cf. Table 5.3).

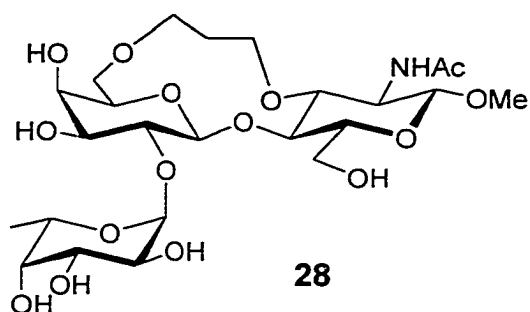
Table 6.1: Interproton distances (Å) derived from experimental NOE values for free and bound H-type 2 trisaccharide.

Proton Pairs	Free H-type 2			Bound H-type 2		
	Relative ROE	Dist. (Å)	Restraint	Relative NOE	Dist. (Å)	Restraint
H1''/H2'	0.77	2.3	Strong	2.17	2.3	Strong
H1''/H3'	0.39	4.8	Medium ^a	0.24	3.4	
H1''/H6a	0.31	2.7	Strong ^a	0.80	2.9	
H1''/H4	1.00	2.2	Medium	0.80	2.9	Medium
H5''/H6a	0.18	3.0	Strong ^a	0.41	3.1	
H5''/H5	0.27	2.8	Strong ^a	1.00	2.7	

^aRestraint had to be weakened.

6.5.3: Determination of the Bound Conformation of Trisaccharide 28

The bound conformation of the tethered H-type 2 trisaccharide **28** with *Ulex europaeus* I was investigated using TRNOESY data to obtain distance restraints for molecular modeling.



6.5.3a: NMR studies of the Bound Conformation of Trisaccharide 28

6.5.3b: Experimental Protocol

Final optimal conditions for the TRNOESY measurement used 0.39 mM of *Ulex europaeus* I in 10mM PBS at pD 7.0 with an optimal 9.14 mM concentration of the tethered H-type 2 trisaccharide **28**. The sugar:protein ratio was 23:1.

One-dimensional analogues of 2D- $T_{1\rho}$ -filtered TRNOESY spectra were acquired on the 600 MHz Varian Inova spectrometer with a starting temperature of 27°C and the temperature was raised in 5 degree steps to a final temperature of 45°C. Temperature was raised in attempts to increase the rate of exchange between the free and bound state of the ligand, in order to eliminated the NOEs of the free ligand. The sugar appeared to be binding too strongly as the desired TRNOE enhancements were not observed. The pD of the sample was then decreased from pD 7.0 to 6.0, and later from 6.0 to 5.0 in order to change the binding affinity of the tethered trisaccharide **28**. At a pH of 5.0 and a temperature of 45°C, respectable TRNOE enhancements were observed but the minimum mixing time required was long (400 ms) and raised concerns that spin-diffusion effects would occur.

These experiments, with the same trisaccharide-protein sample (pH=5.0), were repeated on a 500 MHz Varian Unity⁺ spectrometer but used a starting temperature of 45°C. At this temperature, positive NOESY signals from free sugar were a problem. Therefore, the temperature was raised in 5 degree steps until a final temperature of 65°C was reached and the desired TRNOE enhancements were obtained.

Unfortunately, the resonance peak for H1' of galactose was found under the HOD peak. Since the signal for H1' was of particular interest, the temperature was increased further in order to separate the peak of interest from the HOD peak. An experimental temperature of 75°C was chosen as it resulted in: 1) optimal TRNOE enhancements, 2) the H1' signal was far removed from the HOD peak and 3) NOESY enhancements for the free sugar were absent.

It was also observed that the *Ulex* lectin had resisted denaturation at 45°C over 6 weeks of experimentation, but at a temperature of 75°C, the protein started precipitating after 2 days. Although most proteins are denatured by elevated temperatures, the TRNOESY experiments were performed at 75°C on samples containing a 23 fold excess sugar **28** and using a mixing time of 0.200 s. At the end of all the experiments, the high temperature had caused extensive denaturing of lectin (~60%). Nevertheless, EIA measurements demonstrated activity for ~40% of the protein. Therefore, these NOE data are only given qualitative weight.

6.5.3c: Results

Relative intensities obtained from T_{1ρ}-TRNOESY spectra (Table 6.2) for the protons on the glycosidic linkages for tethered trisaccharide **28** in complex with *Ulex europaeus* I showed some differences to those measured for the free conformation of the trisaccharide **28**. The NOE H1' to H4 distance increased by ~0.5 Å in the bound state while the H1'' to H2' distance decreased (2.7 → 2.3 Å).

In order to verify experimentally that the trisaccharide **28** does not adopt any other higher energy conformations at such an elevated temperature of 75°C, the 1D ¹H-NMR, COSY, and TROESY spectra of the free sugar were acquired at 75°C. These spectra were identical to those recorded at the lower temperature of 27°C and also gave similar ROE values (Table 6.2). Although this indicates that the conformation of bound ligand

adopted at 75°C is similar to that at 27°C, it is expected that a larger range of conformers are being sampled, due to the increase in energy of the system.

Table 6.2: Interproton distances (Å) derived from experimental NOE values for free and bound tethered H-type 2 trisaccharide **28**.

Proton Pairs	Free 28 At 27°C			Free 28 at 75°C	Bound 28 at 75°C		
	Relative ROE	Dist. (Å)	Restr. ^a	Distance (Å)	Relative NOE	Dist. (Å)	Restr. ^a
H1''/H2'	1.00	2.6	S	2.7	1.00 _d	2.3 _d	S
H1''/H3'	0.07	4.0	W ^b	4.0			
H1'/H4	2.57	2.3	S	2.3 _c	0.34 _d	2.7 _d	S
H5''/H6a	0.09	3.1	M				
H5''/H5	0.66	2.8	S ^b	2.9	_d	_d	

^aS=strong, M=medium, W=weak.

^bRestraint had to be weakened.

^cNot reported due to overlapping correlations.

^dNot observed.

6.5.3d: Binding of Native H-type 2 Trisaccharide at 75°C with *Ulex*

The TRNOE experiment for trisaccharide **1** was repeated at 75°C for comparison purposes with the tethered molecule **28** (Table 6.3). In order to determine if the H-type 2 trisaccharide **1** adopts any other higher energy conformations at such an elevated temperature of 75°C, the 1D ¹H-NMR, COSY, and TROESY spectra of the free sugar were acquired at 75°C. By visual inspection, these spectra were identical to those recorded at the lower temperature of 27°C. It is suspected that trisaccharide **1** free in solution may adopt a high energy conformation since NOE H1' to H4 distance increased ~0.5 Å (Table 6.3). The conformation of bound **1** does not seem to change with increased temperature.

Table 6.3: Experimental inter-proton distances for free H-type 2 trisaccharide **1** at 27°C and 75°C, and for **1** bound to *Ulex europaeus* I at 45°C and 75°C.

Proton Pairs	Free 1		Bound 1	
	Dist. (Å) at 27°C	Dist. (Å) at 75°C	Dist. (Å) at 45°C	Dist. (Å) at 75°C
H1''/H2'	2.3	2.6	2.3	2.7
H1''/H3'	2.6	a	3.4	a
H1'/H6a	2.7	2.9	2.9	b
H1'/H4	2.2	2.7	2.9	2.9
H5''/H6a	3.0	3.2	3.1	a
H5''/H5	2.8	a	2.7	a

^aNot observed.

^bNot reported due to overlapping correlations.

6.5.4: Modeling Studies of the Bound Conformation of Trisaccharides **1 and **28****

As was used in the investigation of the solution conformation of **1**, the AMBER^{264,265} forcefield with additional parameters derived for carbohydrates^{266,267} was used in the study of the binding of the H-type 2 trisaccharide **1** and its tethered derivatives to *Ulex europaeus* I.

A model of the complex was generated by superimposing the fucose residue of the minimum energy conformer of bound H-type 2 trisaccharide **1** onto the corresponding geometry of the trisaccharide-*Ulex* coordinates.^{71,131,134} The complex was then minimized by using the conjugate gradient routine.³⁰⁶ The following restraints were applied: 1) the fucose position was constrained in order to avoid expulsion of the trisaccharide from the binding site and 2) the NOE distance restraints derived from TRNOESY data obtained in D₂O for H-type 2 (**1**) (Table 6.1) were applied to the proton pairs about the glycosidic linkages.

The minimization resulted in a trisaccharide **1**-protein complex that is compared with that proposed by Lemieux¹³¹ (Figure 6.2). The Lemieux model docks a GEGOP minimized trisaccharide on the coordinates of the 2-methyl-2,4-pentanediol (cf. Chapter 2). The bound conformation of **1** differs slightly

from the model developed by Lemieux for the docked GEGOP minimum energy conformation of **1**. The $\alpha\text{Fucp}(1\rightarrow2)\beta\text{Galp}$ linkage showed good agreement, while the $\beta\text{Galp}(1\rightarrow4)\text{GlcNac}$ linkage showed a difference of $\sim 30^\circ$ for the ϕ angle (Table 6.4). Although this is a significant movement from the global minimum energy conformation, it remains a relatively modest overall change in the bound state.

Table 6.4: Torsional angles obtained for the solution and bound conformations of trisaccharide **1** and tethered trisaccharide **28**.

Ligand	Free		Bound	
	Fuc→Gal	Gal→GlcNAc	Fuc→Gal	Gal→GlcNAc
	ϕ, ψ	ϕ, ψ	ϕ, ψ	ϕ, ψ
1 calc ^a	58°, 12°	58°, 4°	-	-
1 expt'l	44°, 14°	42°, 4°	56°, 16°	31°, 10°
28 expt'l	49°, 19°	34°, 4°	15°, 31°	32°, 7°

^aH-type 2 structure minimized with GEGOP which was docked in *Ulex*.¹³¹

The same procedure employed to model the structure of the bound trisaccharide **1** was applied to model the structure of the bound tethered trisaccharide **28** with *Ulex*, using NOE distance restraints obtained from the TRNOESY data of **28**. The minimization resulted in a complex with significant deviations of the restrained residues (galactose and *N*-acetylglucosamine) compared to the complex of **1** with *Ulex* (Figure 6.3). When the bound tethered trisaccharide **28** is compared to the conformation of bound **1** (Table 6.4), the conformation about the $\beta\text{Galp}(1\rightarrow4)\text{GlcNac}$ linkages are similar, whereas the $\alpha\text{Fucp}(1\rightarrow2)\beta\text{Galp}$ linkage of **28** displays a large displacement of the ϕ torsional angle when compared to that of bound trisaccharide **1**. This is in marked contrast to the conformation of **28** in the absence of protein, even though this $\alpha\text{Fucp}(1\rightarrow2)\beta\text{Galp}$ linkage did exhibit increased flexibility. The bound conformation of **28** shows a near eclipsed relationship for the fucose C1"-H1" and O1"-C2' bonds. Consequently we feel that the minimization

procedure has failed in the case of the tethered compound **28**. The reasons for this are not clear.

Since it was not clear if a global minimum was attained, further data analysis of the modeling results will not be discussed. Clearly, a more advanced approach to the molecular modeling of these carbohydrate-protein complexes is necessary to determine the bound conformation of the H-type 2 trisaccharides **1** and **28**. It would also be necessary to obtain new transferred NOE data at more reasonable temperatures in the ~40-50°C range.

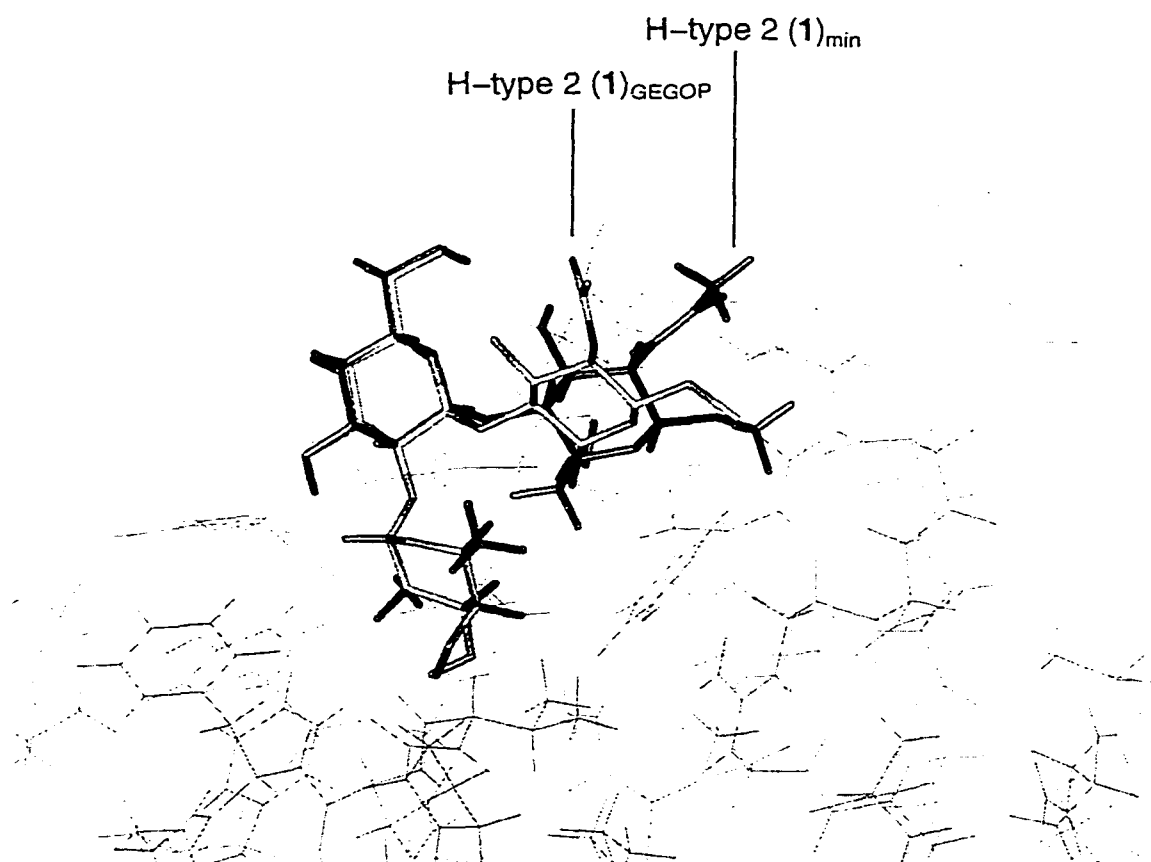


Figure 6.2: Comparison of the model for *Ulex* lectin docked with trisaccharide **1** (GEGOP) and the NMR derived conformation of bound **1**.

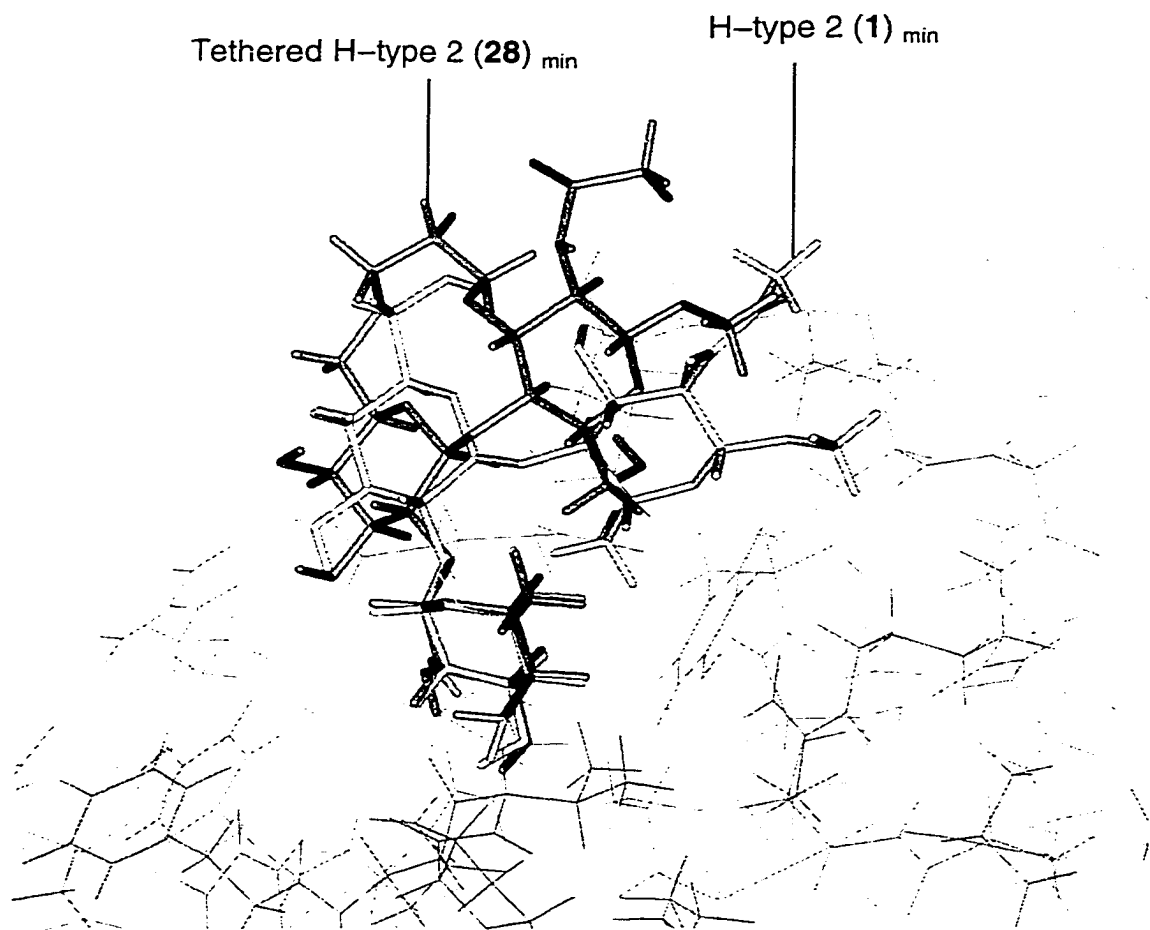


Figure 6.3: Comparison of the models for the bound trisaccharides **1** and **28**.

6.6: Conclusion

Since a qualitative treatment of the TRNOE is reported here, the only main conclusions that may be drawn are:

- ◆ *Ulex europaeus* I binds the native H-type 2 trisaccharide **1** in a conformation similar to its minimum free energy conformation,
- ◆ and a more sophisticated modeling approach must be used to study the carbohydrate-protein interactions of *Ulex europaeus* I with the native H-type 2 trisaccharide (**1**) and its tethered derivatives **28** and **29**.

Conclusions

7.1: Studies of the Carbohydrate-*Ulex* Complexes

The NMR investigation of the conformation of the solution structures of tethered trisaccharides **28** and **29** in Chapter 5, indicates that the overall topography of the H-type 2 trisaccharide **1** was maintained. The conformation of **29** shows a small displacement of the *N*-acetylglucosamine residue relative to that in **28**.

It was demonstrated in Chapter 5 that tethering of the $\beta\text{Galp}(1\rightarrow4)\beta\text{Glc pNAc}$ linkage resulted in decreased flexibility of this glycosidic linkage, whereas the flexibility about the $\alpha\text{Fucp}(1\rightarrow2)\beta\text{Galp}$ linkage increased. Hence, the conformational entropy of the tethered molecules appear to have been redistributed. If the aim was to decrease the overall flexibility of the molecule, tethering was not successful.

The increased entropy experienced by the fucose residue within the tethered trisaccharides would account for the decreased binding affinities, compared to the native trisaccharide **1**. However, since we were not able to make thermodynamic measurements, this entropy argument is unresolved at the present.

The difficulties encountered in the TRNOE experiment which required high temperature and decreased pD in order to observe TRNOEs, leads us to believe that the 'off-rate' of the tethered trisaccharide-lectin complex is fairly slow. Hence, even though the binding affinity is less than that of the native H-type 2 trisaccharide **1**, once the tethered molecule **28** is bound, it remains bound (at lower temperatures and pD=7). The lower off-rate corresponds to a long residence time on the protein. One explanation for this change in kinetics could involve reduced flexibility of the ligand as the cause of slower dissociation; a characteristic attributable to the decrease in flexibility about the $\beta\text{Galp}(1\rightarrow4)\beta\text{Glc pNAc}$ linkage.

From the TRNOE experiments, it was determined that *Ulex europaeus* I binds the H-type 2 trisaccharides **1** and **28** in a conformation similar to their

minimum free energy conformation. Since more in depth work must be done on the analysis of the carbohydrate-*Ulex* complexes, no other comments on the bound conformation of the sugars can be made at this point.

7.2: Binding of the H-type 2 trisaccharides to *Winged Bean*

The dramatic reduction of inhibitory power for **28** and **29** with the *Psophocarpus tetragonolobus* lectin observed by EIA cannot be simply explained by Lemieux's mapping study which suggests that the O-6 of galactose is involved in hydrogen bonding at the periphery of the binding site.¹²² As mentioned earlier, a 6-O-methyl galactose residue for galactose resulted in a $\Delta(\Delta G^\circ) = +0.1 \text{ kcal mol}^{-1}$. Whereas, our tethered compounds resulted in a $\Delta(\Delta G^\circ) = \sim +3 \text{ kcal mol}^{-1}$ indicating that there is more than just a loss in relatively weak hydrogen bonds. Introduction of the tether may result in changes in the rotamer distribution at C'-6, an unfavorable reorganization of the hydrogen bonds that involve structured water molecules or a simple steric clash between the tether and protein. The loss of 3 kcal mol^{-1} is dramatic and could point to an altered rotamer distribution that causes steric penalties.

7.3: Binding of the H-type 2 trisaccharides to *Erythrinia corallodendron*

The poor biological activities observed for the tethered trisaccharides **28** and **29**, and the tethered disaccharides **87** and **88** with *Erythrinia corallodendron* demonstrates the difficulty of trying to increase the binding between a ligand and a protein without knowing the binding topography of the substrate. These 'negative' results indicate that most likely the O'-6 of galactose and/or the O-3 of glucosamine are key polar groups that are involved in the lectin-carbohydrate interaction. Though changes in the rotamer distribution at C'-6, reorganization of structured water molecules and steric clash between the tether and protein may also be in effect.

7.4: Calibration of Heteronuclear Coupling Constants

The tethered disaccharide **82** was synthesized constrained in the *anti*-conformation. The solution behaviour of **82** was determined using T-ROESY and EXSIDE data to obtain distance restraints for molecular modeling and the $^3J_{C,H}$ coupling constants for the determination of the torsional angles. All NMR and computational data confirm that disaccharide **82** adopts the *anti*-conformation.

The study on the *anti*-conformation of **82** is significant, for generally in oligosaccharide modeling, it is difficult to prove that these conformers exist. The $^3J_{C1',H4}$ coupling constant of 7.0 Hz determined here is the largest $^3J_{C,H}$ coupling constant that one may obtain according to the Tvaroska *et al.* derived Karplus curve²⁷² and indicates that ψ is 180°. To the best of our knowledge, this makes the $^3J_{C1',H4}$ of tethered disaccharide **82** the largest measured across a glycosidic linkage. The importance of this work relies in the unique conformation of **82**, which permits the calibration of the heteronuclear three bond coupling constants in the *anti*-conformation.

7.5: Tethering as a Means to Reduce Entropy

These data highlight the difficulty in designing a tether that can effectively constrain an oligosaccharide in a bioactive conformation whilst avoiding unfavourable protein contacts. Even in the best situation, where we had the results of Lemieux's mapping of the carbohydrate,¹²² the crystal structure of the lectin without bound diol, and the modeling indicated that the tethered trisaccharides maintained the overall shape of the binding epitope, increased binding was not attained.

Why is it so difficult?

When trying to design a constrained saccharide not only must the tether position, the conformation of the bioactive epitope, and steric clashes with the surface of the protein be considered, but also the reordering of water due to the change in the balance of the "hydrophobic/hydrophilic character" of the molecule. This is the most difficult phenomenon to take into account.

The tethered di- and trisaccharides synthesized here, compared to the native H-type 2 trisaccharide, underwent a large change in “hydrophobic/hydrophilic character”. Two polar hydroxyl groups have been replaced by ether linkages and an apolar two or three carbon chain. In the case of compounds **28** and **29**, since the tether is not in the binding site of the *Ulex* lectin and therefore exposed to bulk water, the change in the hydrophilicity of the ligand will definitely have a big effect on the arrangement of water molecules around the protein-sugar complex. Changes related to such effects have already been reported.¹¹⁴

The net binding energy is represented by the energy difference between the hydrogen bond energies of the protein and of the sugar with water (solute-solvent interactions), those of the protein and sugar with each other (solute-solute interactions) and new water interactions with the complex. Hence, the manner in which water organizes itself about the ligand in solution is also a determining factor in the binding interaction. Therefore, the difference in the organization of the structured water molecules about the free tethered trisaccharide **28** and the native H-type 2 trisaccharide **1** would affect the net binding energy. This difference would affect not only the solute-solvent interactions but possibly also the final displacement of water molecules when the sugars complex with the protein.

In order to avoid drastic changes in the “hydrophobic/hydrophilic character” of the molecule, very small tethers must be used to minimize any disruption of the water shell around the molecule. One literature example already exists.^{115,116} In that case a methylene-tether was used to replace the intramolecular hydrogen bonds and reduce the flexibility of the trisaccharide while retaining the bioactive conformation of the epitope.^{115,116} Calorimetry data showed that the protein-carbohydrate complexation had a more favorable entropy term but that this term was offset by a smaller enthalpy contribution. Though a smaller tether was used, in this case the binding topography of the ligand was not well defined, therefore the presence of the

methylene group may have disrupted an intermolecular hydrogen bond to the protein.

A second method to avoid changing the “hydrophobic/hydrophilic character” of the molecule is to employ hydrophilic tethers. Tethers which themselves may participate in hydrogen bonding to water, either as donors, acceptors or a combination of the two. The conclusions drawn from binding data of such tethered molecules would be difficult to interpret because there will be a mixture of effects expressed in the binding energy. Calorimetry would be an essential tool in such an investigation.

The hypothesis that loss of conformational entropy on complexation with protein accounts for the low association constants of oligosaccharides thus remains unsubstantiated. An alternative interpretation of the experimental data emphasizes that the *exo*-anomeric effect already imposes conformational preferences on glycosidic linkages and stresses the importance of re-ordering solvent water about polyamphiphilic surfaces.^{5,109} Given the lack of evidence for large gains in binding energy when carbohydrate ligands are pre-organized, it seems quite likely that the solvent effects are more critical than losses in conformational entropy.

Interactions of tethered trisaccharide **28** in the *Ulex* lectin site are the most promising. The solid phase assays reported here show that the free energy of binding changes by only 0.6 kcal mol⁻¹. Published data from van't Hoff plots¹⁰³ show a strong enthalpic contribution to binding ($\Delta H^\circ = 29$ kcal mol⁻¹). Consequently titration calorimetry, which depends upon a large enthalpic term for its sensitivity, should be able to provide useful data to determine the effect of tethering on the entropy of binding. These measurements are the subject of further studies.

Experimental

8.1: Isolation and Purification of Lectins

The *Psophocarpus tetragonolobus* II and *Ulex europaeus* I lectins were isolated from seeds purchased from F. W. Schumacher Co., Inc. Horticulturists (Sandwich, Massachusetts). *Erythrina corallodendron* lectin was isolated from seeds provided by Dr. Nathan Sharon. The procedures followed literature methods of extraction and purification by affinity chromatography.^{27,28,30,307}

Ulex I lectin: *Ulex europaeus* I seeds (100 g) were ground in a coffee grinder and extracted with PBS (500 mL, pH 7.7) for 1 h at rt. The suspension was filtered through a cheese-cloth. The filtrate was spun at 13,000 rpm for 45 min at 4°C. The supernatant was left overnight at 4°C, and then spun again for 45 min at 13,000 rpm at 4°C. The supernatant was filtered through celite 545, then through 0.45 µM and 0.22 µM Millipore filters. If the supernatant remained cloudy, it was spun at 17,000 rpm at 4°C for 40 min. The clear solution was loaded onto the affinity column (fucose-agarose column from Sigma – 3 mL of resin) and washed until the OD₂₈₀ of the effluent was around 0.02. The *Ulex* lectin (extinction coefficient = 1.18) was eluted with a 1% fucose solution in PBS buffer. The lectin was dialyzed extensively against PBS (pH 7.2) and the purity was verified on a SDS PAGE gel (two bands above 31 kD). The lectin solution was concentrated, though to avoid precipitation, concentration should not exceed 4 mg/mL. The procedure maybe repeated on the remaining seed residue to increase the yield of lectin.

Erythrina lectin: Flour of coral tree (40 g) was defatted by stirring with hexane (3x100 mL, 15 min) at 4°C. Once air-dried, the defatted meal (36 g) was stirred with PBS buffer (360 mL, pH 7.2) for 4 h at 4°C. The extract was filtered through cheese-cloth and spun at 13,000 rpm for 20 min. Ammonium sulfate (17.6 g/100 mL) was added to the supernatant (285 mL) and stirred for 1 h at 4°C. The precipitate was spun (10,000 rpm, 20 min, 4°C) and

discarded. More ammonium sulfate (19.8 g/100 mL, 300 mL) was added to the supernatant and was left stirring overnight at 4°C. Once spun (10000 rpm, 20 min, 4°C), the precipitate was collected, dissolved in water (85 mL), and dialyzed against water (3x 2 L) and against PBS (1x 2 L). The *Erythrina coralloidendron* lectin extract (35 mL portions) was purified on a lactose-agarose affinity column (15 mL of resin). After loading, the column was washed until the OD₂₈₀ of the effluent was around 0.02. The *Erythrina coralloidendron* lectin (extinction coefficient = 1.53) was eluted with a 0.2 M lactose solution in PBS buffer (pH 7.2). The lectin was dialyzed extensively against PBS (pH 7.2) and purity was verified on a SDS PAGE gel (one main band around 31 kD).

Wing Bean lectin: Defatted and dried winged-bean seed meal was extracted with PBS buffer (pH 7.2) with continuous stirring for 12 h at 4°C. The extract was spun at 10000 rpm for 30 min, and the clear supernatant was decanted. The ammonium sulfate fraction between 30 and 65% saturation was collected, dissolved in PBS and dialyzed extensively against PBS. The extract was then applied to a 15 mL lactose affinity column and washed with PBS until the OD₂₈₀ was less than 0.005. The *Psophocarpus tetragonolobus* II lectin (extinction coefficient = 1.14) was eluted with a 0.2 M lactose solution in PBS buffer (pH 7.2). The lectin was dialyzed against PBS (pH 7.2) and its purity was verified by SDS PAGE gel (one band around 31 kD).

8.2: Solid Phase Immunoassay

Solid phase immunoassay (EIA) were performed in duplicate as described below using a variant of previously described methods.^{234,235} The dialyzed lectin solutions were used to coat EIA plates. Biotin labeled H-type 2 BSA glycoconjugate²³⁶ was allowed to bind to solid phase lectin in the presence and absence of inhibitors.

Affinity purified lectin dissolved in phosphate buffered saline (PBS) (1 µg/mL) was coated on 96 well ELISA plates overnight at 4°C. The plate was washed 5 times with PBS containing Tween 20 (0.05% v/v), then blocked

with bovine serum albumin (BSA) (Sigma) 2.0% in PBS for 1 h, and then washed 3 times with PBS containing Tween 20 (PBST). A glycoconjugate consisting of H-type 2 trisaccharide conjugated to BSA and biotinylated (0.02-0.3 micrograms per mL) was mixed with inhibitor at concentrations in the range 0.1 nanomolar to 10 millimolar. The duplicate mixtures were added to the coated microtiter plate and incubated at rt for 18 h. Then the plate was washed 5 times with PBST and streptavidin horseradish peroxidase was added and incubated for 1 h at rt. This step was followed by washing 5 times with PBST and then TMB horse radish peroxidase substrate was added. After 2 min the colour reaction was stopped with 1M phosphoric acid. Absorbance was read at 450 nm and percent inhibition was calculated using wells containing no inhibitor as the reference. The data were plotted with Origin[®] software (Microcal Software, Northampton, MA).

8.3: NMR Measurements of Oligosaccharide Solution Conformation

NMR measurements for the determination of oligosaccharide conformation were made at 500 MHz and 600 MHz with Varian Unity⁺ 500 and Varian Inova spectrometers. In both cases a self-shielded z gradient triple resonance probe was used. Chemical shifts were referenced to internal 0.1% external acetone (δ_{H} 2.225 ppm, δ_{C} 31.07 ppm, D₂O), or to CD₃OD (δ_{H} 3.30 ppm, δ_{C} 49.0 ppm, CD₃OD). VNMR software version 5.3 was used for data acquisition and processing. Spectra were recorded under temperature controlled conditions at 300.0 ± 0.1K, unless specified.

The general parameters for homonuclear two dimensional NMR experiments were set as follows: for solutions in D₂O at a field strength of 600 MHz, the spectra were recorded with a spectral width of 3.5 kHz in both dimensions, 512 t_1 increments and 2.8K complex points in t_2 . In CD₃OD at 600 MHz, a spectral width of 6.0 kHz in both dimensions, 512 t_1 increments and 3.5K complex points in t_2 were used. At 500 MHz for D₂O solutions, the spectra were recorded with a spectral width of 5.0 kHz in both dimensions, 512 t_1 increments and 4K data points in t_2 .

Homonuclear ^1H two dimensional (2D) gradient coupling correlated spectroscopy experiments (GCOSY)³⁰⁸ were recorded in magnitude mode with 1-2 scans per increment acquired.

2D Gradient total correlation spectroscopy (GTOCSY)³⁰⁹ experiments were acquired with a spin-lock time of 125 ms, and 1-3 scans per increment accumulated.

The remaining spectra were recorded in the phase-sensitive mode by the States' method³¹⁰ for quadrature detection in t_1 .

Homonuclear 2D transverse rotating-frame nuclear Overhauser effect (T-ROESY) experiment was recorded as described by Hwang and Shaka.^{311,312} The effective field for spin-locking was 3.1 kHz and was applied for a mixing time of 400 ms. A total of 16-20 scans per increment accumulated. T-ROESY peak volumes were measured using the 2D integration routine contained in Varian software.

The general parameters for heteronuclear ^{13}C - ^1H -correlated NMR experiments were set as follows: for solutions in D_2O at a field strength of 600 MHz, the spectra were recorded with a f_1 spectral width of 15 kHz and 3.5 kHz in f_2 , 512 t_1 increments, 2.8K complex points with 2.4K points for zero filling in t_2 and an acquisition time of 247 ms. In CD_3OD at 600 MHz, a f_1 spectral width of 30 kHz and 6 KHz in f_2 , 512 t_1 increments, 3K data points with 1.1K points for zero filling in t_2 , and an acquisition time of 251 ms were used. At 500 MHz for D_2O solutions, the spectra were recorded with a f_1 spectral width of 12.6 kHz and 5 kHz in f_2 , 512 t_1 increments, 1.3K data points with 2.8K points for zero filling in t_2 , and an acquisition time of 256 ms. The refocusing delay for the heteronuclear ^{13}C - ^1H -correlated spectra was based on a $150 \text{ Hz } ^1J_{\text{C,H}}$ value.

^{13}C - ^1H -correlated heteronuclear multiple-quantum coherence (HMQC)³¹³ experiments were acquired with 4-8 scans per increment. ^1H - ^{13}C couplings evolving in t_2 were removed by GARP decoupling.

^{13}C - ^1H -correlated heteronuclear multiple-bond coherence (HMBC)³¹⁴ experiments were acquired with a total of 24 scans per increment.

The excitation-sculptured indirect-detection experiments (EXSIDE)²⁷³ in CD₃OD were recorded at 600 MHz on an Inova Varian spectrometer, using a refocusing delay based on a 5 Hz ³J_{CH} value and at a temperature of 318K. Excitation bandwidth selection was carried out with the Varian software-internal package 'Pandora's Box'³¹⁵ using Q3 inversion pulses²⁷⁴ of duration 12.7 ms. The spectra were acquired with 256 *t*₁ increments, 64 scans per increment with 1K data points in *t*₂, 2.89 kHz ¹³C sweep width, a 1.4 s relaxation and a J-scaling factor of 15.

The EXSIDE experiments in pyridine-d₅ were recorded at 800 MHz on a Varian spectrometer at NANUC (the University of Alberta National NMR Centre). A refocusing delay based on a 5 Hz ³J_{CH} value was used for the determination of the ³J_{C4,H1} (9 Hz for ³J_{C1',H4}) coupling constants. 'SEDUCE' inversion pulses of 5.8 ms (10.8 ms) were used for excitation bandwidth selection. The spectra were also acquired with 256 *t*₁ increments, 64 scans per increment with 2K data points in *t*₂, 2.89 kHz (4.8 kHz) ¹³C sweep width, a 1.3 s relaxation and a J-scaling factor of 15 (10).

8.4: NMR Measurements of Trisaccharides Bound to *Ulex europaeus* I

All experiments performed on the bound sugar at 318K were recorded on a Varian Inova 600 MHz. All experiments performed on the bound sugar at 348K were recorded on a Varian Unity⁺ 500 MHz spectrometer equipped with a Varian proton probe.

To determine the optimal conditions for measuring TRNOEs, a protein solution was prepared in a NMR tube containing 0.44 mM of *Ulex europaeus* I dissolved in 10mM PBS, pD 7.0. To this solution aliquots of trisaccharide were added until the desired TRNOEs were observed. Optimal TRNOEs were measured with a sugar:protein ratio of 6:1 and at a temperature of 318K. 2D T₁ρ-filtered TRNOESY³⁰⁵ (30 ms spin lock) spectra were recorded at different mixing times (100→500 msec). Cross-peaks which arose as a result of spin diffusion were identified by the acquisition of off-set compensated TRROESY spectra.³¹⁶ It has been reported that the acquisition of TRROESY

data alone cannot reliably identify all TRNOESY enhancements which contain a component due to spin-diffusion effects. To further detect the presence of spin-diffusion 2D QUIET-TRNOESY experiments were performed.³¹⁷ Data were acquired using a modified $T_{1\rho}$ -filtered TRNOESY pulse sequence where a Q3 selective inversion pulse was inserted in the middle of the mixing time. Varian's "Pandora's Box" was used to generate the required triple-selective (Q3) pulse shape (selective for anomeric protons downfield of HOD (5.3-4.8ppm), majority of non-exchangeable carbohydrate protons (4.00-3.4ppm), and the methyl protons of fucose (1.40-1.10ppm). Mixing times were identical to that used for the standard TRNOESY experiments.

Inter-molecular NOESY correlations were recorded at 318K using a conventional NOESY pulse sequence with a proton sweep-width of 5 kHz and a mixing time of 400 ms.

The same procedure was followed to obtain the optimal TRNOE as described above for the native H-type 2 trisaccharide **1**. The final conditions which gave optimal TRNOEs for **28** used a sample solution containing 9.14 mM of tethered trisaccharide **28** and 0.39 mM of *Ulex europaeus* I in 10 mM PDS (pD 5.0). This resulted in a sugar:protein ratio of 23:1. $T_{1\rho}$ -TRNOESY experiments were acquired in an identical manner for the H-type 2 trisaccharide (**1**) sample.

The $T_{1\rho}$ -TRNOESY experiments of **1** were repeated at 348K using the same sample of H-type 2 trisaccharide **1** and *Ulex* used in the previous experiments at 318K.

8.5: Molecular Modeling

Computer models were assembled using Biosym's Insight II molecular graphics package (v 2.8, Biosym Technologies, San Diego, CA) running on a Silicon Graphics Indigo 2 Challenge computer.

The minimization calculations for the tethered disaccharides described in Chapter 2 were done with the *Discover*[®] program, using the CVFF

forcefield, and graphical displays were printed out from the *Insight*[®] II molecular modeling program.

Rigid body potential energy calculations were performed for the H-type 2 trisaccharide **1** using the CVFF forcefield, as well as the program GEGOP¹³² that is based upon the HSEA forcefield.²⁵⁴ Monosaccharide coordinates were generated from X-ray or neutron diffraction data. Potential energy maps (ϕ, ψ) were calculated for each glycosidic linkage at 5° intervals. For a given linkage, the map was obtained by choosing the minimum energy for each point (rigid body relaxed map).

Computer modeling calculations described in Chapter 5 for the H-type 2 trisaccharide **1** and its tethered derivatives **28** and **29** were performed on either a Silicon Graphics Indigo 2 Extreme workstation with 64 Mb of memory or a Silicon Graphics Indigo 2 Challenge computer with 128 Mb of memory. Simulated annealing, restrained molecular dynamics, and energy minimization were all generated using the AMBER forcefield^{264,265} with a carbohydrate parameter set developed by Homans^{266,267} as implemented with the Biosym module, Discover 2.9.5. Throughout this work the inter-glycosidic torsion angles are defined as ϕ : H1'-C1'-O-Cx and ψ : C1'-O-Cx-Hx. In accordance with typical AMBER requirements the 1-4 non-bonding interactions were scaled by a factor of 0.5. To mimic solvation effects, a bulk dielectric constant of 80.0 was employed.

Random structures were generated by dynamic quenching. An initial structure was built with pyranose rings in the ⁴C₁ chair conformation and trial values of phi (ϕ) and psi (ψ), and subjected to 100 ps of unrestrained molecular dynamics at 750 K, during which the torsional terms were scaled by a factor of 7 to prevent excessive ring-puckering or ring-flipping. A random structure was saved every 10 ps.

Integrated cross-peak ROE volumes were converted to inter-residue proton-proton distances by comparison with the integrated volumes for reliable intra-residue distance such as β -D-N-acetylglucosamine H1-H5 (2.53 Å) and α -L-fucose H1''-H2'' (2.45 Å). A set of distances was derived for each

internal reference and then was averaged to give the NOE derived proton-proton distances

Constraints from NMR measurements were applied in groups, each with a flat-bottomed potential where there is no force applied within the minimum and maximum allowed distances while a force constant of $10 \text{ kcal mol}^{-1} \text{ \AA}^{-2}$ with a maximum force of $10 \text{ kcal mol}^{-1} \text{ \AA}^{-1}$ is applied outside the allowed distance window. NMR constraints were grouped into three restraint groups, each with a minimum distance set to 1.8 \AA and a maximum set to 2.7 \AA (strong), 3.3 \AA (medium), and 5.0 \AA (weak). Restraints are listed in table 5.2 and 5.6.

Energy minimization by restrained simulated annealing was achieved as follows: models were equilibrated for 10 ps with a thermal bath at temperatures of 500 K, 450 K, 350 K, 300 K, and then successively for 1 ps in decreasing steps of 10 K, followed by a further 1 ps at 5 K. The system was minimized using the steepest decent routine until the maximum derivative was below 0.1 kcal/\AA .

Molecular dynamics were performed with a time-step of 1.0 fs and all systems were equilibrated for 10 ps before a further 5 ns were collected. Theoretical, back-calculated proton-proton distances were analyzed using a full-matrix treatment. The software (MDPROCESS), provided by the Homans group, used a r^{-6} formalism.

In the computer modeling of tethered disaccharide **82**, the forcefield was modified by setting the *exo*-anomeric potentials to zero and to mimic the solvation effects of methanol, a bulk dielectric constant of 33.0 was employed.

In the modeling of the trisaccharide **1** and **28** bound to *Ulex* in Chapter 6, a model of the complex was generated by superimposing the fucose residue of the free H-type 2 trisaccharide **1** minimum energy conformation onto the corresponding geometry of the trisaccharide-*Ulex* coordinates.^{63,131,134} The complex was minimized by the conjugate routine. A dielectric constant of 80.0 was used to mimic the solvation of water. The fucose position was constrained in order to avoid expulsion of the

trisaccharide from the binding site and NOE restraints, obtained from TRNOE data, were applied to the protons about the glycosidic linkages. Constraints were also applied to the protein, only the portion of the protein, which was within 20 Å of the ligand was included in the minimization. The computer modeling of the bound conformer of tethered trisaccharides **28** was performed using this same procedure.

8.6: General methods for Synthesis

All commercial reagents were used as supplied. Solvents used in reactions were dried according to standard methods.³¹⁸ Molecular sieves used in the experiments were flame-dried and then cooled under high vacuum immediately prior to use. TLC was performed on silica gel 60-F₂₅₄ plates (E. Merck, Darmstadt) with detection by charring with 5% sulfuric acid in ethanol. Column chromatography was performed on silica gel 60 (E. Merck 40-60 μM, Darmstadt) with redistilled solvents.

¹H NMR spectra were recorded at either 300, 500, or 600 MHz, and are referenced to internal CHCl₃ (δ 7.24 ppm, CDCl₃), or to 0.1% external acetone (δ 2.225 ppm, D₂O), or to internal (CH₃)₂SO (δ 2.50 ppm, (CH₃)₂SO). ¹³C NMR spectra (HMQC or APT) were recorded either at 75, 120, or 150 MHz, and are referenced to internal CHCl₃ (δ 77.0 ppm, CDCl₃) or to 0.1% external acetone (δ 31.07 ppm, D₂O). Assignments of resonances for the deprotected sugars were made by 2D homonuclear and heteronuclear shift correlation experiments (GCOSY and HMQC). H_{link-2} (C_{link-2}) refers to the central linker methylene, whereas H_{link-1} (C_{link-1}) and H_{link-3} (C_{link-3}) refer to the other two methylenes of the linker. The designation of H_{link-1} is assigned to the most downfield shifted methylene. Verification of the position of glycosidic linkages was made by homonuclear 2D offset compensated rotating-frame nuclear Overhauser effect (ROESY) and ¹³C -¹H-correlated heteronuclear multiple-bond coherence (HMBC) experiments.

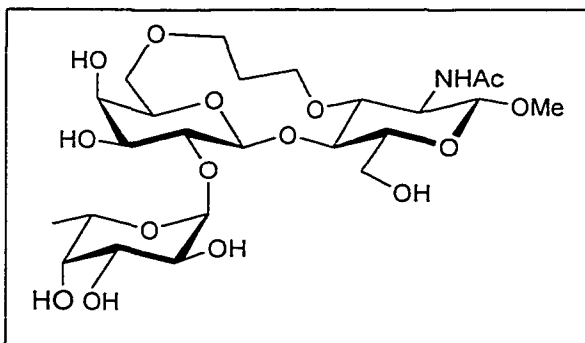
Optical rotations were measured with a Perkin Elmer 241 polarimeter at 22°C. Microanalyses were carried out by the analytical service at this

department, and all samples submitted for elemental analyses were dried overnight under vacuum with phosphorus pentoxide or Drierite at 56°C (refluxing acetone). Electrospray high resolution mass spectra (ES HRMS) of all samples were recorded on a Micromass ZabSpec Hybrid Sector-TOF mass spectrometer.

Purification of final products, deprotected oligosaccharides, was performed by HPLC on a Waters 626 LC System. A semi-preparative column (Beckman Ultrasphere ODS C-18, 80Å pore, particle size 5µm, 10mm x 25cm) was used to perform the reverse phase chromatography. In every case, a flow rate of 2 mL/min was used and the solvent gradient was performed over 30 minutes.

8.7: Synthesis of Constrained H-Type 2 Trisaccharides

Methyl 2-acetamido-2-deoxy-4-O-(2-O-(α -L-fucopyranosyl)- β -D-galactopyranosyl)-3,6'-di-O-(propan-1,3-diyl)- β -D-glucopyranoside (28).

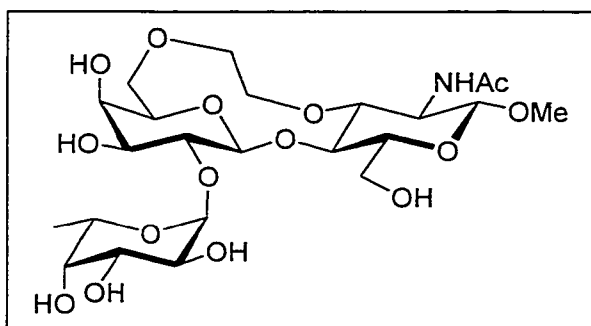


The protected, tethered trisaccharide **61** (7 mg, 0.007 mmol) was dissolved in 90% acetic acid and heated at 65°C for 6 h. The solvents were evaporated and the residue co-evaporated with toluene. The partially protected trisaccharide **62** (R_f

0.13 in 2:3 hexane-acetone) was then dissolved in ethanol (10 mL), to which 20% palladium hydroxide on charcoal was added (10 mg). The mixture was hydrogenated for 18 h under an atmosphere of hydrogen to give **28** as a white solid. The suspension was filtered, concentrated and the crude material was purified by HPLC (water-methanol gradient 0-10%) to give **28** (3.6 mg, 90%). $[\alpha]_D -88.7^\circ$ (c 2.3, H_2O). R_f 0.41 (14:6:1 CH_2Cl_2 -methanol-water). 1H NMR (600 MHz, D_2O): δ 5.39 (d, 1H, $J_{1'',2''}$ 2.0, H-1''), 4.46 (d, 1H, $J_{1',2'}$ 8.1, H-1'), 4.45 (d, 1H, $J_{1,2}$ 8.2, H-1), 4.18 (quartet, 1H, H-5''), 4.13 (dd, 1H, $J_{2,3}$

11.0, H-2), 4.09 (t, $J_{3,4}$ 9.5, $J_{4,5}$ 9.5, H-4), 4.07 (dd, $J_{6a,5}$ 1.8, J_{gem} 11.7, H-6a), 3.87 (H-6'a), 3.87 and 3.44 (H_{link-1}), 3.86 (H-3'), 3.85 (H-6b), 3.84 (H-4''), 3.82 (H-2''), 3.81 (H-3''), 3.79 (H-5'), 3.78 (H-4'), 3.78 and 3.65 (H_{link-3}), 3.77 (H-3), 3.71 (dd, $J_{2',3'}$ 9.5, H-2'), 3.70 (H-6'b), 3.52 (s, 3H, OCH₃), 3.45 (H-5), 2.04 (s, 3H, NHCOCH₃), 1.72-1.79 (m, 2H, H_{link-2}), 1.25 (d, 3H, $J_{5'',6''}$ 6.8, H-6''). ¹³C NMR (125 MHz, D₂O): δ 175.1 (C, NHCOCH₃), 104.0 ($^1J_{C,H}$ 160.7, C-1), 103.0 ($^1J_{C',H'}$ 161.7, C-1'), 100.1 ($^1J_{C'',H''}$ 175.2, C-1''), 79.0 (C-3), 76.4 (C-5), 76.1 (C-2'), 75.6 (C-5'), 75.0 (C-3'), 74.4 (C-4), 72.6, 70.4, 69.0 (C-2'', C-3'', C-4''), 69.9 (C-4'), 69.38 (C-6'), 69.38 (CH₂, C_{link-3}), 67.7 (C-5''), 61.2 (C-6), 58.1 (CH₃O), 57.7 (CH₂, C_{link-1}), 51.2 (C-2), 29.5 (CH₂, C_{link-2}), 22.9 (NHCOCH₃), 16.1 (C-6''). ES HRMS: m/z 606.2373 [M + Na]⁺ \pm 0.1 mDa and 584.3 [M + H]⁺ (C₂₄H₄₁NO₁₅ requires m/z 583.60).

Methyl 2-acetamido-2-deoxy-3,6'-di-O-(ethan-1,2-diyl)-4-O-(2-O-(α -L-fucopyranosyl)- β -D-galactopyranosyl)- β -D-glucopyranoside (29).

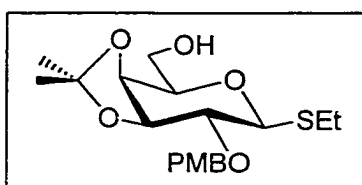


The tethered trisaccharide **85** (53 mg, 0.048 mmol) was dissolved in ethanol (15 mL), to which 20% palladium hydroxide on charcoal was added (55 mg). The mixture was hydrogenated overnight under an

atmosphere of hydrogen. Once filtered, the crude material was purified by HPLC (water-methanol gradient 3-8%). This gave **29** (20 mg, 90%). [α]_D -65.7° (c 12.3, H₂O); ¹H NMR (600 MHz, D₂O): δ 5.48 (d, 1H, $J_{1'',2''}$ 3.5, H-1''), 4.50 (d, 1H, $J_{1,2}$ 8.6, H-1), 4.43 (d, 1H, $J_{1',2'}$ 7.7, H-1'), 4.19 (quartet, 1H, H-5''), 4.13 (dt, 1H, J_{gem} 12.3, J_{link} 1.8, H_{link-1}), 3.94 (H-6'a), 3.93 (H-6a), 3.92 (H_{link-2}), 3.90 (H-3'), 3.88 (dd, 1H, $J_{3'',4''}$ 3.5, $J_{4'',5''}$ 0.9, H-4''), 3.83, 3.81 (H-2'', H-3''), 3.83 (H-4'), 3.80 (H-6b), 3.79 (H-2), 3.75 (dd, 1H, $J_{1',2'}$ 9.3, $J_{2',3'}$ 7.7, H-2'), 3.65 (H-4), 3.64 (H-3), 3.59 (H-6'b), 3.56 (H-5, H_{link-1}), 3.53 (H-5'), 3.51 (H_{link-2} , OCH₃), 2.02 (s, 3H, NHCOCH₃), 1.25 (d, 3H, $J_{5'',6''}$ 6.6, H-6''); ¹³C NMR (150 MHz, D₂O): δ 103.3 (CH, $^1J_{C,H}$ 161.7, C-1'), 101.8 (CH, $^1J_{C,H}$

163.2, C-1), 99.3 (CH, $^1J_{C,H}$ 174.1, C-1''), 82.6 (CH,C-3), 80.8 (CH, C-5), 76.2 (CH, C-5'), 75.6 (CH, C-2'), 75.2 (CH, C-3'), 74.9 (CH, C-4), 72.5 (CH, C-4'), 71.8 (CH₂, C_{link}-2), 71.2 (CH₂, C_{link}-1), 70.3, 69.0 (CH, C-2'', C-3''), 70.1 (CH, C-4''), 69.9 (CH₂, C-6'), 67.6 (CH, C-5''), 62.5 (CH₂, C-6), 57.8 (CH₃, OCH₃), 56.0 (CH, C-2), 22.8 (CH₃, NHCOCH₃), 16.1 (CH₃, C-6''). ES HRMS: m/z 592.222109 [M + Na]⁺ ± 0.4 mDa and 572.3 [M + H]⁺ (C₂₃H₃₉O₁₅N requires m/z 569.56).

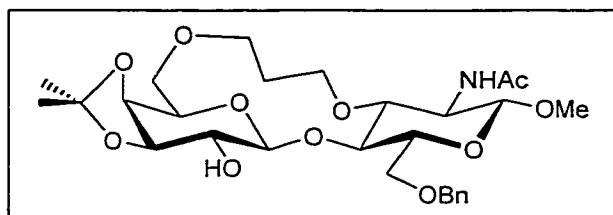
Ethyl 3,4-O-isopropylidene-2-O-p-methoxybenzyl-1-thio-β-D-galactopyranoside (35).



To a mixture of thioglycoside **42**²⁰⁰ (7.86 g, 20.0 mmol) and 2,2-dimethoxypropane (80 mL), was added toluenesulfonic acid (20 mg). The reaction mixture was stirred overnight, neutralized with triethylamine, concentrated and evaporated twice with toluene. The residue was diluted with CH₂Cl₂, washed with brine, dried with anhyd Na₂SO₄ and concentrated. The dried syrup was dissolved in DMF (70 mL) and purged with argon. To the ice cooled solution, NaH (0.58 g, 24.2 mmol) was added portionwise. After stirring for 45 min, *p*-methoxybenzyl chloride (4.10 mL, 30.3 mmol) was added dropwise. After 2 h, another 0.5 equiv of NaH and *p*-methoxybenzyl chloride were added to the reaction mixture. After an additional 2 h, the reaction was complete and diethylamine (1.5 mL) was added to the mixture to destroy excess *p*-methoxybenzyl chloride. The reaction was then quenched with EtOAc containing residual water, diluted with CH₂Cl₂, washed with NaHCO₃, water, and then stirred with 1 M HCl until the mixed acetal (R_f 0.79; 1:1 hexane-EtOAc) had been completely hydrolyzed to **35** (R_f 0.35). The organic layer was then washed with water, NaHCO₃, brine and finally dried over anhyd Na₂SO₄. After removal of the solvent, the crude syrup was chromatographed on silica (5:2 hexane-EtOAc containing 5% triethylamine) to give **35** that crystallized from ether, (3.65 g, 48%) m.p. 90-91°C. [α]_D -2.9° (c 2.8, CHCl₃). ¹H NMR (300 MHz, CDCl₃): δ

7.32, 6.85 (2d, 2H each, J 8.8, ArH), 4.75 (d, 1H, J_{gem} 11.0, $\text{C}_6\text{H}_4\text{CH}_2\text{O}$), 4.67 (d, 1H, $\text{C}_6\text{H}_4\text{CH}_2\text{O}$), 4.40 (d, 1H, $J_{1,2}$ 9.5, H-1), 4.22 (t, 1H, $J_{2,3}$ 6.1, $J_{3,4}$ 5.9, H-3), 4.17 (dd, 1H, $J_{4,5}$ 2.0, H-4), 3.88-3.96 (m, 1H, H-6a or H-6b), 3.74-3.80 (m, 5H, H-5, H-6a or H-6b, $\text{CH}_3\text{OC}_6\text{H}_4$), 3.42 (dd, 1H, H-2), 2.60-2.80 (m, 2H, SCH_2CH_3), 1.43, 1.33 (2s, 3H each, CCH_3), 1.28 (t, 3H, J 7.4, SCH_2CH_3). ^{13}C NMR (75 MHz, CDCl_3): δ 159.3, 130.3 (C, ArC), 130.0, 129.9, 113.8, 113.7 (CH, ArC), 109.9 (C, $(\text{CH}_3)_2\text{C}$), 83.8 (CH, C-1), 79.6 (CH, C-3), 78.8 (CH, C-2), 75.7 (CH, C-5), 74.0 (CH, C-4), 73.3 (CH_2 , $\text{C}_6\text{H}_4\text{CH}_2\text{O}$), 69.4 (CH_2 , C-6), 55.3 (CH_3 , CH_3O), 27.9, 26.4 (CH_3 , $(\text{CH}_3)_2\text{C}$), 24.8 (CH_2 , SCH_2), 15.0 (CH_3 , SCH_2CH_3). Anal. calcd for $\text{C}_{19}\text{H}_{28}\text{O}_6\text{S}$ (384.50): C, 59.35; H, 7.34. Found: C, 59.30; H, 7.41. ES HRMS: m/z 407.149695 [$\text{M} + \text{Na}$] $^+$ \pm 0.7 mDa and 385.2 [$\text{M} + \text{H}$] $^+$ ($\text{C}_{19}\text{H}_{28}\text{O}_6\text{S}$ requires m/z 384.50).

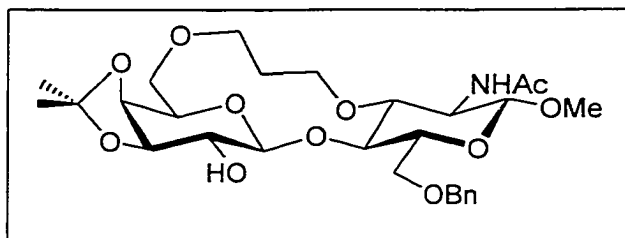
Methyl 2-acetamido-6-O-benzyl-2-deoxy-4-O-(3,4-O-isopropylidene- β -D-galactopyranosyl)-3,6'-di-O-(propan-1,3-diyl)- β -D-glucopyranoside (38).



To compound **59** (36 mg, 0.05 mmol) dissolved in CH_2Cl_2 (1 mL) was added water (0.06 mL) and DDQ (17 mg, 0.08 mmol). The mixture was stirred at rt for 1 h and another 1.5 equiv of DDQ (17 mg, 0.08 mmol) was added. After 1 h the reaction was quenched with a sat. aqueous NaHCO_3 solution. The mixture was diluted with CH_2Cl_2 , washed with NaHCO_3 , brine, dried over anhyd Na_2SO_4 and concentrated. The crude material was chromatographed on silica (1:1 toluene-acetone) and gave **38** (20 mg, 67%) as a white solid. $[\alpha]_D^{+6.8}$ (c 3.7, CHCl_3). ^1H NMR (500 MHz, CDCl_3): δ 7.26-7.36 (5H, ArH), 5.28 (d, 1H, $J_{2,\text{NH}}$ 9.0, NH), 4.65 (d, 1H, J_{gem} 12.1, PhCH_2O), 4.55 (d, 1H, PhCH_2O), 4.33 (d, 1H, $J_{1,2}$ 7.9, H-1), 4.12 (d, 1H, $J_{1,2'}$ 8.4, H-1'), 4.06 (quartet, 1H, $J_{2,3}$ \sim 9.3, H-2), 3.94 (t, $J_{3',4'}$ \sim 5.5, H-3'), 3.88 (H-4'), 3.87 (H-6a), 3.86 (H-4), 3.79 (H-6b), 3.73, 3.68, 3.63, 3.58 ($\text{H}_{\text{link-1}}$, $\text{H}_{\text{link-3}}$, H-6'a, H-6'b), 3.67 (H-3), 3.53 (ddd, 1H, $J_{\text{H,OH}}$ 2.5, $J_{2',3'}$ 6.5, H-2'), 3.45 (H-5, CH_3O), 1.99 (s, 3H, NHCOCH_3), 1.60-1.78 (m, 2H, $\text{H}_{\text{link-2}}$), 1.56, 1.47 (2

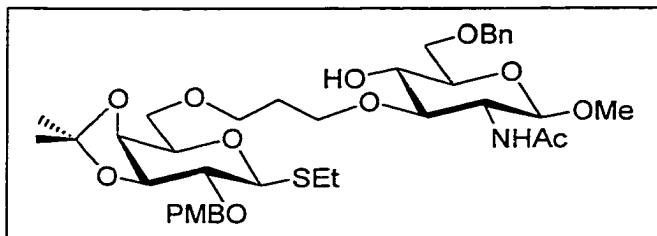
s, 3H each, CCH₃). ¹³C NMR (125 MHz, CDCl₃): δ 128.0, 127.9 (CH, ArC), 105.0 (CH, ¹J_{C,H} 151.4, C-1'), 102.3 (CH, ¹J_{C,H} 163.2, C-1), 79.9 (CH, C-3'), 79.2 (CH, C-3), 77.6 (CH, C-4'), 74.1 (CH, C-5), 73.69 (CH, C-2'), 73.66 (CH₂, PhCH₂O), 73.0 (CH, C-4), 69.3 (CH₂, C-6), 68.3 (CH, C-5'), 66.1 (CH₂, C_{link}-1, C_{link}-3), 59.3 (CH₂, C-6'), 56.4 (CH₃, OCH₃), 52.3 (CH, C-2), 30.7 (CH₂, C_{link}-2), 27.9, 26.1 (CH₃, C(CH₃)₂), 23.5 (CH₃, CH₃CONH). Anal. calcd for C₂₈H₄₁NO₁₁ (567.64): C, 59.25; H, 7.28; N, 2.47. Found: C, 59.56; H, 7.57; N, 2.42.

Methyl 2-acetamido-6-O-benzyl-2-deoxy-4-O-(3,4-O-isopropylidene-β-D-galactopyranosyl)-3,6'-di-O-(propan-1,3-diyl)-β-D-glucopyranoside (38).



Compound **146** (77 mg, 0.13 mmol) was dissolved in (CH₃)₂SO (2 mL) with potassium *t*-butoxide (29 mg, 0.25 mmol). The reaction mixture was heated to 100°C for 1 h, diluted with water, neutralized with dry ice, and the solvents were evaporated. The residue was dissolved in CH₂Cl₂, washed with brine and dried with Na₂SO₄. Once concentrated, the residue was dissolved in a 3:1 acetone and 2M HCl solution (4 mL) and refluxed for 30 min. The reaction was neutralized with saturated NaHCO₃ (aq), evaporated, and chromatographed on silica (2:1 Toluene-Acetone) to give **38** (51 mg, 71%). The spectral data matched that of **38** made from **59**.

Ethyl 3,4-O-isopropylidene-2-O-p-methoxybenzyl-6-O-(3'-O-(methyl 2-acetamido-6-O-benzyl-2-deoxy-β-D-glucopyranos-3-oxy)propyl)-1-thio-β-D-galactopyranoside (39).

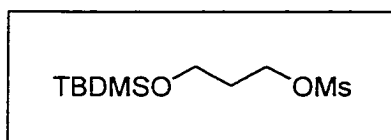


Dry THF (5 mL) was added to a mixture of compound **58** (34 mg, 0.05 mmol), sodium cyanoborohydride (30 mg, 0.5 mmol), dry powdered 3 Å

molecular sieves and methyl orange (1 mg). The suspension was purged with argon. A freshly made saturated solution of HCl in dry ether was added dropwise to the reaction mixture until the evolution of gases ceased and the indicator turned bright pink. A further two fold volume of saturated HCl in ether was added and the reaction was left to stir for 30 min. The reaction mixture was diluted with CH₂Cl₂, filtered through celite, washed with NaHCO₃, brine and dried over Na₂SO₄. After solvent evaporation, column chromatography of the crude material on silica (2:1 toluene-acetone) gave **39** (11.9 mg, 35%). [α]_D -12.1° (c 1.9, CHCl₃). ¹H NMR (500 MHz, CDCl₃): δ 6.84-7.32 (ArH), 5.77 (d, 1H, J_{2',NH} 8.0, NHAc), 4.73 (d, 1H, J_{gem} 11.0, C₆H₄CH₂O), 4.69 (d, 1H, J_{1',2'} 8.2, H-1'), 4.65 (d, 1H, CH₃OC₆H₄CH₂O), 4.59 (d, 1H, J_{gem} 12.1, PhCH₂O), 4.57 (d, 1H, PhCH₂O), 4.36 (d, 1H, J_{1,2} 9.5, H-1), 4.15 (t, 1H, J_{3,4} ~6.0, H-3), 4.11 (dd, 1H, J_{4,5} 1.8, H-4), 3.81 (ddd, 1H, J_{5,6a/b} 6.0, H-5), 3.80 (H-6'a, H-6'b), 3.77 (CH₃OC₆H₄), 3.75, 3.61 (H_{link-3}, H_{link-1}), 3.73 (H-3'), 3.66 (H-6a, H-6b), 3.50 (H-4'), 3.48 (H-5'), 3.46 (s, CH₃O), 3.39 (dd, 1H, J_{2,3} 6.4, H-2), 3.29 (quartet, 1H, J_{2',3'} ~8.2, H-2'), 2.60-2.78 (m, 2H, SCH₂CH₃), 1.97 (s, 3H, NHCOCH₃), 1.70-1.83 (m, 2H, H_{link-2}), 1.40, 1.31 (2 s, 3H each, CCH₃), 1.28 (t, 3H, J 7.4, SCH₂CH₃). ¹³C NMR (125 Hz, CDCl₃): δ 129.8, 127.2, 113.5 (CH, ArCH), 100.9 (CH, J_{C-H} 162.8, C-1), 83.7 (CH, J_{C-H} 154.8, C'-1), 81.2 (CH, C-3), 79.7 (CH, C'-3), 78.4 (CH, C'-2), 75.2 (CH, C'-5), 74.2 (CH, C-4), 74.0 (CH, C'-4), 73.7 (CH₂, PhCH₂O), 73.2 (CH₂, CH₃OC₆H₄CH₂O), 71.8 (CH, C-5), 70.2 (CH₂, C-6, C'-6), 68.7, 68.5 (CH₂, C_{link-3}, C_{link-1}), 56.6 (CH₃, CH₃O), 56.5 (CH, C-2), 55.2 (CH₃, CH₃OC₆H₄),

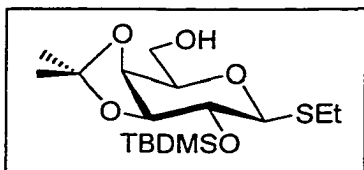
29.6 (CH₂, C_{link}-2), 27.7, 26.1 (CH₃, C(CH₃)₂), 24.6 (CH₂, SCH₂), 23.3 (CH₃, CH₃CONH), 15.1 (CH₃,SCH₂CH₃). Anal. calcd for C₃₈H₅₅NO₁₂S (749.93): C, 60.86; H, 7.39; N, 1.87; S, 4.28. Found: C, 61.07; H, 7.60; N, 1.95; S, 4.23. ES HRMS: m/z 772.334429 [M + Na]⁺ ± 0.2 mDa and 750.3 [M + H]⁺ (C₃₈H₅₅NO₁₂S requires m/z 749.93). The acetylated form of **39** provided a characteristic NMR spectrum showing a downfield shift of the 4-OH signal (4.88 ppm).

1-O-t-butyltrimethylsilyloxy-3-O-methanesulphonyloxy-propane (41).



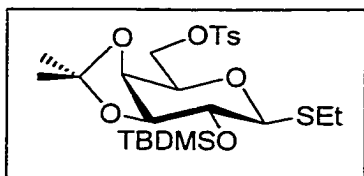
Diol **37** (3.06 g, 40.3 mmol) was added dropwise to a solution of NaH (0.967 g, 40.3 mmol) in dry THF (60 mL) purged with argon. After stirring for 1 h, TBDMSCl (6.06 g, 40.3 mmol) was added portionwise and the reaction was stirred overnight. Triethylamine (8.3 mL, 61.4 mmol) was added followed by slow addition of MsCl (5 mL, 56.0 mmol) in dry THF (5 mL). After 90 min, the reaction was diluted with ether, washed with water, 1 M NaOH, brine, dried over anhyd Na₂SO₄ and concentrated. The residue was chromatographed on silica (10:1 hexane-EtOAc) to give a clear yellow liquid (8.83 g, 81%). IR ν_{\max} (film): 1359.3, 1256.5, 1177.1, 1103.0, 944.2, 836.7, 777.8 cm⁻¹. ¹H NMR (300 MHz, CDCl₃): δ 4.29 (t, 2H, MsOCH₂), 3.67 (t, 2H, TBDMSOCH₂), 2.94 (s, 3H, CH₃SO₃), 1.88 (quintet, 2H, CH₂CH₂CH₂), 0.88 (s, 9H, *t*Bu), 0.05 (s, 6H, (CH₃)₂Si). ¹³C NMR (75 MHz, CDCl₃): δ 67.2 (CH₂), 58.4 (CH₂), 37.2 (CH₃, CH₃SO₃), 32.2 (CH₂, CH₂CH₂CH₂), 25.9 (CH₃, *t*-Bu), -5.4 (CH₃, (CH₃)₂Si). Anal. calcd for C₁₀H₂₄O₄SSi (268.46): C, 44.74; H, 9.01. Found: C, 44.61; H, 9.22. ES HRMS: m/z 291.105761 [M + Na]⁺ ± 0.5 mDa and 269.1 [M + H]⁺ (C₁₀H₂₄O₄SSi requires m/z 268.46).

Ethyl 2-O-*t*-butyldimethylsilyl-3,4-O-isopropylidene-1-thio- β -D-galactopyranoside (44).



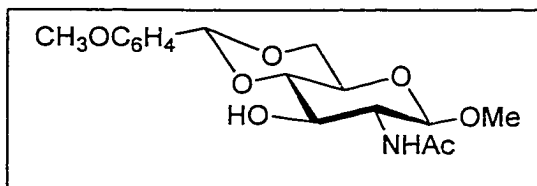
To a mixture of thioglycoside **42**²⁰⁰ (2.69 g, 12.0 mmol) and 2,2-dimethoxypropane (30 mL), was added toluenesulfonic acid (20 mg). The reaction mixture was stirred overnight, neutralized with triethylamine, concentrated and evaporated twice with toluene. The residue was diluted with CH₂Cl₂, washed with brine, dried with anhyd Na₂SO₄ and concentrated. The dried syrup was dissolved in dry THF (50 mL) and purged with argon. To the ice cooled solution, NaH (0.29 g, 12.1 mmol) was added portionwise. After stirring for 45 min, *t*-butyldimethylsilyl chloride (1.81 g, 12.0 mmol) was added portionwise. After 1 h, another 0.5 equiv of NaH and *t*-butyldimethylsilyl chloride were added to the reaction mixture. After an additional 2 h, the reaction was complete and methanol (1 mL) was added to destroy any remaining NaH. The reaction was diluted with CH₂Cl₂, washed with NaHCO₃, water, and then stirred with 1 M HCl until the mixed acetal had been completely hydrolyzed to **44**. The organic layer was then washed with water, NaHCO₃, brine and finally dried over anhyd Na₂SO₄. After removal of the solvent, the crude syrup was chromatographed on silica (5:1 hexane-EtOAc containing) to give **44** (2.50 g, 53%). [α]_D -26.9° (c 26.3, CHCl₃). ¹H NMR (360 MHz, CDCl₃): δ 4.31 (d, 1H, J_{1,2} 9.2, H-1), 4.15 (dd, 1H, J_{3,4} 5.7, J_{4,5} 2.1, H-4), 4.00 (t, 1H, J_{2,3} 6.0, H-3), 3.93 (dd, 1H, J_{5,6a} 6.92, J_{6a,6b} 11.1, H-6a), 3.81 (m, 2H, J_{5,6b} 4.1, H-5, H-6b), 3.57 (dd, 1H, H-2), 2.60-2.80. (m, 2H, SCH₂CH₃), 1.47, 1.32 (2s, 3H each, CCH₃), 1.25 (t, 3H, J 7.4, SCH₂CH₃), 0.89 (s, 9H, (CH₃)₃CSi), 0.13 (s, 6H, (CH₃)₂Si). ¹³C NMR (120 MHz, CDCl₃): δ 110.1 (CH₂), 85.5 (CH), 80.6 (CH), 76.6 (CH), 74.1 (CH), 73.8 (CH), 62.7 (CH₂), 27.9 (CH₃), 26.4 (CH₃), 26.0 (CH₃), 24.6 (CH₂), 18.3 (CH₃), 15.1 (CH₂), -4.2 (CH₃), -4.6 (CH₃). ES HRMS: m/z 401.179717 [M + Na]⁺ \pm 0.3 mDa and 379.2 [M + H]⁺ (C₁₇H₃₄O₅SiS requires m/z 378.60).

Ethyl 2-O-t-butyltrimethylsilyl-3,4-O-isopropylidene-1-thio-6-O-toluenesulphonyl- β -D-galactopyranoside (45).



Toluenesulphonyl chloride (172 g, 0.89 mmol) was added to a mixture of thioglycoside **44** (224 g, 0.58 mmol) and dry pyridine (1 mL). The reaction mixture was diluted with CH_2Cl_2 , washed with K_2CO_3 , brine and then dried with Na_2SO_4 . After co-evaporation with toluene, the residue was filtered through silica (5:1 hexane-EtOAc) to give **45** (0.303 g, 96%), which was immediately used in the coupling reaction with **49**. ^1H NMR (300 MHz, CDCl_3): δ 7.77, 7.31 (2d, 2H each, ArH), 4.29 (d, 1H, $J_{1,2}$ 8.8, H-1), 4.14-4.27 (m, 2H, H-3, H-6a), 4.00 (dd, 1H, $J_{3,4}$ 5.8, $J_{4,5}$ 2.2, H-4), 3.90-4.05 (m, 2H, H-6b, H-5), 3.53 (dd, 1H, $J_{2,3}$ 6.1, H-2), 2.50-2.70. (m, 2H, SCH_2CH_3), 2.43 (s, 3H, CH_3Ph), 1.39 (s, 3H, CCH_3), 1.15-1.30 (m, 6H, CCH_3 , J 7.3, SCH_2CH_3), 0.87 (s, 9H, $(\text{CH}_3)_3\text{CSi}$), 0.09 (s, 6H, $(\text{CH}_3)_2\text{Si}$).

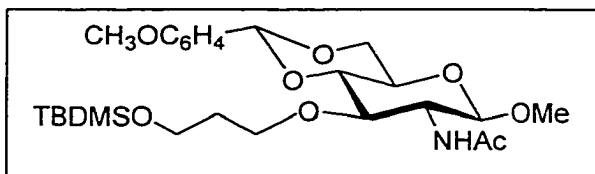
Methyl 2-acetamido-2-deoxy-4,6-O-p-methoxybenzylidene- β -D-glucopyranoside (47).



Toluenesulfonic acid (25 mg) and anisaldehyde dimethyl acetal (1.6 mL, 10.5 mmol) was added to a suspension of methyl 2-acetamido-2-deoxy- β -D-glucopyranoside **46**^{202,203} (1.65 g, 7.02 mmol) in dry acetonitrile (50 mL). The mixture was sonicated and then stirred overnight. Filtration gave benzylidene **47**³¹⁹ as a solid (2.25 g, 90%). ^1H NMR (360 MHz, $(\text{CD}_3)_2\text{SO}$): δ 7.80 (d, 1 H, $J_{2,\text{NH}}$ 8.5, NH), 7.36, 6.91 (2d, 2H each, ArH), 5.53 (s, 1H, $\text{C}_6\text{H}_4\text{CH}$), 4.38 (d, 1H, $J_{1,2}$ 8.0, H-1), 4.18 (dd, 1H, $J_{5,6a}$ 4.8, $J_{6a,6b}$ 10.1, H-6a), 3.74 (s, 3H, $\text{CH}_3\text{OC}_6\text{H}_4$), 3.70 (t, 1H, $J_{5,6b}$ 9.9, H-6b), 3.25-3.60 (m, H-2, H-3, H-4, H-5, OCH_3 , HOD), 1.80 (s, 3H, NHCOCH_3). ^{13}C NMR (120 MHz, $(\text{CD}_3)_2\text{SO}$): δ 127.5, 113.1 (CH, ArC), 100.6 (CH, $\text{CH}_3\text{OC}_6\text{H}_4\text{CH}$), 102.2 (CH, C-1), 92.5, 81.1, 70.6 (CH, C-3, C-4, C-5), 67.5 (CH_2 , C-6), 65.6 (CH, C-2), 55.6 (CH_3 , CH_3O), 55.0 (CH_3 , $\text{CH}_3\text{OC}_6\text{H}_4$), 22.8 (CH_3 , NHAc). ES HRMS: m/z

376.137552 [M + Na]⁺ ± 0.3 mDa and 354.2 [M + H]⁺ (C₁₇H₂₃NO₇ requires m/z 353.37).

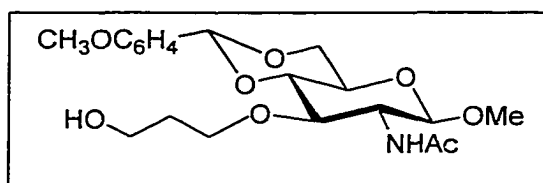
Methyl 2-acetamido-3-O-(3'-O-*t*-butyldimethylsilyloxypropyl)-2-deoxy-4,6-O-*p*-methoxybenzylidene-β-D-glucopyranoside (48).



NaH (40 mg, 1.65 mmol) was added to a solution of alcohol **47** (529 mg, 1.5 mmol) in dry (CH₃)₂SO (15 mL). After stirring for 1 h at 40°C, 1-*O-t*-

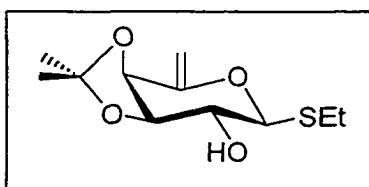
butyldimethylsilyloxy-3-*O*-methanesulphonyloxy-propane (594 mg, 1.65 mmol) was added dropwise. The reaction mixture was stirred at 40°C overnight, after which 0.5 equiv of NaH and 0.4 equiv of linker were added. The reaction was quenched with MeOH, diluted with CH₂Cl₂, and washed with water. The aqueous layer was back extracted with CH₂Cl₂, the combined organic layers were then washed with NaHCO₃, brine and dried over anhyd Na₂SO₄. After concentration, column chromatography of the crude material on silica (1:2 hexane-EtOAc) gave **48** (479 mg, 61%). ¹H NMR (600 MHz, (CD₃)₂SO): δ 7.92 (d, 1 H, J_{2,NH} 9.0, NH), 7.32, 6.89 (2d, 2H each, ArH), 5.56 (s, 1H, C₆H₄CH), 4.40 (d, 1H, J_{1,2} 8.3, H-1), 4.18 (dd, 1H, J_{5,6a} 4.9, J_{6a,6b} 10.1, H-6a), 3.73 (s, 3H, CH₃OC₆H₄), 3.65-3.72 (m, 2H, H-6b, H_{link-1}), 3.30-3.60 (m, H-2, H-3, H-4, H-5, CH₃O, 2xH_{link-3}, H_{link-1}, HOD), 1.81 (s, 3H, NHCOCH₃), 1.75 (m, 2H, H_{link-2}), 0.80 (s, 9H, (CH₃)₃CSi), -0.05 (s, 6H, (CH₃)₂Si). ¹³C NMR (125 MHz, CDCl₃): δ. 129.9, 113.2 (CH, ArC), 102.2 (CH, C-1), 100.1 (CH, C₆H₄CH), 80.9, 79.1 (CH, C-3, C-4), 68.3, 67.7 (C_{link-1}, C-6), 65.6 (CH, C-5), 59.6 (CH, C-2), 55.9, 54.9 (CH₃O, C_{link-3}), 54.3 (CH₃, CH₃OC₆H₄), 33.0 (CH₂, C_{link-2}), 22.8 (CH₃, C(CH₃)₃), 17.7 (CH₃, NHCOCH₃), -5.5 (CH₃, (CH₃)₂Si). ES HRMS: m/z 548.265368 [M + Na]⁺ ± 0.2 mDa and 526.3 [M + H]⁺ (C₂₆H₄₃NO₈Si requires m/z 525.72).

Methyl 2-acetamido-2-deoxy-3-O-(3'-hydroxypropyl)-4,6-O-p-methoxybenzylidene-β-D-glucopyranoside (49).



Compound **48** (128 mg, 0.24 mmol) was stirred for 1 h with a solution of TBAF in THF (1 M, 1 mL). The reaction mixture was evaporated, diluted with CH_2Cl_2 , washed with brine, dried over anhyd Na_2SO_4 and concentrated. The crude syrup was chromatographed on silica (20:1 CH_2Cl_2 -MeOH) to give **49** (78 mg, 78%). ^1H NMR (300 MHz, CDCl_3 & $(\text{CD}_3)_2\text{SO}$): δ 7.30, 6.78 (2d, 2H each, ArH), 6.89 (d, 1 H, $J_{2,\text{NH}}$ 8.1, NH), 5.40 (s, 1H, $\text{C}_6\text{H}_4\text{CH}$), 4.63 (d, 1H, $J_{1,2}$ 8.2, H-1), 4.22 (dd, 1H, $J_{5,6a}$ 4.8, $J_{6a,6b}$ 10.3, H-6a), 3.80-3.92 (m, 2H, H-4, $\text{H}_{\text{link-1}}$), 3.70 (s, 3H, $\text{CH}_3\text{OC}_6\text{H}_4$), 3.52-3.69 (m, 4H, H-6b, $2x\text{H}_{\text{link-3}}$, $\text{H}_{\text{link-1}}$), 3.32-3.48 (m, CH_3O , H-2, H-5, HOD), 1.91 (s, 3H, NHCOCH_3), 1.52-1.78 (m, 2H, $\text{H}_{\text{link-2}}$). ^{13}C NMR (75 MHz, CDCl_3 & $(\text{CD}_3)_2\text{SO}$): δ . 127.1, 113.5 (CH, ArC), 101.8 (CH, C-1), 100.9 (CH, $\text{C}_6\text{H}_4\text{CH}$), 81.6 (CH, C-5), 77.6 (CH, C-4), 69.7 (CH_2 , $\text{C}_{\text{link-1}}$), 68.4 (CH_2 , C-6), 65.8 (CH, C-2), 59.7 (CH_2 , $\text{C}_{\text{link-3}}$), 56.6 (CH_3 , CH_3O), 54.9 (CH_3 , $\text{CH}_3\text{OC}_6\text{H}_4$), 32.2 (CH_2 , $\text{C}_{\text{link-2}}$), 23.1 (CH_3 , NHCOCH_3). ES HRMS: m/z 434.179425 [$\text{M} + \text{Na}$] $^+$ \pm 0.3 mDa and 412.3 [$\text{M} + \text{H}$] $^+$ ($\text{C}_{20}\text{H}_{29}\text{NO}_8$ requires m/z 411.45).

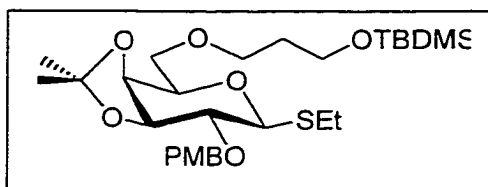
Ethyl 6-deoxy-3,4-O-isopropylidene-1-thio-β-D-galacto-hex-5-enopyranoside (50).



Sodium hydride (4.5 mg, 0.19 mmol) was added to a solution of glucopyranoside **49** (78 mg, 0.19 mmol) in dry DMF (10 mL). The mixture was stirred for 45 min at 60°C under argon. The toluenesulphonate **45** (100 mg, 0.19 mmol) in dry DMF (2 mL) was added and the reaction was stirred at 60°C. No reaction was observed until the reaction was concentrated to approximately 5 mL and an additional equiv of NaH was added. The cooled reaction mixture was quenched with MeOH, diluted with CH_2Cl_2 , washed with water, the aqueous layer was back-extracted with

CH₂Cl₂, and the combined organic layers were washed with NaHCO₃, brine and dried over Na₂SO₄. The concentrated residue was chromatographed on silica (3:1 hexane-EtOAc) and gave the elimination product **50**. No traces of the desired product was found. ¹H NMR (360 MHz, (CD₃)₂SO): δ 5.69 (d, 1H, J_{2,OH} 5.6, OH), 4.88 (d, 1H, J_{1,2} 7.1, H-1), 4.67 (d, 1H, J_{3,4} 6.7, H-4), 4.53 (d, 2H, J_{gem} 12.5, =CH₂), 4.10 (t, 1H, J_{2,3} 5.6, H-3), 3.56 (dd, 1H, H-2), 2.55-2.70 (m, 2H, SCH₂CH₃), 1.43, 1.29 (2s, 3H each, CCH₃), 1.21 (t, 3H, J 7.3, SCH₂CH₃). Addition of D₂O to the sample lead to the disappearance of the peak at 5.69 ppm and verified its assignment as a hydroxyl resonance.

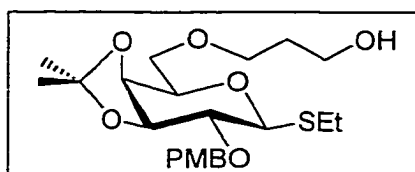
Ethyl 6-O-(3'-O-t-butyltrimethylsilyloxypropyl)-3,4-O-isopropylidene-2-O-p-methoxybenzyl-1-thio-β-D-galactopyranoside (51).



NaH (25 mg, 1.0 mmol) was added to a solution of alcohol **35** (378 mg, 1.0 mmol) in dry THF (4 mL). After stirring for 30 min at 60°C, a solution of 1-O-t-butyltrimethylsilyloxy-3-O-methanesulphonyloxy-propane (360 mg, 1.0 mmol) in dry THF (1 mL) was added dropwise. The reaction mixture was stirred at 60°C for 3 h, then 1 equiv of both NaH and linker were added. The reaction mixture was allowed to concentrate by evaporation of solvent to approximately one third of its original volume by turning off the condenser. Tlc indicated complete conversion of the alcohol. The reaction was quenched with EtOAc containing residual water, diluted with CH₂Cl₂, washed with water, NaHCO₃, brine and then dried over anhyd Na₂SO₄. After concentration, column chromatography of the crude material on silica (8:1 hexane-EtOAc) gave **51** (501 mg, 91%) as an oil. [α]_D -8.8° (c 14.7, CHCl₃). ¹H NMR (300 MHz, CDCl₃): δ 7.32, 6.84 (2d, 2H each, J 8.4, ArH), 4.75 (d, 1H, J_{gem} 11.0, C₆H₄CH₂O), 4.66 (d, 1H, C₆H₄CH₂O), 4.38 (d, 1H, J_{1,2} 9.7, H-1), 4.16 (m, 2H, H-3, H-4), 3.81 (H-5), 3.77 (s, CH₃OC₆H₄), 3.66 (H_{link}-1), 3.60-3.70 (H-6a, H-6b), 3.55 (m, 2H, H_{link}-3), 3.40 (dd, 1H, J_{2,3} 6.1, H-2), 2.58-2.78 (m, 2H, SCH₂CH₃), 1.75 (quintet, 2H, H_{link}-2), 1.42, 1.32 (2s, 3H each, CCH₃), 1.28 (t,

3H, J 7.5, SCH₂CH₃), 0.86 (s, 9H, (CH₃)₃CSi), 0.02 (s, 6H, (CH₃)₂Si).
¹³C NMR (75 MHz, CDCl₃): δ 130.0, 113.8 (CH, ArC), 83.6 (CH, ¹J_{C,H} 152.2, C-1), 79.2 (CH, C-3), 78.4 (CH, C-2), 75.1 (CH, C-5), 73.6 (CH, C-4), 72.9 (CH₂, C₆H₄CH₂O), 69.7 (CH₂, C-6), 67.9 (CH₂, C_{link-3}), 59.7 (CH₂, C_{link-1}), 55.1 (CH₃, CH₃O), 32.5 (CH₂, C_{link-2}), 27.5, 26.0 (CH₃, C(CH₃)₂), 25.7 (CH₃, (CH₃)₃CSi), 24.4 (CH₂, SCH₂), 14.8 (CH₃,SCH₂CH₃), -5.6 (CH₃, (CH₃)₂Si).
 Anal. calcd for C₂₈H₄₈O₇SSi (556.85): C, 60.39; H, 8.69. Found: C, 60.37; H, 8.81. ES HRMS: m/z 579.278341 [M + Na]⁺ ± 0.4 mDa and 558.0 [M + H]⁺ (C₂₈H₄₈O₇SSi requires m/z 556.85).

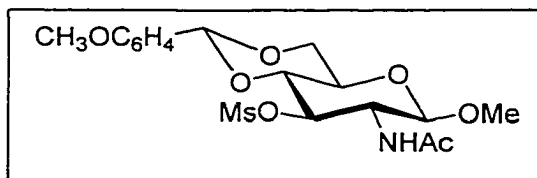
Ethyl 6-O-(3'-hydroxypropyl)-3,4-O-isopropylidene-2-O-p-methoxybenzyl-1-thio-β-D-galactopyranoside (52).



Compound **51** (218 mg, 0.4 mmol) was stirred for 1 h with a solution of TBAF in THF (1 M, 5 mL). The reaction mixture was evaporated, diluted with CH₂Cl₂, washed with brine, dried over anhyd Na₂SO₄ and concentrated. The crude syrup was chromatographed on silica (1:1 hexane-EtOAc) to give **52** (172 mg, 100%) as an oil. [α]_D -9.7° (c 3.2, CHCl₃). ¹H NMR (300 MHz, CDCl₃): δ 7.31, 6.83 (2d, 2H each, J 8.7, ArH), 4.73 (d, 1H, J_{gem} 11.1, C₆H₄CH₂O), 4.65 (d, 1H, C₆H₄CH₂O), 4.38 (d, 1H, J_{1,2} 9.6, H-1), 4.17 (H-3), 4.13 (H-4), 3.83 (m, 1H, H-5), 3.76 (s, CH₃OC₆H₄), 3.74, 3.68 (H_{link-3}, H_{link-1}), 3.66-3.74 (H-6a, H-6b), 3.40 (dd, 1H, J_{2,3} 6.0, H-2), 2.58-2.80 (m, 2H, SCH₂CH₃), 1.79 (m, 2H, H_{link-2}), 1.40, 1.32 (2s, 3H each, CCH₃), 1.27 (t, 3H, J 7.4, SCH₂CH₃). ¹³C NMR (75 MHz, CDCl₃): δ 159.3, 129.9 (C, ArC), 130.0, 113.7 (CH, ArC), 110.0 (C, (CH₃)₂C), 83.7 (CH, ¹J_{C,H} 152.2, C-1), 79.6 (CH, C-3), 78.6 (CH, C-2), 75.4 (CH, C-5), 73.9 (CH, C-4), 73.2 (CH₂, C₆H₄CH₂O), 70.3 (CH₂, C-6), 70.9 (CH₂, C_{link-1}), 61.9 (CH₂, C_{link-3}), 55.3 (CH₃, CH₃O), 31.8 (CH₂, C_{link-2}), 27.9, 26.3 (CH₃, C(CH₃)₂), 24.6 (CH₂, SCH₂), 14.9 (CH₃,SCH₂CH₃). Anal. calcd for C₂₂H₃₄O₇S (442.58): C, 59.70; H, 7.74; S, 7.25. Found: C, 59.51; H, 7.90; S, 7.18. ES HRMS: m/z

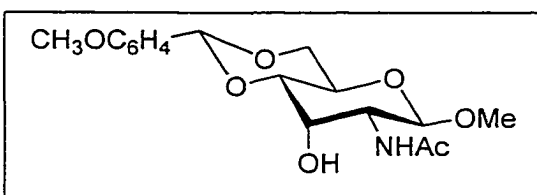
465.192284 [M + Na]⁺ ± 0.0 mDa and 443.2 [M + H]⁺ (C₂₂H₃₄O₇S requires m/z 442.58).

Methyl 2-acetamido-2-deoxy-3-O-methanesulphonyloxy-4,6-O-p-methoxybenzylidene-β-D-glucopyranoside (53).



Triethylamine (0.36 mL, 2.62 mmol) was added to a solution of alcohol **47**³¹⁹ (555 mg, 1.57 mmol) in dry CH₂Cl₂ (10 mL). Methanesulphonyl chloride (0.18 mL, 2.36 mmol) in CH₂Cl₂ (2 mL) was added dropwise. After stirring for 1 h at rt, the solution was diluted with CH₂Cl₂, washed with water, 1 M NaOH, water, brine, and dried over anhyd Na₂SO₄. Evaporation and chromatography on silica (20:1 dichloromethane-methanol) gave **53** (514 mg, 74%). ¹H NMR (300 MHz, (CD₃)₂SO): δ 8.08 (d, 1 H, J_{2,NH} 9.0, NH), 7.35, 6.91 (2d, 2H each, ArH), 5.65 (s, 1H, C₆H₄CH), 4.74 (t, 1H, J_{2,3} 9.7, J_{3,4} 9.7, H-3), 4.59 (d, 1H, J_{1,2} 8.3, H-1), 4.25 (dd, J_{5,6a} 5.0, J_{6a,6b} 10.2, H-6a), 3.20-3.90 (m, H-2, H-4, H-5, H-6b, CH₃O, CH₃OPh, HOD), 3.00 (s, 3H, CH₃SO₃), 1.80 (s, 3H, NHCOCH₃).

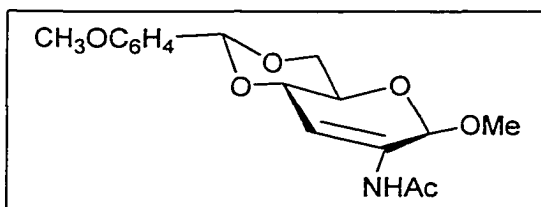
Methyl 2-acetamido-2-deoxy-4,6-O-p-methoxybenzylidene-β-D-allopyranoside (54).



Starting material **53** (0.45 g, 1.04 mmol) was dissolved in 2-methoxy-ethanol (5 mL) with NaOAc (0.43 g, 5.20 mmol) and water (0.25 mL). The reaction mixture was heated to 118°C under argon overnight. Once cooled, the precipitated product was filtered and then dissolved in CH₂Cl₂, washed with water, dried with anhyd Na₂SO₄. Evaporation and chromatography on silica (20:1 dichloromethane-methanol) gave **54** (313 mg, 85%). ¹H NMR (600 MHz, (CD₃)₂SO): δ 7.93 (d, 1 H, J_{2,NH} 8.6, NH), 7.36, 6.90 (2d, 2H each, ArH), 5.57 (s, 1H, C₆H₄CH), 5.42 (d, 1H, J_{3,OH} 4.4, OH), 4.55 (d, 1H, J_{1,2} 8.6, H-1),

4.20 (dd, $J_{5,6a}$ 5.1, $J_{6a,6b}$ 9.9, H-6a), 3.94 (broad quintet, 1H, H-3), 3.83 (ddd, 1H, $J_{4,5}$ 9.9, $J_{5,6b}$ 9.9, H-5), 3.70-3.76 (m, 4H, H-2, $\text{CH}_3\text{OC}_6\text{H}_4$), 3.66 (t, H-6b), 3.58 (dd, 1H, $J_{3,4}$ 2.4, H-4), 3.33 (s, 3H, CH_3O), 1.83 (s, 3H, NHCOCH_3). ^{13}C NMR (150 MHz, $(\text{CD}_3)_2\text{SO}$): δ 127.5, 113.1 (CH, ArC), 100.5 (CH, $\text{C}_6\text{H}_4\text{CH}$), 100.0 (CH, C-1), 78.3 (CH, C-4), 68.1 (CH_2 , C-6), 66.9 (CH, C-3), 62.7 (CH, C-5), 55.8 (CH_3 , CH_3O), 55.0 (CH_3 , $\text{CH}_3\text{OC}_6\text{H}_4$), 52.7 (CH, C-2), 22.5 (CH_3 , NHCOCH_3). ES HRMS: m/z 376.137564 $[\text{M} + \text{Na}]^+ \pm 0.3$ mDa and 354.2 $[\text{M} + \text{H}]^+$ ($\text{C}_{17}\text{H}_{23}\text{NO}_7$ requires m/z 353.37).

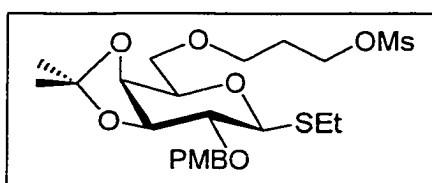
Methyl 2-acetamido-2,3-di-deoxy-4,6-O-p-methoxybenzylidene- β -D-allo-hex-2-enopyranoside (56).



Triethylamine (0.1 mL, 0.72 mmol) was added to a solution of alcohol **54** (171 mg, 0.48 mmol) in dry CH_2Cl_2 (5 mL). Methanesulphonyl chloride (0.06 mL, 0.72 mmol) in CH_2Cl_2 (1 mL) was added dropwise. After stirring for 1 h at rt, the solution was diluted with CH_2Cl_2 , washed with water, 1 M NaOH, water, brine, and dried over anhyd Na_2SO_4 . Evaporation followed by filtration through silica (16:1 dichloromethane-methanol) gave methanesulphonate **55** as an oil which was identified by NMR. This was immediately used in the coupling reaction. Sodium hydride (9.6 mg, 0.40 mmol) was added to a solution of galactopyranoside **52** (177 mg, 0.40 mmol) in dry DMF (3 mL). The mixture was stirred for 45 min at 60°C . The methanesulphonate **55** (170 mg, 0.39 mmol) in dry DMF (2 mL) was added and the reaction was stirred at 60°C until the reaction was complete. Excess NaH was destroyed with MeOH, and the DMF was evaporated. The residue was dissolved in CH_2Cl_2 , washed with water, brine and dried over Na_2SO_4 . The concentrated residue was chromatographed on silica (1:1 hexane-EtOAc) to give **56** (102 mg, 77%). ^1H NMR (300 MHz, $(\text{CD}_3)_2\text{SO}$): δ 8.94 (s, 1 H, NH), 7.34, 6.91 (2d, 2H each, ArH), 6.61 (s, 1H, H-3), 5.65 (s, 1H, $\text{C}_6\text{H}_4\text{CH}$), 5.23 (d, 1H, $J_{1,4}$ 1.7, H-1), 4.33 (ddd, 1H, $J_{3,4}$ 1.8, $J_{4,5}$ 8.5, H-4), 4.15 (dd, $J_{5,6a}$ 4.6, $J_{6a,6b}$ 10.0, H-6a),

3.70-3.86 (m, 4H, H-6b, CH₃O), 3.52-3.64 (m, 1H, H-5), 3.50-3.56 (m, CH₃O, H-2, HOD), 1.97 (s, 3H, NHCOCH₃). ¹³C NMR (125 MHz, (CD₃)₂SO): δ 127.4, 113.0 (CH, ArC), 111.9 (=C, C-3), 103.0 (C, C-2), 100.4 (CH, C₆H₄CH), 97.0 (CH, C-1), 73.3 (CH, C-4), 69.6 (CH, C-5), 67.4 (CH₂, C-6), 54.8 (CH₃, CH₃OC₆H₄), 53.7 (CH₃, CH₃O), 23.3 (CH₃, NHCOCH₃). ES HRMS: m/z 358.126665 [M + Na]⁺ ± 0.0 mDa and 336.1 [M + H]⁺ (C₁₇H₂₁NO₆ requires m/z 335.36).

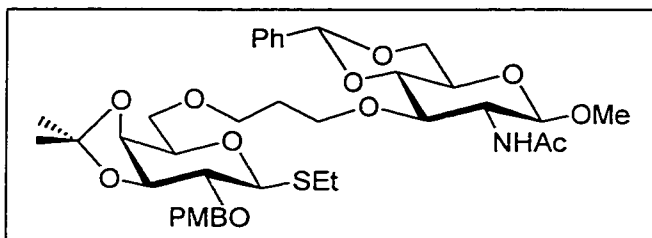
Ethyl 3,4-O-isopropylidene-6-O-(3'-O-methanesulphonyloxypropyl)- 2-O-p-methoxybenzyl-1-thio-β-D-galactopyranoside (57).



Triethylamine (0.11 mL, 0.8 mmol) was added to a solution of alcohol **52** (237 mg, 0.5 mmol) in dry CH₂Cl₂ (4 mL). Methanesulphonyl chloride (0.07 mL, 0.9 mmol) in CH₂Cl₂ (1 mL) was added dropwise. After stirring for 2 h at rt, the solution was diluted with CH₂Cl₂, washed with water, 1 M NaOH, water, brine, and dried over anhyd Na₂SO₄. Evaporation and chromatography on silica (3:2 hexane-EtOAc) gave **57** (263 mg, 93%) as a white solid. [α]_D -6.6° (c 28.8, CHCl₃). ¹H NMR (300 MHz, CDCl₃): δ 7.32, 6.85 (2d, 2H each, J 8.7, ArH), 4.74 (d, 1H, J_{gem} 11.0, C₆H₄CH₂O), 4.66 (d, 1H, C₆H₄CH₂O), 4.38 (d, 1H, J_{1,2} 9.6, H-1), 4.31 (t, 2H, J 6.2, H_{link-1}), 4.17 (J_{2,3} 6.0, J_{3,4} 5.8, H-3), 4.15 (J_{4,5} 2.0, H-4), 3.83 (ddd, 1H, J_{5,6ab} 5.1 & 6.9, H-5), 3.77 (s, 3H, CH₃OC₆H₄), 3.64-3.70 (m, 2H, H-6a, H-6b), 3.52-3.64 (m, 2H, H_{link-3}), 3.40 (dd, 1H, J_{2,3} 6.0, H-2), 2.98 (s, 3H, MsO), 2.58-2.78 (m, 2H, SCH₂CH₃), 1.98 (quintet, 2H, J 6.13, H_{link-2}), 1.42, 1.33 (2s, 3H each, CCH₃), 1.28 (t, 3H, J 7.4, SCH₂CH₃). ¹³C NMR (75 MHz, CDCl₃): δ 129.6, 113.5 (CH, ArC), 83.5 (CH, C-1), 79.3 (CH, C-3), 78.4 (CH, C-2), 75.2 (CH, C-5), 73.6 (CH, C-4), 72.9 (CH₂, C₆H₄CH₂O), 69.9 (CH₂, C-6), 66.8 (CH₂, C_{link-1}), 66.3 (CH₂, C_{link-3}), 55.0 (CH₃, CH₃O), 37.0 (CH₃, CH₃SO₃), 29.1 (CH₂, C_{link-2}), 27.5, 25.9 (CH₃, C(CH₃)₂), 24.4 (CH₂, SCH₂), 14.6 (CH₃, SCH₂CH₃). Anal. calcd for C₂₃H₃₆O₉S₂ (520.67): C, 53.06; H, 6.97; S,

12.32. Found: C, 52.92; H, 7.07; S, 12.59. ES HRMS: m/z 543.169719 [$M + Na$]⁺ \pm 0.1 mDa and 521.2 [$M + H$]⁺ ($C_{23}H_{36}O_9S_2$ requires m/z 520.67).

Ethyl 3,4-O-isopropylidene-2-O-p-methoxybenzyl-6-O-(3'-O-(methyl 2-acetamido-4,6-O-benzylidene-2-deoxy- β -D-glucopyranos-3-oxy)propyl)-1-thio- β -D-galactopyranoside (58).

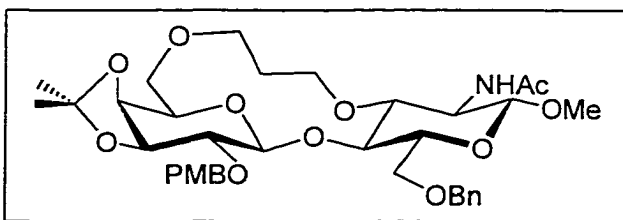


Sodium hydride (9.7 mg, 0.4 mmol) was added to a solution of glucopyranoside **36** (135 mg, 0.4 mmol) in dry THF (3 mL). The mixture was stirred for 30

min at 60°C. The methanesulphonate **57** (146 mg, 0.3 mmol) in dry THF (2 mL) was added and the reaction was stirred at 60°C for 20 min. Dry Me₂SO (0.5 mL) was added and after an additional 2 to 4 h of heating at 60°C, the reaction was complete. The cooled reaction mixture was diluted with CH₂Cl₂, washed with NaHCO₃, brine and dried over Na₂SO₄. The concentrated residue was chromatographed on silica (2:1 hexane-acetone) and gave **58** (174 mg, 83%) as a white solid. $[\alpha]_D^{+17.5}$ (c 5.1, CHCl₃). ¹H NMR (500 MHz, CDCl₃): δ 6.84-7.50 (9H, ArH), 5.93 (d, 1H, $J_{2',NH}$ 8.0, NHAc), 5.51 (s, 1H, PhCHO), 4.70-4.82 (m, 2H, J_{gem} 11.4, $J_{1',2'}$ 8.3, C₆H₄CH₂O and H-1'), 4.65 (d, 1H, C₆H₄CH₂O), 4.36 ($J_{1,2}$ 9.6, H-1), 4.16 (t, 1H, $J_{2,3}$ ~6.0, $J_{3,4}$ ~6.0, H-3), 4.09 (dd, 1H, $J_{4,5}$ 1.9, H-4), 3.98 ($J_{3',4'}$ ~9.6, H-3'), 3.94 (m, 2H, H_{link-1}), 3.76 (H-5'), 3.72-3.82 (m, 4H, CH₃OC₆H₄ and H-5), 3.60-3.70 (H-6'a, H-6'b), 3.59-3.79 (H-6a, H-6b), 3.56 (H-4'), 3.50-3.70 (H_{link-3}), 3.50 (s, OCH₃), 3.50 (H-2'), 3.40 (H-2), 2.56-2.80 (m, 2H, SCH₂CH₃), 2.01 (s, 3H, NHCOCH₃), 1.66-1.82 (m, 2H, H_{link-2}), 1.39, 1.30 (2s, 3H each, CCH₃), 1.26 (t, 3H, J 7.3, SCH₂CH₃). ¹³C NMR (75 MHz, CDCl₃): δ 129.7, 113.6 (CH, ArC), 128.8, 128.0, 125.8 (CH, PhCHO₂), 101.7 (CH, C-1'), 101.0 (CH, PhCHO₂), 83.8 (CH, C-1), 82.3 (CH, C-4'), 79.4 (CH, C-3), 78.3 (CH, C-2), 77.5 (CH, C-3'), 75.5 (CH, C-5), 73.6 (CH, C-4), 72.8 (CH₂, C₆H₄CH₂O), 69.9 (CH₂, C-6), 68.9 (CH₂, C_{link-1}), 68.5 (CH, C-5'), 68.9 (CH₂, C-6'), 67.7 (CH₂, C_{link-3}), 65.7 (CH,

C-2'), 55.1 (CH₃, CH₃OC₆H₄), 56.9 (CH₃, CH₃O), 30.1 (CH₂, C_{link}-2), 27.6, 26.1 (CH₃, C(CH₃)₂), 23.5 (CH₃, CH₃CONH), 24.8 (CH₂, SCH₂), 14.5 (CH₃,SCH₂CH₃). Anal. calcd for C₃₈H₅₃NO₁₂S (747.92): C, 61.03; H, 7.14; N, 1.87. Found: C, 61.36; H, 7.28; N, 1.85. ES HRMS: m/z 770.319525 [M + Na]⁺ ± 0.9 mDa and 748.3 [M + H]⁺ (C₃₈H₅₃NO₁₂S requires m/z 747.92).

Methyl 2-acetamido-6-O-benzyl-2-deoxy-4-O-(3,4-O-isopropylidene-2-O-p-methoxybenzyl-β-D-galactopyranosyl)-3,6'-di-O-(propan-1,3-diyl)-β-D-glucopyranoside (59).



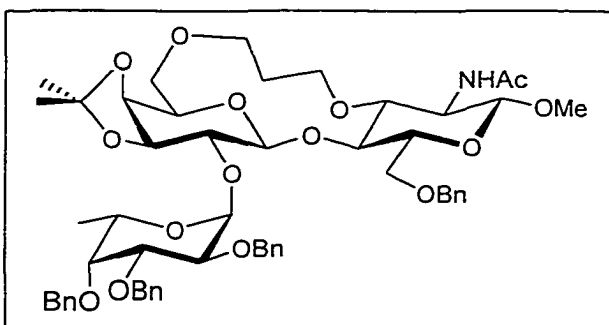
METHOD 1: To a dry mixture of starting material **39** (287 mg, 0.4 mmol) and powdered 4 Å molecular sieves purged with argon, was added dry CH₂Cl₂ (17 mL). Once the reaction flask was covered with aluminum foil, NIS (129 mg, 0.6 mmol) and silver triflate (57 mg, 0.2 mmol) were added. After 30 min, the reaction mixture was diluted with CH₂Cl₂ and the molecular sieves were filtered off. The filtrate was washed with Na₂S₂O₃, NaHCO₃, brine and dried. The concentrated material was chromatographed (2:1 toluene-acetone) to give impure **59** as a white solid that contained the iodinated (**60**) and non-iodinated *p*-methoxybenzyl group (90.2 mg, 35%).

METHOD 2: To a dry mixture of starting material **39** (97 mg, 0.1 mmol), DTBMP (93.1 mg, 0.5 mmol) and powdered 4 Å molecular sieves purged with argon, was added dry CH₂Cl₂ (10 mL). Once the reaction had been stirred for 15 min, methyl triflate (44 μL, 0.4 mmol) was added. After 45 min, the reaction mixture was diluted with CH₂Cl₂ and filtered through celite. The filtrate was washed with NaHCO₃, 0.5 M HCl, NaHCO₃, brine, dried and concentrated. The crude material was chromatographed on silica (2:1 toluene-acetone) to give **59** (44 mg, 50%). The α-anomer of **59** was also isolated (5.6 mg, 7%).

¹H NMR (500 MHz, CDCl₃): δ 6.82-7.32 (ArH), 5.25 (d, 1H, J_{2,NH} 9.2, NHAc), 4.69, 4.58 (2 d, 1H each, J_{gem} 11.1, C₆H₄CH₂O), 4.43, 4.36 (2 d, 1H each, J_{gem} 12.1, PhCH₂O), 4.28 (d, 1H, J_{1,2} 7.9, H-1), 4.20

(quartet, 1H, $J_{2,3} \sim 8.5$, H-2), 4.14 (d, 1H, $J_{1',2'} 8.4$, H-1'), 4.03 (t, 1H, $J_{3',4'} \sim 6.3$, H'-3), 3.96 (t, 1H, $J_{3,4} 9.5$, $J_{4,5} 9.5$, H-4), 3.90 (dd, 1H, $J_{3',4'} 5.5$, $J_{4',5'} 2.0$, H-4'), 3.84 (dd, 1H, $J_{5,6a} 4.3$, $J_{6a,6b} 10.5$, H-6a), 3.77 (s, $\text{CH}_3\text{OC}_6\text{H}_4$), 3.76 (H-5'), 3.73 (H-6b), 3.73, 3.42 ($\text{H}_{\text{link-3}}$, $\text{H}_{\text{link-1}}$), 3.68 (H-3), 3.65-3.80 (H-6'a, H-6'b),, 3.46 (s, 3H, OCH_3), 3.40-3.45 (m, 1H, H-5), 3.37 (dd, 1H, $J_{2',3'} 7.2$, H-2'), 1.99 (s, 3H, NHCOCH_3), 1.60-1.76 (m, 2H, $\text{H}_{\text{link-2}}$), 1.35, 1.27 (2 s, 3H each, CCH_3). ^{13}C NMR (125 Hz, CDCl_3): δ 129.7, 113.4 128.2, 127.6 (CH, ArCH), 104.3 (CH, $^1J_{\text{C,H}} 158.7$, C-1'), 102.4 (CH, $^1J_{\text{C,H}} 158.7$, C-1), 80.2 (CH, C-3'), 79.4 (CH, C-2'), 78.7 (CH, C-3), 75.2 (CH, C-5), 74.9 (CH, C-4), 73.9 (CH, C-5'), 73.5 (CH, C-4'), 72.80 (CH_2 , PhCH_2O), 72.80 (CH_2 , $\text{C}_6\text{H}_4\text{CH}_2\text{O}$), 68.9 (CH_2 , C-6'), 68.1 (CH_2 , C-6), 56.90, 56.86 (CH_2 , $\text{C}_{\text{link-3}}$, $\text{C}_{\text{link-1}}$), 56.3 (CH_3 , CH_3O), 55.0 (CH_3 , $\text{CH}_3\text{OC}_6\text{H}_4$), 51.0 (CH, C-2), 30.5 (CH_2 , $\text{C}_{\text{link-2}}$), 27.5, 26.1 (CH_3 , $\text{C}(\text{CH}_3)_2$), 23.4 (CH_3 , CH_3CONH). ES HRMS: m/z 710.3152 [$\text{M} + \text{Na}$] $^+ \pm 0.1$ mDa and 688.3 [$\text{M} + \text{H}$] $^+$ ($\text{C}_{36}\text{H}_{49}\text{NO}_{12}$ requires m/z 687.80).

Methyl 2-acetamido-6-O-benzyl-4-O-(2-O-(2,3,4-tri-O-benzyl- α -L-fucopyranosyl)-3,4-O-isopropylidene- β -D-galactopyranosyl)-2-deoxy-3,6'-di-O-(propan-1,3-diyl)- β -D-glucopyranoside (61).

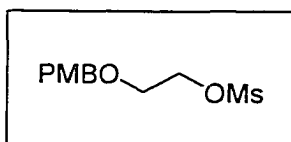


A mixture of disaccharide **38** (50 mg, 0.09 mmol) and the fucose thioglycoside **40**²⁰⁸ (44 mg, 0.09 mmol) in dry CH_2Cl_2 (2 mL) was prepared and purged with argon. This solution of sugars **38** and **40**

was transferred via canula to a mixture of DMTST (60 mg, 0.2 mmol), DTBMP (57 mg, 0.3 mmol), and 4 Å molecular sieves in dry CH_2Cl_2 (2 mL) at -68°C purged with argon. The reaction mixture was allowed to warm up to rt. After stirring for 2 h the reaction was diluted with CH_2Cl_2 , washed with NaHCO_3 , brine, dried over Na_2SO_4 and concentrated. The crude material was chromatographed on silica (3:2 hexane-acetone) and gave **61** (47.6 mg, 55%) as a white solid. ^1H NMR (500 MHz, CDCl_3): δ 7.26-7.43 (m, 20H, ArH), 5.59

(d, 1H, $J_{1'',2''}$ 3.8, H-1''), 5.25 (d, 1H, $J_{2,NH}$ 9.2, NH), 4.92, 4.61 (2d, 2H, J_{gem} 11.6, PhCH₂O), 4.77, 4.61 (2d, 2H, J_{gem} 11.9, PhCH₂O) 4.78, 4.74 (2d, 2H, J_{gem} 11.6, PhCH₂O) 4.52, 4.48 (2d, 2H, J_{gem} 12.0, PhCH₂O), 4.26 (d, 1H, $J_{1,2}$ 7.9, H-1), 4.18 (quartet, 1H, $J_{2,3}$ 9.6, H-2), 4.11 (d, $J_{1',2'}$ 8.6, H-1'), 4.09 ($J_{3',4'}$ 6.6, H-3'), 4.05 (dd, $J_{2'',3''}$ 10.1, H-2''), 3.95 (quartet, 1H, H-5''), 3.89 (t, 1H, $J_{3,4}$ 9.2, $J_{4,5}$ 9.3, H-4), 3.85 (dd, 1H, $J_{4',5'}$ 5.5, H-4'), 3.82 (dd, 1H, $J_{3'',4''}$ 2.6, H-3''), 3.78 (H-6a, H-6b), 3.75 (H-2'), 3.70 (H-5'), 3.69-3.76 (H_{link-1}, H_{link-3}), 3.67 (H-3), 3.62 (d, 1H, $J_{4'',5''}$ 2.3, H-4''), 3.47 (s, 3H, CH₃O), 3.34-3.40 (m, 1H, H-6'a), 3.25 (m, 1H, H-5), 1.99 (s, 3H, NHCOCH₃), 1.64-1.74 (m, 2H, H_{link-2}), 1.44, 1.28 (2 s, 3H each, CCH₃), 1.09 (d, 3H, $J_{5'',6''}$ 6.4, H-6''). ¹³C NMR (125 MHz, CDCl₃): δ 126.0-130.0 (CH, ArC), 102.5 (CH, ¹J_{C,H} 156.6, C-1'), 102.3 (CH, ¹J_{C,H} 159.0, C-1), 95.6 (CH, ¹J_{C,H} 172.6, C-1''), 80.5 (CH, C-3'), 78.9 (CH, C-3''), 78.3 (CH, C-3), 77.3 (CH, C-4''), 76.1 (CH, C-2''), 76.0 (CH, C-5), 75.1 (CH, C-2'), 74.5 (CH₂, PhCH₂), 74.1 (CH, C-5'), 73.6 (CH, C-4, C-4'), 73.2 (CH₂, PhCH₂), 72.5 (CH₂, 2xPhCH₂), 68.3, 68.0 (CH₂, C_{link-1}, C_{link-3}), 66.1 (CH, C-5''), 56.3 (CH₃, OCH₃), 56.2 (CH, C-6, C-6'), 50.4 (CH, C-2), 30.0 (CH₂, C_{link-2}), 27.6, 26.2 (CH₃, CCH₃), 23.1 (CH₃, COCH₃), 16.4 (CH₃, C-6''). ES HRMS: m/z 1006.4577 [M + Na]⁺ ± 1.2 mDa and 984.5 [M + H]⁺ (C₅₅H₆₉NO₁₅ requires m/z 984.17).

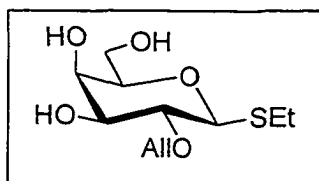
1-O-methanesulphonyloxy-2-O-p-methoxybenzyloxy-ethane (64).



METHOD 1: Diol **63** (5.00 g, 80.6 mmol) was added dropwise to a solution of NaH (1.94 g, 80.6 mmol) in dry THF (100 mL) purged with argon. After stirring for 45 min, PMBCl (13.1 mL, 96.8 mmol) was added portionwise and the reaction mixture was stirred overnight. Triethylamine (16.8 mL, 120.9 mmol) was added followed by slow addition of MsCl (10.0 mL, 120.9 mmol) in dry THF (20 mL). After 90 min, the reaction was diluted with ether, washed with water, 1 M NaOH, brine, dried over anhyd Na₂SO₄ and concentrated. The residue was chromatographed (4:1→1:1 hexane-EtOAc) to give a clear liquid (8.11 g, 39%).

METHOD 2: A solution of diol **63** (4.00 g, 64.5 mmol) in anhyd toluene (90 mL) was refluxed for 4 h in the presence of dibutyltin oxide (17.67 g, 71.0 mmol), with azeotropic removal of water. The solution was concentrated to approximately 30 mL and cooled to rt. Tetrabutylammonium iodide (23.98 g, 65 mmol) and PMBCl (13.1 mL, 96.8 mmol) were then added, and the mixture was heated at reflux overnight. After the evaporation of the solvent, the residue was dissolved in dry CH₂Cl₂ (90 mL) and triethylamine (16.8 mL, 120.9 mmol) was added, followed by slow addition of MsCl (10.0 mL, 120.9 mmol) in dry CH₂Cl₂ (10 mL). After 90 min, the reaction was diluted with ether, washed with water, 1 M NaOH, brine, dried over anhyd Na₂SO₄ and concentrated. Chromatography on silica (4:1 → 1:1 hexane-EtOAc) yielded compound **64** as a clear liquid (7.50 g, 45%). IR ν_{\max} (film): 1612.5, 1585.8, 1514.0, 1352.2, 1248.7, 1174.7, 923.2. ¹H NMR (300 MHz, CDCl₃): δ 7.2-3, 6.86 (2d, 2H each, ArH), 4.35 (A₂B₂, 2H, CH₂OMs), 3.78 (s, 3H, C₆H₄OCH₃), 3.68 (A₂B₂, 2H, TBDMSOCH₂), 2.99 (s, 3H, SO₂CH₃). ¹³C NMR (75 MHz, CDCl₃): δ 159.4 (C, ArC), 129.4, 113.9 (CH, ArC), 72.9 (CH₂), 69.2 (CH₂), 67.5 (CH₂), 55.3 (CH₃), 37.6 (CH₃). Anal. calcd for C₁₁H₁₆O₅S (260.30): C, 50.76; H, 6.20; S, 12.32. Found: C, 50.45; H, 6.29; S, 12.27. ES HRMS: m/z 283.061280 [M + Na]⁺ ± 0.3 mDa and 261.1 [M + H]⁺ (C₁₁H₁₆O₅S requires m/z 260.30).

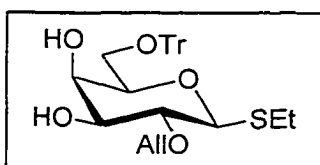
Ethyl 2-O-allyl-1-thio-β-D-galactopyranoside (65).



To a mixture of thioglycoside **42**²⁰⁰ (1.77 g, 7.9 mmol) and 2,2-dimethoxypropane (40 mL), was added toluenesulfonic acid (20 mg). The reaction mixture was stirred overnight, neutralized with triethylamine, concentrated and evaporated twice with toluene. The residue was diluted with CH₂Cl₂, washed with brine, dried with anhyd Na₂SO₄ and concentrated. The dried syrup was dissolved in THF (30 mL) and purged with argon. To the ice cooled solution, NaH (0.20 g, 8.0 mmol) was added portionwise. After stirring for 45 min, allyl bromide (0.70 mL, 8.0 mmol) was added dropwise.

The reaction was then quenched with MeOH containing residual water, diluted with CH₂Cl₂, washed with NaHCO₃, water, and concentrated. The residue was then dissolved in 80% AcOH and heated to 65°C for 2 h. After removal of the solvent, the crude material was chromatographed on silica (1:1 hexane-EtOAc) to give **65**²⁰⁰ (1.48 g, 71%). [α]_D +18.0° (c 6.9, CHCl₃); ¹H NMR (600 MHz, CDCl₃): δ 5.96 (ddt, 1H, =CH), 5.30 (dddd, 1H, =CH₂), 5.20 (dd, 1H, =CH₂), 4.42, 4.19 (2xddd, 1H each, H₂C=CHCH₂), 4.36 (d, 1H, J_{1,2} 9.7, H-1), 4.04 (t, 1H, J_{3,4}, J_{4,5} 2.4, 2.8, H-4), 3.90-3.94, 3.81-3.86 (m, 2H, H-6a, H-6b), 3.60 (ddd, 1H, J_{3,OH} 3.7, J_{3,4} 3.5, J_{2,3} 10.0, H-3), 3.51 (t, 1H, J 5.5, 5.0, H-5), 3.42 (t, 1H, J_{2,3} 9.4, H-2), 2.87 (d, 1H, OH-4), 2.60-2.84 (m, 3H, OH-3, SCH₂CH₃), 2.22 (t, 1H, OH-6), 1.29 (t, 3H, J 7.5, SCH₂CH₃); ¹³C NMR (150 MHz, CDCl₃): δ 134.0 (CH, =CH), 117.8 (CH₂, =CH₂), 85.0 (CH, C-1), 78.4 (CH, C-2), 77.8 (CH, C-5), 74.9 (CH, C-3), 74.0 (CH₂, H₂C=CHCH₂), 69.7 (CH, C-4), 63.2 (CH₂, C-6), 24.7 (CH₂, SCH₂CH₃), 15.0 (CH₃, SCH₂CH₃). ES HRMS: m/z 287.092455 [M + Na]⁺ \pm 0.5 mDa and 265.12 [M + H]⁺ (C₁₁H₂₀O₅S requires m/z 264.34).

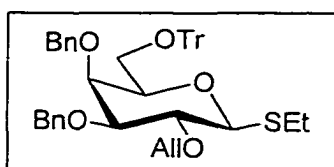
Ethyl 2-O-allyl-6-O-trityl-1-thio- β -D-galactopyranoside (66).



Thioglycoside **65**²⁰⁰ (5.16 g, 19.6 mmol) and trityl chloride (6.56 g, 23.5 mmol) were dissolved in dry pyridine (100 mL) and stirred overnight. After dilution in CH₂Cl₂, the mixture was washed with water, NaHCO₃, and brine. After concentration and chromatography on silica (5:1 Hexane-EtOAc), compound **66** was obtained as an oil (9.40 g, 95%). [α]_D +17.0° (c 13.2, CHCl₃); ¹H NMR (300 MHz, CDCl₃): δ 7.10-7.40 (m, ArH), 5.96 (ddt, 1H, =CH), 5.29 (dddd, 1H, =CH₂), 5.20 (dd, 1H, =CH₂), 4.40, 4.19 (2xddd, 1H each, H₂C=CHCH₂), 4.32 (d, 1H, J_{1,2} 9.5, H-1), 4.04 (t, 1H, J_{3,4}, J_{4,5} 3.5, 3.8, H-4), 3.56 (ddd, 1H, J_{3,OH} 6.0, J_{3,4} 3.0, J_{2,3} 9.0, H-3), 3.48 (H-5), 3.39 (H-2), 3.30-3.50 (m, 2H, H-6a, H-6b), 2.60-2.84 (m, 2H, SCH₂CH₃), 2.56 (d, 1H, OH), 2.30 (d, 1H, OH), 1.30 (t, 3H, J 7.3, SCH₂CH₃); ¹³C NMR (150 MHz, CDCl₃): δ 134.5 (CH, =CH), 127.0-129.0 (CH, ArC), 117.4 (CH₂, =CH₂), 84.5 (CH, C-1), 78.2 (CH, C-2),

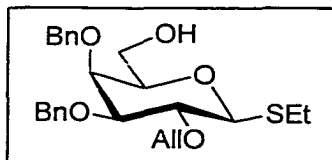
77.0 (CH, C-5), 74.8 (CH, C-3), 74.1 (CH₂, H₂C=CHCH₂), 69.0 (CH, C-4), 62.5 (CH₂, C-6), 24.5 (CH₂, SCH₂CH₃), 14.9 (CH₃, SCH₂CH₃). ES HRMS: m/z 529.202749 [M + Na]⁺ and 507.9 [M + H]⁺ (C₃₀H₃₄O₅S₁ requires m/z 506.66).

Ethyl 2-O-allyl-3,4-di-O-benzyl-6-O-trityl-1-thio-β-D-galactopyranoside
(67).



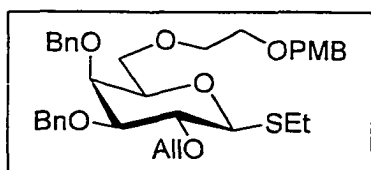
Thioglycoside **66** (9.3 g, 18.4 mmol) was dissolved in DMF (50 mL) and purged with argon. To the ice cooled solution, NaH (2.04 g, 84.7 mmol) was added portionwise. After stirring for 45 min at rt, benzyl bromide (8.2 mL, 68.1 mmol) was added dropwise. The reaction mixture was quenched with EtOAc containing residual water, then diluted with CH₂Cl₂, washed with NaHCO₃, brine, and dried over anhyd Na₂SO₄. After removal of the solvent, the crude material was chromatographed on silica (12:1 hexane-EtOAc) to give **67** (11.9 g, 94%). [α]_D -12.9° (c 6.2, CHCl₃); ¹H NMR (300 MHz, CDCl₃): δ 7.0-7.5 (m, ArH), 5.96 (ddt, 1H, =CH), 5.25 (dddd, 1H, =CH₂), 5.13 (dd, 1H, =CH₂), 4.79, 4.75, 4.67, 4.46 (4d, 1H each, J_{gem} 11.9, 11.6, 2xPhCH₂), 4.20-4.36 (m, 3H, J_{1,2} 9.6, H-1, H₂C=CHCH₂), 3.86 (d, 1H, J 2.8, H-4), 3.63 (t, 1H, J_{2,3} 9.3, J_{1,2} 9.5, H-2), 3.40-3.50 (m, 2H, H-3, H-5), 3.31 (t, 1H, J_{6a,6b} 6.9, J_{5,6a} 5.8, H-6a), 3.17 (dd, 1H, J_{5,6b} 9.2, H-6b), 2.58-2.80 (m, 2H, SCH₂CH₃), 1.25 (t, 3H, J 7.4, SCH₂CH₃); ¹³C NMR (125 MHz, CDCl₃): δ 134.7 (CH, =CH), 126.0-130.0 (CH, ArC), 116.9 (CH₂, =CH₂), 85.0 (CH, C-1), 83.8 (CH, C-3), 78.1 (CH, C-2), 77.5 (CH, C-5), 74.4 (CH₂, H₂C=CHCH₂), 74.1, 73.75 (CH₂, C₆H₅CH₂), 73.75 (CH, C-4), 62.5 (CH₂, C-6), 24.4 (CH₂, SCH₂CH₃), 14.7 (CH₃, SCH₂CH₃). ES HRMS: m/z 709.296444 [M + Na]⁺ ± 0.1 mDa and 688.5 [M + H]⁺ (C₄₄H₄₆O₆S requires m/z 686.91).

Ethyl 2-O-allyl-3,4-di-O-benzyl-1-thio- β -D-galactopyranoside (68).



Compound **67** (1.20 g, 1.79 mmol) was dissolved in a 9:1 MeOH-EtOAc solution (15 mL) with TsOH (20 mg). The mixture was heated to 35°C until the removal of the trityl group was complete (tlc). The reaction mixture was neutralized with triethylamine and then concentrated. The residue was dissolved in CH₂Cl₂, washed with water, NaHCO₃, brine and dried with Na₂SO₄. After evaporation, chromatography (2:1 Hexane-EtOAc) of the residue on silica gave thioglycoside **68** (0.465 g, 77%). [α]_D -62.7° (c 1.5, CHCl₃); R_f 0.45 (1:1 Hexane-EtOAc); ¹H NMR (300 MHz, CDCl₃): δ 7.20-7.40 (m, ArH), 5.98 (ddt, 1H, =CH), 5.28 (dddd, 1H, =CH₂), 5.17 (dd, 1H, =CH₂), 4.92, 4.79, 4.72, 4.62 (4d, 1H each, J_{gem} 11.9, 11.9, 2xPhCH₂), 4.25-4.41 (m, 3H, J_{1,2} 9.5, H₂C=CHCH₂, H-1), 3.78 (d, 1H, J 2.2, H-4), 3.75 (m, 1H, H6a), 3.69 (t, 1H, J_{1,2} 9.5, J_{2,3} 9.4, H-2), 3.50 (dd, 1H, J_{2,3} 9.2, J_{3,4} 2.8, H-3), 3.34-3.48 (m, 2H, H-5, H-6b), 2.60-2.80 (m, 2H, SCH₂CH₃), 1.47 (dd, 1H, OH), 1.27 (t, 3H, J 7.5, SCH₂CH₃); ¹³C NMR (75 MHz, CDCl₃): δ 134.1 (CH=CH), 128.3, 127.1 (CH, ArC), 116.9 (CH₂, =CH₂), 85.4 (CH, C-1), 83.8 (CH, C-3), 78.3 (CH, C-5), 77.9 (CH, C-2), 74.2 (CH₂, H₂C=CHCH₂); 74.0 (CH₂, PhCH₂), 72.9 (CH & CH₂, C-4 & PhCH₂), 62.1 (CH₂, C-6), 24.2 (CH₂, SCH₂CH₃), 15.0 (CH₃, SCH₂CH₃). Anal. Calcd for C₂₅H₃₂O₅S (444.59): C, 67.54; H, 7.26; S, 7.21. Found: C, 67.33; H, 7.19; S, 7.43. ES HRMS: m/z 467.186677 [M + Na]⁺ \pm 0.1 mDa and 445.2 [M + H]⁺ (C₂₅H₃₂O₅S requires m/z 444.59).

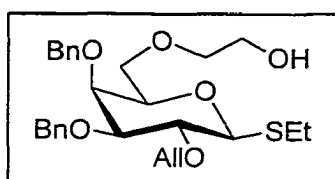
Ethyl 2-O-allyl-3,4-di-O-benzyl-6-O-(2'-O-p-methoxybenzyloxyethyl)-1-thio- β -D-galactopyranoside (69).



NaH (115.3 mg, 4.79 mmol) was added to a solution of alcohol **68** (2.01 g, 4.79 mmol) in dry THF (13 mL). After stirring for 30 min at 60°C, the linker (1.62 g, 6.23 mmol) was added with dry THF (2 mL) dropwise. The reaction mixture was stirred at 60°C for 3 h, then 1

equiv of both NaH and linker were added. At this point the condenser was turned off and the reaction was allowed to concentrate to approximately one third of its original volume. The reaction was quenched with EtOAc, diluted with CH₂Cl₂, washed with water, NaHCO₃, brine and then dried with anhyd Na₂SO₄. After solvent evaporation, column chromatography of the crude material on silica (5:1 hexane-EtOAc) gave **69** (2.27 g, 83%). [α]_D -19.7° (c 25.4, CHCl₃); R_f 0.69 (1:1 hexane-EtOAc); ¹H NMR (600 MHz, CDCl₃): δ 7.20-7.40, 6.84 (ArH), 5.97 (ddt, 1H, =CH), 5.26 (dddd, 1H, =CH₂), 5.14 (dd, 1H, =CH₂), 4.90 (d, 1H, J_{gem} 11.7, PhCH₂), 4.71, 4.68 (2d, 2H, J_{gem} 11.9, PhCH₂), 4.62 (d, 1H, J_{gem} 11.7, PhCH₂), 4.45, 4.43 (2d, 2H, J_{gem} 12.1, PhCH₂), 4.26-4.36 (m, 3H, J_{1,2} 9.5, H-1, H₂C=CHCH₂), 3.91 (d, 1H, J 2.8, H-4), 3.76 (s, 3H, CH₃OC₆H₄), 3.67 (t, 1H, J_{2,3} 9.3, H-2), 3.44-3.59 (m, 8H, H-3, H-5, H-6a, H-6b, 2xH_{link-1}, 2xH_{link-2}), 2.62-2.76 (m, 2H, SCH₂CH₃), 1.26 (t, 3H, J 7.5, SCH₂CH₃); ¹³C NMR (150 MHz, CDCl₃): δ 134.8 (CH=CH), 127.0-130.0, 113.6 (CH, ArC), 116.9 (CH₂, =CH₂), 85.1 (CH, ¹J_{C,H} 153.3, C-1), 83.8 (CH, C-3), 78.0 (CH, C-2), 76.9 (CH, C-5), 74.3 (CH₂, H₂C=CHCH₂); 74.1, 72.7, 72.4 (CH₂, 2xPhCH₂, PMB), 73.4 (CH, C-4), 70.6 (CH₂, C-6), 69.3, 68.5 (CH₂, C_{link-1}, C_{link-2}), 55.1 (CH₃, CH₃OPh), 24.4 (CH₂, SCH₂CH₃), 14.1 (CH₃, SCH₂CH₃). Anal. Calcd for C₃₅H₄₄O₇S (608.79): C, 69.05; H, 7.29; S, 5.27. Found: C, 68.77; H, 7.44; S, 5.24. ES HRMS: m/z 631.271409 [M + Na]⁺ ± 0.9 mDa and 609.9 [M + H]⁺ (C₃₅H₄₄O₇S requires m/z 608.79).

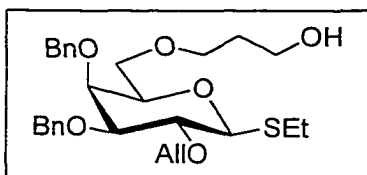
Ethyl 2-O-allyl-3,4-di-O-benzyl-6-O-(2'-hydroxyethyl)-1-thio- β -D-galactopyranoside (71).



Water (1.1 mL) and DDQ (1.34 g, 5.75 mmol) were added to compound **69** (2.27 g, 3.83 mmol) dissolved in CH₂Cl₂ (20 mL). The mixture was stirred at rt for 1 h. Another 1.5 equiv of DDQ (1.00 g, 4.29 mmol) was added. After another hour the reaction was quenched with NaHCO₃. The mixture was diluted with CH₂Cl₂, washed with NaHCO₃, brine, dried with anhyd Na₂SO₄ and concentrated. The crude syrup was chromatographed on

silica (2:1 hexane-EtOAc) to give **71** (1.04 g, 58%). $[\alpha]_D -6.9^\circ$ (c 1.6, CHCl₃); R_f 0.33 (2:1 hexane-EtOAc); ¹H NMR (600 MHz, CDCl₃): δ 7.20-7.42 (m, ArH), 5.98 (ddt, 1H, =CH), 5.27 (dddd, 1H, =CH₂), 5.16 (dd, 1H, =CH₂), 4.93 (d, 1H, J_{gem} 11.8, PhCH₂), 4.76, 4.71 (2d, 2H, J_{gem} 11.8, PhCH₂), 4.61 (d, 1H, PhCH₂), 4.17-4.40 (m, 3H, $J_{1,2}$ 9.6, H-1, H₂C=CHCH₂), 3.83 (d, 1H, J 2.8, H-4), 3.36-3.74 (m, 9H, H-2, H-3, H-5, H-6a, H-6b, 2xH_{link}-1, 2xH_{link}-2), 2.60-2.80 (m, 2H, SCH₂CH₃), 1.27 (t, 3H, J 7.4, SCH₂CH₃); ¹³C NMR (125 MHz, CDCl₃): δ 135.0 (CH,=CH), 128.4, 128.2, 128.1, 127.7, 127.6, 127.5 (CH, ArC), 116.0 (CH₂, =CH₂), 85.4, 84.1 (CH, C-1, C-3), 78.2 (CH, C-2), 76.4 (CH, C-5), 74.5, 74.3, 73.1, 72.9, 72.4, 61.7 (CH₂, H₂C=CHCH₂, C_{link}-1, C_{link}-2, C-6, 2xPhCH₂); 73.7 (CH, C-4), 24.4 (CH₂, SCH₂CH₃), 14.2 (CH₃, SCH₂CH₃). Anal. Calcd for C₂₇H₃₆O₆S (488.64): C, 66.37; H, 7.43. Found: C, 65.89; H, 7.52. ES HRMS: m/z 511.212435 [M + Na]⁺ \pm 0.6 mDa and 489.3 [M + H]⁺ (C₂₇H₃₆O₆S requires m/z 488.64).

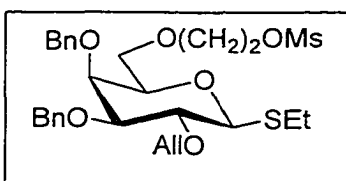
Ethyl 2-O-allyl-3,4-di-O-benzyl-6-O-(3'-hydroxypropyl)-1-thio- β -D-galactopyranoside (72).



NaH (56 mg, 2.34 mmol) was added to a solution of alcohol **68** (1.00 g, 2.34 mmol) in dry THF (6 mL). After stirring for 30 min at 60°C, the linker (820 mg, 3.04 mmol) was dissolved in dry THF (2 mL) was added dropwise. The reaction mixture was stirred at 60°C for 3 h, then 1 equiv of both NaH and linker were added. At this point the condenser was turned off and the reaction was allowed to concentrate to approximately one third of its original volume. The reaction was quenched with EtOAc, diluted with CH₂Cl₂, washed with water, NaHCO₃, brine and then dried with anhyd Na₂SO₄. After solvent evaporation, the syrup was treated with 1M TBAF in THF (10 mL). The mixture was stirred at rt for 1 h. After concentration, the crude syrup was chromatographed on silica (2:1 Hexane-EtOAc) to give **72** (877 mg, 77%) as an oil. $[\alpha]_D -29.3^\circ$ (c 3.0, CHCl₃); ¹H NMR (500 MHz, CDCl₃): δ 7.20-7.40 (m, ArH), 5.97 (ddt, 1H, =CH), 5.26 (dddd, 1H, =CH₂),

5.15 (dd, 1H, =CH₂), 4.93 (d, 1H, J_{gem} 11.8, PhCH₂), 4.75, 4.71 (2d, 1H each, J_{gem} 11.8, PhCH₂), 4.59 (d, 1H, PhCH₂), 4.24–4.38 (m, 3H, J_{1,2} 9.6, H-1, H₂C=CHCH₂), 3.82 (d, 1H, J 2.6, H-4), 3.64–3.72 (m, 3H, H-2, H_{link}-1), 3.42–3.58 (m, 6H, H_{link}-3, H-6a, H-6b, H-5, H-3), 2.63–2.77 (m, 2H, SCH₂CH₃), 1.74 (quintet, 2H, H_{link}-2), 1.27 (t, 3H, J 7.4, SCH₂CH₃); ¹³C NMR (125 MHz, CDCl₃): δ 134.8 (CH=CH), 126.0–130.0 (CH, ArC), 117.0 (CH₂, =CH₂), 85.1 (CH, ¹J_{C,H} 143.5, C-1), 83.7 (C-3), 77.9 (CH, C-2), 77.0 (CH, C-5), 74.3 (CH₂, H₂C=CHCH₂), 74.0, 72.7 (CH₂, 2xPhCH₂), 73.6 (CH, C-4), 70.1 (CH₂, C_{link}-3), 69.7 (CH₂, C-6), 61.5 (CH₂, C_{link}), 31.7 (CH₂, C_{link}-2), 24.5 (CH₂, SCH₂CH₃), 14.6 (CH₃, SCH₂CH₃). Anal. Calcd for C₂₈H₃₈O₆S (502.67): C, 66.90; H, 7.62; S, 6.38. Found: C, 66.72; H, 7.45; S, 6.30. ES HRMS: m/z 525.229066 [M + Na]⁺ ± 0.4 mDa and 503.2 [M + H]⁺ (C₂₈H₃₈O₆S requires m/z 502.67).

Ethyl 2-O-allyl-3,4-di-O-benzyl-6-O-(2'-O-methanesulphonyloxyethyl)-1-thio-β-D-galactopyranoside (73).

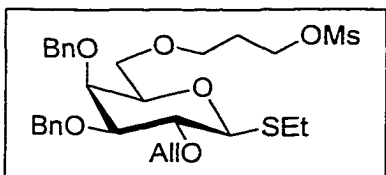


Triethylamine (0.47 mL, 3.36 mmol) was added to a solution of alcohol **71** (1.04 g, 2.24 mmol) in dry CH₂Cl₂ (25 mL). Methanesulphonyl chloride (0.3 mL, 3.36 mmol) in CH₂Cl₂ (0.7 mL) was added dropwise.

After stirring for 2 h at rt, the solution was diluted with CH₂Cl₂, washed with water, 1 M NaOH, water, brine, and dried with anhyd Na₂SO₄. Evaporation and chromatography on silica (4:1 Hexane-EtOAc) gave **73** (1.12 g, 93%) as a clear oil. [α]_D -19.9° (c 13.5, CHCl₃); R_f 0.59 (1:1 Hexane-EtOAc); ¹H NMR (500 MHz, CDCl₃): δ 7.20–7.40 (m, ArH), 5.97 (ddt, 1H, =CH), 5.27 (dddd, 1H, =CH₂), 5.15 (dd, 1H, =CH₂), 4.94 (d, 1H, J_{gem} 11.9, PhCH₂), 4.77, 4.72 (2d, 2H, J_{gem} 11.8, PhCH₂), 4.60 (d, 1H, PhCH₂), 4.16–4.38 (m, 5H, J_{1,2} 9.8, H-1, MsOCH₂, H₂C=CHCH₂), 3.83 (d, 1H, J 2.7, H-4), 3.44–3.70 (m, 7H, H-2, H-3, H-5, H-6a, H-6b, 2xH_{link}-1, 2xH_{link}-2), 2.95 (s, 3H, SO₂CH₃), 2.62–2.76 (m, 2H, SCH₂CH₃), 1.26 (t, 3H, J 7.4, SCH₂CH₃); ¹³C NMR (125 MHz, CDCl₃): δ 134.8 (CH=CH), 126.0–129.0 (CH, ArC), 116.9 (CH₂, =CH₂), 85.1 (CH, ¹J_{C,H} 155.4, C-1), 83.8 (CH, C-3), 77.9 (CH, C-2), 77.0 (CH, C-5), 74.3 (CH₂,

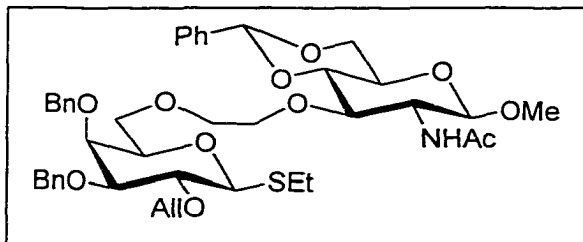
H₂C=CHCH₂) 74.0, 72.9 (CH₂, 2xPhCH₂), 73.4 (CH, C-4), 69.8 (CH₂, C-6), 68.9, 68.6 (CH₂, C_{link}-1, C_{link}-2), 37.4 (CH₃, SO₂CH₃), 24.5 (CH₂, SCH₂CH₃), 14.6 (CH₃, SCH₂CH₃). Anal. Calcd for C₂₈H₃₈O₈S₂ (566.72): C, 59.34; H, 6.76; S, 11.31. Found: C, 58.85; H, 6.72; S, 11.50. ES HRMS: m/z 589.190794 [M + Na]⁺ ± 0.2 mDa and 567.3 [M + H]⁺ (C₂₈H₃₈O₈S₂ requires m/z 566.72).

Ethyl 2-O-allyl-3,4-di-O-benzyl-6-O-(3'-O-methanesulphonyloxypropyl)-1-thio-β-D-galactopyranoside (74).



Triethylamine (0.35 mL, 2.52 mmol) was added to a solution of alcohol **72** (817 mg, 1.68 mmol) in dry CH₂Cl₂ (20 mL) and methanesulphonyl chloride (0.23 mL, 2.52 mmol) in CH₂Cl₂ (0.7 mL) was added dropwise. After stirring for 2 h at rt, the solution was diluted with CH₂Cl₂, washed with water, 1 M NaOH, water, brine, and dried with anhyd Na₂SO₄. Evaporation and chromatography on silica (2:1 Hexane-EtOAc) gave **74** (832 mg, 88%) as a oil. [α]_D -22.5° (c 4.0, CHCl₃); ¹H NMR (600 MHz, CDCl₃): δ 7.20-7.40 (m, ArH), 5.97 (ddt, 1H, =CH), 5.26 (dddd, 1H, =CH₂), 5.15 (dd, 1H, =CH₂), 4.93 (d, 1H, J_{gem} 11.7, PhCH₂), 4.76, 4.72 (2d, 1H each, J_{gem} 11.7, PhCH₂), 4.59 (d, 1H, PhCH₂), 4.21-4.36 (m, 5H, J_{1,2} 9.5, H-1, H_{link}-1, H₂C=CHCH₂), 3.83 (d, 1H, J 2.7, H-4), 3.67 (t, 1H, J_{2,3} 9.3, H-2), 3.44-3.52 (m, 5H, H-3, H-5, H-6a, H-6b, H_{link}-3), 2.94 (s, 3H, SO₂CH₃), 2.63-2.75 (m, 2H, SCH₂CH₃), 1.84-1.94 (m, 2H, H_{link}-2), 1.26 (t, 3H, J 7.5, SCH₂CH₃); ¹³C NMR (150 MHz, CDCl₃): δ 134.8 (CH,=CH), 126.0-129.0 (CH, ArC), 116.8 (CH₂, =CH₂), 85.0 (CH, ¹J_{C,H} 154.6, C-1), 83.8 (C-3), 77.9 (CH, C-2), 76.8 (CH, C-5), 74.2 (CH₂, H₂C=CHCH₂), 74.1, 72.7 (CH₂, 2xPhCH₂), 73.4 (CH, C-4), 69.4 (CH₂, C-6), 66.7 (CH₂, C_{link}-1), 66.3 (CH₂, C_{link}-3), 37.0 (CH₃, SO₂CH₃), 28.9 (CH₂, C_{link}-2), 24.5 (CH₂, SCH₂CH₃), 14.6 (CH₃, SCH₂CH₃). Anal. Calcd for C₂₉H₄₀O₈S₂ (580.75): C, 59.98; H, 6.94; S, 11.04. Found: C, 59.93; H, 6.94; S, 11.00. ES HRMS: m/z 603.206614 [M + Na]⁺ ± 0.4 mDa and 583.4 [M + H]⁺ (C₂₉H₄₀O₈S₂ requires m/z 580.75).

Ethyl 2-O-allyl-3,4-di-O-benzyl-6-O-(2'-O-(methyl 2-acetamido-4,6-O-benzylidene-2-deoxy-β-D-glucopyranos-3-oxy)ethyl)-1-thio-β-D-galactopyranoside (75).

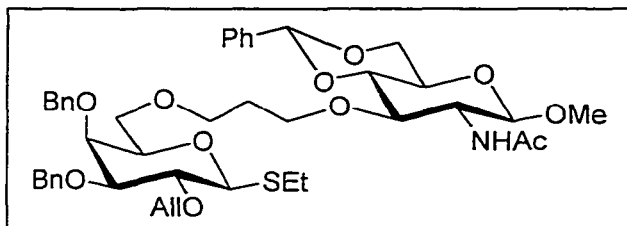


Sodium hydride (17 mg, 0.70 mmol) was added to a solution of glucopyranoside **36** (235 mg, 0.73 mmol) in dry THF (3 mL). The mixture was stirred for 30 min at 60°C. The

methanesulphonate **73** (282 mg, 0.52 mmol) in dry THF (3 mL) was added and 5 min later, (CH₃)₂SO (0.5 mL) was added to the reaction. After 3 h of heating, the reaction was complete. The cooled reaction mixture was diluted with CH₂Cl₂, washed with NaHCO₃, brine and dried with Na₂SO₄. The concentrated residue was chromatographed on silica (50:1 CH₂Cl₂-MeOH) and gave **75** (350 mg, 85%). [α]_D -12.7° (c 2.6, CHCl₃); R_f 0.46 (16:1 CH₂Cl₂-MeOH); ¹H NMR (500 MHz, CDCl₃): δ 7.20-7.50 (m, ArH), 6.13 (d, 1H, J_{2',NH} 8.1, NHAc), 5.97 (ddt, 1H, =CH), 5.50 (s, 1H, PhCH), 5.27 (dd, 1H, =CH₂), 5.15 (dd, 1H, =CH₂), 4.92 (d, 1H, J_{gem} 11.8, PhCH₂), 4.72-4.78 (m, 2H, J_{1',2'} 8.2, J_{gem} 13.0, H-1', PhCH₂), 4.69 (d, 1H, PhCH₂), 4.53 (d, 1H, PhCH₂), 4.31 (H_{link-1}), 4.27 (J_{1,2} 9.8, H-1), 4.26-4.40 (CH₂=CHCH₂), 4.05 (t, 1H, H-3'), 3.78 (H-5'), 3.75 (H-4), 3.74 (H_{link-1}), 3.70 (H-2), 3.59 (H-6a), 3.52 (H-4', H-5), 3.48 (H-2'), 3.46 (OCH₃, H-3), 3.45 (H-6'a), 3.40 (H_{link-2}), 3.36 (H-6'b), 3.28 (dd, 1H, J_{6a,6b} 9.5, J_{5,6b} 4.1, H-6b), 2.64-2.78 (m, 2H, SCH₂CH₃), 1.92 (s, 3H, NHCOCH₃), 1.26 (t, 3H, J 7.3, SCH₂CH₃). ¹³C NMR (125 MHz, CDCl₃): δ 134.5 (CH, =CH), 125.0-130.0 (CH, ArC), 116.9 (CH₂, =CH₂), 102.0 (CH, ¹J_{C,H} 163.2, C-1'), 100.9 (CH, PhCH), 85.3 (CH, ¹J_{C,H} 163.2, C-1), 83.8 (CH, C-3), 82.5 (CH, C-4'), 78.3 (CH, C-3'), 77.8 (CH, C-2, C-5), 74.3 (CH₂, CH₂=CHCH₂), 74.0 (CH, C-4), 74.0, 72.8 (CH₂, 2xPhCH₂), 72.4 (CH₂, C-6'), 70.9 (CH, C-5'), 70.5 (CH₂, C-6), 68.6 (CH₂, C_{link-1}), 65.6 (CH₂, C_{link-2}), 56.6 (CH₃, OCH₃), 56.5 (CH, C-2'), 24.1 (CH₂, SCH₂CH₃), 23.3 (CH₃, NHCOCH₃), 14.5 (CH₃, SCH₂CH₃). Anal. Calcd for C₄₃H₅₅O₁₁NS (793.97): C, 65.05; H,

6.98; N, 1.76; S, 4.04. Found: C, 64.94; H, 6.94; N, 1.79; S, 4.01. ES HRMS: m/z 816.340717 $[M + Na]^+ \pm 1.4$ mDa and 794.3 $[M + H]^+$ ($C_{43}H_{55}O_{11}NS$ requires m/z 793.97).

Ethyl 2-O-allyl-3,4-di-O-benzyl-6-O-(3'-O-(methyl 2-acetamido-4,6-O-benzylidene-2-deoxy- β -D-glucopyranos-3-oxo)propyl)-1-thio- β -D-galactopyranoside (76).

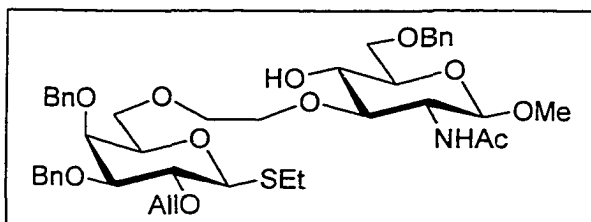


Sodium hydride (34.2 mg, 1.43 mmol) was added to a solution of glucopyranoside **36** (477 mg, 1.48 mmol) in dry THF (6 mL) and the mixture was stirred for 30 min at

60°C. The methanesulphonate **74** (641 mg, 1.14 mmol) in dry THF (3 mL) was added and after 5 min, dry Me_2SO (0.5 mL) was added. After heating overnight, the cooled reaction mixture was diluted with CH_2Cl_2 , washed with $NaHCO_3$, brine and dried with Na_2SO_4 . The concentrated residue was chromatographed on silica (60:1 CH_2Cl_2 - $MeOH$) to give **76** (707.3 mg, 77%). $[\alpha]_D -35.4^\circ$ (c 2.4, $CHCl_3$); R_f 0.63 (1:1 Toluene-Acetone); 1H NMR (600 MHz, $CDCl_3$): δ 7.20-7.50 (m, ArH), 5.96 (ddt, 1H, =CH), 5.69 (d, 1H, $J_{2',NH}$ 7.7, NHAc), 5.49 (s, 1H, PhCH), 5.26 (dd, 1H, = CH_2), 5.14 (dd, 1H, = CH_2), 4.90 (d, 1H, J_{gem} 11.5, Ph CH_2), 4.82 (d, 1H, $J_{1,2'}$ 8.4, H-1'), 4.73, 4.69, 4.54 (3d, 3H, J_{gem} 11.7, Ph CH_2), 4.26-4.36 (m, 4H, $J_{1,2}$ 9.6, H-6'a, H-1', $CH_2=CHCH_2$), 4.01 (t, 1H, J 9.5, 9.4, H-3'), 3.85-3.89 (m, 1H, H_{link-1}), 3.79 (d, 1H, $J_{3,4}$ 2.8, H-4), 3.74 (t, 1H, J 10.2, H-6'b), 3.66 (t, 1H, $J_{2,3}$ 9.0, H-2), 3.57-3.62 (m, 1H, H_{link-1}), 3.52 (t, 1H, J 9.2, H-4'), 3.38-3.49 (m, 9H, H-5', H-3', H-5', H-6'a, H-6'b, H_{link-3} , OCH₃), 3.29-3.33 (m, 1H, H_{link-3}), 3.26 (dd, 1H, $J_{2',3'}$ 8.2, H-2'), 2.64-2.75 (m, 2H, SCH_2CH_3), 1.93 (s, 3H, $NHCOCH_3$), 1.62-1.74 (m, 2H, H_{link-2}), 1.26 (t, 3H, J 7.5, SCH_2CH_3). ^{13}C NMR (150 MHz, $CDCl_3$): δ 134.9 (CH, =CH), 125.0-129.0 (CH, ArC), 116.9 (CH_2 , = CH_2), 101.4 (CH, $^1J_{C,H}$ 162.0, C-1'), 100.9 (CH, PhCH), 85.2 (CH, $J_{C,H}$ 151.6, C-1), 83.7 (CH, C-3), 82.2 (CH, C-4'), 77.8 (CH, C-2), 77.1 (CH, C-3'), 77.1, 69.4, 67.7, 67.6, 65.5

(C-5', C-5, C-6, C_{link}-3), 74.0, 72.5, (CH₂, 2xPhCH₂), 74.1 (CH₂, CH₂=CHCH₂), 73.7 (CH, C-4), 69.0 (CH₂, C_{link}-1), 68.5 (CH₂, C-6'), 57.2 (CH, C-2'), 56.7 (CH₃, OCH₃), 29.9 (CH₂, C_{link}-2), 25.6 (CH₂, SCH₂CH₃), 23.2 (CH₃, NHCOCH₃), 14.6 (CH₃, SCH₂CH₃). Anal. Calcd for C₄₄H₅₇O₁₁NS (808.00): C, 65.41; H, 7.11; N, 1.73; S, 3.98. Found: C, 65.25; H, 7.10; N, 1.74; S, 3.81. ES HRMS: m/z 830.356520 [M + Na]⁺ ± 1.5 mDa and 809.1 [M + H]⁺ (C₄₄H₅₇O₁₁NS requires m/z 808.00).

Ethyl 2-O-allyl-3,4-di-O-benzyl-6-O-(2'-O-(methyl 2-acetamido-6-O-benzyl-2-deoxy-β-D-glucopyranos-3-oxy)ethyl)-1-thio-β-D-galactopyranoside (77).

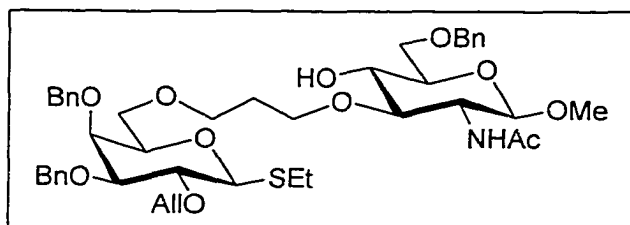


Dry THF (5 mL) was added to a mixture of compound **75** (332 mg, 0.42 mmol), sodium cyanoborohydride (158 mg, 2.52

mmol), dry powdered 3 Å molecular sieves and methyl orange (3 mg) which was purged with argon. A solution of freshly made concd HCl in dry ether was added dropwise to the reaction mixture until the evolution of gases ceased and the indicator turned bright pink. Approximately twice the original volume of HCl ethereal solution was again added and the reaction was left to stir for 60 min. The reaction mixture was diluted with CH₂Cl₂, filtered through celite, washed with NaHCO₃, brine and dried with Na₂SO₄. After solvent evaporation, column chromatography of the crude material on silica (60:1 CH₂Cl₂-MeOH) gave **77** (197 mg, 60%). [α]_D -12.7° (c 13.2, CHCl₃); R_f 0.38 (16:1 CH₂Cl₂-MeOH); ¹H NMR (500 MHz, CDCl₃): δ 7.20-7.40 (m, ArH), 5.97 (ddt, 1H, =CH), 5.74 (d, 1H, J_{2',NH} 7.9, NHAc), 5.27 (dd, 1H, =CH₂), 5.15 (dd, 1H, =CH₂), 4.92 (d, 1H, J_{gem} 11.8, PhCH₂), 4.70 (J_{1',2'} 8.7, H-1'), 4.68-4.76 (m, 2H, J_{gem} 11.9, PhCH₂), 4.54-4.60 (m, 3H, PhCH₂), 4.31 (J_{1,2} 9.8, H-1), 4.25-4.38 (CH₂=CHCH₂), 3.83 (H-3'), 3.79 (H-4), 3.66 (H-2), 3.49 (H-5), 3.47 (H-4', H-3), 3.46 (OCH₃), 3.37-3.90 (H-5', H-6'a, H-6'b, H-6a, H-6b, H_{link}-1, H_{link}-2), 3.23 (H-2'), 2.62-2.76 (m, 2H, SCH₂CH₃), 1.96 (s, 3H, NHCOCH₃), 1.25 (t,

3H, J 7.5, SCH₂CH₃). ¹³C NMR (125 MHz, CDCl₃): δ 134.8 (CH, =CH), 126.0-130.0 (CH, ArC), 116.9 (CH₂, =CH₂), 100.7 (CH, ¹J_{C,H} 163.7, C-1'), 85.0 (CH, ¹J_{C,H} 153.7, C-1), 83.8 (CH, C-3), 82.3 (CH, C-3'), 77.8 (CH, C-2), 77.2 (CH, C-5), 74.9, 73.4, 72.7 (CH₂, 3xPhCH₂), 74.4 (CH, C-4'), 74.2 (CH₂, CH₂=CHCH₂), 73.6 (CH, C-4), 71.7, 71.0, 70.9, 70.5, 70.0 (C-5', C-6', C-6, C_{link}-1, C_{link}-2), 56.7 (CH, C-2'), 56.4 (CH₃, OCH₃), 24.3 (CH₂, SCH₂CH₃), 23.4 (CH₃, NHCOCH₃), 14.6 (CH₃, SCH₂CH₃). ES HRMS: m/z 818.356340 [M + Na]⁺ ± 1.3 mDa and 796.4 [M + H]⁺ (C₄₃H₅₇O₁₁NS requires m/z 795.99). The acetylated form of **77** provided a characteristic NMR spectrum showing a downfield shift of the 4-OH signal (4.86 ppm).

Ethyl 2-O-allyl-3,4-di-O-benzyl-6-O-(3'-O-(methyl 2-acetamido-6-O-benzyl-2-deoxy-β-D-glucopyranos-3-oxo)propyl)-1-thio-β-D-galactopyranoside (78).

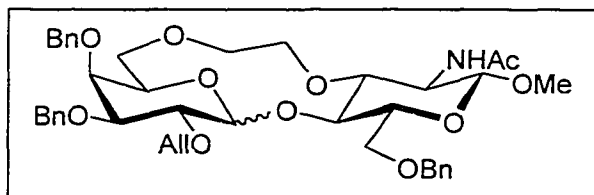


Dry THF (20 mL) was added to a mixture of compound **76** (647 mg, 0.8 mmol), sodium cyanoborohydride (352 mg, 5.6 mmol), dry powdered 3 Å

molecular sieves and methyl orange (10 mg) purged with argon. A solution of freshly made concd HCl in dry ether was added dropwise to the reaction mixture until the evolution of gases ceased and the indicator turned bright pink. Approximately twice the original volume of ethereal HCl solution was added and the reaction was left to stir for 90 min. The reaction mixture was diluted with CH₂Cl₂, filtered through celite, washed with NaHCO₃, brine and dried with Na₂SO₄. After solvent evaporation, column chromatography of the crude material (60:1 CH₂Cl₂-MeOH) on silica gave a white solid **78** (66 mg, 63%). [α]_D -14.0° (c 4.8, CHCl₃); R_f 0.53 (1:1 Toluene-Acetone); ¹H NMR (600 MHz, CDCl₃): δ 7.22-7.36 (m, ArH), 5.97 (ddt, 1H, =CH), 5.59 (d, 1H, J_{2',NH} 7.7, NHAc), 5.26 (dddd, 1H, =CH₂), 5.14 (dddd, 1H, =CH₂), 4.91 (d, 1H, J_{gem} 11.9, PhCH₂), 4.67-4.74 (m, 3H, J_{1',2'} 8.6, H-1', PhCH₂), 4.54-4.60 (m,

3H, PhCH₂), 4.25–4.36 (m, 3H, J_{1,2} 9.5, H-1, CH₂=CHCH₂), 3.82 (d, 1H, J_{3,4} 2.4, H-4), 3.63–3.78 (m, 6H, H-3', H-2, H-6'a, H-6'b, 2xH_{link-1}), 3.44–3.54 (m, 10H, OCH₃, H-3, H-4', H-5', H-5, H-6b, 2xH_{link-3}), 3.42 (dd, 1H, J_{5,6a} 5.9, J_{6a,6b} 9.2, H-6a), 3.22 (dd, 1H, J_{2,3} 8.1, H-2), 2.64–2.76 (m, 2H, SCH₂CH₃), 1.95 (s, 3H, NHCOCH₃), 1.62–1.80 (m, 2H, H_{link-2}), 1.26 (t, 3H, J 7.5, SCH₂CH₃). ¹³C NMR (150 MHz, CDCl₃): δ 134.8 (CH, =CH), 126.5–129.0 (CH, ArC), 116.9 (CH₂, =CH₂), 100.7 (CH, ¹J_{C,H} 161.0, C-1'), 85.2 (CH, ¹J_{C,H} 152.6, C-1), 83.9 (CH, C-3), 81.1 (CH, C-3'), 78.0, 74.2, 72.1 (CH, C-4', C-5', C-5), 77.9 (CH, C-2), 74.1, 73.4, 72.7 (CH₂, 3xPhCH₂), 74.2 (CH₂, CH₂=CHCH₂), 73.6 (CH, C-4), 70.2 (CH₂, C-6'), 69.7 (CH₂, C-6), 69.1 (CH₂, C_{link-1}), 68.4 (CH₂, C_{link-3}), 56.9 (CH, C-2'), 56.5 (CH₃, OCH₃), 29.5 (CH₂, C_{link-2}), 24.6 (CH₂, SCH₂CH₃), 23.4 (CH₃, NHCOCH₃), 14.8 (CH₃, SCH₂CH₃). Anal. Calcd for C₄₄H₅₉O₁₁NS (810.01): C, 65.24; H, 7.34; N, 1.73; S, 3.96. Found: C, 64.84; H, 7.31; N, 1.80; S, 3.96. ES HRMS: m/z 832.370137 [M + Na]⁺ ± 0.5 mDa and 811.5 [M + H]⁺ (C₄₄H₅₉O₁₁NS requires m/z 810.01).

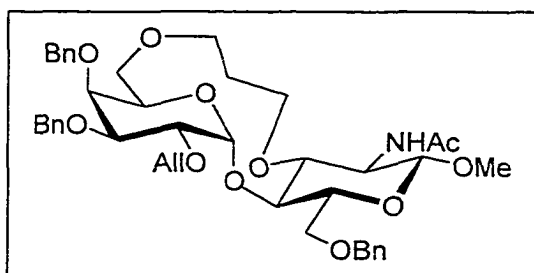
Methyl 2-acetamido-4-O-(2-O-allyl-3,4-di-O-benzyl- α/β -D-galactopyranosyl)-6-O-benzyl-2-deoxy-3,6'-di-O-(ethan-1,2-diyl)- β -D-glucopyranoside (79).



To a dry mixture of **77** (1.04 g, 1.3 mmol), DTBMP (907 mg, 4.4 mmol) and powdered 4 Å molecular sieves purged with argon, was added dry CH₂Cl₂ (40 mL). The reaction was stirred for 15 min and methyl triflate (430 μL, 3.8 mmol) was added. After 45 min, the reaction mixture was diluted with CH₂Cl₂ and filtered through celite. The filtrate was washed with NaHCO₃, 0.5 M HCl, NaHCO₃, brine and dried. The crude material was chromatographed on silica (2:1 Toluene-Acetone) and gave **79** as an inseparable α/β mixture which was used in the next step (381 mg, 40%). β -anomer: ¹H NMR (500 MHz, CDCl₃): δ 7.00–7.55 (m, ArH), 5.89 (ddt, 1H, =CH), 5.70 (d, 1H, J_{2,NH} 8.0, NHAc), 5.26 (dd, 1H, =CH₂), 5.14 (dd, 1H,

=CH₂), 4.85 (d, 1H, *J*_{gem} 12.1, PhCH₂), 4.79 (d, 1H, *J*_{1,2} 6.4, H-1), 4.72, 4.67 (2d, 1H each, *J*_{gem} 12.0, PhCH₂), 4.52-4.60 (m, 3H, PhCH₂), 4.24 (*J*_{1',2'} 7.8, H-1'), 4.19 (H-6a), 4.18-4.28 (CH₂=CHCH₂), 3.94 (t, 1H, *J* 6.5, H-4'), 3.87 (m, 1H, H-5), 3.70 (H-3, H-5'), 3.66 (H-6'), 3.64 (H-4), 3.63 (H-2'), 3.53 (H-6b), 3.47 (H_{link-1}), 3.43 (H-2, H-3', OCH₃), 3.40 (H_{link-2}), 1.98 (s, 3H, NHCOCH₃). ¹³C NMR (125 MHz, CDCl₃): δ 134.6 (CH, =CH), 126.0-130.0 (CH, ArC), 116.3 (CH₂, =CH₂), 104.3 (CH, ¹*J*_{C,H} 158.6, C-1'), 99.6 (CH, ¹*J*_{C,H} 164.5, C-1), 83.0 (CH, C-3'), 81.1 (CH, C-3), 79.8 (CH, C-4'), 78.9 (CH, C-2'), 75.2 (CH₂, C_{link-2}), 73.9 (CH₂, CH₂=CHCH₂), 73.7, 73.3, 73.0 (CH₂, 3xPhCH₂), 73.5 (CH, C-5'), 73.3 (CH, C-4), 70.4 (CH, C-5), 70.4 (CH₂, C-6'), 69.8 (CH₂, C-6, C_{link-1}), 56.1 (CH, C-2), 56.1 (CH₃, OCH₃), 21.5 (CH₃, NHCOCH₃). ES HRMS: *m/z* 756.335744 [M + Na]⁺ ± 0.2 mDa and 734.3 [M + H]⁺ (C₄₁H₅₁O₁₁NS requires *m/z* 733.86).

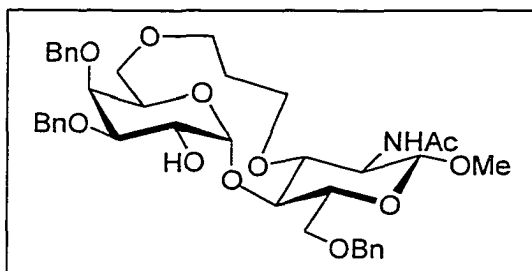
Methyl 2-acetamido-4-O-(2-O-allyl-3,4-di-O-benzyl- α -D-galactopyranosyl)-6-O-benzyl-2-deoxy-3,6'-di-O-(propan-1,3-diyl)- β -D-glucopyranoside (80).



A dry mixture of starting material **78** (286 mg, 0.35 mmol), DTBMP (256 mg, 1.24 mmol) and powdered 4 Å molecular sieves was purged with argon and dry CH₂Cl₂ (24 mL) was added. The reaction was stirred for 15 min, and then methyl triflate (120 μL, 1.06 mmol) was added. After 45 min, the reaction mixture was diluted with CH₂Cl₂ and filtered through celite. The filtrate was washed with NaHCO₃, 0.5 M HCl, NaHCO₃, brine and dried. The crude material was chromatographed on silica (2:1 Toluene-Acetone) to give **80** (142 mg, 54%). Only the α -anomer **80** was isolated. [α]_D +30.0° (*c* 1.6, CHCl₃); *R*_f 0.44 (1:1 Toluene-Acetone); ¹H NMR (300 MHz, CDCl₃): δ 7.20-7.41 (m, ArH), 5.88 (ddt, 1H, =CH), 5.66 (d, 1H, *J*_{2,NH} 8.2, NHAc), 5.06-5.26 (m, 2H, H-1', =CH₂), 5.10 (dd, 1H, =CH₂), 4.91 (d, 1H, *J*_{gem} 11.7, PhCH₂), 4.73, 4.66 (2d, 2H, *J*_{gem} 11.9, PhCH₂), 4.56-4.64 (m,

3H, H-1, PhCH₂), 4.52 (d, J_{gem} 11.6, PhCH₂), 4.39 (d, 1H, J_{5,6} 9.8, H-5'), 3.98-4.26 (m, 4H, H-3, H-6a, CH₂=CHCH₂), 3.94 (H-2', H-6'a), 3.88, 3.82 (H-4, H-3'), 3.86, 3.71 (H_{link-1}), 3.85 (H-6b), 3.64 (H_{link-3}), 3.62 (H-5), 3.61 (H-4'), 3.54 (H-2), 3.44 (OCH₃), 3.24-3.32 (m, 1H, H_{link-3}), 3.13 (dd, 1H, J_{6'a,6'b} 12.4, J_{6'b,5'} 1.8, H-6'b), 1.95 (s, 3H, NHCOCH₃), 1.54-1.78 (m, 2H, H_{link-2}). ¹³C NMR (75 MHz, CDCl₃): δ 134.9 (CH, =CH), 125.0-129.0 (CH, ArC), 117.1 (CH₂, =CH₂), 100.0 (CH, ¹J_{C,H} 162.9, C-1), 92.8 (CH, ¹J_{C,H} 165.3, C-1'), 79.0, 75.5 (CH, C-3', C-4), 76.9 (CH, C-3), 76.1 (CH, C-2'), 74.7 (CH, C-4'), 74.3, 73.2, 72.5 (CH₂, 3xPhCH₂), 72.8 (CH₂, CH₂=CHCH₂), 72.7 (CH, C-5), 69.7 (CH₂, C-6), 67.7 (CH₂, C-6'), 65.8 (CH₂, C_{link-1}), 64.7 (CH, C-5'), 60.0 (CH₂, C_{link-3}), 57.9 (CH, C-2), 56.1 (CH₃, OCH₃), 29.8 (CH₂, C_{link-2}), 23.2 (CH₃, NHCOCH₃). Anal. Calcd for C₄₂H₅₃O₁₁N (747.88): C, 67.45; H, 7.14; N, 1.87. Found: C, 66.78; H, 7.10; N, 1.89. ES HRMS: m/z 770.351000 [M + Na]⁺ ± 0.6 mDa and 748.4 [M + H]⁺ (C₄₂H₅₃O₁₁N requires m/z 747.88).

Methyl 2-acetamido-6-O-benzyl-4-O-(3,4-di-O-benzyl- α -D-galactopyranosyl)-2-deoxy-3,6'-di-O-(propan-1,3-diyl)- β -D-glucopyranoside (81).

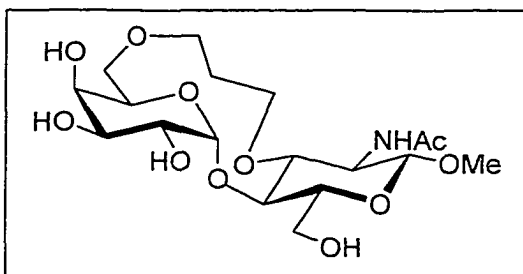


Compound **80** (134 mg, 179 μ mol) was dissolved in (CH₃)₂SO (6 mL) with potassium *t*-butoxide (40 mg, 0.36 μ mol) and the reaction mixture was heated to 100°C for 1 h. The mixture was diluted

with water, neutralized with dry ice, and the solvents were evaporated. The residue was dissolved in CH₂Cl₂, washed with brine and dried with Na₂SO₄. Once concentrated, the residue was dissolved in a 3:1 acetone and 2M HCl solution (4 mL) and refluxed for 30 min. The reaction was neutralized with NaHCO₃, evaporated, and chromatographed on silica (1:1 Hexane-Acetone) to give **81** (90 mg, 71%). [α]_D +10.0° (c 2.7, CHCl₃), ¹H NMR (500 MHz, CDCl₃): δ 7.20-7.40 (m, ArH), 5.72 (d, 1H, J_{2,NH} 8.7, NHAc), 5.24 (d, 1H, J_{1',2'} 3.8, H-1'), 4.85 (d, 1H, J_{gem} 11.6, PhCH₂), 4.51-4.62 (m, 4H, J_{gem} 11.9,

PhCH₂), 4.49 (d, 1H, PhCH₂), 4.52 (d, 1H, J_{gem} 11.6, PhCH₂), 4.46 (d, 1H, J_{1,2} 7.2, H-1), 4.41 (d, 1H, J 9.3, H-5'), 4.14 (ddd, 1H, J_{2',3'} 9.1, J_{2',OH} 6.6, H-2'), 4.04 (t, 1H, J 8.4, 8.7, H-3), 3.79-3.99 (m, 4H, H-6a, H-4, H-6'a, H_{link-1}), 3.75 (dd, 1H, J 4.7, J 10.1, H-6b), 3.61-3.72 (m, 5H, H-6b, H-5, H-4', H-3', H_{link-1}, H_{link-3}, H-2), 3.39 (s, 3H, OCH₃), 3.27-3.33 (m, 1H, H_{link-3}), 3.20 (d, 1H, J_{6'a,6'b} 11.9, H-6'b), 2.98 (d, 1H, OH), 1.95 (s, 3H, NHCOCH₃), 1.59-1.73 (m, 2H, H_{link-2}). ¹³C NMR (125 MHz, CDCl₃): δ 126.0-129.0 (CH, ArC), 100.5 (CH, ¹J_{C,H} 158.4, C-1), 93.8 (CH, ¹J_{C,H} 166.0, C-1'), 79.6 (CH, C-3'), 77.3 (CH, C-3, C-4), 74.1, 73.3, 72.4 (CH₂, 3xPhCH₂), 73.9 (CH, C-4'), 71.5 (CH₂, C-6), 71.7 (CH, C-5), 68.8 (CH, C-2'), 67.8 (CH₂, C-6'), 65.6 (CH₂, C_{link-1}), 65.3 (CH, C-5'), 60.4 (CH₂, C_{link-3}), 56.8 (CH, C-2), 56.2 (CH₃, OCH₃), 29.8 (CH₂, C_{link-2}), 23.3 (CH₃, NHCOCH₃). ESMS: m/z 730.9 [M + Na]⁺ and 708.5 [M + H]⁺ (C₃₉H₄₉O₁₁N requires m/z 707.82).

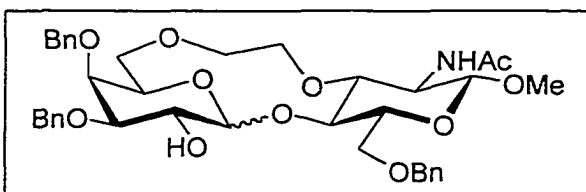
Methyl 2-acetamido-2-deoxy-4-O- α -D-galactopyranosyl-3,6'-di-O-(propan-1,3-diyl)- β -D-glucopyranoside (82).



The tethered disaccharide **81** (30.4 mg, 0.04 mmol) was dissolved in ethanol (15 mL), to which 20% palladium hydroxide on charcoal was added (60 mg). The mixture was hydrogenated overnight under an atmosphere of hydrogen. Once filtered, the crude material was purified by HPLC (water-methanol gradient 0-8%). This gave **82** (16.7 mg, 89%). [α]_D +76.0° (c 1.5, H₂O); ¹H NMR (500 MHz, D₂O): δ 5.31 (d, 1H, J_{1',2'} 3.1, H-1'), 4.55 (dd, 1H, J_{5',6'b} 2.1, J_{5',6'a} 11.1, H-5'), 4.45 (d, 1H, J_{1,2} 8.5, H-1), 4.14 (d, 1H, J_{6a,6b} 11.3, H-6a), 3.97 (m, 1H, H-3), 3.91, 3.69 (H_{link-1}), 3.89 (H-4', H-6b), 3.89, 3.86 (H-2', H-3'), 3.88 (H-6a), 3.79 (H-2), 3.74 (H-4), 3.73, 3.46 (H_{link-3}), 3.73 (H-5), 3.58 (dd, 1H, J_{6'a,6'b} 13.0, H-6'b), 3.49 (OCH₃), 2.03 (s, 3H, NHCOCH₃), 1.65-1.80 (m, 2H, H_{link-2}). ¹³C NMR (125 MHz, D₂O): δ 101.1 (CH, ¹J_{C,H} 161.1, C-1), 94.6 (CH, ¹J_{C,H} 165.5, C-1'), 78.0 (CH, C-3), 75.8 (CH, C-4), 73.2 (CH, C-5), 69.4, 69.1 (CH, C-2', C-3'), 68.2 (CH, C-4'),

67.5 (CH₂, C-6'), 67.0 (CH₂, C_{link}-1), 65.1 (CH, C-5'), 61.6 (CH₂, C-6), 60.5 (CH₂, C_{link}-3), 56.7 (CH, C-2), 57.4 (CH₃, OCH₃), 29.3 (CH₂, C_{link}-2), 22.6 (CH₃, NHCOCH₃). ES HRMS: m/z 460.179242 [M + Na]⁺ ± 0.2 mDa and 437.2 [M + H]⁺ (C₁₈H₃₁NO₁₁ requires m/z 437.44).

Methyl 2-acetamido-6-O-benzyl-4-O-(3,4-di-O-benzyl-β-D-galactopyranosyl)-2-deoxy-3,6'-di-O-(ethan-1,2-diyl)-β-D-glucopyranoside (83).



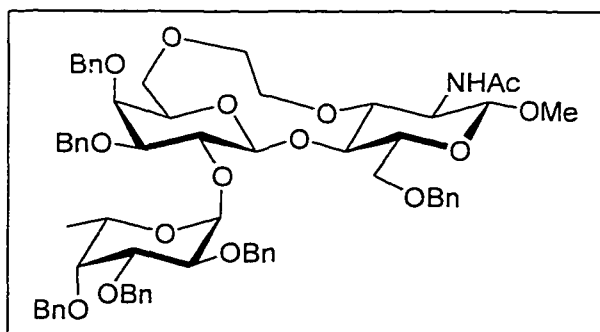
Compound **79** (250 mg, 0.34 mmol) was dissolved in (CH₃)₂SO (4 mL) with potassium *t*-butoxide (114 mg, 1.02 mmol). The reaction mixture

was heated to 100°C for 1 h. The mixture was diluted with water, neutralized with dry ice, and the solvents were evaporated. The residue was dissolved in CH₂Cl₂, washed with brine and dried with Na₂SO₄. Once concentrated, the residue was dissolved in a 3:1 acetone and 2M HCl solution (4 mL) and refluxed for 30 min. After 30 min, the reaction was neutralized with NaHCO₃, evaporated, and chromatographed on silica (2:1 Toluene-Acetone) to give **83** (150 mg, 64%). At this stage, the α/β mixture was separated and a 1:1 ratio of the anomers was observed. β-anomer: [α]_D +8.6° (c 5.6, CHCl₃); ¹H NMR (500 MHz, CDCl₃): δ 7.20-7.40 (m, ArH), 5.67 (d, 1H, J_{2,NH} 7.5, NHAc), 4.81 (d, 1H, J_{gem} 12.1, PhCH₂), 4.78 (d, 1H, J_{1,2} 6.4, H-1), 4.70, 4.65 (2d, 1H each, J_{gem} 11.9, PhCH₂), 4.52-4.62 (m, 3H, PhCH₂), 4.20 (J_{1,2'} 7.8, H-1'), 4.20 (H-5'), 3.96 (t, 1H, J 7.0, H-3), 3.88 (H-6'a), 3.85 (H-2'), 3.80 (H-6a), 3.73 (H-4), 3.71 (H-6b), 3.68 (H-4'), 3.50-3.59 (H-6'b, H_{link}-1, H_{link}-2), 3.40-3.44 (H-2, H-5, OCH₃), 3.35 (dd, 1H, J_{3',4'} 3.1, J_{2',3'} 9.5, H-3'), 1.94 (s, 3H, NHCOCH₃). ¹³C NMR (125 MHz, CDCl₃): δ 126.5-129.5 (CH, ArC), 104.8 (CH, ¹J_{C,H} 157.2, C-1'), 99.7 (CH, ¹J_{C,H} 163.9, C-1), 83.1 (CH, C-3'), 81.5 (CH, C-4), 79.5 (CH, C-3), 75.8 (CH, C-5), 73.7, 73.2, 72.6 (CH₂, 3xPhCH₂), 72.7 (CH, C-4'), 71.6 (CH, C-2'), 70.8 (CH₂, C-6'), 70.4 (CH₂, C-6), 70.2 (CH, C-5'), 69.8 (CH₂, C_{link}-1, C_{link}-2), 58.5 (OCH₃, C-2), 23.3 (CH₃, NHCOCH₃). ES

HRMS: m/z 716.304736 $[M + Na]^+ \pm 0.1$ mDa and 694.3 $[M + H]^+$ ($C_{38}H_{47}O_{11}N$ requires m/z 693.79).

α -anomer: 1H NMR (600 MHz, $CDCl_3$): δ 7.20-7.40 (m, ArH), 5.60 (b, 1H, $J_{2,NH}$ 7.4, NHAc), 5.23 (s, 1H, H-1'), 4.85 (d, 1H, J_{gem} 10.8, PhCH₂), 4.46-4.72 (m, 6H, J_{gem} 11.4, $J_{1,2}$ 7.9, H-1, PhCH₂), 4.29 (d, 1H, J 9.0, H-5'), 4.23, 3.92 (H-3, H-4), 3.62-4.12 (m, H-6, H-6', H-3', H-5, H_{link-1}, H_{link-2}), 3.72 (H-4'), 3.63 (H-2), 3.32-3.55 (m, H-2', OCH₃, H-6b), 1.95 (s, 3H, NHCOCH₃). ^{13}C NMR (150 MHz, $CDCl_3$): δ 126.0-130.0 (CH, ArC), 100.3 (CH, $^1J_{C,H}$ 165.4, C-1), 93.4 (CH, $^1J_{C,H}$ 172.3, C-1'), 79.8 (CH, C-3'), 77.4, 76.5 (CH, C-3, C-4), 74.5 (CH, C-4'), 73.8, 73.2, 72.5 (CH₂, 3xPhCH₂), 70.9 (CH, C-5'), 70.8, 70.5, 70.3, 69.5, 68.7 (C-6, C-6', C-5, C_{link-1}, C_{link-2}), 57.8 (CH, C-2'), 57.2 (CH, C-2), 56.0 (CH₃, OCH₃), 23.3 (CH₃, NHCOCH₃). ES HRMS: m/z 716.305468 $[M + Na]^+ \pm 0.8$ mDa and 694.2 $[M + H]^+$ ($C_{38}H_{47}O_{11}N$ requires m/z 693.79).

Methyl 2-acetamido-6-O-benzyl-4-O-(3,4-di-O-benzyl-2-O-(2,3,4-tri-O-benzyl- α -L-fucopyranosyl)- β -D-galactopyranosyl)-2-deoxy-3,6'-di-O-(ethan-1,2-diyl)- β -D-glucopyranoside (85).

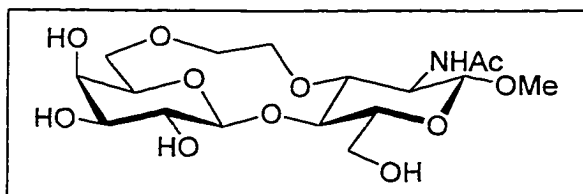


Bromine (~0.001 mL) was added to the thioglycoside **40**²⁰⁸ (90 mg, 0.19 mmol) dissolved in dry CH_2Cl_2 (1 mL) with 4 Å molecular sieves while purged with argon. After 30 min, the reaction was quenched with enough

cyclohexene to make the red color of bromine disappear. In a second reaction flask, a mixture of disaccharide **83** (60 mg, 0.087 mmol), DTBMP (20 mg, 0.1 mmol), tetrabutylammonium bromide (16.5 mg, 0.051 mmol), dry DMF (0.03 mL), 4 Å molecular sieves and dry CH_2Cl_2 (1 mL) was prepared and purged with argon. The freshly generated glycosyl bromide **84** was then added to the second reaction flask via a canula. Every 24 h a tlc was run, and an additional 1 equivalent of freshly prepared bromide was added. After

stirring for 3 days, the reaction was quenched with triethylamine, diluted with CH_2Cl_2 , filtered through celite, washed with NaHCO_3 , brine and dried with Na_2SO_4 . The crude material was chromatographed on silica (4:1 Toluene-Acetone) and gave **85** (53 mg, 55%) which still remained slightly impure. ^1H NMR (600 MHz, CDCl_3): δ 6.90-7.40 (m, ArH), 5.81 (d, 1H, $J_{2,\text{NH}}$ 7.5, NHAc), 5.61 (d, 1H, $J_{1'',2''}$ 3.7, H-1''), 4.89 (d, 1H, $J_{1,2}$ 7.7, H-1), 4.60-4.74 (m, 6H, PhCH₂), 4.54 (d, 1H, J_{gem} 11.4, PhCH₂), 4.42-4.50 (m, 5H, H-1', PhCH₂), 4.34 (d, 1H, PhCH₂), 4.22 (H-2'), 4.20 (H-5''), 4.18 (H_{link-1}), 4.10 (dd, 1H, J 7.8, J 9.0, H-3), 4.03-4.07 (m, 1H, $J_{6a,6b}$ 10.8, H-6a), 3.96 (H-2''), 3.95 (H_{link-2}), 3.90 (dd, 1H, $J_{2'',3''}$ 10.3, $J_{3'',4''}$ 2.6, H-3''), 3.75 (d, 1H, J 1.8, H-4'), 3.71 (dd, 1H, $J_{2',3'}$ 9.0, $J_{3',4'}$ 3.0, H-3'), 3.67 (d, 1H, J 1.8, H-4''), 3.63 (H-6'), 3.62 (H-5, H-6b), 3.55 (H-5'), 3.54 (H-6'), 3.48 (H_{link-1}), 3.44 (CH₃O), 3.41 (H-4), 3.39 (H_{link-2}), 3.22 (dd, 1H, $J_{2,3}$ 6.8, H-2), 1.97 (s, 3H, NHCOCH₃), 1.18 (d, 3H, $J_{5'',6''}$ 6.6, H-6''); ^{13}C NMR (150 MHz, CDCl_3): δ 126.0-129.0 (CH, ArC), 102.8 (CH, $^1J_{\text{C,H}}$ 161.7, C-1'), 99.3 (CH, $^1J_{\text{C,H}}$ 163.8, C-1), 97.4 (CH, $^1J_{\text{C,H}}$ 174.3, C-1''), 83.4 (CH, C-3'), 81.2 (CH, C-4), 79.6 (CH, C-3), 79.1 (CH, C-3''), 77.7 (CH, C-4''), 76.5 (CH, C-5), 74.7, 73.6, 73.4, 72.7, 72.1, 71.3 (CH, PhCH₂), 74.4 (CH, C-5'), 73.0 (CH, C-2''), 72.3 (CH, C-2'), 71.8 (CH, C-4'), 71.2 (CH₂, C-6), 70.4 (CH₂, C_{link-2}), 70.1 (CH₂, C_{link-1}), 68.8 (CH₂, C-6'), 66.0 (CH, C-5''), 57.8 (CH, C-2), 56.2 (CH₃, OCH₃), 23.3 (CH₃, NHCOCH₃), 16.1 (CH₃, C-6''). ES HRMS: m/z 1132.504583 $[\text{M} + \text{Na}]^+ \pm 1.1$ mDa and 1111.6 $[\text{M} + \text{H}]^+$ ($\text{C}_{65}\text{H}_{75}\text{O}_{15}\text{N}$ requires m/z 1110.31).

Methyl 2-acetamido-2-deoxy-3,6'-di-O-(ethan-1,2-diyl)-4-O- β -D-galactopyranosyl- β -D-glucopyranoside (87).

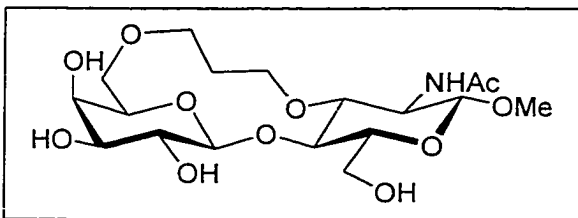


The tethered disaccharide **83** (25 mg, 0.04 mmol) was dissolved in ethanol (8 mL), to which 20% palladium hydroxide on charcoal was added (26

mg). The mixture was hydrogenated overnight under an atmosphere of hydrogen. Once filtered, the crude material was purified by HPLC (water-

methanol gradient 0-8%) to give **87** (14.2 mg, 93%). $[\alpha]_D +7.6^\circ$ (*c* 5.4, CHCl₃); ¹H NMR (600 MHz, D₂O): δ 4.51 (d, 1H, *J*_{1,2} 7.7, H-1), 4.31 (d, 1H, *J*_{1',2'} 7.9, H-1'), 4.16, 3.98, 3.90, 3.92, 3.80-3.84, 3.54, 3.53 (H-6a, H-6b, H-6'a, H-6'b, H_{link}-1, H_{link}-3), 3.91 (H-4'), 3.77 (broad, 1H, H-2), 3.65 (dd, 1H, *J* 3.5, *J* 9.7, H-3'), 3.59 (H-3, H-4, H-5, H-2', H-5'), 3.51 (s, 3H, OCH₃), 2.02 (s, 3H, NHCOCH₃); ¹³C NMR (125 MHz, D₂O): δ 175.1 (CO, NHCOCH₃), 105.2 (CH, ¹*J*_{C,H} 161.0, C-1'), 102.0 (CH, ¹*J*_{C,H} 157.5, C-1), 82.7, 81.3, 75.5, 75.3 (CH, C-3, C-4, C-5, C-5'), 74.4 (CH, C-3'), 72.1 (CH, C-2'), 71.9, 71.5, 69.7, 61.7 (CH₂, C_{link}-1, C_{link}-3, C-6, C-6'), 69.5 (CH, C-4'), 57.7 (CH₃, OCH₃), 56.2 (CH, C-2), 22.9 (CH₃, NHCOCH₃). ES HRMS: *m/z* 446.164063 [*M* + Na]⁺ ± 0.2 mDa (C₁₇H₂₉NO₁₁ requires *m/z* 423.42).

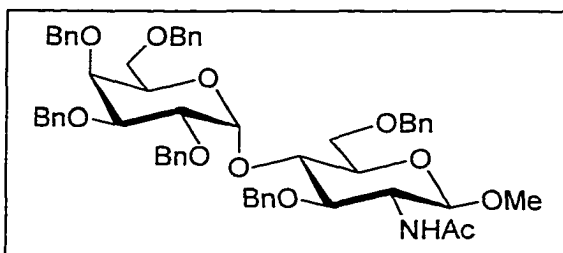
Methyl 2-acetamido-2-deoxy-4-O-β-D-galactopyranosyl-3,6'-di-O-(propan-1,3-diyl)-β-D-glucopyranoside (88).



The tethered disaccharide **38** (14.9 mg, 0.02 mmol) was dissolved in ethanol (15 mL), to which 20% palladium hydroxide on charcoal was added (30 mg). The mixture was hydrogenated overnight under an atmosphere of hydrogen. Once filtered, the crude material was purified by HPLC (water-methanol gradient 0-8%) to give **88** (8.6 mg, 92%). ¹H NMR (500 MHz, D₂O): δ 4.48 (d, 1H, *J*_{1,2} 8.4, H-1), 4.40 (d, 1H, *J*_{1',2'} 7.9, H-1'), 4.04-4.10 (m, 2H, H-6a, H-2), 4.00 (t, 1H, *J* 9.5, 9.6, H-4), 3.89 (dd, 1H, *J*_{6a,6b} 12.2, *J*_{5,6b} 5.5, H-6b), 3.79-3.84 (m, 5H, H-4', H-5', H-6'a, H_{link}-1, H_{link}-3), 3.67-3.74 (m, 2H, H-3, H_{link}-1), 3.49-3.66 (m, 8H, H-2', H-3', H-6'b, H-5, H_{link}-3, OCH₃), 2.03 (s, 3H, NHCOCH₃), 1.64-1.80 (m, 2H, H_{link}-2). ¹³C NMR (125 MHz, D₂O): δ 102.2 (CH, C-1), 105.9 (CH, C-1'), 78.1 (CH, C-3), 76.4 (CH, C-4), 75.2 (CH, C-5), 74.3, 68.5 (CH, C-4', C-5'), 73.2 (CH, C-3'), 71.2 (CH, C-2'), 68.5, 67.3 (CH₂, C_{link}-1, C_{link}-3), 60.5 (CH₂, C-6), 59.3 (CH₂, C-6'), 57.3 (CH₃, OCH₃), 51.5 (CH, C-2), 29.7 (CH₂, C_{link}-2), 22.2 (CH₃, NHCOCH₃). ES

HRMS: m/z 460.178665 $[M + Na]^+ \pm 0.8$ mDa and 437.2 $[M + H]^+$ ($C_{18}H_{31}NO_{11}$ requires m/z 437.44).

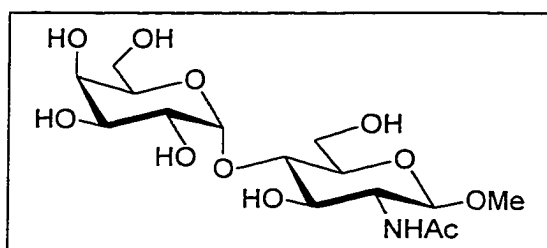
Methyl 2-acetamido-3,6-di-O-benzyl-4-O-(2,3,4,6-tetra-O-benzyl- α -D-galactopyranosyl)-2-deoxy- β -D-glucopyranoside (91).



Thioglycoside **89**²¹⁰ (465 mg, 0.8 mmol), the acetamido derivative **90**²¹¹ (254 mg, 0.61 mmol) and 4 Å molecular sieves were mixed in dry CH_2Cl_2 (6 mL) and purged with argon.

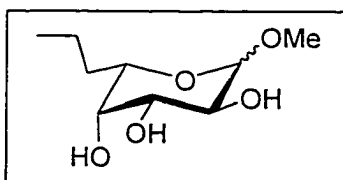
After stirring for 30 min, NIS (192 mg, 0.85 mmol), and silver triflate (63 mg, 0.24 mmol) were added and the flask was covered with aluminum foil. After 45 min, the reaction mixture was diluted with CH_2Cl_2 and the molecular sieves were filtered off. The filtrate was washed with $Na_2S_2O_3$, $NaHCO_3$, brine and dried. The concentrated material was chromatographed on silica (10:1→3:1 Toluene-EtOAc) to give **91** (131 mg, 23%). $[\alpha]_D +26.7^\circ$ (c 26.6, $CHCl_3$); 1H NMR (500 MHz, $CDCl_3$): δ 7.10-7.40 (m, ArH), 6.85 (d, 1H, $J_{2,NH}$ 8.0, NHAc), 4.88 (d, 1H, J_{gem} 11.3, $PhCH_2$), 4.84 (d, 1H, $J_{1',2'}$ 3.8, H-1'), 4.46-4.72 (m, 9H, H-1, $PhCH_2$), 4.42 (d, 1H, J_{gem} 11.9, $PhCH_2$), 4.37, 4.30 (2d, 1H each, J_{gem} 11.8, $PhCH_2$), 4.13-4.17 (m, 1H, H-2), 3.90-4.01 (m, 5H, H-2', H-5', H-4, H-5, H-6a/H-6a'), 3.86 (dd, 1H, $J_{2',3'}$ 10.2, $J_{3',4'}$ 2.6, H-3'), 3.79 (dd, 1H, $J_{5,6b}$ 5.3, $J_{6a,6b}$ 9.4, H-6b/H-6'b), 3.57 (broad t, 1H, H-3), 3.52 (t, 1H, J 7.6, H-6'a/H-6a), 3.40-3.46 (m, 4H, CH_3O , H-6'b/H-6b), 1.58 (s, 3H, $NHCOCH_3$). ^{13}C NMR (125 MHz, $CDCl_3$): δ 126.0-130.0 (CH, ArC), 100.9 (CH, $^1J_{C,H}$ 168.9, C-1), 97.4 (CH, $^1J_{C,H}$ 170.0, C-1'), 78.6 (CH, C-3'), 75.9, 75.2, 74.5, 70.9 (CH, C-2', C-5', C-4, C-5), 73.6 (CH, C-3), 70.5, 68.1 (CH_2 , C-6, C-6'), 56.2 (CH_3 , OCH_3), 49.1 (CH, C-2), 22.5 (CH_3 , $NHCOCH_3$). ES HRMS: m/z 960.429580 $[M + Na]^+ \pm 0.3$ mDa and 938.5 $[M + H]^+$ ($C_{57}H_{63}NO_{11}$ requires m/z 938.13).

Methyl 2-acetamido-2-deoxy-4-O- α -D-galactopyranosyl- β -D-glucopyranoside (92).



The disaccharide **91** (100 mg, 0.11 mmol) was dissolved in ethanol (35 mL), to which 20% palladium hydroxide on charcoal was added (120 mg). The mixture was hydrogenated overnight under an atmosphere of hydrogen. Once filtered, the crude material was purified by HPLC (water-methanol gradient 0-8%) to give **92** (38 mg, 89%). $[\alpha]_D^{25} +68.3^\circ$ (c 3.0, H₂O); $^1\text{H NMR}$ (600 MHz, CD₃OD): δ 5.21 (d, 1H, $J_{1,2}$ 3.8, H-1'), 4.32 (d, 1H, $J_{1,2}$ 7.9, H-1), 3.88-3.92 (m, 2H, H-6a, H-5'), 3.87 (d, 1H, J 3.3, H-4'), 3.81-3.88 (m, 2H, H-6b, H-2'), 3.65-3.75 (m, 5H, H-2, H-3, H-3', H-6'a, H-6'b), 3.56 (t, 1H, J 9.5, H-4), 3.45 (s, 3H, CH₃O), 3.36 (ddd, 1H, J 1.8, 4.7, 10.0, H-5), 1.96 (s, 3H, NHCOCH₃). $^{13}\text{C NMR}$ (150 MHz, CD₃OD): δ 175.5 (C, NHCOCH₃), 103.1 (CH, $^1J_{\text{C,H}}$ 162.0, C-1), 102.7 (CH, $^1J_{\text{C,H}}$ 174.0, C-1'), 81.1 (CH, C-4), 76.4 (CH, C-5), 75.4 (CH, C-3), 73.1 (CH, C-5'), 71.1 (CH, C-3'), 70.6 (CH, C-4'), 70.5 (CH, C-2'), 62.5 (CH₂, C-6'), 61.9 (CH₂, C-6), 57.2 (CH₃, OCH₃), 56.4 (CH, C-2), 22.4 (CH₃, NHCOCH₃). ES HRMS: m/z 420.148206 [$\text{M} + \text{Na}$]⁺ \pm 0.0 mDa (C₁₅H₂₇NO₁₁ requires m/z 397.38).

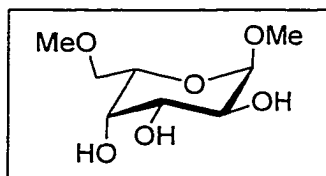
Methyl 6-C-ethyl- α/β -L-fucopyranoside (93).



Acetonide **102** (58.8 mg, 0.22 mmol) was dissolved in acetic acid (15 mL) and water (7 mL), and heated to 80°C overnight. Once concentrated and co-evaporated with toluene, the white powdery residue was mixed with methanol (20 mL), 1.5% TFA (0.3 mL) and refluxed overnight. Once neutralized with Dowex resin (OH⁻), filtered and chromatographed on silica (15:1 CH₂Cl₂-MeOH), compound **93** was obtained (15 mg, 36%). R_f 0.57 (7:2 EtOAc-MeOH); $^1\text{H NMR}$ (360 MHz, CD₃OD): δ 4.77 (d, 1H, $J_{1,2}$ 2.8, α H-1), 4.11 (d, 1H, $J_{1,2}$ 6.9, β H-1), 3.38-3.85 (m, 14H, H-2, H-3, H-4, H-5, H-6, OCH₃ for α - and β -anomers), 0.8-1.85 (m, 7H, H-6, H-7, H-8). ES HRMS:

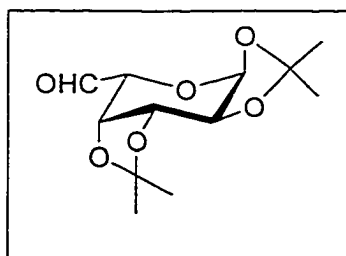
m/z 229.105086 [M + Na]⁺ ± 0.1 mDa and 207.1 [M + H]⁺ (C₉H₁₈O₅ requires m/z 206.24).

Methyl 6-O-methyl- α -L-galactopyranoside (94).



Compound **103** (310 mg, 1.1 mmol) was dissolved in acetic acid (10 mL) and water (3 mL), and heated to 80°C overnight. Once concentrated and co-evaporated with toluene, the white powdery residue was mixed with methanol (20 mL), 1.5% TFA (0.2 mL) and refluxed overnight. The solution was neutralized with Dowex resin (OH⁻), the filtrate was concentrated and chromatographed on silica (50:1→30:1 CH₂Cl₂-MeOH) to give compound α **94** and β **94** (108 mg, 46%). α -anomer: $[\alpha]_D^{+116.9^\circ}$ (c 6.0, CH₃OH); ¹H NMR (600 MHz, CDCl₃): δ 4.91 (d, 1H, J_{1,2} 1.4, H-1), 4.03-4.07 (m, 2H, H-2, H-3), 3.92-3.97 (m, 2H, H-4, H-5), 3.62 (dd, 1H, J_{5,6a} 3.8, J_{6a,6b} 10.8, H-6a), 3.56 (dd, 1H, J_{5,6b} 7.5, H-6b), 3.42, 3.41 (2s, 6H, 2xOCH₃); ¹³C NMR (150 MHz, CDCl₃): δ 109.0 (CH, ¹J_{C,H} 170.8, C-1), 83.8, 69.6 (CH, C-4, C-5), 81.4, 77.3 (CH, C-2, C-3), 74.0 (CH₂, C-6), 59.0, 55.7 (CH₃, OCH₃). ES HRMS: m/z 231.084381 [M + Na]⁺ ± 0.1 mDa (C₈H₁₆O₆ requires m/z 208.21).

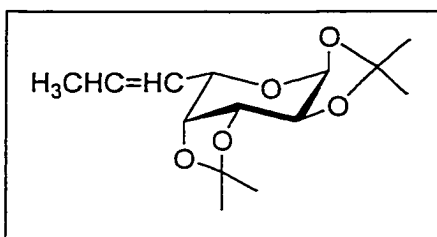
1,2,3,4-O-di-isopropylidene- α -L-galacto-hexadialdose (100).



To a mixture of oxalyl chloride (0.17 mL, 2.0 mmol) in dry CH₂Cl₂ (3 mL) cooled to -60°C was added (CH₃)₂SO (0.28 mL, 4.0 mmol). After 10 min, a solution of the acetonide **99**³²⁰ (433 mg, 1.7 mmol) in CH₂Cl₂ (3 mL) was added. The mixture was then stirred for 15 min, and triethylamine (1.1 mL, 8.0 mmol) was added. After 10 min, the reaction mixture was diluted with CH₂Cl₂, washed with HCl (1M), back-extracted with CH₂Cl₂, the combine organic layers were washed with brine and then dried with Na₂SO₄. Once concentrated, the residue was chromatographed on silica (3:1 Pentane-EtOAc) which gave **100** as an oil (308 mg, 72%). R_f 0.49 (1:1 Pentane-EtOAc); ¹H NMR (300 MHz, CDCl₃): δ

9.62 (s, 1H, HC=O), 5.66 (d, 1H, $J_{1,2}$ 5.0, H-1), 4.61 (dd, 1H, $J_{2,3}$ 2.3, $J_{3,4}$ 7.8, H-3), 4.64 (dd, 1H, $J_{4,5}$ 2.1, H-4), 4.38 (dd, 1H, H-2), 4.18 (d, 1H, H-5), 1.48 (s, 3H, $(\text{CH}_3)_2\text{C}$), 1.42 (s, 3H, $(\text{CH}_3)_2\text{C}$), 1.33(s, 3H, $(\text{CH}_3)_2\text{C}$), 130 (s, 3H, $(\text{CH}_3)_2\text{C}$).

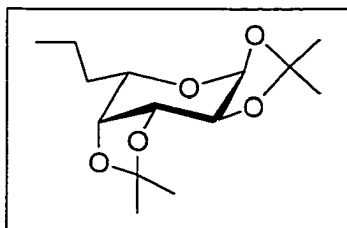
6,7,8-tri-deoxy-1,2,3,4-O-di-isopropylidene- α -L-galacto-octo-6-enopyranose (101).



The Wittig reagent was prepared by heating (ethyl)triphenylphosphonium bromide (374 mg, 1 mmol) and sodium hydride (24 mg, 1 mmol) in dry THF (4 mL) to 62°C for 5 h. A solution of the aldehyde **100** (201 mg, 0.78 mmol), TDA-1

(25 μL) in THF (4 mL) was added to the Wittig reagent and was stirred at 62°C overnight. Once cooled, the reaction mixture was filtered through celite, and evaporated. The residue was chromatographed on silica (6:1 Pentane-EtOAc) to give **101** (167 mg, 80%). R_f 0.88 (Hexane-EtOAc); ^1H NMR (360 MHz, CDCl_3): δ 5.65 (dd, 1H, =CH), 5.56 (ddt, 1H, $\text{CH}_3\text{CH}=\text{C}$), 5.49 (d, 1H, $J_{1,2}$ 5.1, H-1), 4.53-4.57 (m, 2H, H-5, H-3/H-4), 4.25 (dd, 1H, $J_{2,3}$ 2.4, H-2), 4.10 (dd, 1H, J 2.0, 7.8, H-4/H-3), 1.65 (dd, 3H, J 1.6, 6.8, CH_3), 1.51 (s, 3H, $(\text{CH}_3)_2\text{C}$), 1.41(s, 3H, $(\text{CH}_3)_2\text{C}$), 1.28 (s, 6H, $(\text{CH}_3)_2\text{C}$).

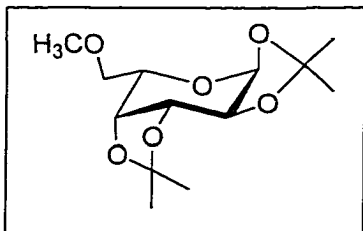
6-C-ethyl-1,2,3,4-O-di-isopropylidene- α -L-fucopyranoside (102).



Enopyranose **101** (59 mg, 0.22 mmol) and 10% palladium on charcoal (24 mg) were mixed in acetic acid (15 mL) and the mixture was hydrogenated overnight under an atmosphere of hydrogen. Once the reaction was complete, the mixture was filtered, concentrated and chromatographed on silica (13:1 Hexane-EtOAc) to give compound **102** (58.8 mg, 99%). R_f 0.30 (12:1 Hexane-EtOAc); ^1H NMR (360 MHz, CDCl_3): δ 5.51 (d, 1H, $J_{1,2}$ 5.1, H-1), 4.55 (dd, 1H, $J_{2,3}$ 2.2, $J_{3,4}$ 7.9, H-3),

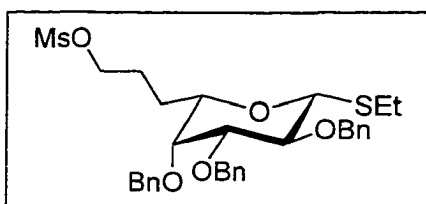
4.26 (dd, 1H, H-2), 3.68-3.80 (m, 2H, H-4, H-5), 1.98-2.19 (m, 2H, H-6a, H-6b), 1.20-1.75 (m, 14H, 2x(CH₃)₂C, H-7a, H-7b), 0.91 (t, 3H, CH₃).

1,2,3,4-O-di-isopropylidene-6-O-methyl- α -L-galactopyranose (103).



Acetonide **99**³²⁰ (350 mg, 1.4 mmol) was mixed with sodium hydride (48 mg, 2.1 mmol) in dry DMF (10 mL) and stirred for 30 min under argon. Iodomethane (180 μ L, 2.7 mmol) was added dropwise. The reaction mixture was quenched with MeOH, partitioned between water and CH₂Cl₂, washed with NaHCO₃, brine, and dried with Na₂SO₄. After evaporation and chromatography on silica (8:1 Toluene-EtOAc), compound **103** was obtained (310 mg, 84%). [α]_D +61.7° (c 13.5, CHCl₃); R_f 0.49 (4:1 Hexane-EtOAc); ¹H NMR (600 MHz, CDCl₃): δ 5.52 (d, 1H, J_{1,2} 5.1, H-1), 4.58 (dd, 1H, J_{2,3} 2.6, J_{3,4} 8.1, H-3), 4.29 (dd, 1H, H-2), 4.22 (dd, 1H, J_{4,5} 2.0, H-4), 3.95 (ddd, 1H, J_{4,5} 2.0, J_{5,6a} 5.5, J_{5,6b} 6.9, H-5), 3.58 (dd, 1H, J_{6a,6b} 10.1, H-6a), 3.52 (dd, 1H, J_{5,6b} 7.0, H-6b), 3.37 (s, 3H, CH₃O), 1.52, 1.43, 1.32, 1.31 (4s, 3H each, (CH₃)₂C); ¹³C NMR (150 MHz, CDCl₃): δ 96.2 (CH, ¹J_{C,H} 180.0, C-1), 71.0 (CH, C-4), 71.0 (CH₂, C-6), 70.4 (CH, C-3), 70.2 (CH, C-2), 66.3 (CH, C-5), 58.8 (CH₃, OCH₃), 25.7, 25.0 (CH₃, (CH₃)₂C). ES HRMS: m/z 297.131298 [M + Na]⁺ \pm 0.1 mDa and 275.1 [M + H]⁺ (C₁₃H₂₂O₆ requires m/z 274.31).

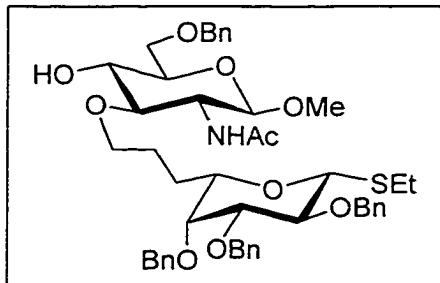
Ethyl 2,3,4-tri-O-benzyl-6,7-di-deoxy-8-O-methanesulphonyl-1-thio- β -L-galacto-octo-pyranoside (104).



Triethylamine (0.09 mL, 0.68 mmol) was added to a solution of alcohol **123** (238 mg, 0.46 mmol) in dry CH₂Cl₂ (5 mL) and methanesulphonyl chloride (0.06 mL, 0.68 mmol) in CH₂Cl₂ (1 mL) was added dropwise over 2 min. After stirring overnight at rt, the solution was diluted with CH₂Cl₂, washed with water, 1 M NaOH, water, brine, and dried with anhyd Na₂SO₄. Evaporation and chromatography on silica (2:1 Hexane-

EtOAc) gave **104** (367 mg, 90%) as an oil. $^1\text{H NMR}$ (300 MHz, CDCl_3): δ 7.20-7.42 (m, ArH), 4.99 (d, 1H, J_{gem} 11.8, PhCH_2), 4.87 (d, 1H, J_{gem} 10.2, PhCH_2), 4.70-4.81 (m, 3H, PhCH_2), 4.63 (d, 1H, J_{gem} 11.7, PhCH_2), 4.38 (d, 1H, $J_{1,2}$ 9.6, H-1), 4.06-4.22 (m, 2H, H-8), 3.80 (t, 1H, J 9.4, H-2), 3.64 (d, 1H, $J_{3,4}$ 2.3, H-4), 3.54 (dd, 1H, $J_{2,3}$ 9.3, H-3), 3.26 (dd, 1H, J 3.6, 8.4, H-5), 2.94 (s, 3H, CH_3SO_2), 2.60-2.81 (m, 2H, SCH_2CH_3), 1.74-1.94 (m, 2H, H-6a, H-7a), 1.49-1.67 (m, 1H, H-7b), 1.32-1.46 (m, 1H, H-6b), 1.28 (t, 3H, J 7.5, SCH_2CH_3); $^{13}\text{C NMR}$ (75 MHz, CDCl_3): δ 126.0-130.0 (CH, ArC), 84.9 (CH, $^1J_{\text{C,H}}$ 152.9, C-1), 84.2 (CH, C-3), 78.3 (CH, C-2), 77.6 (CH, C-5), 75.5, 74.1, 72.8 (CH_2 , PhCH_2), 75.1 (CH, C-4), 69.5 (CH_2 , C-8), 37.0 (CH_3 , CH_3SO_2), 24.4 (CH_2 , SCH_2CH_3), 14.7 (CH_3 , SCH_2CH_3). ES HRMS: m/z 623.211710 [$\text{M} + \text{Na}$] $^+ \pm 0.4$ mDa and 602.1 [$\text{M} + \text{H}$] $^+$ ($\text{C}_{32}\text{H}_{40}\text{O}_7\text{S}_2$ requires m/z 600.79).

Ethyl 2,3,4-tri-O-benzyl-6,7-di-deoxy-8-O-(methyl 2-acetamido-6-O-benzyl-2-deoxy- β -D-glucopyranos-3-oxy)-1-thio- β -L-galacto-octopyranoside (105).

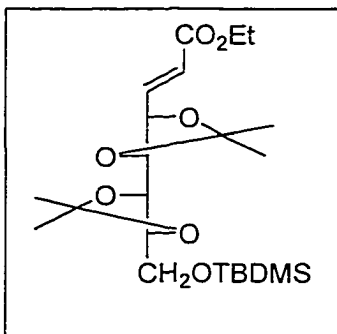


Dry THF (5 mL) was added to a mixture of compound **124** (170 mg, 0.21 mmol), sodium cyanoborohydride (78 mg, 1.23 mmol), dry powdered 3 Å molecular sieves and methyl orange (2 mg) and the suspension was purged with argon. A freshly made saturated solution of

HCl in dry ether was added dropwise to the reaction mixture until the evolution of gases ceased and the indicator turned bright pink. A further two fold volume of saturated HCl in ether was added and the reaction was left to stir for 30 min. The reaction mixture was diluted with CH_2Cl_2 , filtered through celite, washed with NaHCO_3 , brine and dried over Na_2SO_4 . Column chromatography of the crude material on silica (70:1 CH_2Cl_2 -MeOH) gave compound **105** (115 mg, 66%). $[\alpha]_{\text{D}} -0.8^\circ$ (c 59.0, CHCl_3); $^1\text{H NMR}$ (600 MHz, CDCl_3): δ 7.25-7.39 (m, 20H, ArH), 5.40 (d, 1H, $J_{2,\text{NH}}$ 7.7, NHAc), 4.86, 4.70 (2d, 1H each, J_{gem} 11.7, 10.2, PhCH_2), 4.70-4.79 (m, 4H, PhCH_2 , H-1'), 4.54-

4.68 (m, 3H, PhCH₂), 4.36 (d, 1H, J_{1,2} 9.7, H-1), 3.72-3.80 (m, 3H, H-2, H-3', H-5'), 3.60-3.67 (m, 2H, H-4, H-6'a), 3.47-3.56 (m, 5H, H-3, H-8a, H-8b, H-4', H-6'b), 3.45 (s, 3H, OCH₃), 3.23 (dd, 1H, J_{5,6a/b} 4.4, 8.4, H-5), 3.17 (quartet, 1H, J 8.0, H-2'), 2.64-2.77 (m, 2H, SCH₂CH₃), 1.92 (s, 3H, NHCOCH₃), 1.78-1.86 (m, 1H, H-6a), 1.54-1.64 (m, H-7a, HOD), 1.32-1.44 (m, 2H, H-6b, H-7b), 1.27 (t, 3H, J 7.4, SCH₂CH₃); ¹³C NMR (150 MHz, CDCl₃): δ 126.0-130.0 (CH, ArC), 100.5 (CH, ¹J_{C,H} 160.1, C-1'), 84.8 (CH, ¹J_{C,H} 154.9, C-1), 83.0 (CH, C-3), 80.3 (CH, C-3'), 78.3 (CH, C-2, C-5), 75.4, 74.0, 73.3, 72.5 (CH₂, PhCH₂), 75.1 (CH, C-4), 73.5 (CH, C-4'), 72.5 (CH₂, C-8), 71.3 (CH₂, C-6'), 70.2 (CH, C-5'), 56.7 (CH, C-2'), 56.4 (CH₃, OCH₃), 27.3 (CH₂, C-6), 26.4 (CH₂, C-7), 24.3 (CH₂, SCH₂CH₃), 23.3 (CH₃, NHCOCH₃), 14.5 (CH₃, SCH₂CH₃). ES HRMS: m/z 852.374720 [M + Na]⁺ ± 1.0 mDa and 831.4 [M + H]⁺ (C₄₇H₅₉NO₁₀S requires m/z 830.05).

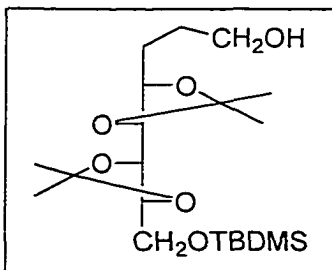
Methyl 8-O-t-butyldimethylsilyl-4,5:6,7-di-O-isopropylidene-D-galactoocto-2-en-ate (111).



A solution of ethyl diethylphosphonoacetate (740 mg, 3.52 mmol) in DME (3 mL) was added dropwise to a suspension of sodium hydride (77 mg, 3.20 mmol) in DME (15 mL). After 1 h, the reaction flask was cooled to 0°C, and a solution of aldehyde **110**²²¹ (600 mg, 1.60 mmol) in DME (3x2 mL) was added. The reaction mixture was evaporated after 2-3 h, the residue was dissolved in CH₂Cl₂, washed with 1 M HCl, NaHCO₃, brine, and dried over Na₂SO₄. Chromatography on silica (6:1 toluene-ethyl acetate), compound **111** as a syrup (678 mg, 98%). [α]_D -1.11° (c 4.5, CHCl₃); R_f 0.83 (2:1 toluene-ethyl acetate); ¹H NMR (300 MHz, CDCl₃): δ 6.98 (dd, 1H, J_{3,4} 4.6, J_{2,3} 15.8, H-3), 6.15 (dd, 1H, J_{3,4} 1.7, H-2), 4.58 (ddd, 1H, J_{4,5} 7.6, H-4), 3.94-4.02 (m, 2H, H-6, H-7), 3.85 (dd, 1H, H-8a), 3.78 (H-5), 3.73 (OCH₃), 3.71 (H-8b), 1.40, 1.39, 1.36 (3s, 12H, CCH₃), 0.88 (s, 9H, tBu), 0.056, 0.054 (2s, 6H, SiCH₃); ¹³C NMR (125 MHz, CDCl₃): δ 145.2 (CH, C-3), 121.0 (CH,

C-2), 81.4 (CH, C-5), 80.6, 77.4 (CH, C-6, C-7), 78.4 (CH, C-4), 62.9 (CH₂, C-8), 51.5 (CH₃, OCH₃), 26.6 (CH₃, C(CH₃)₂), 25.6 (CH₃, *t*Bu), -5.55 (CH₃, (CH₃)₂Si). Anal. Calcd for C₂₁H₃₈O₇Si (430.63): C, 58.57; H, 8.90. Found: C, 58.12; H, 8.65. ES HRMS: *m/z* 453.226300 [M + Na]⁺ ±2.2 mDa and 431.1 [M + H]⁺ (C₂₁H₃₈O₇Si requires *m/z* 430.63).

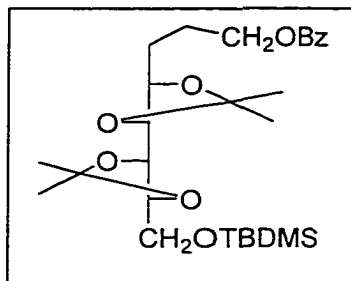
1-O-*t*-butyldimethylsilyl-6,7-di-deoxy-2,3:4,5-di-O-isopropylidene-L-galacto-octitol (113).



Sugar **111** (678 mg, 1.6 mmol) was dissolved in 95% ethanol (10 mL) and bismuth(III) chloride (252 mg, 0.8 mmol) was added. The reaction flask was cooled on ice, then NABH₄ (238 mg, 6.3 mmol) was added portionwise. The reaction was stirred at rt for 3 h.

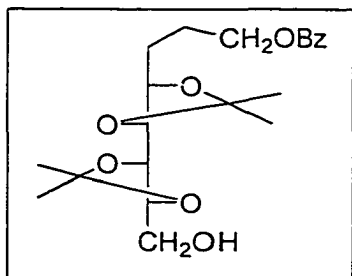
The reaction was quenched with water, neutralized with 1 M HCl, extracted with CH₂Cl₂, washed with brine and dried with Na₂SO₄. Solvent was evaporated and the residue pumped dry for 90 min, and then added to a suspension of LAH (67 mg, 1.77 mmol) in ether (24 mL). After stirring for 45 min, the reaction was quenched with K₂CO₃, washed with water, NaHCO₃, brine, and dried with Na₂SO₄. Chromatography on silica (4:1 toluene-ethyl acetate) gave compound **113** (573.3 mg, 88%) as a syrup. [α]_D -1.67° (*c* 5.4, CHCl₃); R_f 0.27 (4:1 toluene-ethyl acetate); ¹H NMR (500 MHz, CDCl₃): δ 4.01 (ddd, 1H, J 3.0, 7.4, J_{7,8b} 4.1, H-7), 3.97 (dt, 1H, J_{3,4} 3.1, J_{4,5} 8.1, H-4), 3.86 (H-6, H-8a), 3.70 (dd, 1H, J_{8a,8b} 11.1, H-8b), 3.67 (H1), 3.61 (t, J 7.6, H-5), 1.87-1.94 (m, 1H, H-3a), 1.73 (quintet, 2H, J 6.5, H-2), 1.56-1.64 (m, 1H, H-3b), 1.38, 1.35, 1.33 (3s, 12H, CCH₃), 0.88 (s, 9H, *t*Bu), 0.054, 0.050 (2s, 6H, SiCH₃); ¹³C NMR (125 MHz, CDCl₃): δ 81.7 (CH, C-5), 81.2 (CH, C-7), 80.4 (CH, C-4), 77.1 (CH, C-6), 63.0 (CH₂, C-8), 62.5 (CH₂, C-1), 30.0 (CH₂, C-3), 29.1 (CH₂, C-2), 26.8 (CH₃, C(CH₃)₂), 25.5 (CH₃, *t*Bu), -5.53 (CH₃, (CH₃)₂Si). Anal. Calcd for C₂₀H₄₀O₆Si (404.63): C, 59.37; H, 9.96. Found: C, 59.41; H, 10.04. ES HRMS: *m/z* 427.13 [M + Na]⁺ and 405.265400 [M + H]⁺ ± 1.8 mDa (C₂₀H₄₀O₆Si requires *m/z* 404.63).

8-O-benzoyl-1-O-*t*-butyldimethylsilyl-6,7-di-deoxy-2,3:4,5-di-O-isopropylidene-L-galacto-octitol (114).



Alcohol **113** (564 mg, 1.39 mmol) was dissolved in dry pyridine (15 mL) and benzoyl chloride (0.19 mL, 1.67 mmol) was added to the cooled solution. The reaction was stirred at rt for 2 h, then poured on ice, extracted with CH_2Cl_2 , washed with NaHCO_3 , brine, and dried with Na_2SO_4 . Once concentrated, the residue was chromatographed on silica (11:1 Hexane-EtOAc) to give compound **114** (651 mg, 92%) obtained as a syrup. $[\alpha]_D -3.6^\circ$ (c 6.7, CHCl_3); R_f 0.80 (4:1 toluene-ethyl acetate); $^1\text{H NMR}$ (300 MHz, CDCl_3): δ 8.02, 7.66, 7.41 (5H, ArH), 4.35 (t, 2H, $J_{1,2}$ 6.4, H-1), 3.82-4.40 (m, 4H, H-4, H-6, H-7, H-8a), 3.70 (dd, 1H, $J_{8a,8b}$ 4.3, $J_{8a,8b}$ 11.3, H-8b), 3.62 (t, 1H, J 7.7, H-5), 1.60-2.40 (m, 4H, H-2a, H-2b, H-3a, H-3b), 1.37, 1.35, 1.33, 1.32 (4s, 3H each, $\text{C}(\text{CH}_3)_2$), 0.88 (s, 9H, $\text{C}(\text{CH}_3)_3$), 0.05 (s, 6H, $\text{Si}(\text{CH}_3)_2$); $^{13}\text{C NMR}$ (300 MHz, CDCl_3): δ 134.3, 129.3, 128.0 (CH, ArC), 81.6 (CH, C-5), 81.5, 79.8, 77.1 (CH, C-4, C-6, C-7), 64.4 (CH_2 , C-1), 62.9 (CH_2 , C-8), 29.8 (CH_2 , C-3), 26.7 (CH_3 , $\text{C}(\text{CH}_3)_2$), 25.6 (CH_3 , *t*Bu), 24.9 (CH_2 , C-2), -5.53 (CH_3 , $(\text{CH}_3)_2\text{Si}$). ES HRMS: m/z 531.275846 $[\text{M} + \text{Na}]^+$ and 509.3 $[\text{M} + \text{H}]^+$ ($\text{C}_{27}\text{H}_{44}\text{O}_7\text{Si}$ requires m/z 508.73).

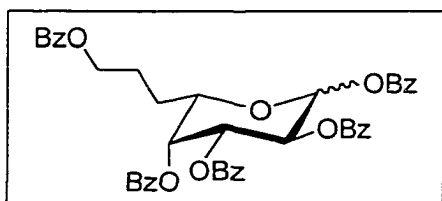
1-O-benzoyl-2,3-di-deoxy-4,5:6,7-di-O-isopropylidene-D-galacto-octitol (115).



Benzoate **114** (651 mg, 1.28 mmol) was stirred with 1 M solution of TBAF in THF for 1 h, the solution was concentrated and chromatographed on silica (4:1 toluene-ethyl acetate) to give **115** (503 mg, 99%) as a syrup. $[\alpha]_D -10.7^\circ$ (c 5.7, CHCl_3); R_f 0.21 (3:1 Hexane-EtOAc); $^1\text{H NMR}$ (600 MHz, CDCl_3): δ 8.02, 7.53, 7.41 (5H, ArH), 4.36 (t, 2H, $J_{1,2}$ 6.2, H-1), 3.98-4.04 (m, 4H, H-4, H-7), 3.79 (dd, 1H, $J_{8a,8b}$ 5.0, $J_{8a,8b}$ 11.7, H-8a), 3.69-3.75 (m, 2H, H-6, H-8b), 3.58 (dd, 1H, J 7.5, 8.6, H-5),

1.88-2.03 (m, 3H, H-2a, H-2b, H-3a), 1.65-1.73 (m, 1H, H-3b), 1.38, 1.35, 1.34, 1.32 (4xs, 12H, C(CH₃)₂); ¹³C NMR (150 MHz, CDCl₃): δ 136.6, 129.2, 123.0 (CH, ArC), 81.0 (CH, C-5), 80.7 (CH, C-4, C-7), 79.2 (CH, C-6), 64.2 (CH, C-1), 62.4 (CH, C-8), 29.3 (CH₂, C-3), 26.9, 26.6 (CH₃, C(CH₃)₂), 24.9 (CH₂, C-2). Anal. Calcd for C₂₁H₃₀O₇ (394.46): C, 63.94; H, 7.67; O, 28.39. Found: C, 64.00; H, 7.72. ES HRMS: m/z 417.188853 [M + Na]⁺ and 395.2 [M + H]⁺ (C₂₁H₃₀O₇ requires m/z 394.46).

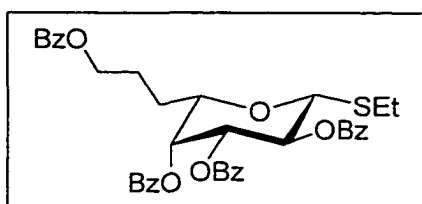
1,2,3,4,8-penta-O-benzoyl-6,7-di-deoxy- α/β -L-galacto-octo-pyranoside (117).



(CH₃)₂SO (0.31 mL, 4.33 mmol) was added to a cooled solution (-60°C) of oxalyl chloride (0.16 ml, 1.83 mmol) in dry CH₂Cl₂. After 10 min, alcohol **115** (706.6 mg, 1.79 mmol) was dissolved in dry CH₂Cl₂ (5 mL) and added to the reaction mixture. After stirring the reaction mixture for 15 min, triethylamine (1.17 mL, 8.42 mmol) was added and the reaction was stirred for 90 min. (Note that the R_f of the starting material is the same as that of the product aldehyde.) Water (10 mL) was added to quench the reaction. After stirring for 10 min at rt, the reaction mixture was diluted with CH₂Cl₂, washed with water, back extracted with CH₂Cl₂, washed with brine and dried over Na₂SO₄. Once concentrated, the residue was mixed with acetic acid (24 mL) and water (6 mL) and refluxed for 2 h. The mixture was co-evaporated with toluene and dried under vacuum. The residue and DMAP (20 mg) were then dissolved in pyridine (13 mL) and cooled to 0°C and benzoyl chloride (1.66 mL, 14.3 mmol) was added dropwise. The reaction mixture was allowed to warm to rt and was left to stir overnight. CH₂Cl₂ (10 mL) and water (5 mL) were added to the reaction mixture and stirred for 2 h. The reaction mixture was diluted with CH₂Cl₂, washed with water, NaHCO₃, and brine, and then dried with Na₂SO₄. Chromatography on silica (16:1 Toluene-EtOAc), gave a mixture of anomeric benzoates **117** as a syrup. β-anomer: ¹H NMR (600 MHz, CDCl₃): δ 7.22-

8.13 (m, ArH), 6.22 (d, 1H, $J_{1,2}$ 8.4, H-1), 6.08 (dd, 1H, $J_{2,3}$ 10.4, H-2), 5.91 (d, 1H, $J_{3,4}$ 3.7, H-4), 5.74 (dd, 1H, H-3), 4.27-4.37 (m, 2H, H-8a, H-8b), 4.21 (dd, 1H, $J_{5,6a/b}$ 4.4, 7.3, H-5), 1.80-2.02 (m, 4H, H-6a, H-6b, H-7a, H-7b); ^{13}C NMR (150 MHz, CDCl_3): δ 128.0-134.0 (CH, ArC), 96.2 (CH, $^1J_{\text{C,H}}$ 164.1, C-1), 74.3 (CH, C-5), 71.7 (CH, C-3), 69.6 (CH, C-4), 68.6 (CH, C-2), 63.9 (CH_2 , C-8), 26.7, 24.5 (CH_2 , C-6, C-7). ES HRMS: m/z 751.215341 $[\text{M} + \text{Na}]^+ \pm 0.2$ mDa and 730.1 $[\text{M} + \text{H}]^+$ ($\text{C}_{43}\text{H}_{36}\text{O}_{11}$ requires m/z 728.76). α -anomer: ^1H NMR (600 MHz, CDCl_3): δ 7.20-8.20 (m, ArH), 6.90 (d, 1H, $J_{1,2}$ 3.7, H-1), 6.09 (dd, 1H, $J_{2,3}$ 10.8, H-3), 5.99-6.02 (m, 2H, H-2, H-4), 4.51 (dd, 1H, $J_{5,6a/b}$ 5.7, 8.1, H-5), 4.24-4.32 (m, 2H, H-8a, H-8b), 1.75-1.98 (m, 4H, H-6a, H-6b, H-7a, H-7b); ^{13}C NMR (150 MHz, CDCl_3): δ 128.0-134.0 (CH, ArC), 90.5 (CH, $^1J_{\text{C,H}}$ 178.5, C-1), 71.1 (CH, C-5), 70.0, 67.4 (CH, C-2, C-4), 68.9 (CH, C-3), 64.1 (CH_2 , C-8), 26.6, 24.5 (CH_2 , C-6, C-7). ES HRMS: m/z 751.216283 $[\text{M} + \text{Na}]^+ \pm 0.8$ mDa ($\text{C}_{43}\text{H}_{36}\text{O}_{11}$ requires m/z 728.76).

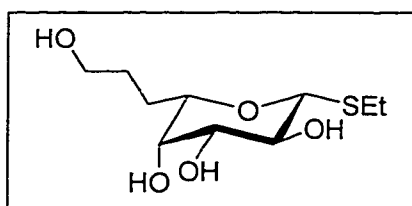
Ethyl 2,3,4,8-tetra-O-benzoyl-6,7-di-deoxy-1-thio- β -L-galacto-octopyranoside (119).



The anomeric benzoates **117** (1.8 g) dissolved in dry CH_2Cl_2 (10 mL) and HBr in acetic acid (10 mL) was stirred for 1-2 h. The reaction mixture was then concentrated and co-evaporated with toluene. Ethanethiol (0.53 mL, 7 mmol) was added dropwise to a suspension of NaH (158 mg, 6.5 mmol) in dry DMF (5 mL). After 15 min, the bromide dissolved in THF (5-10 mL) was added dropwise to the thiolate solution. After 20 min, the mixture was diluted in EtOAc, washed with water, the aqueous layer was back extracted, and the combined organic layers were washed with brine and dried with Na_2SO_4 . Chromatography on silica (18:1 Toluene-EtOAc) gave compound **119** (514 mg, 43% from compound **115**). $[\alpha]_{\text{D}} -120.2^\circ$ (c 9.1, CHCl_3); R_f 0.48 (8:1 toluene-ethyl acetate); ^1H NMR (500 MHz, CDCl_3): δ 7.10-8.10 (m, ArH), 5.74-5.86 (m, 2H, $J_{1,2}$ 9.9, H-2, H-4), 5.58 (dd, 1H, $J_{2,3}$ 10.0, $J_{3,4}$ 3.4, H-3), 4.78 (d, 1H, H-1), 4.24-4.40 (m, 2H, H-8), 3.95

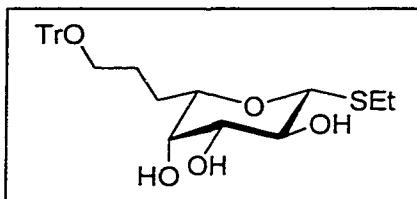
(dd, 1H, J 5.6, 6.5, H-5), 2.72-2.92 (m, 2H, SCH₂CH₃), 1.70-2.06 (m, 4H, H-6, H-7), 1.31 (t, 3H, J 7.5, SCH₂CH₃); ¹³C NMR (125 MHz, CDCl₃): δ 133.4, 133.2, 133.0, 130.0, 129.6, 128.6, 128.2 (CH, ArC), 83.7 (CH, ¹J_{C,H} 153.4, C-1), 77.2 (CH, C-5), 73.1 (CH, C-3), 70.1 (CH, C-4), 68.1 (CH, C-2), 64.1 (CH₂, C-8), 27.4, 24.8 (CH₂, C-6, C-7), 24.1 (CH₂, SCH₂CH₃), 14.7 (CH₃, SCH₂CH₃). ES HRMS: m/z 691.197961 [M + Na]⁺ ± 0.2 mDa and 670.4 [M + H]⁺ (C₃₈H₃₆O₉S₁ requires m/z 668.77).

Ethyl 6,7-di-deoxy-1-thio-β-L-galacto-octo-pyranoside (120).



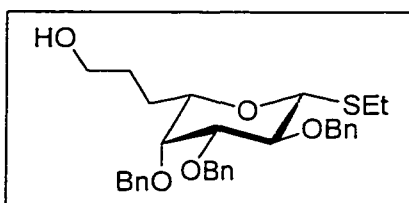
Thioglycoside **119** (750 mg, 1.12 mmol) was dissolved in dry methanol (20 mL). A catalytic amount of freshly prepared sodium methoxide was added and the reaction mixture was heated to 60°C. When deacylation was complete, the solution was neutralized with dry ice. Chromatography on silica (5:1 EtOAc-MeOH) gave compound **120** (268 mg, 95%). [α]_D +16.9° (c 1.6, CHCl₃); ¹H NMR (600 MHz, CD₃OD): δ 4.30 (d, 1H, J_{1,2} 9.5, H-1), 3.71 (dd, 1H, J_{3,4} 3.7, J_{4,5} 0.9, H-4), 3.55-3.60 (m, 2H, H-8), 3.50 (t, 1H, J 9.3, H-2), 3.42-3.47 (m, 2H, H-3, H-5), 2.63-2.78 (m, 2H, SCH₂CH₃), 1.73-1.83 (m, 1H, H-6a), 1.63-1.73 (m, 1H, H-7a), 1.55-1.63 (m, 2H, H-6b, H-7b), 1.28 (t, 3H, J 7.5, SCH₂CH₃); ¹³C NMR (150 MHz, CD₃OD): δ 87.1 (CH, ¹J_{C,H} 152.1, C-1), 79.8, 76.3 (CH, C-3, C-5), 72.0 (CH, C-4), 71.3 (CH, C-2), 62.6 (CH₂, C-8), 29.7 (CH₂, C-7), 28.1 (CH₂, C-6), 24.8 (CH₂, SCH₂CH₃), 15.3 (CH₃, SCH₂CH₃). Anal. Calcd for C₁₀H₂₀O₅S₁ (252.34): C, 47.60; H, 7.99. Found: C, 48.04; H, 7.83. ES HRMS: m/z 275.092209 [M + Na]⁺ ± 0.7 mDa and 253.1 [M + H]⁺ (C₁₀H₂₀O₅S₁ requires m/z 252.34).

Ethyl 6,7-di-deoxy-1-thio-8-O-trityl- β -L-galacto-octo-pyranoside (121).



Thioglycoside **120** (200 mg, 0.79 mmol) and trityl chloride (355 mg, 1.27 mmol) were dissolved in dry pyridine (8 mL) and stirred overnight. After dilution in CH_2Cl_2 , the mixture was washed with water, NaHCO_3 , and brine. Chromatography on silica (1:2 Hexane-EtOAc) gave compound **121** (304 mg, 78%). $[\alpha]_D^{25} +7.8^\circ$ (c 1.8, CHCl_3); R_f 0.19 (1:2 Hexane-EtOAc); ^1H NMR (600 MHz, CDCl_3): δ 7.39-7.43, 7.25-7.30, 7.19-7.23 (m, ArH), 4.15 (d, 1H, $J_{1,2}$ 9.5, H-1), 3.77 (broad, 1H, H-4), 3.58 (t, $J_{2,3}$ 8.8, H-2), 3.50 (broad, 1H, H-3), 3.30 (broad dd, 2H, $J_{5,6a/b}$ 4.9, 8.6, H-5, OH), 3.04-3.13 (m, 2H, H-8a, H-8b), 2.94 (s, OH), 2.60-2.70 (m, 2H, SCH_2CH_3), 2.54 (d, 1H, $J_{4,\text{OH}}$ 3.6, OH), 1.62-1.87 (m, 4H, H-6a, H-6b, H-7a, H-7b), 1.25 (t, 3H, J 7.5, SCH_2CH_3); ^{13}C NMR (150 MHz, CDCl_3): δ 128.5, 127.6, 126.7 (CH, ArC), 85.7 (CH, $^1J_{\text{C,H}}$ 153.9, C-1), 78.0 (CH, C-5), 74.8 (CH, C-3), 70.4 (CH, C-2), 70.3 (CH, C-4), 62.5 (CH_2 , C-8), 27.2, 25.5 (CH_2 , C-6, C-7), 24.4 (CH_2 , SCH_2CH_3), 14.9 (CH_3 , SCH_2CH_3). Anal. Calcd for $\text{C}_{29}\text{H}_{34}\text{O}_5\text{S}_1$ (494.65): C, 70.42; H, 6.93; S, 6.48. Found: C, 70.05; H, 7.07; S, 6.44. ES HRMS: m/z 517.202320 $[\text{M} + \text{Na}]^+ \pm 0.0$ mDa and 494.8 $[\text{M} + \text{H}]^+$ ($\text{C}_{29}\text{H}_{34}\text{O}_5\text{S}_1$ requires m/z 494.65).

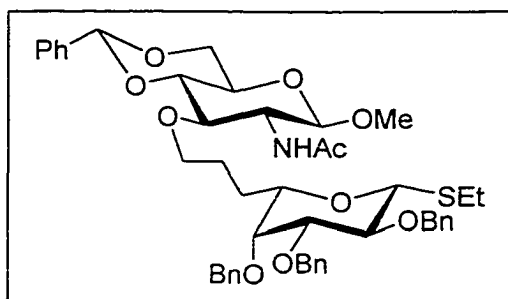
Ethyl 2,3,4-tri-O-benzyl-6,7-di-deoxy-1-thio- β -L-galacto-octo-pyranoside (123).



Thioglycoside **121** (304 mg, 0.62 mmol) was dissolved in DMF (10 mL) and the flask purged with argon. To the ice cooled solution, NaH (45 mg, 1.86 mmol) was added portionwise. After stirring for 45 min at rt, benzyl bromide (0.29 mL, 2.48 mmol) was added dropwise. The reaction mixture was quenched with EtOAc containing residual water, diluted with CH_2Cl_2 , brine, and dried over anhyd Na_2SO_4 . After evaporation, the crude syrup was dissolved in 9:1 MeOH-EtOAc (10 mL) solution with TsOH (10 mg). The mixture was heated to 35°C until the

removal of the trityl group was complete (tlc). The reaction mixture was neutralized with triethylamine and then concentrated. The residue was dissolved in CH_2Cl_2 , washed with water, NaHCO_3 , brine and dried with Na_2SO_4 . After evaporation, the chromatography (2:1 Hexane-EtOAc) of the residue on silica gave thioglycoside **123** (288 mg, 89%). $[\alpha]_D^{25} +4.3^\circ$ (c 1.4, CHCl_3); R_f 0.14 (2:1 Hexane-EtOAc); $^1\text{H NMR}$ (600 MHz, CDCl_3): δ 7.25-7.40 (m, 15H, ArH), 4.97, 4.87 (2d, 1H each, J_{gem} 11.9, 10.0, PhCH_2), 4.71-4.79 (m, 3H, PhCH_2), 4.66 (d, 1H, J_{gem} 11.7, PhCH_2), 4.38 (d, 1H, $J_{1,2}$ 9.7, H-1), 3.81 (t, 1H, $J_{2,3}$ 9.3, H-2), 3.66 (d, 1H, $J_{3,4}$ 2.2, H-4), 3.52-3.59 (m, 3H, H-3, H-8a, H-8b), 3.26 (dd, 1H, $J_{5,6a/b}$ 3.5, 9.0, H-5), 2.66-2.78 (m, 2H, SCH_2CH_3), 1.79-1.86 (m, 1H, H-6a), 1.52-1.62 (m, 1H, H-7a), 1.39-1.46 (m, 2H, H-6b, H-7b), 1.28 (t, 3H, J 7.3, SCH_2CH_3); $^{13}\text{C NMR}$ (150 MHz, CDCl_3): δ 127.0-129.0 (CH, ArC), 84.9 (CH, $^1J_{\text{C,H}}$ 156.1, C-1), 84.3 (CH, C-3), 78.3 (CH, C-5), 78.2 (CH, C-2), 75.4 (CH, C-4), 75.4, 74.2, 72.7 (CH_2 , PhCH_2), 62.4 (CH_2 , C-8), 28.9 (CH_2 , C-7), 27.6 (CH_2 , C-6), 24.4 (CH_2 , SCH_2CH_3), 14.6 (CH_3 , SCH_2CH_3). Anal. Calcd for $\text{C}_{31}\text{H}_{38}\text{O}_5\text{S}_1$ (522.70): C, 71.23; H, 7.33; S, 6.13. Found: C, 71.24; H, 7.47; S, 6.18. ES HRMS: m/z 545.233801 $[\text{M} + \text{Na}]^+ \pm 0.5$ mDa and 525.2 $[\text{M} + \text{H}]^+$ ($\text{C}_{31}\text{H}_{38}\text{O}_5\text{S}_1$ requires m/z 522.70).

Ethyl 2,3,4-tri-O-benzyl-6,7-di-deoxy-8-O-(methyl 2-acetamido-4,6-O-benzylidene-2-deoxy- β -D-glucopyranos-3-oxo)-1-thio- β -L-galacto-octopyranoside (124).

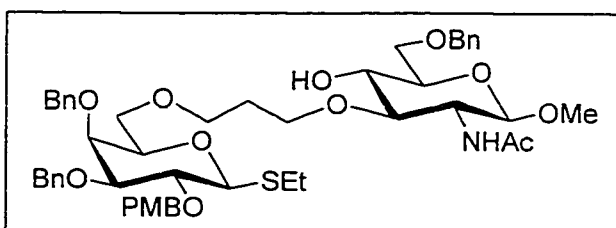


Sodium hydride (14.4 mg, 0.60 mmol) was added to a solution of 2-acetamido-2-deoxy-glucopyranoside **36** (195 mg, 0.60 mmol) in dry THF (2 mL). The mixture was stirred for 30 min at 60°C , followed by addition of the methanesulphonate **104** (240 mg, 0.4 mmol) in dry THF (3 mL). After the reaction mixture had been stirred at 60°C for 1 h, dry $(\text{CH}_3)_2\text{SO}$ (0.05 mL) was added and after an additional 7 h of heating, the reaction was complete. The cooled reaction

mixture was diluted with CH₂Cl₂, washed with NaHCO₃, brine and dried with Na₂SO₄. The concentrated residue was chromatographed on silica (60.1 CH₂Cl₂-MeOH) and gave **124** (331 mg, 78%) as a white solid. $[\alpha]_D -14.2^\circ$ (c 1.9, CHCl₃), ¹H NMR (600 MHz, CDCl₃): δ 7.20-7.45 (m, ArH), 5.57 (d, 1H, J 7.3, NHAc), 5.49 (s, 1H, PhCH), 4.93 (d, 1H, J_{gem} 11.7, PhCH₂), 4.90 (d, 1H, J_{1,2} 8.2, H-1'), 4.85 (d, 1H, J_{gem} 10.3, PhCH₂), 4.76 (d, 1H, PhCH₂), 4.72 (d, 1H, J_{gem} 12.1, PhCH₂), 4.68 (d, 1H, PhCH₂), 4.59 (d, 1H, PhCH₂), 4.25-4.34 (m, 2H, H-1, H-6'a), 4.10 (t, 1H, J 9.0, H-3'), 3.70-3.79 (m, 3H, H-6'b, H-8a, H-2), 3.59 (d, 1H, J_{3,4} H-4), 3.42-3.52 (m, 7H, OCH₃, H-8b, H-4', H-5', H-3), 3.18 (dd, 1H, J 5.1, 7.3, H-5), 3.09 (quartet, 1H, J 8.2, H-2'), 2.61-2.74 (m, 2H, SCH₂CH₃), 1.92 (s, 3H, NHCOCH₃), 1.74-1.82, 1.50-1.60, 1.34-1.43, 1.22-1.34 (4xm, 7H, H-6a, H-6b, H-7a, H-7b, SCH₂CH₃); ¹³C NMR (150 MHz, CDCl₃): δ 125.0-129.0 (CH, ArC), 101.0 (CH, PhCH), 100.9 (CH, ¹J_{C,H} 161.4, C-1'), 84.7 (CH, C-1), 84.3, 82.2, 65.7 (CH, C-4', C-5', C-3), 78.2 (CH, C-2, C-5), 76.6 (CH, C-3'), 75.1, 74.0, 72.6 (CH₂, PhCH₂), 75.0 (CH, C-4), 72.0 (CH₂, C-8), 68.3 (CH₂, C-6'), 58.0 (CH, C-2'), 56.8 (CH₃, OCH₃), 26.7, 25.6 (CH₂, C-6, C-7), 23.8 (CH₂, SCH₂CH₃), 22.9 (CH₃, NHCOCH₃), 6.0 (CH₃, SCH₂CH₃). ES HRMS: m/z 850.360736 [M + Na]⁺ ± 0.6 mDa and 829.0 [M + H]⁺ (C₄₇H₅₇NO₁₀S requires m/z 828.03).

8.8: Investigation of the Intramolecular Glycosylation

Ethyl 3,4-di-O-benzyl-2-O-p-methoxybenzyl-6-O-(2'-O-(methyl 2-acetamido-6-O-benzyl-2-deoxy-β-D-glucopyranos-3-oxy)propyl)-1-thio-β-D-galactopyranoside (131).



Thioglycoside **139** (105 mg, 0.13 mmol) was dissolved in DMF (2 mL) and the flask was purged with argon. To the ice cooled solution, NaH (3.1 mg, 0.13 mmol) was

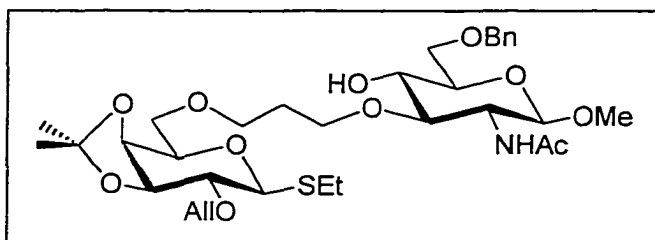
added portionwise. After stirring for 45 min at 0°C, benzyl bromide (15 μL,

0.13 mmol) was added dropwise and the reaction mixture was kept at 0°C overnight. The reaction was quenched and worked up in the usual way. The crude material was chromatographed on silica (60:1 CH₂Cl₂-MeOH) to give **131** (35 mg, 27%), its regioisomer **140** (58 mg, 44%), and fully benzylated product **141** (21 mg, 16%). Target component **131** gave: $[\alpha]_D +1.9^\circ$ (*c* 1.6, CHCl₃); ¹H NMR (500 MHz, CDCl₃): δ 7.20-7.39, 6.81 (19H, ArH), 5.63 (d, 1H, J_{2',NH} 7.7, NHAc), 4.94, 4.79 (2d, 1H each, J_{gem} 11.7, 9.9, PhCH₂), 4.68-4.74 (m, 3H, H-1', PhCH₂), 4.53-4.61 (m, 3H, PhCH₂), 4.38 (d, 1H, J_{1,2} 9.6, H-1), 3.85 (d, 1H, J_{3,4} 2.7, H-4), 3.66-3.80 (m, 9H, CH₃O, 2xH_{link-1}, H-2, H-3', 2xH-6a/H-6'a), 3.41-3.55 (m, 11H, 2xH-6'/H-6, H-4', H-5', H-5, H-3, OCH₃, 2xH_{link-3}), 3.23 (dd, 1H, J_{1',2'} 8.1, H-2'), 2.66-2.78 (m, 2H, SCH₂CH₃), 1.95 (s, 3H, CH₃CONH), 1.62-1.82 (m, H_{link-2}, HOD), 1.28 (t, 3 H, J 7.4, SCH₂CH₃); ¹³C NMR (125 MHz, CDCl₃): δ 126.0-130.0, 113.8 (CH, ArC), 100.6 (CH, ¹J_{C,H} 162.3, C-1'), 85.2 (CH, ¹J_{C,H} 151.6, C-1), 83.9 (CH, C-3), 81.1 (CH, C-2), 77.9 (CH, C-3'), 77.1, 74.1, 72.0 (CH, C-4', C-5', C-5), 75.2, 74.1, 73.3, 72.6 (CH₂, PhCH₂), 73.6 (CH, C-4), 70.2, 69.7 (CH₂, C-6/C-6'), 69.1 (CH₂, C_{link-1}), 68.5 (CH₂, C_{link-3}), 56.7 (CH, C-2'), 56.4 (CH₃, OCH₃), 54.8 (CH₃, OCH₃), 29.6 (CH₂, C_{link-2}), 24.6 (CH₂, SCH₂CH₃), 23.6 (CH₃, NHCOCH₃), 14.8 (CH₃, SCH₂CH₃). ES HRMS: *m/z* 912.396480 [M + Na]⁺ ± 0.4 mDa and 890.5 [M + H]⁺ (C₄₉H₆₃O₁₂NS requires *m/z* 890.10).

Regioisomer **140** gave: $[\alpha]_D +5.0^\circ$ (*c* 1.6, CHCl₃); ¹H NMR (500 MHz, CDCl₃): δ 7.20-7.40, 6.81 (19H, ArH), 5.70 (d, 1H, J_{2',NH} 8.0, NHAc), 4.93 (d, 1H, J_{gem} 11.6, PhCH₂), 4.68-4.80 (m, 6H, H-1', PhCH₂), 4.56-4.62 (m, 2H, J_{gem} 11.9, 11.3, PhCH₂), 4.35 (d, 1H, J_{1,2} 9.6, H-1), 3.75-3.87 (m, 8H, CH₃O, H_{link-1}, H-4, H-2, H-3', H-6'/H-6), 3.60-3.72 (m, 2H, H_{link-1}, H-6'/H-6), 3.28-3.52 (m, 12H, 2xH-6'/H-6, H-5, H-5', H-4', H-2', H-3, OCH₃, 2xH_{link-3}), 2.63-2.78 (m, 2H, SCH₂CH₃), 1.94 (s, 3H, CH₃CONH), 1.56-1.78 (m, H_{link-2}, HOD), 1.27 (t, 3 H, J 7.5, SCH₂CH₃); ¹³C NMR (125 MHz, CDCl₃): δ 127.0-130.0, 113.6 (CH, ArC), 100.8 (CH, ¹J_{C,H} 160.5, C-1'), 85.2 (CH, ¹J_{C,H} 151.0, C-1), 83.9 (CH, C-3), 80.6 (CH, C-3'), 78.0 (CH, C-2), 78.0, 77.2, 74.9 (CH, C-4', C-5', C-5), 75.2, 74.1, 74.3, 72.6 (CH₂, PhCH₂), 73.7 (CH, C-4), 69.4, 69.1, 67.8 (CH₂,

C-6, C-6', C_{link}-3), 61.7 (CH₂, C_{link}-1), 56.9 (CH, C-2'), 56.7 (CH₃, OCH₃), 55.0 (CH₃, OCH₃), 30.1 (CH₂, C_{link}-2), 24.5 (CH₂, SCH₂CH₃), 23.3 (CH₃, NHCOCH₃), 14.8 (CH₃, SCH₂CH₃). ES MS: 891.3 [M + H]⁺ (C₄₉H₆₃O₁₂NS requires m/z 890.10).

Ethyl 2-O-allyl-3,4-O-isopropylidene-6-O-(3'-O-(methyl 2-acetamido-6-O-benzyl-2-deoxy-β-D-glucopyranos-3-oxy)propyl)-1-thio-β-D-galactopyranoside (132).

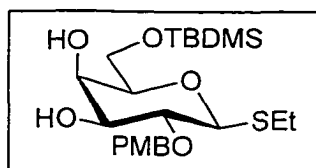


Dry THF (8 mL) was added to a mixture of compound **145** (387 mg, 0.58 mmol), sodium cyanoborohydride (220 mg, 3.47 mmol), dry powdered 3 Å

molecular sieves and methyl orange (3 mg). The suspension was purged with argon and a freshly prepared saturated solution of HCl in dry ether was added dropwise to the reaction mixture until the evolution of gases ceased and the indicator turned bright pink. A further two fold volume of saturated HCl in ether was added and the reaction was left to stir for 30 min. The reaction mixture was diluted with CH₂Cl₂, filtered through celite, washed with NaHCO₃, brine and dried over Na₂SO₄. Column chromatography of the crude material on silica (60:1 CH₂Cl₂-MeOH) gave a white solid **132** (256 mg, 66%). [α]_D -9.5° (c 7.9, CHCl₃); ¹H NMR (600 MHz, CDCl₃): δ 7.24-7.38 (m, ArH), 5.92 (ddt, 1H, HC=), 5.28 (ddd, 1H, HC=), 5.17 (ddd, 1H, HC=), 4.72 (d, 1H, J_{1',2'} 8.3, H-1'), 4.60 (d, 1H, J_{gem} 12.1, PhCH₂), 4.56 (d, 1H, PhCH₂), 4.33 (d, 1H, J_{1,2} 9.5, H-1), 4.26, 4.20 (2ddt, 2H, H₂C=CHCH₂), 4.08-4.12 (m, 2H, H-3, H-4), 3.81 (ddd, 1H, J_{4,5} 1.6, J_{5,6a&6b} 6.6, H-5), 3.46 (s, 3H, OCH₃), 3.46-3.80 (m, 11H, H-6a, H-6b, H-6'a, H-6'b, H-4', H-5', H-3', H_{link}-1, H_{link}-3), 3.35 (dd, 1H, J_{2,3} 6.0, H-2), 3.28 (quartet, 1H, J 9.7, H-2'), 2.64-2.76 (m, 2H, SCH₂CH₃), 1.68-1.86 (m, 2H, H_{link}-2), 1.47, 1.39 (2s, 3H each, (CH₃)₂C), 1.27 (t, 3H, SCH₂CH₃); ¹³C NMR (150 MHz, CDCl₃): δ 134.2 (CH, =CH), 128.6, 127.7, 126.3 (CH, ArC), 117.6 (CH₂, =CH₂), 100.8 (CH, ¹J_{C,H} 160.8, C-1'), 83.6 (CH,

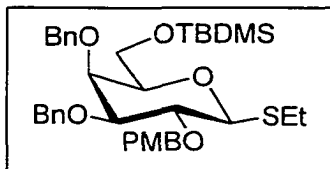
C-1), 81.2 (CH, C-3'), 79.2, 73.7 (CH, C-3, C-4), 78.5 (CH, C-2), 75.3 (CH, C-5), 74.2, 72.0 (CH, C-4', C-5'), 73.4 (CH₂, PhCH₂), 72.3 (CH₂, H₂C=CHCH₂), 70.1, 70.0, 68.8, 68.6 (CH₂, C-6, C-6', C_{link}-1, C_{link}-3), 56.8 (CH₃, OCH₃), 56.7 (CH, H-2'), 29.4 (CH₂, C_{link}-2), 27.5, 26.1 (CH₃, C(CH₃)₂), 24.5 (CH₂, SCH₂CH₃), 14.8 (CH₃, SCH₂CH₃). ES HRMS: m/z 692.306900 [M + Na]⁺ ± 1.2 mDa and 670.2 [M + H]⁺ (C₃₃H₅₁NO₁₁S requires m/z 669.83).

Ethyl 6-O-*t*-butyldimethylsilyl-2-O-*p*-methoxybenzyl-1-thio-β-D-galactopyranoside (133).



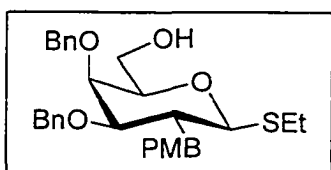
Thioglycoside **35** (2.0 g, 5.2 mmol) was dissolved in dry methanol (22 mL) with tetrafluoroboric acid (200 μL) and stirred overnight at 0°C. After neutralization with triethylamine and removal of solvent, the crude material was diluted in CH₂Cl₂, washed with water, NaHCO₃, and brine. Once concentrated, the residue (860 mg, ~2.5 mmol), *t*-butyldimethylsilyl chloride (395 mg, 2.63 mmol) and imidazole (179 mg, 2.63 mmol) were dissolved in dry DMF (25 mL) and stirred overnight. After dilution in CH₂Cl₂, the mixture was washed with water, NaHCO₃, and brine. Chromatography on silica (4:1 Hexane-EtOAc) gave compound **133** (1.05 g, 44%). ¹H NMR (500 MHz, CDCl₃): δ 7.32, 6.87 (2d, 4H, J 8.6, ArH), 4.87 (d, 1H, J 10.7, PhCH₂), 4.62 (d, 1H, PhCH₂), 4.38 (d, 1H, J_{1,2} 9.5, H-1), 4.04 (m, 1H, H-4), 3.87 (dd, 1H, J_{5,6a} 6.0, J_{6a,6b} 10.4, H-6a), 3.82 (dd, 1H, J_{5,6b} 5.0, H-6b), 3.78 (s, 3H, CH₃O), 3.55-3.59 (m, 1H, H-3), 3.50 (t, 1H, J_{2,3} 9.0, H-2), 3.44 (dt, 1H, J_{4,5} 0.9, H-5), 2.72 (OH), 2.65-2.85 (m, 2 H, SCH₂CH₃), 2.39 (d, 1H, J 5.4, OH), 1.30 (t, 3 H, J 7.5, SCH₂CH₃), 0.87 (s, 9H, (CH₃)₃C), 0.06 (s, 6H, (CH₃)₂Si); ¹³C NMR (125 MHz, CDCl₃): δ 130.1 (C, ArC), 130.0, 114.1 (CH, ArC), 85.2 (CH, C-1), 78.2, 77.8, 74.7, 69.8 (CH, C-2, C-3, C-4, C-5), 74.9 (CH₂, PhCH₂), 63.0 (CH₂, C-6), 55.3 (CH₃, OCH₃), 25.08 (CH₃, C(CH₃)₃), 25.06 (CH₂, SCH₂CH₃), 15.0 (CH₃, SCH₂CH₃), -5.1 (CH₃, (CH₃)₂Si).

Ethyl 3,4-di-O-benzyl-6-O-t-butyldimethylsilyl-2-O-p-methoxybenzyl-1-thio-β-D-galactopyranoside (134).



Thioglycoside **133** (1.17 g, 2.55 mmol) was dissolved in DMF (20 mL) and purged with argon. To the ice cooled solution, NaH (245 mg, 10.2 mmol) was added portionwise and after stirring for 45 min at rt, benzyl bromide (1.8 mL, 15.3 mmol) was added dropwise. Once the reaction was complete, it was quenched with EtOAc containing residual water, the mixture was diluted with CH₂Cl₂, washed with NaHCO₃, brine, and dried over anhyd Na₂SO₄. The crude reaction material was chromatographed on silica (12:1 Hexane-EtOAc) to give **134** (1.06 g, 65%). [α]_D -11.6° (c 4.5, CHCl₃); ¹H NMR (600 MHz, CDCl₃): δ 7.25-7.40, 6.83 (14H, J 8.6, ArH), 4.96 (d, 1H, J 11.6, PhCH₂), 4.70-4.81 (m, 4H, PhCH₂), 4.63 (d, 1H, J 11.5, PhCH₂), 4.39 (d, 1H, J_{1,2} 9.8, H-1), 3.91 (d, 1H, J 1.7, H-4), 3.81 (t, 1H, J_{2,3} 9.5, H-2), 3.78 (s, 3H, CH₃O), 3.65-3.72 (m, 2H, H-6), 3.54 (dd, 1H, J_{3,4} 2.7, H-3), 3.38 (t, 1H, J 6.2, H-5), 2.64-2.80 (m, 2 H, SCH₂CH₃), 1.28 (t, 3 H, J 7.4, SCH₂CH₃), 0.86 (s, 9H, (CH₃)₃C), 0.02 (s, 6H, (CH₃)₂Si); ¹³C NMR (150 MHz, CDCl₃): δ 126.5-130.0, 113.6 (CH, ArC), 85.0 (CH, ¹J_{C,H} 157.4, C-1), 83.9 (CH, C-3), 78.7 (CH, C-5), 78.1 (CH, C-2), 75.2, 74.4, 72.6 (CH₂, PhCH₂), 73.5 (CH, C-4), 61.5 (CH₂, C-6), 55.3 (CH₃, OCH₃), 25.6 (CH₃, C(CH₃)₃), 24.3 (CH₂, SCH₂CH₃), 15.2 (CH₃, SCH₂CH₃), -5.5 (CH₃, (CH₃)₂Si). ES HRMS: m/z 661.299514 [M + Na]⁺ ± 0.0 mDa (C₃₆H₅₀O₆SSi requires m/z 638.94).

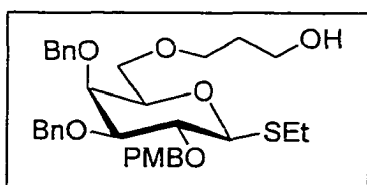
Ethyl 3,4-di-O-benzyl-2-O-p-methoxybenzyl-1-thio-β-D-galactopyranoside (135).



Compound **134** (1.04 mg, 1.63 mmol) was stirred for 1 h with a solution of TBAF in THF (1 M, 16 mL). The mixture was evaporated, diluted with CH₂Cl₂, washed with brine, dried over anhyd Na₂SO₄ and concentrated. The crude syrup was chromatographed on silica (5:4 Hexane-EtOAc) to give **135** (694 mg, 81%) as an oil. [α]_D -30.0° (c 0.2, CHCl₃); ¹H

NMR (600 MHz, CDCl₃): δ 7.25-7.40, 6.83 (14H, J 8.5, ArH), 4.96 (d, 1H, J 11.7, PhCH₂), 4.72-4.81 (m, 4H, PhCH₂), 4.65 (d, 1H, J 11.8, PhCH₂), 4.41 (d, 1H, J_{1,2} 9.7, H-1), 3.74-3.85 (m, 6H, H-2, H-4, H-6, OCH₃), 3.55 (dd, 1H, J_{2,3} 9.3, J_{3,4} 2.9, H-3), 3.45-3.50 (m, 1H, H-6a), 3.39 (dt, 1H, J 6.6, 0.9, H-5), 2.67-2.80 (m, 2 H, SCH₂CH₃), 1.30 (t, 3 H, J 7.3, SCH₂CH₃); ¹³C NMR (150 MHz, CDCl₃): δ 127.0-130.0, 113.7 (CH, ArC), 85.2 (CH, ¹J_{C,H} 154.2, C-1), 84.0 (CH, C-3), 78.4 (CH, C-5), 77.9 (CH, C-2), 75.2, 74.0, 72.9 (CH₂, PhCH₂), 73.0 (CH, C-4), 61.2 (CH₂, C-6), 55.1 (CH₃, OCH₃), 24.7 (CH₂, SCH₂CH₃), 15.0 (CH₃, SCH₂CH₃). ES HRMS: m/z 547.213521 [M + Na]⁺ \pm 0.5 mDa and 525.3 [M + H]⁺ (C₃₀H₃₆O₆S requires m/z 524.67).

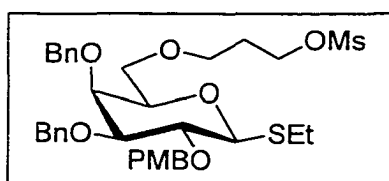
Ethyl 3,4-di-O-benzyl-6-O-(3'-hydroxypropyl)-2-O-p-methoxybenzyl-1-thio- β -D-galactopyranoside (136).



NaH (38 mg, 1.59 mmol) was added to a solution of alcohol **135** (694 mg, 1.33 mmol) in dry THF (6 mL). After stirring for 30 min at 60°C, a solution of 1-O-t-butyltrimethylsilyloxy-3-O-methanesulphonyloxypropane (470 mg, 1.73 mmol) in dry THF (1 mL) was added dropwise. The reaction mixture was stirred at 60°C for 3 h, when the tlc indicated complete reaction of the alcohol, the reaction was quenched with EtOAc containing residual water, the mixture was diluted with CH₂Cl₂, washed with water, NaHCO₃, brine and then dried over anhyd Na₂SO₄. After concentration, the residue was stirred for 30 min with a solution of TBAF in THF (1 M, 5 mL). The reaction mixture was evaporated, diluted with CH₂Cl₂, washed with brine, dried over anhyd Na₂SO₄ and concentrated. The crude syrup was chromatographed on silica (1:1 Hexane-EtOAc) to give **136** (544 mg, 94%). $[\alpha]_D -5.0^\circ$ (c 3.0, CHCl₃); ¹H NMR (500 MHz, CDCl₃): δ 7.25-7.40, 6.81 (14H, J 8.6, ArH), 4.96 (d, 1H, J 11.7, PhCH₂), 4.79 (d, 1H, J 9.7, PhCH₂), 4.69-4.77 (m, 3H, PhCH₂), 4.61 (d, 1H, J 11.7, PhCH₂), 4.39 (d, 1H, J_{1,2} 9.8, H-1), 3.84 (d, 1H, J 2.6, H-4), 3.76-3.82 (m, 4H, H-2, CH₃O), 3.70 (quartet, 2H, J 5.5, H_{link}-1), 3.43-3.58 (m, 6H, H-3, H-5, H-6a, H-6b, H_{link}-3), 2.65-2.79 (m, 2 H,

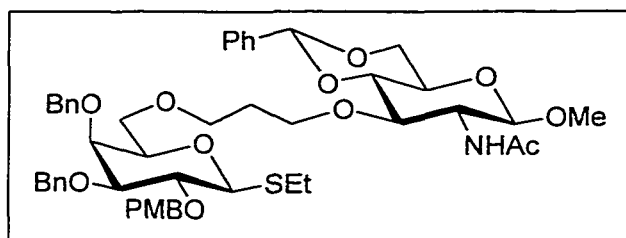
SCH₂CH₃), 1.75 (quintet, 2H, J 5.6, H_{link-2}), 1.28 (t, 3 H, J 7.5, SCH₂CH₃); ¹³C NMR (150 MHz, CDCl₃): δ 127.0-130.0, 113.4 (CH, ArC), 85.0 (CH, ¹J_{C,H} 154.1, C-1), 83.9 (CH, C-3), 77.7 (CH, C-2), 76.9 (CH, C-5), 75.0, 74.1, 72.6 (CH₂, PhCH₂), 73.5 (CH, C-4), 69.6 (CH₂, C-6), 69.7, 61.4 (CH₂, C_{link-1}, C_{link-2}), 55.2 (CH₃, OCH₃), 25.6 (CH₃, C(CH₃)₃), 24.3 (CH₂, SCH₂CH₃), 15.2 (CH₃, SCH₂CH₃), -5.5 (CH₃, (CH₃)₂Si). ES HRMS: m/z 605.254097 [M + Na]⁺ ± 0.8 mDa and 583.5 [M + H]⁺ (C₃₃H₄₂O₇S requires m/z 582.75).

Ethyl 3,4-di-O-benzyl-6-O-(3'-O-methanesulfonyloxypropyl)-2-O-p-methoxybenzyl-1-thio-β-D-galactopyranoside (137).



Triethylamine (0.19 mL, 1.4 mmol) was added to a solution of alcohol **136** (544 mg, 0.93 mmol) in dry CH₂Cl₂ (15 mL) and methanesulfonyl chloride (0.125 mL, 1.4 mmol) in CH₂Cl₂ (1 mL) was added dropwise. After stirring for 1 h at rt, the solution was diluted with CH₂Cl₂, washed with water, 1 M NaOH, water, brine, and dried over anhyd Na₂SO₄. Chromatography on silica (3:1 Hexane-EtOAc) gave **137** (557 mg, 90%). [α]_D +5.2° (c 21.2, CHCl₃); ¹H NMR (500 MHz, CDCl₃): δ 7.25-7.39, 6.82 (14H, J 8.6, ArH), 4.97 (d, 1H, J 11.7, PhCH₂), 4.69-4.81 (m, 3H, PhCH₂), 4.61 (d, 1H, J 11.7, PhCH₂), 4.39 (d, 1H, J_{1,2} 9.7, H-1), 4.22-4.28 (m, 2H, H_{link-1}), 3.86 (d, 1H, J 2.8, H-4), 3.76-3.81 (m, 4H, H-2, CH₃O), 3.55 (dd, 1H, J_{2,3} 9.2, J_{3,4} 2.8, H-3), 3.37-3.53 (m, 5H, H-5, H-6a, H-6b, 2xH_{link-3}), 2.94 (s, 3H, SO₂CH₃), 2.64-2.98 (m, 2 H, SCH₂CH₃), 1.86-1.95 (m, 2H, H_{link-2}), 1.29 (t, 3 H, J 7.5, SCH₂CH₃); ¹³C NMR (150 MHz, CDCl₃): δ 126.0-130.0, 113.6 (CH, ArC), 85.0 (CH, ¹J_{C,H} 153.4, C-1), 83.8 (CH, C-3), 77.9 (CH, C-2), 76.7 (CH, C-5), 75.0, 73.9, 72.6 (CH₂, PhCH₂), 73.3 (CH, C-4), 69.4 (CH₂, C-6), 66.6 (CH₂, C_{link-1}), 66.2 (CH₂, C_{link-3}), 55.2 (CH₃, OCH₃), 36.9 (CH₃, SO₂CH₃), 29.3 (CH₂, C_{link-2}), 24.3 (CH₂, SCH₂CH₃), 15.2 (CH₃, SCH₂CH₃), -5.5 (CH₃, (CH₃)₂Si). ES HRMS: m/z 683.233505 [M + Na]⁺ ± 1.1 mDa (C₃₄H₄₄O₉S₂ requires m/z 660.84).

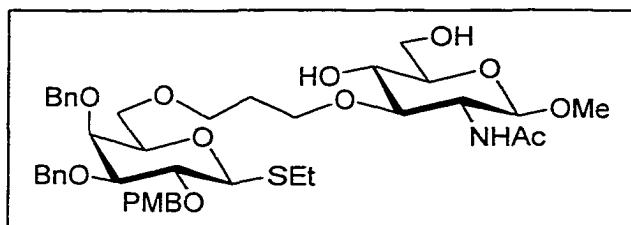
Ethyl 3,4-di-O-benzyl-2-O-p-methoxybenzyl-6-O-(3'-O-(methyl 2-acetamido-4,6-O-benzylidene-2-deoxy- β -D-glucopyranos-3-oxo)propyl)-1-thio- β -D-galactopyranoside (138).



Sodium hydride (27 mg, 1.13 mmol) was added to a solution of glucopyranoside **36** (380 mg, 1.18 mmol) in dry THF (4 mL). The mixture was stirred for 30 min at

60°C and the methanesulphonate **137** (557 mg, 0.84 mmol) in dry THF (4 mL) was added followed 5 min later by (CH₃)₂SO (0.5 mL). After heating overnight, the cooled reaction mixture was diluted with CH₂Cl₂, washed with NaHCO₃, brine and dried with Na₂SO₄. The concentrated residue was chromatographed on silica (50:1 CH₂Cl₂-MeOH) to give **138** (573 mg, 77%). [α]_D -6.4° (c 14.1, CHCl₃); ¹H NMR (500 MHz, CDCl₃): δ 7.20-7.46, 6.82 (19H, ArH), 5.73 (d, 1H, J_{2',NH} 7.6, NHAc), 5.49 (s, 1H, PhCH), 4.93 (d, 1H, J 11.6, PhCH₂), 4.82 (d, 1H, J_{1,2} 8.2, H-1'), 4.68-4.84 (m, 4H, PhCH₂), 4.56 (d, 1H, J 11.7, PhCH₂), 4.36 (d, 1H, J_{1,2} 9.6, H-1), 4.32 (dd, 1H, J 4.7, 10.4, H-6'a), 4.01 (t, 1H, J_{2,3} 9.3, H-3'), 3.88 (m, 1H, H_{link-1}), 3.82 (d, 1H, J_{3,4} 2.4, H-4), 3.72-3.80 (m, 5H, H-2, H-6', OCH₃), 3.57-3.64 (m, 1H, H_{link-1}), 3.40-3.55 (m, 10H, H-4', H-5', H-3, H-6a, H-6b, OCH₃, H_{link-3}), 3.25-3.35 (m, 2H, H-2', H_{link-3}), 2.62-2.78 (m, 2H, SCH₂CH₃), 1.93 (s, 3H, CH₃CONH), 1.60-1.76 (m, H_{link-2}, HOD), 1.27 (t, 3H, J 7.5, SCH₂CH₃); ¹³C NMR (150 MHz, CDCl₃): δ 125.0-130.0, 113.5 (CH, ArC), 101.0 (CH, PhCH), 101.5 (CH, ¹J_{C,H} 161.3, C-1'), 85.3 (CH, ¹J_{C,H} 152.5, C-1), 84.0, 82.3 (CH, C-3, C-4'), 78.0 (CH, C-2), 77.3 (CH, C-3', C-5'), 75.2, 74.1, 72.4 (CH₂, PhCH₂), 73.8 (CH, C-4), 69.6 (CH₂, C-6), 68.9 (CH₂, C_{link-1}), 68.6 (CH₂, C-6'), 67.8 (CH₂, C_{link-3}), 65.6 (CH, C-5), 57.3 (CH, C-2'), 56.8 (CH₃, OCH₃), 55.1 (CH₃, OCH₃), 30.0 (CH₂, C_{link-2}), 24.7 (CH₂, SCH₂CH₃), 23.4 (CH₃, NHCOCH₃), 14.9 (CH₃, SCH₂CH₃). ES HRMS: m/z 910.378750 [M + Na]⁺ ± 2.5 mDa and 888.4 [M + H]⁺ (C₄₉H₆₁O₁₂NS requires m/z 888.08).

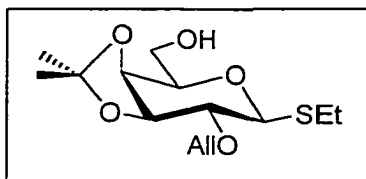
Ethyl 3,4-di-O-benzyl-2-O-p-methoxybenzyl-6-O-(3'-O-(methyl 2-acetamido-2-deoxy- β -D-glucopyranos-3-oxo)propyl)-1-thio- β -D-galactopyranoside (139).



Thioglycoside **138** (547 mg, 0.62 mmol) was dissolved in a mixture of dry methanol (10 mL) and dry CH_2Cl_2 (10 mL) containing tetrafluoroboric acid (60 μL) and

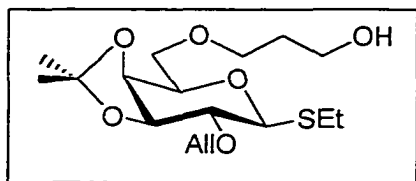
stirred overnight at 0°C . Since the reaction had not gone to completion, additional tetrafluoroboric acid (60 μL) was added. After another 24 h, a third addition followed. Neutralization with triethylamine on the fourth day and removal of solvent gave the crude product that was diluted in CH_2Cl_2 , washed with water, 0.5 M HCl, 0.5 M NaOH, and brine. After concentration and chromatography on silica (60:1 \rightarrow 20:1 CH_2Cl_2 -MeOH), compound **139** was obtained (390 mg, 79%). $[\alpha]_D^{25} +7.4^\circ$ (c 4.7, CHCl_3); ^1H NMR (500 MHz, CDCl_3): δ 7.20-7.40, 6.81 (14H, ArH), 5.85 (d, 1H, $J_{2',\text{NH}}$ 7.5, NHAc), 4.95 (d, 1H, J_{gem} 11.6, PhCH_2), 4.66-4.82 (m, 5H, H-1', PhCH_2), 4.59 (d, 1H, J_{gem} 11.8, PhCH_2), 4.38 (d, 1H, $J_{1,2}$ 9.6, H-1), 3.82-3.88 (m, 2H, H-6'a, H-4), 3.64-3.82 (m, 8H, OCH_3 , H-3', H-6'b, H-2, $\text{H}_{\text{link-1}}$), 3.51-3.58 (m, 2H, H-3, $\text{H}_{\text{link-3}}$), 3.40-3.51 (m, 6H, OCH_3 , H-4', H-5, $\text{H}_{\text{link-3}}$), 3.34-3.39 (m, 1H, H-5'), 3.29 (dd, 1H, $J_{1',2'}$ 8.4, H-2'), 2.63-2.80 (m, 2 H, SCH_2CH_3), 1.98 (s, 3H, CH_3CONH), 1.62-1.84 (m, $\text{H}_{\text{link-2}}$, HOD), 1.28 (t, 3 H, J 7.3, SCH_2CH_3); ^{13}C NMR (125 MHz, CDCl_3): δ 126.0-130.0, 113.5 (CH, ArC), 101.2 (CH, $^1J_{\text{C,H}}$ 159.3, C-1'), 85.1 (CH, $^1J_{\text{C,H}}$ 152.2, C-1), 83.9 (CH, C-3), 78.0 (CH, C-2), 81.3, 77.8 (CH, C-3', C-2), 77.1, 70.9 (CH, C-4', C-5), 75.3, 74.1, 72.7 (CH_2 , PhCH_2), 74.8 (CH, C-5'), 73.6 (CH, C-4), 69.7, 68.4 (CH_2 , C-6, $\text{C}_{\text{link-3}}$), 69.0 (CH_2 , $\text{C}_{\text{link-1}}$), 62.5 (CH_2 , C-6'), 56.7 (CH_3 , OCH_3), 56.5 (CH, C-2'), 55.1 (CH_3 , OCH_3), 29.1 (CH_2 , $\text{C}_{\text{link-2}}$), 24.5 (CH_2 , SCH_2CH_3), 23.2 (CH_3 , NHCOCH_3), 14.9 (CH_3 , SCH_2CH_3). ES HRMS: m/z 822.350286 $[\text{M} + \text{Na}]^+ \pm 0.4$ mDa and 800.4 $[\text{M} + \text{H}]^+$ ($\text{C}_{42}\text{H}_{57}\text{O}_{12}\text{NS}$ requires m/z 799.97).

Ethyl 2-O-allyl-3,4-O-isopropylidene-1-thio- β -D-galactopyranoside (142).



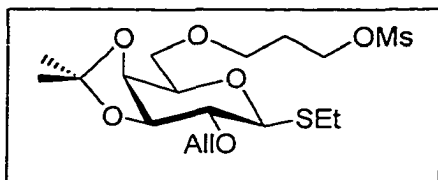
Toluenesulfonic acid (20 mg) was added to a mixture of thioglycoside **42**²⁰⁰ (0.886 g, 3.95 mmol) and 2,2-dimethoxypropane (20 mL) and stirred overnight. The reaction mixture was neutralized with triethylamine, concentrated and co-evaporated toluene (2x). The crude material was diluted with CH₂Cl₂, washed with brine, dried with anhyd Na₂SO₄ and concentrated. After the syrup has been dried on the pump for 2 h, it was dissolved in THF (15 mL) and purged with argon. NaH (0.096 g, 4 mmol) was added portionwise and after stirring for 30 min, allyl bromide (0.35 mL, 4 mmol) was added dropwise. After stirring 18h, another 1 eq of NaH and allyl bromide are added to the reaction mixture. The reaction was quenched with MeOH (2 mL), the mixture was diluted with CH₂Cl₂, washed with NaHCO₃, water, and then stirred with 0.3 M HCl until the mixed acetal has been completely hydrolyzed (tlc). The organic layer was washed with water, NaHCO₃, brine and dried with anhyd Na₂SO₄. The crude syrup was chromatographed on silica (3:1 hexane-EtOAc) to give **142** as a white solid (0.857 g, 71%). $[\alpha]_D -4.4^\circ$ (c 11.4, CHCl₃); R_f 0.34 (1:1 hexane-EtOAc); ¹H NMR (300 MHz, CDCl₃): δ 5.92 (ddt, 1 H, HC=), 5.28 (dd, 1 H, ³J_E 17.2, ²J 1.4, HC=), 5.17 (dd, 1 H, ³J_Z 10.3, HC=), 4.36 (d, 1 H, J_{1,2} 9.6, H-1), 4.1-4.3 (m, 4 H, H-3, H-4, =CHCH₂O), 3.88-3.98 (m, 1 H, H-6a), 3.70-3.86 (m, 2 H, H-5, H-6b), 3.37 (dd, 1 H, J_{2,3} 5.6, H-2), 2.71 (m, 2 H, SCH₂), 1.33, 1.49 (2 s, 6 H, (CH₃)₂CO₂), 1.27 (t, 3 H, SCH₂CH₃); ¹³C NMR (300 MHz, CDCl₃): δ 134.7 (CH, =CH), 117.7 (CH₂, =CH₂), 83.4 (CH, ¹J_{C,H} 152.7, C-1), 79.3, 73.8 (CH, C-3, C-4), 78.4 (CH, C-2), 76.4 (CH, C-5), 72.3 (CH₂, H₂C=CHCH₂), 62.5 (CH₂, C-6), 27.5, 26.0 (CH₃, C(CH₃)₂), 24.6 (CH₂, SCH₂CH₃), 14.7 (CH₃, SCH₂CH₃). ES HRMS: m/z 327.124484 [M + Na]⁺ \pm 0.3 mDa and 305.2 [M + H]⁺ (C₁₄H₂₄O₅S requires m/z 304.41).

Ethyl 2-O-allyl-6-O-(3'-hydroxypropyl)-3,4-O-isopropylidene-1-thio- β -D-galactopyranoside (143).



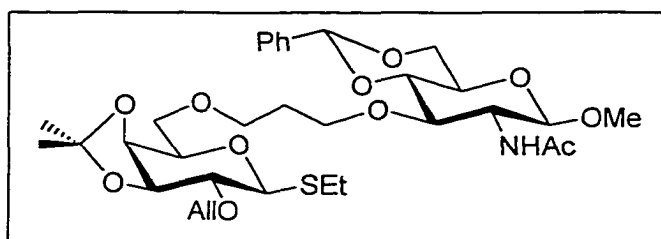
NaH (18.2 mg, 0.76 mmol) was added to a solution of alcohol **142** (210 mg, 0.69 mmol) in dry THF (8 mL). After stirring for 50 min at 60°C, the linker **41** (480 mg, 1.38 mmol) was diluted with dry THF (4 mL) and added dropwise to the alkoxide. The reaction mixture was stirred at 60°C for 2 h, then 1 eq of NaH was added. Once the reaction was completed, the mixture was quenched with EtOAc, diluted with CH₂Cl₂, washed with water, NaHCO₃, brine and then dried with anhyd Na₂SO₄. After solvent evaporation, the residue was stirred with a 1 M TBAF solution in THF (1.5 mL) for 1 h. The mixture was evaporated, diluted with CH₂Cl₂, washed with brine, dried with anhyd Na₂SO₄ and concentrated. The crude syrup was chromatographed on silica (2:1 hexane-EtOAc) to give **143** (105.7 mg, 73%). $[\alpha]_D -14.5^\circ$ (c 8.3, CHCl₃), ¹H NMR (600 MHz, CDCl₃): δ 5.91 (ddt, 1H, HC=), 5.27 (ddd, 1H, HC=), 5.16 (ddd, 1H, HC=), 4.34 (d, 1H, J_{1,2} 9.7, H-1), 4.18-4.28 (m, 2 H, =CHCH₂O), 4.14 (dd, 1H, J_{4,5} 2.0, J_{3,4} 5.7, H-4), 4.12 (t, 1H, H-3), 3.82 (ddd, 1H, J_{4,5} 2.0, J_{5,6a&6b} 7.0, 5.3, H-5), 3.64-3.75 (m, 6H, H-6a, H-6b, H_{link-1}, H_{link-3}), 3.36 (dd, 1H, J_{2,3} 6.2, H-2), 2.64-2.75 (m, 2H, SCH₂CH₃), 1.74-1.84 (m, 2H, H_{link-2}), 1.47, 1.31 (2 s, 6H, (CH₃)₂CO₂), 1.26 (t, 3H, SCH₂CH₃); ¹³C NMR (150 MHz, CDCl₃): δ 134.4 (CH, =CH), 117.6 (CH₂, =CH₂), 83.5 (CH, C-1), 79.2 (CH, C-3), 78.5 (CH, C-2), 75.2 (CH, C-5), 73.7 (CH, C-4), 72.4 (CH₂, H₂C=CHCH₂), 70.8, 70.0, 61.7 (CH₂, C-6, C_{link-3}, C_{link-1}), 31.7 (CH₂, C_{link-2}), 27.6, 26.1 (CH₃, C(CH₃)₂), 24.5 (CH₂, SCH₂CH₃), 14.7 (CH₃, SCH₂CH₃). ES HRMS: m/z 385.166394 [M + Na]⁺ \pm 0.3 mDa and 363.1 [M + H]⁺ (C₁₇H₃₀O₆S requires m/z 362.49).

Ethyl 2-O-allyl-3,4-O-isopropylidene-6-O-(3'-O-methanesulphonyloxypropyl)-1-thio-β-D-galactopyranoside (144).



Triethylamine (0.06 mL, 0.44 mmol) was added to a solution of alcohol **143** (105.7 mg, 0.29 mmol) in dry CH_2Cl_2 (3 mL) and methanesulphonyl chloride (0.035 mL, 0.44 mmol) in CH_2Cl_2 (1 mL) was added dropwise. After stirring for 1 h at rt, the solution was diluted with CH_2Cl_2 , washed with water, 1 M NaOH, water, brine, and dried with anhyd Na_2SO_4 . Evaporation and chromatography on silica (2:1 hexane-EtOAc) gave **144** (120.5 mg, 94%) as an oil. R_f 0.45 (1:1 hexane-EtOAc); ^1H NMR (500 MHz, CDCl_3): δ 5.93 (ddt, 1 H, $\text{HC}=\text{C}$), 5.28 (ddd, 1 H, 3J_E 17.3, 2J 3.2, 4J 1.6, $\text{HC}=\text{C}$), 5.17 (ddd, 1 H, 3J_Z 9.2, 4J 1.1, $\text{HC}=\text{C}$), 4.35 (d, 1 H, $J_{1,2}$ 9.7, H-1), 4.27-4.35 (t, 2 H, $\text{H}_{\text{link-3}}$), 4.20-4.28 (m, 2 H, $=\text{CHCH}_2\text{O}$), 4.15-4.18 (m, 2 H, H-3, H-4), 3.83 (m, 1 H, $J_{4,5}$ 1.7, $J_{5,6a\&6b}$ 5.1, 6.8, H-5), 3.63-3.74 (m, 2 H, H-6a, H-6b), 3.54-3.64 (m, 2 H, $\text{H}_{\text{link-1}}$), 3.37 (dd, 1 H, $J_{2,3}$ 5.9, H-2), 2.99 (s, 3 H, CH_3SO_3), 2.70 (m, 2 H, SCH_2), 1.98 (quintet, 2 H, J 6.23, $\text{H}_{\text{link-2}}$), 1.33, 1.49 (2 s, 6 H, $(\text{CH}_3)_2\text{CO}_2$), 1.28 (t, 3 H, SCH_2CH_3); ^{13}C NMR (125 MHz, CDCl_3): δ 134.4 (CH, $=\text{CH}$), 117.7 (CH_2 , $=\text{CH}_2$), 83.6 (CH, C-1), 79.2 (CH, C-3), 78.4 (CH, C-2), 75.1 (CH, C-5), 73.6 (CH, C-4), 72.3 (CH_2 , $\text{H}_2\text{C}=\text{CHCH}_2$), 69.9 (CH_2 , C-6), 66.8 (CH_2 , $\text{C}_{\text{link-1}}$), 66.4 (CH_2 , $\text{C}_{\text{link-3}}$), 37.0 (CH_3 , CH_3SO_2), 28.9 (CH_2 , $\text{C}_{\text{link-2}}$), 27.5, 26.2 (CH_3 , $\text{C}(\text{CH}_3)_2$), 25.7 (CH_3 , $\text{C}(\text{CH}_3)_3$), 24.5 (CH_2 , SCH_2CH_3), 14.6 (CH_3 , SCH_2CH_3). Anal. Calcd for $\text{C}_{18}\text{H}_{32}\text{O}_8\text{S}_2$ (440.59): C, 49.07; H, 7.32; O, 29.05; S, 14.56. Found: C, 49.59; H, 7.59. ES HRMS: m/z 463.143570 [$\text{M} + \text{Na}$] $^+$ \pm 0.1 mDa and 442.9 [$\text{M} + \text{H}$] $^+$ ($\text{C}_{18}\text{H}_{32}\text{O}_8\text{S}_2$ requires m/z 440.59).

Ethyl 2-O-allyl-3,4-O-isopropylidene-6-O-(3'-O-(methyl 2-acetamido-4,6-O-benzylidene-2-deoxy- β -D-glucopyranos-3-oxo)propyl)-1-thio- β -D-galactopyranoside (145).

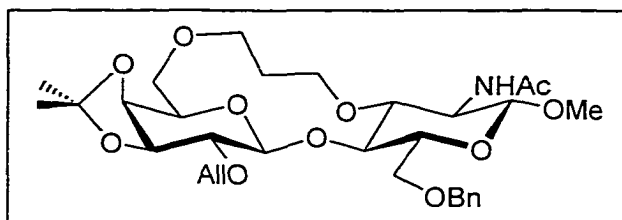


Sodium hydride (4 mg, 0.17 mmol) was added to a solution of glucopyranoside **36** (66 mg, 0.19 mmol) in dry THF (3 mL) and the mixture was stirred for

30 min at 60°C. The methanesulphonate **144** (42 mg, 0.10 mmol) in dry THF (1.5 mL) was added and the reaction mixture was stirred at 60°C for 1 h. Dry (CH₃)₂SO (0.5 mL) was added and after an additional 7 h of heating, the reaction was complete. The cooled reaction mixture was diluted with CH₂Cl₂, washed with NaHCO₃, brine and dried with Na₂SO₄. The concentrated residue was chromatographed on silica (30:1 CH₂Cl₂-MeOH) to give **145** (43.1 mg, 65%) as a white solid. $[\alpha]_D -31.6^\circ$ (*c* 18.5, CHCl₃); ¹H NMR (600 MHz, CDCl₃): δ 7.43-7.46, 7.31-7.36 (m, 5H, ArH), 5.89-5.96 (ddt, 1H, HC=), 5.87 (d, 1H, *J*_{2,NH} 8.1, NHAc), 5.52 (s, 1H, PhCH), 5.28 (ddd, 1H, HC=), 5.17 (ddd, 1H, HC=), 4.80 (d, 1H, *J*_{1,2} 8.2, H-1'), 4.29-4.34 (m, 2H, H-1, H-6'a), 4.27, 4.21 (2ddt, 1H each, H₂C=CHCH₂), 4.07-4.12 (m, 2H, H-3, H-4), 3.98 (t, 1H, *J* 9.4, H-3'), 3.90-3.95 (m, 1H, H_{link}-1), 3.73-3.79 (m, 2H, H-5, H-6'b), 3.61-3.67 (m, 2H, H-6a, H_{link}-1), 3.53-3.61 (m, 3H, H-6b, H-4', H_{link}-3), 3.43-3.50 (m, 5H, OCH₃, H_{link}-3, H-5'), 3.39 (quartet, 1H, *J* 8.3, H-2'), 3.34 (dd, 1H, *J* 6.2, 9.7, H-2), 2.64-2.76 (m, 2H, SCH₂CH₃), 2.02 (s, 3H, NHCOCH₃), 1.68-1.80 (m, 2H, H_{link}-2), 1.46, 1.30 (2s, 3H each, (CH₃)₂C), 1.26 (t, 3H, *J* 7.5, SCH₂CH₃); ¹³C NMR (150 MHz, CDCl₃): δ 135.1 (CH, HC=), 127.0-129.0, 125.8 (CH, ArC), 117.4 (CH, HC=), 101.6 (CH, ¹*J*_{C,H} 164.3, C-1'), 100.9 (CH, PhCH), 83.8 (CH, ¹*J*_{C,H} 154.0, C-1), 82.2 (CH, C-4'), 79.3 (CH, C-3), 78.5 (CH, C-2), 77.4 (CH, C-3'), 75.4 (CH, C-5), 73.7 (CH, C-4), 72.2 (CH₂, H₂C=CHCH₂), 69.9 (CH₂, C-6), 68.9 (CH₂, C_{link}-1), 68.5 (CH₂, C-6'), 67.7 (CH₂, C_{link}-3), 65.6 (CH, C-5'), 57.1 (CH, C-2'), 56.7 (CH₃, OCH₃), 29.9 (CH₂, C_{link}-2), 27.4, 25.8 (CH₃, (CH₃)₂C), 24.6 (CH₂, SCH₂CH₃), 23.4 (CH₃,

NHCOCH₃), 14.7 (CH₃, SCH₂CH₃). Anal. Calcd for C₃₃H₄₉NO₁₁S (667.8): C, 59.35; H, 7.40; N, 2.10; O, 26.35; S, 4.80. Found: C, 59.46; H, 7.39; N, 2.16; S, 4.79. ES HRMS: m/z 690.292627 [M + Na]⁺ ± 0.2 mDa and 668.3 [M + H]⁺ (C₃₃H₄₉NO₁₁S requires m/z 667.3).

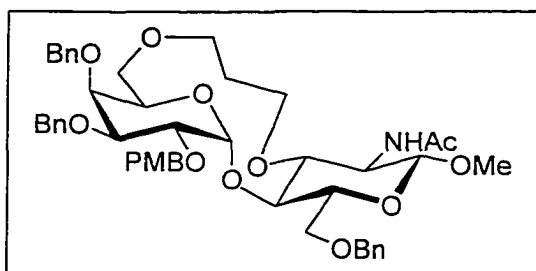
Methyl 2-acetamido-4-O-(2-O-allyl-3,4-O-isopropylidene-β-D-galactopyranosyl)-6-O-benzyl-2-deoxy-3,6'-di-O-(propan-1,3-diyl)-β-D-glucopyranoside (146).



To a dry mixture of **132** (168 mg, 0.25 mmol), DTBMP (179 mg, 0.88 mmol) and powdered 4 Å molecular sieves purged with argon, was added dry CH₂Cl₂ (6 mL). Once the reaction had been stirred for 15 min, methyl triflate (85 μL, 0.75 mmol) was added. After 45 min, the reaction mixture was diluted with CH₂Cl₂ and filtered through celite. The filtrate was washed with NaHCO₃, 0.5 M HCl, NaHCO₃, brine, dried and concentrated. The crude material was chromatographed on silica (2:1 Toluene-Acetone) to give **146** (81 mg, 53%). Some α-anomer was also isolated (4 mg, 3%). [α]_D +10.0° (c 0.4, CHCl₃); ¹H NMR (500 MHz, CDCl₃): δ 7.25-7.38 (m, 5H, ArH), 5.88 (ddt, 1H, HC=), 5.25 (ddd, 1H, HC=), 5.21 (d, 1H, J_{2,NH} 9.2, NHAc), 5.13 (ddd, 1H, HC=), 4.63 (d, 1H, J_{gem} 12.2, PhCH₂), 4.58 (d, 1H, PhCH₂), 4.28 (d, 1H, J_{1,2} 8.0, H-1), 4.14-4.24 (m, 3H, H-2, =CHCH₂), 4.12 (d, 1H, J_{1',2'} 8.4, H-1'), 3.91-4.02 (m, 3H, H-3', H-4, H-6a), 3.89 (dd, 1H, J_{3,4} 5.4, J_{4,5} 1.1, H-4'), 3.65-3.85 (m, 9H, H-3, H-6b, H-5', H-6'a, H-6'b, H_{link-1}, H_{link-3}), 3.47 (s, 3H, CH₃O), 3.39-3.46 (m, 1H, H-5), 3.31 (t, 1H, J_{2',3'} 7.3, H-2'), 1.99 (s, 3H, NHCOCH₃), 1.60-1.78 (m, 2H, H_{link-2}), 1.46, 1.28 (2 s, 3H each, CCH₃); ¹³C NMR (600 MHz, CDCl₃): δ 134.2 (CH, HC=), 128.0, 127.9 (CH, ArC), 116.8 (CH, HC=), 104.3 (CH, ¹J_{C,H} 158.7, C'-1), 102.3 (CH, ¹J_{C,H} 158.2, C-1), 79.8 (CH, C-3'), 78.8 (CH, C-3), 73.4 (CH, C-4'), 75.1 (CH, C-5), 79.4 (CH, C-2'), 72.8 (CH₂, H₂C=CHCH₂), 73.0 (CH₂, PhCH₂O), 74.3 (CH, C-4), 68.1 (CH₂, C-6), 78.3 (CH, C-5'), 67.9, 68.9 (CH₂, C-6', C_{link-1}, C_{link-3}), 56.4 (CH₃, OCH₃),

50.5 (CH, C-2), 30.4 (CH₂, C_{link-2}), 27.9, 26.1 (CH₃, C(CH₃)₂), 23.6 (CH₃, CH₃CONH). ES HRMS: m/z 630.288628 [M + Na]⁺ ± 0.4 mDa and 608.3 [M + H]⁺ (C₃₁H₄₅NO₁₁ requires m/z 607.70).

Methyl 2-acetamido-6-O-benzyl-4-O-(3,4-di-O-benzyl-2-O-p-methoxybenzyl- α -D-galactopyranosyl)-2-deoxy-3,6'-di-O-(propan-1,3-diyl)- β -D-glucopyranoside (147).



To a dry mixture of **131** (29 mg, 0.03 mmol), DTBMP (24 mg, 0.12 mmol) and powdered 4 Å molecular sieves which was purged with argon, was added dry CH₂Cl₂ (1 mL). Once the reaction was stirred for 15 min, methyl triflate (11 μ L, 0.1 mmol) was added. After 45 min the reaction mixture was diluted with CH₂Cl₂ and filtered through celite. The filtrate was washed with NaHCO₃, 0.5 M HCl, NaHCO₃, brine and dried. The crude material was chromatographed on silica (2:1 Toluene-Acetone) and gave **147** (10 mg, 37%). Only the α -anomer of **147** was isolated. $[\alpha]_D^{+16.0^\circ}$ (*c* 0.5, CHCl₃), ¹H NMR (600 MHz, CDCl₃): δ 7.19-7.38, 6.77 (m, ArH), 5.58 (d, 1H, NHAc), 5.04 (d, 1H, *J*_{1',2'} 2.8, H-1'), 4.92 (d, 1H, *J*_{gem} 11.5, PhCH₂), 4.65-4.76 (m, 3H, PhCH₂), 4.48-4.56 (m, 4H, H-1, PhCH₂), 4.44 (d, 1H, *J*_{gem} 12.2, PhCH₂), 4.38 (d, 1H, *J*_{5,6} 9.2, H-5'), 3.98-4.26 (m, 2H, H-3, H-2'), 3.72-3.95 (m, 9H, H-3', H-4, 2XH-6, H-6'A, OCH₃, H_{link-1}), 3.52-3.70 (m, 4H, H-2, H_{link-3}, H_{link-1}, H-4'), 3.42-3.49 (m, 4H, H-5, OCH₃), 3.25-3.30 (m, 1H, H_{link-3}), 3.13 (d, 1H, *J*_{6'a,6'b} 12.5, H-6'), 1.97 (s, 3H, NHCOCH₃), 1.50-1.70 (m, H_{link-2}, HOD). ¹³C NMR (150 MHz, CDCl₃): δ 127.0-130.0, 113.4 (CH, ArC), 100.1 (CH, ¹*J*_{C,H} 161.5, C-1), 93.1 (CH, ¹*J*_{C,H} 165.6, C-1'), 79.3 (CH, C-3'), 77.0, 75.7 (CH, C-3, C-2'), 75.2 (CH, C-4), 74.7 (CH, C-4'), 74.1, 73.7, 73.3, 72.6 (CH₂, 4xPhCH₂), 73.0 (CH, C-5), 69.4 (CH₂, C-6), 68.0 (CH₂, C-6'), 65.7 (CH₂, C_{link-1}), 64.8 (CH, C-5'), 60.0 (CH₂, C_{link-3}), 57.6 (CH, C-2), 56.1, 55.1 (CH₃, 2xOCH₃), 29.7 (CH₂, C_{link-2}), 23.3 (CH₃, NHCOCH₃). ES HRMS: m/z 850.378143 [M + Na]⁺ ± 0.3 mDa (C₄₇H₅₇O₁₂N requires m/z 827.97).

References

- 1 Stryer, L. In *Biochemistry* – 3rd edition; W. H. Freeman and Company: New York, 1988; p. 344-346.
- 2 Wassarman, P. M. *Fertilization in Mammals Sci. Am.* **1988**, *259*, 78-85.
- 3 Watson, K. A.; Mitchell, E. P.; Johnson, L. N.; Son, J. C.; Bichard, C. J. F.; Orchard, M. G.; Fleet, G. W. J.; Oikonomakos, N. G.; Leonidas, D. D.; Kontou, M.; Papageorgiou, A. *Biochemistry* **1994**, *33*, 5745-5758.
- 4 Lindth, I.; Hindsgaul, O. *J. Am. Chem. Soc.* **1991**, *113*, 216-223.
- 5 Lemieux, R. U. *Acc. Chem. Res.* **1996**, *29*, 373-380.
- 6 Isbister, B. D.; St. Hilaire, P. M.; Toone, E. J. *J. Am. Chem. Soc.* **1995**, *117*, 12877-12878.
- 7 Izumi, M.; Tsuruta, O.; Hashimoto, H.; Yazawa, S. *Tetrahedron Lett.* **1996**, *37*, 1809-1812.
- 8 Gohier, A.; Espinosa, J. F.; Jimenez-Barbero, J.; Carrupt, P.-A.; Perez, S.; Imberty, A. *J. Mol. Graphics* **1996**, *14*, 322-327.
- 9 Lemieux, R. U. *Chem. Soc. Rev.* **1989**, *18*, 347-374.
- 10 Bundle, D. R.; Altman, E.; Auzanneau, F.-I.; Baumann, H.; Eichler, E. and Sigurskgold, B. W. In "Complex Carbohydrates in Drug Research", Alfred Benzon Symposium no.36, eds K. Bock and H. Clausen, Munksgaard, Copenhagen, 1994.
- 11 Mulligan, M. S.; Paulson, J. C., Defrees, S.; Zheng, Z.-L.; Lowe, J. B.; Ward, P. A. *Nature* **1993**, *364*, 149-151.
- 12 Von Itzstein, M. et al. *Nature* **1993**, *363*, 418-423.
- 13 Livingston, P. O. *Immunol. Rev.* **1995**, *145*, 147-166.
- 14 Balfour, J. A.; McTavish, D. *Drugs* **1993**, *46*, 1025-1054.
- 15 Johnston, P. S.; Coniff, R. F.; Hoogwerf, B. J.; Santiago, J. V.; Pi-Sunyer, F. X.; Krol, A. *Diabetes Care* **1994**, *17*, 20-29.
- 16 Jacob, G. S. *Curr. Opinion Struct. Biol.* **1995**, *5*, 605-611 and references therein.

- 17 Fischl, M. A.; Resnick, L.; Coombs, R.; Kremer, A. B.; Pottage, J. C.; Fass, R. J.; Fife, K. H.; Powderly, W. G.; Collier, A. C.; Aspinall, R. L. *et al. J. Acquir. Immun. Defic. Syndr.* **1994**, *7*, 139-147.
- 18 Lian, R.H.; Kotwal, G.J.; Wellhausen, S.R.; Hunt, L.A.; Justus, D.E. *J. Immunology* **1996**, *157*, 864-873.
- 19 Hoppensteadt, D.A.; Jeske, W.; Fareed, J.; Nicolaidis, A.N. *International Angiology* **1996**, *15*, 39-46.
- 20 Avila, M.A.; Velasco, J.A.; Cho, C.; Lupu, R.; Wen, D.Z.; Notario, V. *Oncogene* **1995**, *10*, 963-971.
- 21 Chamberlain, J.; Shah, M.; Ferguson, M.W.J. *J. Anatomy* **1995**, *186*, 87-96.
- 22 Lafont, J.; Baroukh, B.; Meddahi, A.; Caruelle, J.P.; Barritault, D.; Saffar, J.L. *Cells and Materials* **1994**, *4*, 219-230.
- 23 Bade, J.J.; Mensink, H.J.A.; Laseur, M. *British J. Urology* **1995**, *75*, 260.
- 24 Simanek, E. E.; McGarvey, G. J.; Jablonowski, J. A.; Wong, C.-H. *Chem. Rev.* **1998**, *98*, 833-862.
- 25 Wong, C.-H; Moris-Varas, F.; Hung, S.-C.; Marron, T. G.; Lin, C.-C.; Gong, K. W.; Weitz-Schmidt, G. *J. Am. Chem. Soc.* **1997**, *119*, 8152-8158.
- 26 Kolb, H. C.; Ernst, B. *Chem. Eur. J.* **1997**, *3*, 1571-1578.
- 27 Allen, H. J.; Johnson, A. A. *Carbohydr. Res.* **1977**, *58*, 253-265; Frost, R. G.; Reitherman, R. W.; Miller, A. L.; O'Brien, J. S. *Anal. Biochem.* **1975**, *69*, 170-179.
- 28 Patanjali, S. R.; Sajjan, S. U.; Surolia, A. *Biochemistry J.* **1988**, *252*, 625-631. Schwarz, F. P.; Puri, K.; Surolia, A. *J. Biol. Chem.* **1991**, *266*, 24344-24350.
- 29 Le Pendu, J.; Gerard, G.; Lambert, F.; Mollicone, R.; Oriol, R. *Glycoconjugate J.* **1986**, *3*, 203-216.
- 30 Lis, H.; Joubert, F. J.; Sharon, N. *Phytochemistry* **1985**, *24*, 2803-2809. Surolia, A.; Sharon, N.; Schwarz, F. P. *J. Biol. Chem.* **1996**, *271*, 17697-17703.

- 31 Loris, R.; Hamelryck, T.; Bouckaert, J.; Wyns, L. *Biochimica et Biophysica Acta* **1998**, *1383*, 9-36.
- 32 Darnell, J.; Lodish, H.; Baltimore, D. In *Molecular Cell Biology* second edition – Scientific American Books, New York, 1990.
- 33 Kornfeld, R.; Kornfeld, S. *Annu. Rev. Biochem.* **1985**, *54*, 631-664.
- 34 Paulson, J. C. *Trends Biochem. Sci.* **1989**, *14*, 272-276.
- 35 Rademacher, T. W.; Parekh, R. B.; Dwek, R. A. *Annu. Rev. Biochem.* **1988**, *57*, 785-838.
- 36 Finne, J.; Breimer, M.E.; Hansson, G. C.; Karlsson, K.-A.; Leffler, H.; Vliegthart, J. F. G.; Van Halbeek, H. *J. Biol. Chem.* **1989**, *264*, 5720-5735.
- 37 Hakomori, S. *Adv. Cancer Res.* **1989**, *52*, 257-331 and references therein.
- 38 Linsley, P. S.; Ochs, V.; Laska, S.; Horn, D.; Ring, D. B.; Frankel, A. E.; Brown, J. P. *Cancer Res.* **1986**, *46*, 5444-5450.
- 39 Jentoft, N. *Trends Biochem. Sci.* **1990**, *15*, 291-294.
- 40 Hakomori, S. In: *Sphingolipid Biochemistry* – Kanfer, J. N. and Hakomori, S. (Eds.), Plenum Press, New York, **1983**, vol 3, 1-165.
- 41 Karlsson, K. A. In: *Biological Membranes* – Chapman, D (Ed.), Academic Press, London, **1982**, vol 4, 1-75.
- 42 Crook, S. J.; Boggs, J. M.; Vistnes, A. I.; Koshy, K. M. *Biochemistry* **1986**, *25*, 7488-7494.
- 43 Kannagi, R.; Nudelman, E.; Hakomori, S. *Proc. Natl. Acad. Sci. USA* **1982**, *79*, 3470-3474.
- 44 Nyholm, P.-G.; Pascher, I.; Sundell, S. *Chem. Phys. Lipids* **1990**, *52*, 1-10.
- 45 Strömberg, N.; Karlsson, K.-A. *J. Biol. Chem.* **1990**, *265*, 11244-11250.
- 46 Hirschberg, C.; Snider, M. D. *Annu. Rev. Biochem.* **1987**, *56*, 63-87.
- 47 Schwarzmann, G.; Sandhoff, K. *Biochemistry* **1990**, *29*, 10865-10871.
- 48 Bundle, D. R. "Recognition of carbohydrate antigens by antibody binding sites" In "Carbohydrates" edited S. Hecht, Oxford University Press Inc., Oxford, **1998**, 370-594.
- 49 Kolter, T.; Sandhoff, K. *Angew. Chem. Int. Ed.* **1999**, *38*, 1532-1568.

- 50 Hakomori, S.; Young, W. W. Jr. In: *Sphingolipid Biochemistry* – Kanfer, J. N. and Hakomori, S. (Eds.), Plenum Press, New York, **1983**, vol 3, 381-436.
- 51 Clausen, H.; Hakomori, S. *Vox Sang.* **1989**, *56*, 1-20.
- 52 Oriol, R.; Le Pendu, J.; Mollicone, R. *Vox. Sang.* **1986**, *51*, 161-171.
- 53 Watkins, W. M. *Advances in human genetics* - Harris, H.; Hirschholm, K. (Eds.), Plenum Press, New York, 1980, 1-136.
- 54 Johnson, P. H.; Yates, A. D.; Watkins, W. M. *Biochem. Biophys. Res. Commun.* **1981**, *100*, 1611-1618.
- 55 Prieels, J. P.; Monnom, D.; Dolmans, M.; Beyer, T. A.; Hill, R. L. *J. Biol. Chem.* **1981**, *256*, 10456-10463.
- 56 Breimer, M. E.; Jovall, P.-A. *FEBS Lett.* **1985**, *179*, 165-172.
- 57 Clausen, H.; Watanabe, K.; Kannagi, R.; Levery, S. B.; Nudelman, E.; Arao-Tomono, Y.; Hakomori, S. *Biochem. Biophys. Res. Commun.* **1984**, *124*, 523-529.
- 58 Kannagi, R. Levery, S. B.; Hakomori, S. *FEBS Lett.* **1984**, *175*, 397-401.
- 59 Karlsson, K.-A.; Larson, G. *J. Biol. Chem.* **1981**, *256*, 3512-3524.
- 60 Yamamoto, F.; Clausen, H.; White, T.; Marken, J.; Hakomori, S. *Nature* **1990**, *345*, 229-233.
- 61 Yamamoto, F.; Hakomori, S. *J. Biol. Chem.* **1990**, *265*, 19257-19262.
- 62 Lis, L.; Sharon, N. *Chem. Rev.* **1998**, *98*, 637-674, and references therein.
- 63 Sharon, N; Lis, H. *Essays Biochem.* **1995**, *30*, 59.
- 64 Rini, J. M. *Annu. Rev. Biophys. Biomol. Struct.* **1995**, *24*, 551.
- 65 Weis, W.; Drickamer, K. *Annu. Rev. Biochem.* **1996**, *65*, 441.
- 66 Cambillau, C. In *Glycoproteins I*; Montreuil, J., Schachter, H., Vliegthart, J. F. G., Eds.; Elsevier Science B.V.: Amsterdam, 1995; p 29.
- 67 Sharon, N; Lis, H. In *Glycoproteins II*; Vliegthart, J. F. G., Montreuil, J., Schachter, H., Eds.; Elsevier Science B.V.: Amsterdam, 1997; p 475.
- 68 Gabius, H.-J. *Eur. J. Biol.* **1997**, *243*, 543.
- 69 Barondes, S. H. *Science* **1984**, *223*, 1259-1264.

- 70 Lemieux, R. U.; Spohr, U. *Adv. Carbohydr. Chem. Biochem.* **1994**, *50*, 1-20.
- 71 Vandonselaar, M.; Delbaere, L. T. J. *J. Mol. Biol.* **1994**, *243*, 345-346.
- 72 Adar, R.; Sharon, N. *Eur. J. Biochem.* **1996**, *239*, 668.
- 73 Imberty, A.; Lasset, F.; Gegg, C.V.; Etzler, M. E.; Perez, S. *Glycoconjugate J.* **1994**, *11*, 400.
- 74 Mammen, M.; Choi, S.-K.; Whitesides, G. M. *Angew. Chem. Int. Ed.* **1998**, *37*, 2754-2794.
- 75 Dimick, S. M.; Powell, S. C.; McMahon, S. A.; Moothoo, D. N.; Naismith, J.H.; Toone, E. J. On the Meaning of Affinity: Cluster Glycoside Effects and Concanavalin A. *J. Am. Chem. Soc.* 1999, In Press.
- 76 Bhattacharyya, L.; Kahn, M. I.; Frant, J.; Brewer, C. F. *Biochemistry* **1988**, *27*, 8762-8767.
- 77 Bhattacharyya, L.; Kahn, M. I.; Brewer, C. F. *J. Biol. Chem.* **1989**, *264*, 11543-11545.
- 78 Mandal, D. K.; Brewer, C. F. *Biochemistry* **1992**, *31*, 12602-12609.
- 79 Schrevel, J.; Gros, D.; Monsigny, M. *Prog. Histochem. Cytochem.* **1981**, *14*(2), 1-269.
- 80 Roth, J. *Exp. Pathol. (Suppl. 3)* **1978**, 1-186.
- 81 Rhodes, J. M.; Milton, J. D.; Eds; In *Lectin Methods and Protocols*; Humana Press Inc.: Totowa, New Jersey, 1998, p. 616.
- 82 Mesulam, M. In *Tracing Neural Connections with Horseradish Peroxidase*; Wiley, New York, 1982, p 251.
- 83 Doyle, R. J.; Keller, K. F. *Eur. J. Clin. Microbiol.* **1984**, *3*, 4-9.
- 84 Doyle, R. J.; Nedjat-Haiem, F.; Keller, K. F.; Frasch, C. E.; *J. Clin. Microbiol.* **1984**, *19*, 383-387.
- 85 Graham, K.; Keller, K.; Ezzell, J.; Doyle, R. J. *Eur. J. Clin. Microbiol.* **1984**, *3*, 210-212.
- 86 Delucca, A. J. II *Can. J. Microbiol.* **1984**, *30*, 1100-1104.
- 87 Debray, H.; Montreuil, J. *Adv. Lectin Res.* **1991**, *4*, 51.
- 88 Reisner, Y.; Sharon, N. *Methods Enzymol.* **1984**, *108*, 168-179.

- 89 Maekawa, M.; Nishimune, Y.; *Biol. Reprod.* **1985**, *32*, 419-425.
- 90 Reisner, Y.; Ravid, A.; Sharon, N. *Biochem. Biophys. Res. Commun.* **1976**, *72*, 1585-1591.
- 91 Aversa, F.; Tabillo, A.; Terenzi, A.; Velardi, A. et al. *Blood*, **1994**, *84*, 3948.
- 92 Reisner, Y.; Kapoor, N.; Kirkpatrick, D.; Pollack, M. S.; Cunningham-Rundles, S. et al. *Blood*, **1983**, *61*, 341-348.
- 93 Kilpatrick, D. C.; Green, C. *Adv. Lectin Res.* **1992**, *5*, 51.
- 94 Oriol, R. *Biochem. Soc. Transac.* **1987**, *15*, 596-599.
- 95 Le Pendu, J.; Lemieux, R. U.; Lambert, F.; Dalix, A.; Oriol, R. *Am. J. of Human Genetics* **1982**, *34*, 402-415.
- 96 Quioco, F. A. *Biochem. Soc. Trans.* **1993**, *21*, 442.
- 97 Toone, E. J. *Current Opinion in Structural Biology* **1994**, *4*, 719-728
- 98 Bundle, D. R.; Baumann, H.; Brisson, J.-R.; Gagne, S. M.; Zdanov, A.; Cygler, M. *Biochem.* **1994**, *33*, 5183-5192.
- 99 Milton, M. J.; Bundle, D. R. *J. Am. Chem. Soc.* **1998**, *120*, 10547-10548.
- 100 Dunitz, J. D. *Science*, **1994**, *264*, 670.
- 101 Gupta, D.; Dam, T. K.; Oscarson, S.; Brewer, C. F. *J. Biol. Chem.* **1997**, *272*, 6388.
- 102 Carver, J. P. *Pure Appl. Chem.* **1993**, *65*, 763-770.
- 103 Hindsgaul, O.; Khane, D. P.; Bach, M.; Lemieux, R. U. *Can. J. Chem.* **1985**, *63*, 2653-2658.
- 104 Carver, J. P.; Michnick, S. W.; Imberty, A.; Cumming, D. A. In *Carbohydrate Recognition in Cellular Function*; Ciba Foundation Symposium 145; Wiley: Chichester, **1989**; Vol. 145.
- 105 Chervenak, M. C.; Toone, E. J. *J. Am. Chem. Soc.* **1994**, *116*, 10533-10539.
- 106 Lemieux, R. U.; Delbaere, L. T. J.; Beierbeck, H.; Spohr, U. In *Host-Guest Molecular Interactions: From Chemistry to Biology*, Ciba Foundation Symposium; Wiley: Chichester, 1991; Vol. 158, pp 231-248.
- 107 Sturtevant, J. M. *Proc. Natl. Acad. Sci. USA*, **1977**, *74*, 2236-2240.
- 108 Oas, T. G.; Toone, E. J. *Adv. Biophysical Chem.* **1997**, *6*, 1-52.

- 109 Lemieux, R. U.; Delbaere, L. T. J.; Beierbeck, H.; Spohr, U. In *Host-Guest Molecular Interactions: From Chemistry to Biology*, Ciba Foundation Symposium; Wiley: Chichester, 1991; Vol. 158, pp 231-248.
- 110 Searle, M. S.; Williams, D. H. *J. Am. Chem. Soc.* **1992**, *114*, 10690-10697.
- 111 Finkelstein, A. V.; Janin, J. *Protein Eng.* **1989**, *3*, 1-3.
- 112 Wilstermann, M.; Balogh, J.; Magnusson, G. *J. Org. Chem.* **1997**, *62*, 3659-3665.
- 113 Alibes, R.; Bundle, D. R. *J. Org. Chem.* **1998**, *63*, 6288-6301.
- 114 Bundle, D. R.; Alibes, R.; Nilar, S.; Otter, A.; Warwas, M.; Zhang, P. *J. Am. Chem. Soc.* **1998**, *120*, 5317-5318.
- 115 Navarre, N.; van Oijen, A. H.; Boons, G. J. *Tetrahedron Lett.* **1997**, *38*, 2023.
- 116 Navarre, N.; Amiot, N.; van Oijen, A. H.; Imberty, A.; Poveda, A.; Jiménez-Barbero, J.; Cooper, A.; Nutley, M. A.; Boons, G. J. *Eur. J. Chem.* **1999**, *5*, 2281-2294.
- 117 Kolb, H. C. *Bioorg. Med. Chem.* **1997**, *7*, 2629-2634.
- 118 Kolb, H. C.; Ernst, B. *Chem. Eur. J.* **1997**, *3*, 1571-1578.
- 119 Ernst, B.; Kolb, H. C. *Pure Appl. Chem.* **1997**, *69*, 1879-1884.
- 120 Shaanan, B.; Lis, H.; Sharon, N. *Science*, **1991**, *254*, 862-866.
- 121 Hindsgaul, O.; Norberg, T.; Le Pendu, J.; Lemieux, R. U. *Carb. Res.* **1982**, *109*, 109-142.
- 122 Du, M.-H.; Spohr, U.; Lemieux, R.U. *Glycoconjugate J.* **1994**, *11*, 443-461.
- 123 Spohr, U.; Paszkiewicz-Hnatiw, E.; Morishima, N.; Lemieux, R. U. *Can. J. Chem.* **1992**, *70*, 254-271.
- 124 Cromer, R.; Spohr, U.; Khare, D. P.; LePendou, J.; Lemieux, R. U. *Can. J. Chem.* **1992**, *70*, 1511-1530.
- 125 Lemieux, R. U.; Du, M.-H.; Spohr, U.; Acharya, S.; Surolia, A. *Can. J. Chem.* **1994**, *72*, 158-163.
- 126 Bush, A. C. *Curr. Opin. Struct. Biol.* **1992**, *2*, 655.

- 127 Homans, S. W. In *Molecular Glycobiology*; Fukuda, M., Hindsgaul, O., Eds.; Oxford University Press: Oxford, **1994**; p 230.
- 128 Homans, S. W.; Rutherford, T. *Biochem. Soc. Trans.* **1993**, *21*, 449.
- 129 Imberty, A.; Bourne, Y.; Cambillau, C.; Rouge, P.; Perez, S. *Adv. Biophys. Chem.* **1993**, *3*, 61.
- 130 Rice, K. G.; Wu, P. Brand, L.; Lee, Y. C. *Curr. Opin. Struct. Biol.* **1993**, *3*, 669.
- 131 Lemieux – personal communication.
- 132 Stuike-Prill, R.; Meyer, B. *Eur. J. Biochem.* **1990**, *194*, 903-919.
- 133 Milton, M.; Bundle, D. R. – unpublished results.
- 134 Delbaere, L. T. J. *et al* – unpublished results.
- 135 Dauber-Osguthorpe, P.; Roberts, V. A.; Osguthorpe, D. J.; Wolff, J.; Genest, M.; Hagler, A. T. *Proteins: Structure, Function and Genetics* **1988**, *4*, 31-47.
- 136 Delbaere, L. T. J.; Vandonselaar, M.; Prasad, L.; Quail, J. W.; Nikrad, P. V.; Pearlstone, J. R.; Carpenter, M. R.; Smillie, L. B.; Spohr, U.; Lemieux, R. U. *Can. J. Chem.* **1990**, *68*, 1116-1121.
- 137 Paulsen, H. *Angew. Chem. Int. Ed. Engl.* **1982**, *21*, 155-173.
- 138 A. Vasella *Pure Appl. Chem.* **1993**, *5*, 731, and references therein.
- 139 Greene, T. W., Wuts, P. G. M. In *Protective Groups in Organic Synthesis*, 2nd ed., Wiley, New York **1991**.
- 140 Frejd, T. *Acta. Pharm. Suec.* **1986**, *23*, 323-369.
- 141 Brinkley, R. In *Modern Carbohydrate Chemistry*, M. Dekker, New York, **1988**.
- 142 Lemieux, R. U. *Adv. Carbohydr. Chem.* **1954**, *9*, 1.
- 143 Lemieux, R. U.; Brice, C.; Huber, G. *Can. J. Chem.* **1955**, *33*, 134.
- 144 Schmidt, R. R.; Behrendt, M.; Toepfer, A. *Synlett* **1990**, 694-696.
- 145 Vankar, Y. D.; Vankar, P. S.; Behrendt, M.; Schmidt, R. R. *Tetrahedron* **1991**, *47*, 9985-9992.
- 146 Ratcliffe, A. J.; Fraser-Reid, B. *J. Chem. Soc. Perkin Trans. 1* **1990**, 747-750.

- 147 Lemieux, R. U.; Chu, P. *Abstr. Pap. Am. Chem. Soc.* **1958**, 133, 31N.
- 148 Lemieux, R. U. In *Molecular rearrangements*, ed. P. de Mayo, Interscience Publishers, New York, **1964**, p709.
- 149 Praly, J. P.; Lemieux, R. U. *Can. J. Chem.* **1987**, 65, 212-223.
- 150 Ziegler, T.; Lau, R. *Tet. Lett.* **1995**, 36, 1417-1420.
- 151 Ziegler, T.; Lemanski, G.; Rakoczy, A. *Tet. Lett.* **1995**, 36, 8973-8976.
- 152 Ziegler, T.; Schüle, G. *Liebigs Ann.* **1996**, 1599-1607.
- 153 Ziegler, T.; Ritter, A.; Hürttlen, J. *Tet. Lett.* **1997**, 38, 3715-3718.
- 154 Ziegler, T.; Lemanski, G. *Eur. J. Org. Chem.* **1998**, 163-170.
- 155 Lau, R.; Schüle, G.; Schwaneberg, U.; Ziegler, T. *Liebigs Ann, Chem.* **1995**, 1745-1754.
- 156 Barresi, F.; Hindsgaul, O. *J. Am. Chem. Soc.* **1991**, 113, 9376-9377.
- 157 Barresi, F.; Hindsgaul, O. *Synlett* **1992**, 759-761.
- 158 Barresi, F.; Hindsgaul, O. *Can. J. Chem.* **1994**, 72, 1447-1465.
- 159 Valverde, S.; Gómez, A. M.; Hernández, A.; Herradón, B.; López, J. C. *J. Chem. Soc. Chem. Commun.* **1995**, 2005-2006.
- 160 Valverde, S.; Gómez, A. M.; Herradón, B.; López, J. C. *Tet. Lett.* **1996**, 37, 1105-1108.
- 161 Paulsen, H.; Lockhoff, O. *Chem. Ber.* **1981**, 114, 3102-3114.
- 162 Iversen, T.; Bundle, D. R. *Carbohydr. Res.* **1980**, 84, C13-C15.
- 163 Paulsen, H.; Kutschker, W.; Lockhoff, O. *Chem. Ber.* **1981**, 114, 3233-3241.
- 164 Garegg, P. J.; Ossowski, P. *Acta. Chem. Scand. Ser. B* **1983**, 37, 249-250.
- 165 Paulsen, H.; Lebuhn, R.; Lockhoff, O. *Carbohydr. Res.* **1983**, 103, C7.
- 166 Gorin, P. A. J.; Perlin, A. S.; *Can. J. Chem.* **1961**, 39, 2474-2485.
- 167 Lichtenthaler, F. W.; Kaji, E. *Liebigs Ann. Chem.* **1985**, 1659-1668.
- 168 Günther, W.; Kunz, H. *Carbohydr. Res.* **1992**, 228, 21 and 217.
- 169 Srivastava, V. K.; Schurch, C. J. *J. Org. Chem.* **1981**, 46, 1121-1126.
- 170 Garegg, P. J.; Hallgren, C. J. *Carbohydr. Chem.* **1992**, 11, 425.
- 171 Ogawa, T.; Kitajima, T.; Nukada, T. *Carbohydr. Res.* **1983**, 123, C5.

- 172 David, S.; Malleron, A.; Dini, C. *Carbohydr. Res.* **1989**, 188, 193.
- 173 Auge, C.; Warren, C. D.; Jeanloz, R. W. *Carbohydr. Res.* **1980**, 82, 85.
- 174 Ekborg, G.; Lindberg, B.; Lonngren, J. *Acta. Chem. Scand.* **1972**, 26, 3287.
- 175 Klimov, E. M.; Demchenko, A. V.; Malysheva, N. N.; Kochetkov, N. *Bioorg. Khim.* **1991**, 17, 1660.
- 176 Tebbe, F. N.; Parshall, G. W.; Reddy, G. S. *J. Am. Chem. Soc.* **1978**, 100, 3611. Ali, M. H.; Collins, P. M.; Overend, W. G. *Carb. Res.* **1990**, 205, 428. Cannizo, L. F.; Grubbs, R. H. *J. Org. Chem.* **1985**, 50, 2386.
- 177 Ito, Y.; Ogawa, T. *Angew. Chem. Int. Ed. Engl.* **1994**, 33, 1765-1767.
- 178 Dan, A.; Ito, Y.; Ogawa, T. *Tet. Lett.* **1995**, 36, 7487-7490.
- 179 Dan, A.; Ito, Y.; Ogawa, T. *J. Org. Chem.* **1995**, 60, 4680-4681.
- 180 Ito, Y.; Ohnishi, Y.; Ogawa, T.; Nakahara, Y. *Synlett* **1998**, 1102.
- 181 Lergenmuller, M.; Nukada, T.; Kuramochi, K.; Dan, A.; Ogawa, T.; Ito, Y. *Eur. J. Org. Chem.* **1999**, 1367-1376.
- 182 Ito, Y.; Ogawa, T. *J. Am. Chem. Soc.* **1997**, 119, 5562-5566.
- 183 Stork, G.; Suh, H. S.; Kim, G. *J. Am. Chem. Soc.* **1991**, 113, 7054-7056.
- 184 Stork, G.; Kim, G. *J. Am. Chem. Soc.* **1992**, 114, 1087-1088.
- 185 Stork, G.; LaClair, J. J. *J. Am. Chem. Soc.* **1996**, 118, 247-248.
- 186 Kahne, D.; Walker, S.; Cheng, Y.; Van Engen, D. *J. Am. Chem. Soc.* **1989**, 111, 6881.
- 187 Bols, M. *J. Chem. Soc. Chem. Commun.* **1992**, 913-914.
- 188 Bols, M. *Acta Chemica Scand.* **1993**, 47, 829-834.
- 189 Bols, M. *J. Chem. Soc. Chem. Commun.* **1993**, 791.
- 190 Bols, M. *Tet. Lett.* **1993**, 49, 10049-10060.
- 191 Bols, M.; Hansen, H. C. *Chem. Lett.* **1994**, 1049.
- 192 Bols, M.; Skrydstrup, T. *Chem. Rev.* **1995**, 95, 1253-1277.
- 193 Hansen, H. C.; Hindsgaul, O.; Bols, M. *Tet. Lett.* **1996**, 36, 4211-4212.
- 194 Nakata, M.; Tamai, T.; Kamio, T.; Kinoshita, M.; Tatsuta, K. *Bull. Chem. Soc. Jpn.* **1994**, 67, 3057-3066.

- 195 Nakata, M.; Tamai, T.; Kamio, T.; Kinoshita, M.; Tatsuta, K. *Tet. Lett.* **1994**, *35*, 3099-3102.
- 196 Huchel, U.; Schmidt, R. R. *Tetrahedron Lett.* **1998**, *39*, 7693-7694.
- 197 Müller, M.; Huchel, U.; Geyer, A.; Schmidt, R. R. *J. Org. Chem.* **1999**, *64*, 6190-6201.
- 198 Garegg, P. J. *Adv. Carb. Chem. Biochem.* **1997**, *38*, 3715-3718.
- 199 McDougal, P. G.; Rico, J. G.; Oh, Y.-I.; Condon, B. D. *J. Org. Chem.* **1986**, *51*, 3388-3390.
- 200 Thijssen, M. J. L.; van Rijswijk, M. N.; Kamerling, J. P. ; Vliegenthart, J. F. G. *Carbohydr. Res.* **1998**, *306*, 93-110.
- 201 Catelani, G.; Colonna, F.; Marra, A. *Carbohydr. Res.* **1988**, *182*, 297-300.
- 202 Kuhn; Baer *Chem. Ber.* **1953**, *86*; 724-726; Moggridge; Neuberger *J. Chem. Soc.* **1938**; 745-748; Freudenberg, K.; Eich, H.; Knoevenagel, C.; Westphal, W. *Chem. Ber.* **1940**, *73*, 441-447.
- 203 Golik, J.; Liu, H.-W.; Dinovi, M.; Furukawa, J.; Nakanishi, K. *Carbohydr. Res.* **1983**, *118*; 135-146; Yoshikawa, M.; Kamigauchi, T.; Ikeda, Y.; Kitagawa, I. *Chem. Pharm. Bull.* **1981**, *29*; 2582-2586; Defaye, J.; Gadelle, A.; Pedersen, C. *Carbohydr. Res.* **1989**, *186*, 177-188; Sabesan, S.; Paulson, J. C. *J. Am. Chem. Soc.* **1986**, *108*; 2068-2080.
- 204 Richardson, A. C. *Carbohydr. Res.* **1969**, *10*, 395-402.
- 205 Meyer zu Reckendork, W. *Chem. Ber.* **1969**, *102*, 4207.
- 206 Jeanloz, R. W. *J. Am. Chem. Soc.* **1957**, *79*, 2591-2592.
- 207 Sabesan, S.; Paulson, J. C. *J. Am. Chem. Soc.* **1986**, *108*, 2068-2080.
- 208 Sprengard, U.; Kretzschmar, G.; Bartnik, E.; Huels, C.; Kunz, H. *Angew. Chem.* **1995**, *107*, 1104-1107.
- 209 David, S. In *Preparative Carbohydrate Chemistry*, ed. Hanessian, S.; Marcel Dekker Inc., New York, 1997, 69-83.
- 210 Kihlberg, J. O.; Leigh, D. A.; Bundle, D. R. *J. Org. Chem.* **1990**, *55*; 2860-2863.
- 211 Cromer, R.; Spohr, U.; Khare, D. P.; LePendu, J.; Lemieux, R. U.; *Can. J. Chem.* **1992**, *70*; 1511-1530.

- 212 Bock, K.; Lundt, I.; Pedersen, C. *Carbohydr. Chem.* **1981**, *90*, 7-16;
Wolfrom, M. L.; Anno, K. *J. Am. Chem. Soc.* **1952**, *74*, 5583-5584.
- 213 Sufrin, J. R.; Bernacki, R. J.; Morin, M. J.; Korytnyk, W.; *J. Med. Chem.*
1980, *23*; 143-149; Danishefsky, S.; Maring, C. *J. Am. Chem. Soc.* **1985**,
107; 7762-7764.
- 214 Swern, D. *Tetrahedron* **1978**, 1651-1660.
- 215 Maercker, A. In *Organic Reactions*, ed. A. C. Cope, John Wiley and Sons,
Inc., N. Y., **1965**, vol 14, 270-434.
- 216 Stafford, J. A.; McMurry, J. E. *Tetrahedron. Lett.* **1988**, *29*, 2531-2534.
- 217 Bergmann, D. *J. Org. Chem.* **1958**, *23*, 1245. Wittig, W. *Liebigs Ann.*
Chem. **1957**, 1.
- 218 Dejter-Juszynski, M.; Flowers, H. M. *Carbohydr. Res.* **1973**, *28*, 144-146.
- 219 Vogel, C.; Bergemann, C.; Ott, A.-J.; Lindhorst, T. K.; Thiem, J.; Dahlhoff,
W. V.; Hällgren, C.; Palcic, M. M.; Hindsgaul, O. *Liebigs Ann./Recueil*
1997, 601-612.
- 220 Wolfrom, M. L. *J. Am. Chem. Soc.* **1930**, *52*, 2464.
- 221 McAuliffe, J. C.; Hindsgaul, O. *J. Org. Chem.* **1997**, *62*, 1234-1239.
- 222 Bhattacharya, A. K.; Thyagarajan, G. *Chem. Rev.* **1981**, *81*, 415-430.
Kosolapoff, J. *J. Am. Chem. Soc.* **1946**, *68*, 1104.
- 223 Ren, P. D.; Pan, S. F.; Dong, T. W.; Wu, S. H. *Synth. Commun.* **1995**, *25*,
3395.
- 224 Zhang, Y.-M.; Esnault, J.; Mallet, J.-M.; Sinay, P. *J. Carbohydr. Chem.*
1999, *18*, 419-427.
- 225 Fukuzawa, A.; Sato, H.; Masamune *Tetrahedron Lett.* **1987**, *28*, 4303.
- 226 Depre, D.; Düffels, A.; Green, L. G.; Lenz, R.; Ley, S. V.; Wong, C.-H.
Chem. Eur. J. submitted.
- 227 Frechét, J. M.; Schuerch, C. *J. Am. Chem. Soc.* **1972**, *94*, 604.
- 228 Baeschlin, D. K.; Chaperon, A. R.; Charbonneau, V.; Green, L. G.; Ley, S.
V.; Lücking, U.; Walter, E. *Angew. Chem. Int. Ed. Engl.* **1998**, *37*, 3423.
- 229 Mayer, T. G.; Krazer, B.; Schmidt, R. R. *Angew. Chem. Int. Ed. Engl.*
1994, *33*, 2177.

- 230 Kim, W. S.; Hosono, S.; Sasai, H.; Shibasaki, M. *Heterocycles* **1996**, *42*, 795.
- 231 Douglas, N. L.; Ley, S. V.; Lücking, U.; Warriner, S. L. *J. Chem. Soc., Perkin Trans. 1*, **1998**, 51-65.
- 232 Green, L.; Hinzen, B.; Ince, S. J.; Langer, P.; Ley, S. V.; Warriner, S. L. *Synlett* **1998**, 440.
- 233 Gervay, J.; McReynolds, K. D. *Curr. Med. Chem.* **1999**, *6*, 129-153.
- 234 Meikle, P. J.; Young, N. M.; Bundle, D. R. *J. Immunol. Meth.* **1990**, *132*, 255-261.
- 235 Bundle, D. R.; Eichler, E.; Gidney, M. A. J.; Meldal, M.; Ragauskas, A.; Sigurskjold, B. W.; Sinnot, B.; Watson, D. C.; Yaguchi, M.; Young, N. M. *Biochemistry* **1994**, *33*, 5172-5182.
- 236 Wilchek, M.; Bayer, E. A. In *Methods in Enzymology: Avidin-Biotin Technology*, Academic Press, inc. New York, 1990, Vol. 184, pp 138-149.
- 237 Woods, R. J.; Edge, C. J.; Dwek, R. A. In *Modeling the Hydrogen Bond*. ACS Symposium Series. Edited by Smith D. Washington: ACS; **1993**, *569*, 252-268.
- 238 Edward, J. T. *Chem. Ind.* **1955**, 1102.
- 239 Pérez, S.; Marchessault, R. H. *Carbohydr. Res.* **1978**, *65*, 114-120.
Jeffrey, G. A. *Acta. Cryst.* **1990**, *B46*, 89-103.
- 240 Lemieux, R. U. *Abstr. Pap. Am. Chem. Soc.* **1959**, *135*, 5E.
- 241 Lemieux, R.U., Bock, K.; Delbaere, L. T. J.; Koto, S.; Rao, V. S. *Can. J. Chem.* **1980**, *58*, 631-653.
- 242 Jeffrey, G. A. *Acta Crystallogr. Sect. B* **1990**, *46*, 89-103.
- 243 Pérez, S.; Kouwijzer, M.; Mazeau, K.; Engelsen, S. B. *J. Mol. Graphics* **1996**, *14*, 307-321.
- 244 Imberty, A. *Curr. Opin. Struct. Biol.* **1997**, *7*, 617-623.
- 245 Melberg, S.; Rasmussen, K. *Carbohydr. Res.* **1979**, *69*, 27-38.
- 246 Imberty, A.; Gerber, S.; Tran, V.; Pérez, S. *Glycoconjugate J.* **1990**, *7*, 27-54.

- 247 Imberty, A.; Mikros, E.; Koca, J.; Mollicone, R.; Oriol, R.; Pérez, S. *Glycoconjugate J.* **1995**, *12*, 331-349.
- 248 Hardy, B. J.; Gutierrez, A.; Lesiak, K.; Seidl, E.; Widmalm, G. *J. Phys. Chem.* **1996**, *100*, 9187-9192.
- 249 Landersjö, C.; Stenutz, R.; Widmalm, G. *J. Am. Chem. Soc.* **1997**, *119*, 8695-8698.
- 250 Lemieux, R. U.; Koto, S. *Tetrahedron* **1974**, *30*, 1933-1944.
- 251 Espinosa, J. F.; Montero, E.; Vian, A.; Garcia, J. L.; Dietrich, H.; Schmidt, R. R.; Martin-Lomas, M.; Imberty, A.; Canada, F. J.; Jimenez-Barbero, J. *J. Am. Chem. Soc.* **1998**, *120*, 1309-1318.
- 252 Cumming, D. A.; Carver, J. P. *Biochemistry* **1987**, *26*, 6655-6663; 6664-6676; 6676-6683.
- 253 Homans, S. W. In *A Dictionary of Concepts in NMR* (revised edition), Oxford University Press, **1992**.
- 254 Thøgersen, H.; Lemieux, R. U.; Bock, K.; Meyer, B. *Can. J. Chem.* **1982**, *60*, 44-57.
- 255 Rees, D. A.; Skerrett, R. J. *Carbohydr. Res.* **1968**, *7*, 334.
- 256 Kitaygorodsky, A. I. *Tetrahedron* **1961**, *14*, 230.
- 257 Lemieux, R. U.; Bock, K. *Arch. Biochem. Biophys.* **1983**, *221*, 125-134.
- 258 Peters, T.; Meyer, Struik-Prill, R.; Somorjai, R.; Brisson, J. R. *Carbohydr. Res.* **1993**, *238*, 49-73.
- 259 Ott, K.-H.; Meyer, B. *J. Comput. Chem.* **1996**, *17*, 1068-1084. Ott, K.-H.; Meyer, B. *Carbohydr. Res.* **1996**, *281*, 11-34.
- 260 Homans, S. W. – MDPROCESS software analyses back-calculated proton-proton distances using an r^6 formalism.
- 261 Woods, R. J. *Curr. Opin. Struct. Biol.* **1995**, *5*, 591-598.
- 262 Hwang, T.-L.; Shaka, A. J. *J. Am. Chem. Soc.* **1992**, *114*, 3157-3159.
- 263 Hwang, T.-L.; Shaka, A. J. *Magn. Reson. Ser. B* **1993**, *102*, 155-165.
- 264 Singh, U. C.; Weiner, P.; Caldwell, J.; Kollman, P. A.; AMBER 3.0, University of California, San Francisco, 1996.

- 265 Weiner, S. J.; Kollman, P. A.; Case, D. A.; Singh, U. C.; Ghio, C.; Alagona, G.; Profeta, S. Jr.; Weiner, P. *J. Am. Chem. Soc.* **1984**, *106*, 765-784.
- 266 Homans, S. W. *Prog. NMR Spec.* **1990**, *22*, 55-81.
- 267 Homans, S. W. *Biochemistry*, **1990**, *29*, 9110-9118.
- 268 Neuhaus, D.; Williamson, M. In *The Nuclear Overhauser Effect in Structural and Conformational Analysis*, VCH Publishers, Inc., **1989**.
- 269 Bock, K.; Thøgersen, H. *Ann. Rep. NMR Spectroscopy* **1982**, *13*, 1-57.
- 270 Lemieux, R. U.; Nagabhushan, T. L.; Paul, B. *Can. J. Chem.* **1972**, *50*, 773-776.
- 271 Delbaere, L. T. J.; James, M. N. G.; Lemieux, R. U. *J. Am. Chem. Soc.* **1973**, *95*, 7866-7868.
- 272 Tvaroska, I.; Hricovini, M.; Petrakova, E. *Carbohydr. Res.* **1989**, *189*, 359-362.
- 273 Krishnamurthy, V. V. *US Patent* **1996**, 4 137, 401.
- 274 Emsley, L.; Bodenhausen, G. *J. Magn. Reson.* **1992**, *97*, 135-148.
- 275 Geyer, A.; Müller, M.; Schmidt, R. R. *J. Am. Chem. Soc.* **1999**, *121*, 6312-6313.
- 276 Poveda, A.; Jiménez-Barbero, J. *Chem. Soc. Rev.* **1998**, *27*, 133-143 and references therein.
- 277 Kronis, K. A.; Carver, J. P. *Biochemistry* **1985**, *24*, 826.
- 278 Asensio, J. L.; Canada, F. J.; Bruix, M.; Rodriguez-Romero, A.; Jiménez. *J. Eur. J. Biochem.* **1995**, *230*, 621.
- 279 Hom, K.; Gochin, M.; Peumans, W. J.; Shine, N. *FEBS Lett.* **1995**, *361*, 157.
- 280 Johnson, P. E.; Joshi, M. D.; Tomme, P.; Kilburn, D. G.; McIntosh, L. P. *Biochemistry* **1996**, *35*, 14381.
- 281 Mullin, N. P.; Hitchen, P. G.; Taylor, M. E. *J. Biol. Chem.* **1997**, *272*, 5668.
- 282 Mikhailov, D.; Mayo, K. H.; Pervin, A.; Lindhardt, R. J. *Biochem. J.* **1996**, *315*, 447.

- 283 Siebert, H. C.; Von der Lieth, C. W.; Kaptein, R.; Beintema, J. J.; Dijkstra, K.; van Nuland, N.; Soedjanaamadja, U. M.; Rice, A.; Vliegthart, J. F. G.; Wright, C. S.; Gabius, H. J. *Proteins* **1997**, *28*, 268.
- 284 Mattinen, M. L.; Kontelli, M.; Kerovuo, J.; Linder, M.; Annala, A.; Lindeberg, G.; Reinikainen, T.; Drakenberg, T. *Protein Sci.* **1997**, *6*, 294.
- 285 Siebert, H. C.; Von der Lieth, C. W.; Dong, X.; Reuter, G.; Schauer, R.; Gabius, H. J.; Vliegthart, J. F. G. *Glycobiology* **1996**, *6*, 561.
- 286 Clore, G. M.; Gronenborn, A.M. *J. Magn. Reson.* **1982**, *48*, 402.
- 287 Clore, G. M.; Gronenborn, A.M. *J. Magn. Reson.* **1982**, *53*, 423.
- 288 Feeney, J.; Birdsall, B.; Roberts, G. C. K.; Burgen, A. S. V. *Biochemistry* **1983**, *22*, 628.
- 289 Casset, F.; Peters, T.; Etzler, M.; Korchagina, E.; Nifant'ev, N.; Perez, S.; Imberty, A. *Eur. J. Biochem.* **1996**, *239*, 710.
- 290 Peters, T.; Pinto, B. M. *Curr. Opin. Struct. Biol.* **1996**, *6*, 710.
- 291 Asensio, J. L.; Canada, F. J.; Jiménez, J. *Eur. J. Biochem.* **1995**, *233*, 618.
- 292 Weimar, T.; Peters, T. *Angew. Chem. Int. Ed. Engl.* **1994**, *33*, 88.
- 293 Casset, F.; Imberty, A.; Perez, S.; Etzler, M.; Paulsen, H.; Peters, T. *Eur. J. Biochem.* **1997**, *244*, 242.
- 294 Meyer, B.; Weimar, T.; Peters, T. *Eur. J. Biochem.* **1997**, *246*, 705.
- 295 Glaudemans, C. P. J.; Lerner, L. E.; Daves, D. G.; Kovac, P. Jr; Venable, R.; Bax, A. *Biochemistry* **1990**, *29*, 906.
- 296 Arepalli, S. R.; Glaudemans, C. P. J.; Bax, A. *J. Mag. Res. Series B* **1995**, *106*, 195.
- 297 Imberty, A.; Hardman, K. D.; Carver, J. P.; Perez, S. *Glycobiology* **1991**, *1*, 456.
- 298 Perez, S. **1978**, DSc Thesis, University of Grenoble, France.
- 299 Allinger, N. L.; Yuh, Y. H.; Lii, J. H. *J. Am. Chem. Soc.* **1989**, *111*, 8551-8556.
- 300 Brooks, B. R.; Brucoleri, R. E.; Olafson, B. D.; States, D. J.; Swaminathan, S.; Karplus, M. *J. Comp. Chem.* **1983**, *4*, 187-217.

- 301 Blondel, A.; Karplus, M. *J. Comp. Chem.* **1996**, *17*, 1132-1141.
- 302 van Gunsteren, W. F.; Berendsen, H. J. C. *Angew. Chem., Int. Ed. Engl.* **1990**, *29*, 992-1023.
- 303 Clark, M.; Cramer, III, R. D.; Van Opdenbosch, N. *J. Comp. Chem.* **1989**, *10*, 982-1012.
- 304 Cornell, W. D.; Cieplak, P.; Bayly, C. I.; Gould, I. R.; Merz, Jr.; K. M.; Ferguson, D. M.; Spellmeyer, D. C.; Fox, T.; Caldwell, J. W.; Kollman, P. A. *J. Am. Chem. Soc.* **1995**, *117*, 5179-5197.
- 305 Scherf, T.; Anglister, J. (1993) *Biophys. J.* *64*, 754-761.
- 306 Discover® User Guide, part 1 – versions 2.9.7 and 95.0/3.00 – Biosym/MSI, San Diego, 1995, pp. 4-1 to 4-27.
- 307 Iglesias, J. L.; Lis, H., Nathan, S. *J. Biochem.* **1982**, *123*, 247-252.
- 308 Hurd, R. E. *J. Mag. Res.* **1990**, *87*, 422-428.
- 309 Brüschweiler, R.; Griesinger, C.; Sorensen, O.W.; Ernst, R. R. *J. Magn. Res.* **1988**, *78*, 178-185.
- 310 States, D. J.; Haberkon, R. A.; Ruben, D. J. *J. Magnetic Res.* **1982**, *48*, 286-292.
- 311 Hwang, T.-L.; Shaka, A. J. *J. Am. Chem. Soc.* **1992**, *114*, 3157-3159.
- 312 Hwang, T.-L.; Shaka, A. J. *Magn. Reson. Ser. B* **1993**, *102*, 155-165.
- 313 Bax, A.; Subramanian, S. *J. Mag. Res.* **1986**, *67*, 565-569.
- 314 Bax, A.; Summer, F. *J. Am. Chem. Soc.* **1986**, *108*, 2093-2094.
- 315 Kupce, E; Freeman, R. *J. Magn. Reson. Ser. A* **1993**, *105*, 234-238.
- 316 Arepalli, S. R., Glaudemans, C. P. J., Daves, G. D, Kovac, P., & Bax, A. *J. Magn. Reson. B.* **1995**, *106*, 195-198.
- 317 Vincent, S. J. F., Zwahlen, C., Bodenhausen, G. *Proc. Natl. Acad. Sci. U.S.A.* **1997**, *94*, 4383-4388.
- 318 Perrin, D. D.; Armarego, W. L. F.; Perrin, D. R. In *Purification of Laboratory Chemicals*; 2nd edition; Pergamon Press: New York, **1980**.
- 319 Pozagay, V.; Brisson, J.-R.; Jennings, H. J. *J. Org. Chem.* **1991**, *56*, 3377-3385.

320 Sufrin, J. R.; Bernacki, R. J.; Morin, M. J.; Korytnyk, W. J. *Med. Chem.*
1980, 23, 143-149.